DNA methylation, cell differentiation and genetic factors involved in radiosensitivity

Thesis submitted for the degree of

Doctor of Philosophy

at the University of Leicester

by

George Giotopoulos

Department of Genetics

University of Leicester

August 2008

for Mark

Table of contents

Acknowledgements

I would like to thank all the people in the Department of Genetics, who provided support and advice during this PhD. Special thanks goes to Ila Patel for securing some extra funding for me during the write-up period. Many thanks to the animal house staff for their help and excellent care of the mice, and Ruth Barber for all her help with the project licence. I would also like to thank the Hope Foundation for funding this project.

Many thanks to our collaborators, especially Dr Paul Symonds and Prof. Robert Brown, for their invaluable contributions to this project. I am grateful to Yuri Dubrova for his advice and support, countless cigarette breaks, and for being crazy enough to read through this thesis and adopt me as his student. Chris Talbot and Cristina Tufarelli (in alphabetical order) for all their feedback, help and advice, and simply for being amazing people. Aline for (once more) countless breaks and tonnes of hot chocolate during the last months of writing up.

A big ‘thank you’ to the people in my group: Abi for introducing me to the evil ways of lab work, and Christine for being a great colleague and for putting up with me. Finally, Mays for all the training and advice, and for being a great person to work with. Above all, a big ‘thank you’ Mays, for being there when things went a bit wrong and for your invaluable friendship.

I am grateful to my family for their unconditional love and support. You guys are a big part of this thesis; thank you.

Most importantly, I would like to express my sincere gratitude to my supervisor and friend Mark Plumb, for giving me the chance to work on this project, and for his excellent guidance and continuous support during this PhD. I really hope he would have enjoyed reading through this thesis. After all, all (good) ideas in it were his. Thank you for everything Mark, I am grateful I got to work with you.

Abstract

George Giotopoulos: DNA methylation, cell differentiation and genetic factors involved in radiosensitivity

Despite its benefits in cancer treatment, ionising radiation (IR) can induce a series of adverse acute and/or long term effects. Studies on A-bomb survivors and radiotherapy patients have shown that acute whole-body exposure results in an increased risk for radiation-induced Acute Myeloid Leukaemia (r-AML), a bone marrow (BM) malignancy; whereas local-radiotherapy patients run the risk of developing acute and/or long term normal tissue reactions.

Irradiated BM cells manifest persistent radiation-induced genomic instability. BM is one of the most susceptible tissues to radiation-induced cancer and one of the most radiosensitive tissues, which proposes a link between cancer susceptibility, genomic instability and radiosensitivity. The exact mechanism by which exposure of BM cells to IR leads to malignant transformation is still unclear, but the non-targeted nature of radiation-induced damage and genomic instability could suggest that an epigenetic mechanism is also involved; and DNA methylation is a good candidate.

This thesis investigated genetic and epigenetic factors that may be involved in biological responses to ionising radiation exposure. Stem cell frequency is genetically determined in mouse haemopoiesis and is possibly part of the equation that defines cancer risk. Global DNA methylation levels were assessed in control haemopoietic tissues and radiation-induced leukaemias. The methylation status of haemopoietic malignancies reflects that of their untransformed tissue. Additionally, DNA methylation levels of untransformed haemopoietic tissues were found to correlate with their relative radiosensitivity *in vivo*.

In vivo responses to ionising radiation were found to be under the influence of both genetic and epigenetic factors, highlighting the complexity of such biological reactions.

List of Tables

List of Figures

Abbreviations

•OH	Hydroxyl radical
5-^{Me}C	5-methyldeoxycytosine
95%CI	95% confidence intervals
AHS	Adult health study
ALL	Acute Lymphoblastic Leukaemia
AML	Acute Myeloid Leukaemia
ASO	Allele Specific Oligonucleotide
AT	Ataxia telangiectasia
ATM	Mutated gene in Ataxia Telangiectasia
BER	Base excision repair
BL	B-cell leukaemia
BM	Bone marrow
bp	Base pairs
(BXD)R1	C57BL/6 x DBA recombinant mice
CAFC	Cobblestone Area Forming Cell
CFU-A	Agar-Colony forming unit
CFU-S	Spleen-Colony forming unit
CHO	Chinese Hamster Ovary (cells)
CLL	Chronic Lymphoid Leukaemia
cM	Centi-Morgan
CML	Chronic Myeloid Leukaemia
dH_2O	Distilled water
DHFR	Dihydrofolate Reductase
DNA	Deoxyribonucleic acid
DNMT	DNA methyltransferase
E/NE	Erythroid/non-erythroid
ECM	Extracellular matrix
EORTC	European Organization for Research and Treatment of Cancer
EPO	Erythropoietin
EPO-R	Erythropoietin receptor
ESTR	Expanded simple-tandem repeat
EtOH	Ethanol
F_1	CBA/H x C57BL/6 cross
F_2	F_1 x F_1
FACS	Fluorescence activated cell sorting/scanning
Gy	Gray
HPLC	High Performance Liquid Chromatography
HRR	Homologous recombination repair
HSC	Haemopoietic Stem Cell
IAP	Intracisternal A Particle

ICF	Immunodeficiency, centromeric instability, facial anomalies syndrome
IR	Ionising radiation
JAK2	Janus Kinase 2
$L^-S^+K^+$	Lin^- $Sca\text{-}1^+$ $c\text{-}Kit^+$
LENT-SOMA	Late Effects of Normal Tissue-Subjective Objective Management Analytical
LET	Linear energy transfer
Lin	Lineage
LINE-1	Long Interspersed Nucleotide Element-1
LOD	Logarithm of the odds
LSS	Life span study
LT-HSC	Long-term self-renewing Haemopoietic Stem Cell
LTC-IC	Long Term Culture Initiating Cell
LTR	Long-term repopulating (assay)
MDS	Myelodysplastic syndrome
MPP	Multipotent Progenitor Cell
MTHFR	Methylenetetrahydrofolate Reductase
MTR	5-Methyltetrahydrofolate-homocysteine methyltransferase
NHL	Non-Hodgkin's Lymphoma
OR	Odds ratio
***p*-ABG**	*p*-aminobenzoglutamic acid
PCR	Polymerase Chain Reaction
pRBC	Peripheral red blood cell
QTL	Quantitative Trait Loci
r-AML	Radiation-induced Acute Myeloid Leukaemia
RBMC	Red bone marrow cell
RERF	Radiation effects research foundation
RFLP	Restriction fragment length polymorphism
RNA	Ribonucleic acid
ROS	Reactive oxygen species
RTOG	Radiation Therapy Oncology Group
SAM	S-adenosyl methionine
Scfr	Stem cell frequency regulator (1 and 2)
SCID	Severe combined immunodeficiency
SNP	Single nucleotide polymorphism
ST-HSC	Short-term self-renewing Haemopoietic Stem Cell
Sv	Sievert
t-AML	Therapy-related Acute Myeloid Leukaemia
TGF*β*-1	Transforming Growth Factor beta-1
TL	Thymic lymphoma
UV	Ultraviolet (light)
WBMC	White bone marrow cell
XRCC	X-ray Repair Cross Complementing (1 and 2)

Chapter 1:

General Introduction

1.1 Radiation.

Radiation is a generic term describing a flux of energy in the form of electromagnetic waves (photons of light) or subatomic particles. The energy deposited by these electromagnetic waves and particles determines the effect radiation has on the cell/organism.

High energy particles and electromagnetic waves are able to remove electrons upon collision with atoms or molecules, thus producing ions within a cell (ionising radiation). The energy content of non-ionising radiation [e.g. microwaves and extremely low-frequency electric and magnetic fields (ELF-EMF)] is not high enough to overcome the binding energy that keeps electrons in their orbital shells and does not produce ionisation (reviewed in Wakeford, 2004).

1.2 Ionising Radiation.

As the name implies, ionising radiation (IR) contains energy high enough to create electrically charged ion pairs (ionisation). Electrons and positrons (β-particles), protons, neutrons, and α-particles belong to this category of radiation. β-particles have a very high speed and very little mass. Depending on the emitting isotope, β-particles have a characteristic amount of energy which may vary from low (e.g. ^{3}H) to high (e.g. ^{32}P). α-particles (large subatomic particles consisting of two protons and two neutrons) and protons have a larger mass, but a lower speed. They deposit large amounts of energy over a relatively short distance (reviewed in Dainiak, 2002). Neutrons are particles with a mass similar to that of a proton. Contrary to α-particles and protons, which have a net positive charge, neutrons are uncharged particles. For this reason, neutrons are highly penetrating compared to charged particles of similar mass and energy (Hall, 2000).

In contrast to the aforementioned types of radiation, X-rays and γ-rays have no mass or charge. These types of IR are less efficient at creating ions, but are able to penetrate more deeply into tissues. The rate at which the energy is deposited along the track of radiation further classifies the various types of IR into high- or low-LET (linear energy transfer). Neutrons and α-particles are forms of high-LET and produce dense ionisation tracks, whereas X-rays and γ-rays are forms of low-LET as they produce sparse ionisation tracks (Wakeford, 2004).

The energy deposited by the radiation in a unit mass of matter is called the absorbed dose of ionising radiation and is measured in Gray (Gy, 1Gy=1Joule/Kg). Given the difference in the density of ionisation tracks between high- and low-LET, the effective dose is also used as a way to add and/or compare the effects of different types of radiation delivered to different parts of the body. The effective dose is measured in Sievert (Sv), where 1Gy=1Sv in the case of sparsely ionising radiations (e.g. X-rays). This is not the case for radiations that produce dense ionisation tracks (high-LET). For example, 1Gy=20Sv in the case of α-particles (Wakeford, 2004). X-rays were used in all experiments in this thesis. Additionally all murine leukaemias analysed (see **Chapter 4**) arose following exposure to X-rays. This thesis will therefore focus on the effects of exposure to low-LET types of ionising radiation; X-rays in particular.

1.3 The biological effects of ionising radiation.

Exposure of a biological system to ionising radiation induces a series of processes that differ in time-scale. As seen in **Figure 1.1** these effects can be divided into three phases (according to Steel, 1993).

The physical phase ($0\text{-}10^{-8}$ seconds) involves the interactions between the charged particles and the atoms/molecules in the irradiated tissue. Electron excitation (rising to higher energy levels) and ionisation (ejection from orbital shells) occurs during this phase. These energetic electrons may excite or ionise other atoms, giving rise to a chain of ionisations. Free radicals, damaged atoms and molecules react with other cellular components during the chemical phase (10^{-12}-100 seconds). Free radicals are atoms or molecules carrying an un-paired orbital electron in the outer shell, which results in high chemical reactivity. They result from the direct interaction of ionising radiation with

atoms or molecules in the cell (primarily with water as ~80% of a cell is composed of water) and are then able to induce DNA damage (indirect effects of ionising radiation) (see section 1.3.2).

All subsequent effects are included in the biological phase which commences at approximately 1 second post-irradiation and may cover the entire lifespan. The biological phase includes recognition of damage and subsequent repair of damaged organelles and molecules. Improper repair might lead to mutations, whereas in cases when substantial damage has occurred, the cells might undergo apoptosis (programmed cell death). This increase in cell death can lead to the development of early/acute effects, which are the manifestations of cell loss. Increased cell death is followed by compensatory cell proliferation, which aims to restore tissue cellularity. Finally, exposure to ionising radiation may lead to late tissue effects such as fibrosis and telangiectasia and/or the formation of cancer many years after exposure, suggesting that the effects of ionising radiation can persist for life (Steel, 1993). These effects will be discussed separately (see sections 1.3.1, 1.3.2, 1.3.3 and 1.3.4).

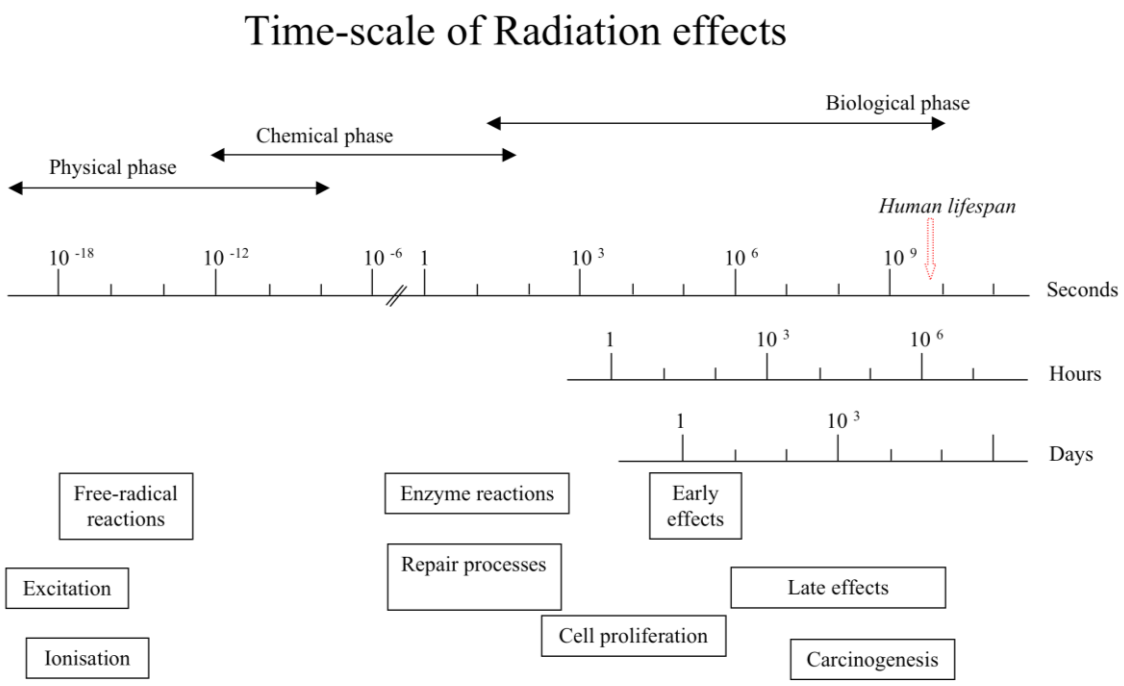

Figure 1.1: The time-scale of radiation effects (adapted from Steel, 1993).

Very high doses of IR are lethal, which constitutes ionising radiation as a relatively weak carcinogen (this is why radiotherapy is so effective). In contrast, moderate-to-high doses of ionising radiation have been found to have direct, indirect, as well as delayed effects on the cell and its DNA (**Figure 1.2**; see sections 1.3.2, 1.3.3 and 1.3.4). At the tissue level, exposure to ionising radiation may lead to the development of acute and/or long term effects (**Figure 1.2**; see section 1.3.1).

For the purposes of this thesis, the murine haemopoietic system has been used to investigate the direct/indirect and delayed effects of ionising radiation on the cell and its DNA (see sections 1.3.2, 1.3.3 and 1.3.4; **Chapters 3** and **4**).

The acute and long term tissue effects of ionising radiation have been assessed in a group of female breast cancer patients that have received radiotherapy as part of their treatment (see section 1.3.1; **Chapter 5**).

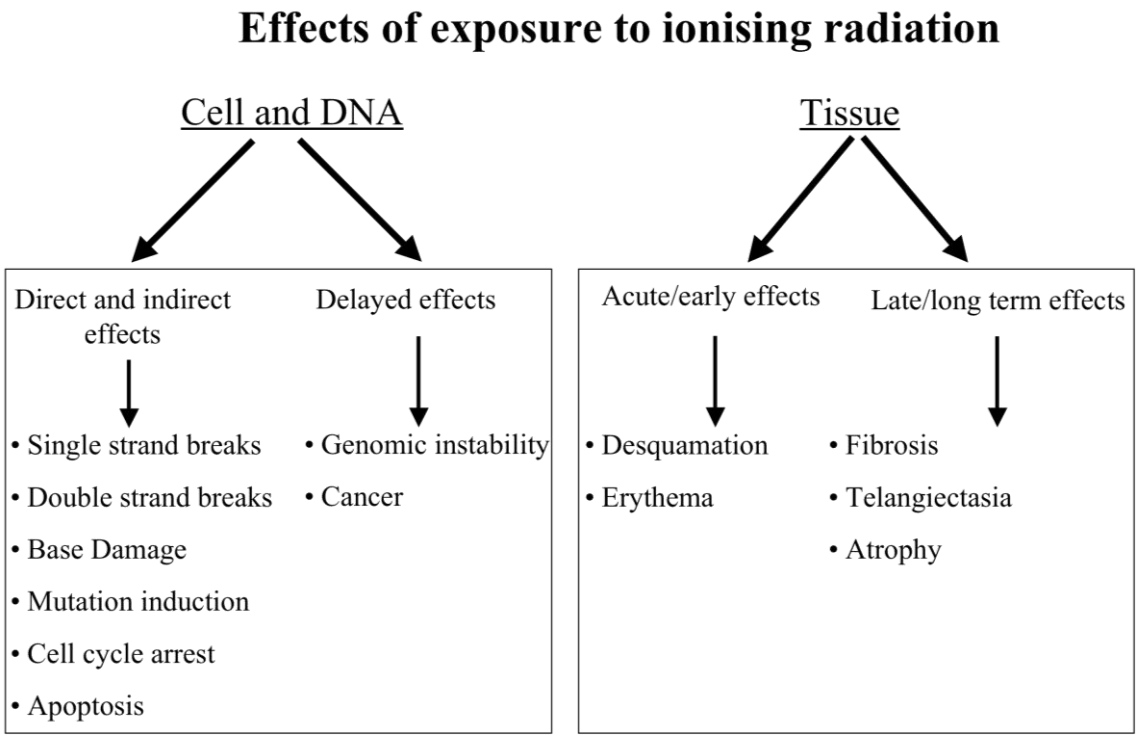

Figure 1.2: The effects on ionising radiation on the cell/DNA and tissue level.

1.3.1 Normal tissue damage.

Due to its high efficiency at cell killing, ionising radiation is widely used in cancer treatment. Approximately 50% of patients with solid malignant tumours will be offered radiotherapy with either curative or palliative intent (Bentzen, 2006). However, radiotherapy has been associated with a range of adverse reactions, seen in the unavoidably exposed normal tissue surrounding the irradiated area. These effects (**Figure 1.2**) are known as normal tissue damage and are further classified as either acute/early or late/long term. In this thesis, normal tissue damage has been assessed in a group of breast cancer patients treated with radiotherapy (**Chapter 5**) and only normal tissue reactions associated with this specific site will be discussed.

The early/acute effects are seen within 90 days from the start of treatment and are the manifestations of radiation-induced cell killing (Van der Kogel, 1993). They are mainly seen in highly proliferating hierarchical tissues such as bone marrow (BM), skin, and the intestinal tract and reflect stem/progenitor cell depletion. Hierarchical tissues show a clearly recognisable separation between the stem cell compartment and the compartment of post-mitotic functional cells and are usually rapidly proliferating (Van der Kogel, 1993). Desquamation (skin shedding) and erythema (redness of the skin) are acute responses often seen in breast cancer radiotherapy patients. Within the dose range of standard radiotherapy schedules (40-60Gy delivered in ~2Gy fractions for breast cancer patients), acute responses tend to be transient and show no strong dependence on the total dose received. However, high doses may lead to slower healing of the injury sustained (Bentzen and Overgaard, 1993).

As the name implies, late/long term effects have a longer latency period (>90 days from the beginning of the treatment, but usually develop after months or years) and are rarely reversible (Bentzen, 2006). Exposure to higher doses correlates with reduced latency and usually increased levels of injury sustained (Bentzen and Overgaard, 1993).

Long term normal tissue damage may include telangiectasia, atrophy, and fibrosis. Given their long latency period, these reactions are scored at least 2 years following treatment. Telangiectasia refers to small, dilated blood vessels, which can be seen under the surface of the skin. Atrophy refers to loss of tissue cellularity. Fibrosis is the most studied long term normal tissue damage and the major constraint of dose in fractionated

radiotherapy. It is clinically defined by overgrowth and hardening (reduced tissue flexibility) of the exposed tissue due to excess deposition of extracellular matrix (ECM) components (Rodemann and Bamberg, 1995). Normal tissue is gradually replaced by mesenchymal cells which over-produce ECM (including collagen), ultimately giving rise to the fibrotic phenotype (Li *et al.*, 1999). This type of long term normal tissue damage is considered to be the endpoint of chronic inflammatory reactions involving a large number of cytokines and chemokines, which act as regulators of fibrosis (Rodemann and Bamberg, 1995; Li *et al.*, 1999; Wynn, 2008). These chronic inflammatory reactions may also lead to the development of heart disease such as myocardial infarction or other ischaemic heart diseases (Schultz-Hector and Trott, 2007). For example, radiation-induced pericardial and epicardial inflammation can lead to the development of pericarditis as early as one year following exposure (Hendry *et al.*, 2008).

Radiotherapy patients may present with all, none, or different combinations of both acute and late reactions. Empirical clinical evidence has demonstrated that normal tissue reactions (both early and late) vary significantly between patients, even after strictly identical treatment schedules (Bentzen, 2006), raising the possibility that normal tissue responses to radiation may be under genetic control (see section 1.9).

1.3.2 Direct and indirect effects of ionising radiation on the cell and its DNA.

The direct effects of ionising radiation arise from the interaction of DNA with the radiation energy, whereas the indirect effects arise from the interaction of DNA with radiation-formed reactive species. Reactive oxygen species (ROS) are predominantly formed following radiolysis of water resulting in the formation of hydroxyl radicals (•OH). Most DNA damage is induced by •OH radicals (~65%) rather than damage induced by direct ionisation (Friedberg *et al.*, 1995). Radiation-induced DNA damage includes DNA base damage, single and double strand breaks. Exposure of one cell to 1Gy of ionising radiation will result in ~1000 single strand breaks and ~40 double strand breaks (Ward, 1988). Radiation-induced single strand breaks are usually readily repaired using the opposite DNA strand as a template. Radiation-induced double strand breaks are the most biologically important DNA lesions, as they are usually accompanied by extensive base damage, a phenomenon termed ‘locally multiply

damaged site(s)' (Ward, 1985). If un-repaired, radiation-induced double strand breaks can lead to cell death and if mis-repaired they can lead to chromosome deletions and/or translocations (King, 2000).

Upon irradiation and subsequent DNA damage, the cell cycle machinery arrests at specific checkpoints in G1, S, G2 and M phase. This enables repair of DNA damage and prevents lesions from turning into permanent mutations (Hoeijmakers, 2001). The cells employ DNA repair mechanisms which are specific to the nature of damage incurred. There are five major DNA repair pathways: Base excision repair (BER) removes and corrects damaged bases and single strand breaks, nucleotide excision repair (NER) removes pyrimidine dimers and large chemical adducts and mismatch repair (MMR) removes and corrects any mismatched bases resulting from replication mistakes. Finally, homologous recombination repair (HRR) and non-homologous end joining (NHEJ) are employed to repair double strand breaks (reviewed in Hoeijmakers, 2001).

In cases when the damage incurred is too significant, cells undergo apoptosis (programmed cell death). The direct and indirect effects of ionising radiation on the cell/DNA level are therefore mainly comprised of DNA damage and cell death. The levels of radiation-induced apoptosis vary between different tissues and are usually higher in hierarchical tissues (**Figure 1.3**). These tissues (e.g. bone marrow, skin) are high-turnover and enriched for clearly recognisable immature stem cells. Tissues such as skeletal muscle and brain exhibit a less clearly defined separation between the stem and mature cell compartments, are slowly renewing, show decreased levels of radiation-induced cell death and a dose-dependant latency to radiation-induced effects (Van der Kogel, 1993; Midgley *et al.*, 1995; MacCallum *et al.*, 1996).

Midgley *et al.* (1995) reported increased p53 induction and apoptosis in the bone marrow and spleen, but not the liver of irradiated mice. Similarly, another study reported radiation-induced apoptosis in murine spleen, BM and intestine, but not liver, skeletal muscle and brain (MacCallum *et al.*, 1996). BM was identified by these *in vivo* experiments as one of the most radiosensitive murine tissues, which is in agreement with the increased BM radiosensitivity seen in humans (**Figure 1.3**) and the paradigm of increased radiosensitivity of hierarchical tissues.

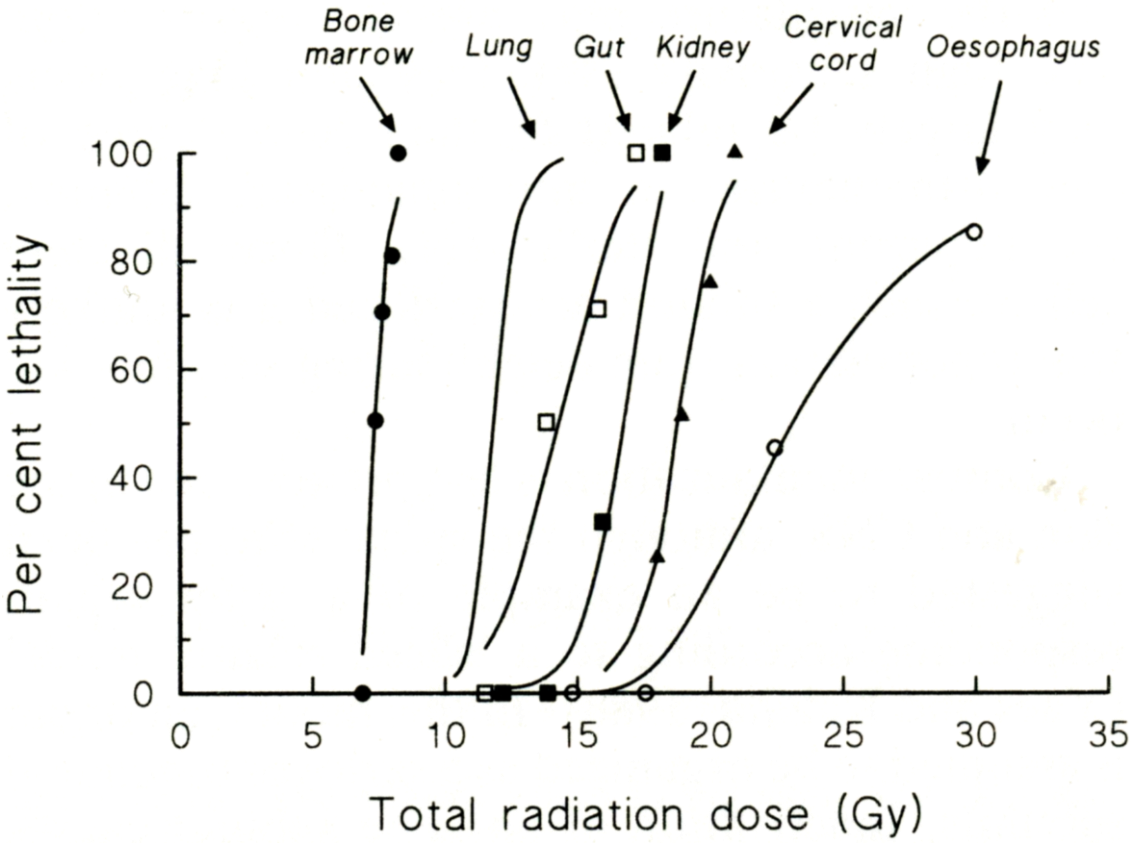

Figure 1.3: Dose response curves of irradiated normal tissues, employing lethality as an endpoint (Figure 13.7 from Steel, 1993). Lethality endpoints are based on patient death due to specific tissue injury following exposure to ionising radiation (Van der Kogel, 1993). Bone marrow (a hierarchical tissue) is one of the most radiosensitive adult tissues.

1.3.3 Radiation-induced genomic instability.

For many years, the central dogma in radiobiology has been that radiation-induced DNA damage is solely caused by the direct and indirect effects of ionising radiation. According to this, if the initial damage was repaired, then all the clonal descendants of irradiated cells should appear normal (**Figure 1.4a**). Similarly, if the initial damage remained un-repaired (or was mis-repaired), then all clonal descendants should exhibit the same genetic alterations (**Figure 1.4b**). However, the presence of non-clonal chromosome aberrations and mutations in descendants of irradiated cells (Chang and Little, 1992; Kadhim *et al.*, 1992 and 1994; Marder and Morgan, 1993; Grosovsky *et al.*, 1996; Harper *et al.*, 1997; Watson *et al.*, 2001) challenged the dogma that all radiation-induced effects occur shortly after exposure (**Figure 1.4c**) and introduced the concept of radiation-induced genomic instability.

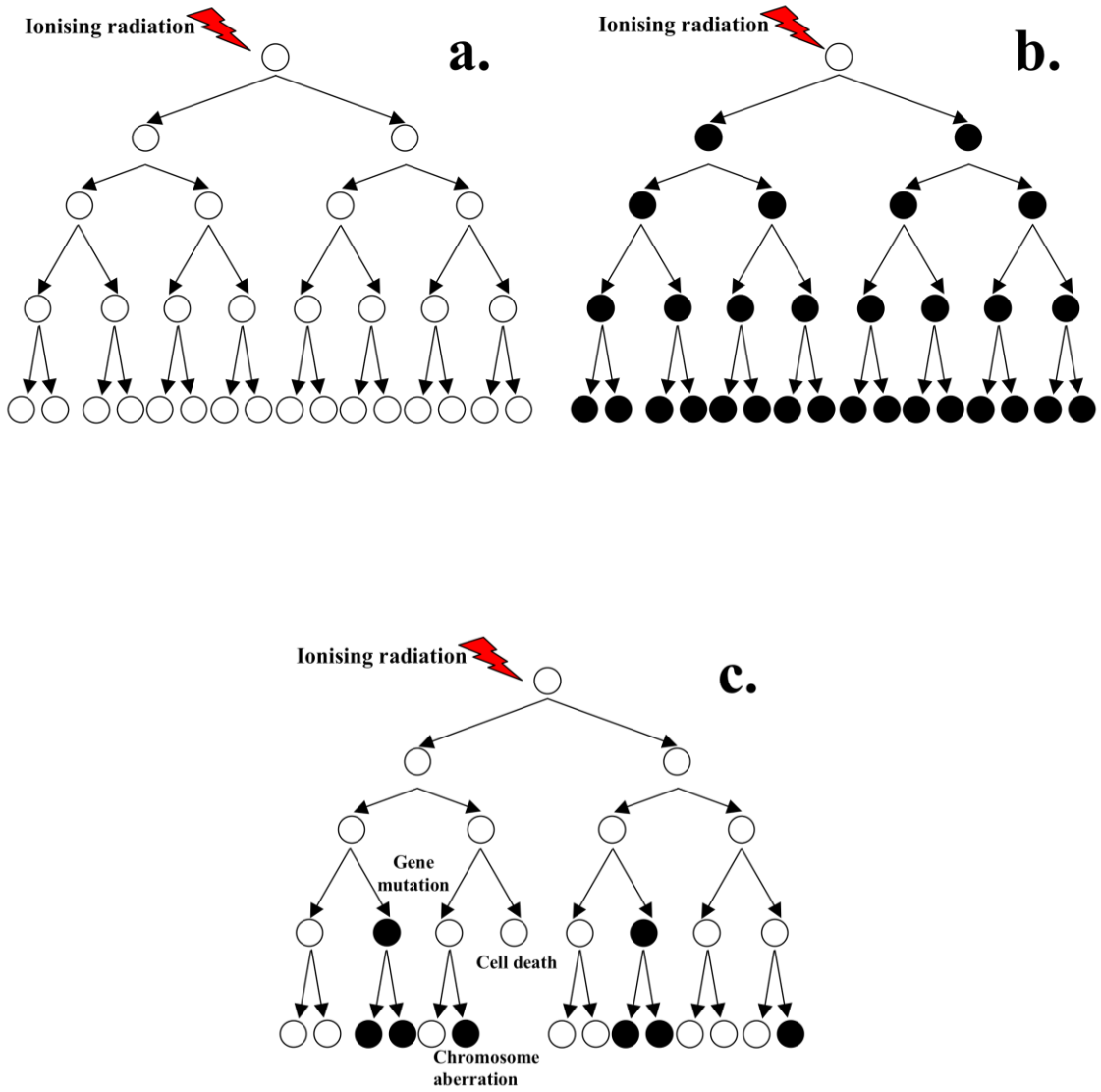

Figure 1.4: Contrary to the central dogma that radiation-induced damage is either repaired (a), or present in all clonal descendants of irradiated cells (b), exposure to ionising radiation results in genomic instability (c) seen in the un-irradiated progeny of the irradiated cell, multiple generations following the initial insult. Radiation-induced genomic instability is a genome-wide process characterised by non-clonal genomic alterations and increased rates of cell death in the descendants of irradiated cells. The resulting cellular phenotype is similar to that seen in chromosome instability disorders. In contrast to those inherited syndromes, genomic instability following exposure to ionising radiation does not result from mutation of genome maintenance genes (figure adapted from Lorimore *et al.*, 2003).

The term radiation-induced genomic instability refers to an increase in the rates of a variety of genomic alterations, including gene mutations and chromosomal destabilization, as well as an increase in the rates of cell death in the unexposed progeny of irradiated cells (reviewed in Lorimore *et al.*, 2003; Morgan, 2003a and 2003b). This unstable phenotype is also seen in un-irradiated cells that have come in contact with either irradiated cells or factors produced by irradiated cells (bystander effect) (reviewed in Lorimore *et al.*, 2003). Radiation-induced genomic instability is persistent and similar to that seen in chromosome instability disorders (**Table 1.1**). The effects of ionising radiation are non-targeted (i.e. it is extremely unlikely that ionising radiation induces the same DNA damage/mutations in all irradiated cells/studies) and delayed (i.e. the genetic damage arises in un-irradiated descendants of irradiated but phenotypically normal cells).

Table 1.1

Genetic syndrome	Gene	Function	Phenotype	Cancer predisposition
Ataxia telangiectasia	*ATM*	DNA damage response	Chromosomal instability Radiosensitivity	Leukaemia and lymphoma
Nijmegen breakage syndrome	*NBS1*	DNA repair	Chromosomal instability Radiosensitivity	Leukaemia and lymphoma
Bloom's syndrome	*BLM*	DNA replication	Chromosomal instability	Wide range of cancers
Fanconi anaemia	*FA*[a]	DNA damage response	Chromosomal instability Increased sensitivity to DNA crosslinking agents	Leukaemia and solid tumours
ICF*	*DNMT3b*	*de novo* DNA methylation	Chromosomal instability Radiosensitivity	N/A

Table 1.1: These genetic syndromes are characterised by genomic instability, radiosensitivity and predisposition to specific cancer types (adapted from Little, 2003).

* Immunodeficiency, centromeric instability and facial anomalies syndrome

The mouse haemopoietic system (later discussed in section 1.6) has been extensively used as an experimental system to study the delayed effects of ionising radiation. Genomic instability arose in clonal descendants of haemopoietic immature cells

exposed to alpha irradiation, with 40-60% of the colonies produced by irradiated BM cells exhibiting karyotypic abnormalities (Kadhim *et al.*, 1992). More significantly, these genomic abnormalities were non-clonal, as evidenced by the fact that cells within individual colonies (up to 50% of scored metaphases) carried different aberrations (Kadhim *et al.*, 1992). Further *in vitro* studies have demonstrated that this increased incidence of *de novo* genomic alterations and apoptosis can persist for many generations (Chang and Little, 1992; Lyng *et al.*, 1996; reviewed in Lorimore *et al.*, 2003).

Radiation-induced genomic instability in mice has also been demonstrated *in vivo* (Watson *et al.*, 1996; Ullrich and Davis, 1999) and the manifestation of delayed effects varies significantly among different mouse strains (see section 1.8; Ponnaiya *et al.*, 1997; Watson *et al.*, 1997; Lorimore *et al.*, 2003).

Increased ROS production and oxidative stress have been proposed as a possible mechanism for radiation-induced genomic instability (Clutton *et al.*, 1996; Limoli *et al.*, 2001). It is well established that ionising radiation results in oxidative stress via the production of ROS (see section 1.3.2). Oxidative stress has been associated with the resulting unstable phenotype (Clutton *et al.*, 1996), whilst increased levels of ROS correlate with an increase in radiation-induced cell death in Chinese Hamster Ovary (CHO) cells (Limoli *et al.*, 2001). A large number of studies have associated oxidative stress with a wide range of cancers, including cancers of the lung, stomach, prostate and breast (reviewed in Loft and Poulsen, 1996). However, oxidative stress alone can not explain the trans-generational genomic instability reported by a number of *in vivo* studies (see section 1.4; Dubrova *et al.*, 2000; Barber *et al.*, 2002; Barber *et al.*, 2006) and the exact mechanism of radiation-induced genomic instability is still unclear.

Genomic instability is a hallmark of cancer cells and many genomic instability syndromes are associated with specific cancer types (**Table 1.1**), supporting the notion that it is involved in the process of carcinogenesis. As previously discussed, radiation-induced genomic instability is similar to that seen in these syndromes. More importantly, exposure to ionising radiation is associated with an increased cancer risk (see section 1.3.4). Irrespective of its exact induction mechanism, radiation-induced genomic instability appears to play an important role in radiation-carcinogenesis. The

increased cancer risk following exposure to ionising radiation will be discussed in the following section.

1.3.4 Ionising radiation and carcinogenesis.

On August 6th 1945, the US Air Force dropped an A-bomb on Hiroshima. A similar bomb was dropped on Nagasaki, instantly killing over 74,000 people. Five years later, the Radiation Effects Research Foundation (RERF) was founded, focusing on studies on long term health effects of radiation in the survivors of the atomic bombings in both cities. The Life Span Study (LSS) and the Adult Health Study (AHS) are two major clinical research programs conducted under the supervision of the RERF. The LSS includes approximately 120,000 subjects from Hiroshima and Nagasaki (93,000 A-bomb survivors and 27,000 unexposed individuals). The AHS involves 20,000 individuals selected from the LSS and has been collecting information on the health status of the A-bomb survivors through biennial health examinations since 1958 (http://www.rerf.or.jp).

Along with studies on occupational, accidental, and/or therapy-related exposure to radiation, the LSS and AHS are major sources of ionising radiation exposure data in humans. Acute whole-body exposure to radiation has been associated with a number of diseases. For example, cardiovascular disease (CVD) and hyperparathyroidism have been linked to exposure to ionising radiation (Kodama *et al.*, 1996). In addition to an increased risk for thyroid cancer, cases of other solid cancers were elevated among the survivors, including basal cell carcinoma, lung, and breast cancer (in females) (Pierce *et al.*, 1996; Ron, 1998).

Significantly, an increased incidence of haemopoietic malignancies (leukaemias, lymphomas, and myelomas) was reported for the LSS population (Pierce *et al.*, 1996). Acute whole-body exposure to ionising radiation resulted in a high excess relative risk of radiation-induced Acute Myeloid Leukaemia (r-AML) (see section 1.7.2) which was materially greater than that for solid cancers (**Figure 1.5**; Pierce *et al.*, 1996).

Most leukaemias occurred within the first 5-15 years of exposure in contrast to solid cancers where incidence was more consistent with the age-specific cancer risks (Pierce

et al., 1996). Given the 5 year gap between the bombings and the establishment of the RERF, there is no data available regarding this early period following exposure, so r-AML risk may have actually been underestimated. In fact, a notable excess of leukaemia was observed by clinicians as early as 3 years after the bombings (Wakeford, 2004). Misclassification (false diagnosis of non-cancer blood disease as leukaemia) could not explain the excess risk for r-AML and thus a direct association between acute whole-body exposure to ionising radiation and r-AML was concluded (Shimizu *et al.*, 1999).

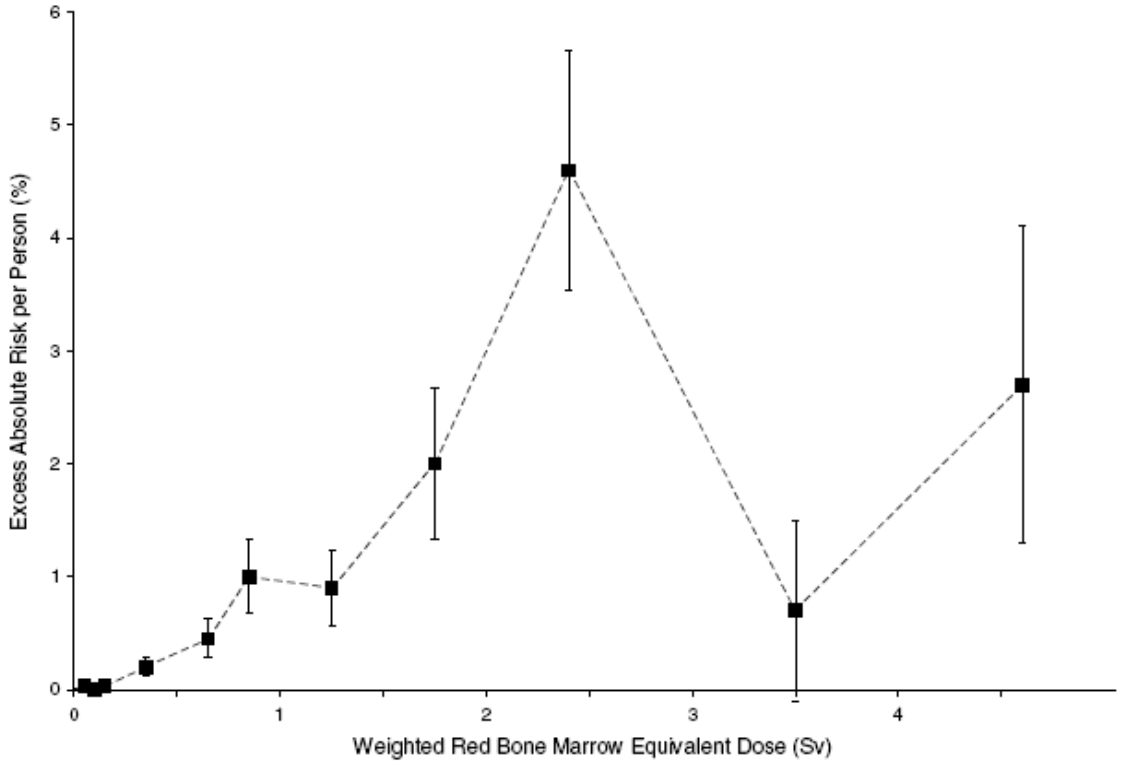

Figure 1.5: Excess absolute risk for r-AML following whole-body exposure to ionising radiation (Pierce *et al.*, 1996). A sub-linear curve is seen in the moderate dose region. Exposure to high doses of ionising radiation may result in increased cell death as a direct effect, which accounts for the declined risk at higher doses of ionising radiation.

Cancer patients treated with whole-body radiotherapy also run the risk of developing therapy-related Acute Myeloid Leukaemia (t-AML) as a secondary cancer following treatment (Plumb, 2003). Unlike most cases of *de novo* AMLs (which mainly exhibit chromosomal translocations), most cases of radiation/therapy-induced AMLs exhibit

deletions of the long arm of chromosome 5 and/or 7 (as well as monosomy 7) (Pedersen-Bjergaard *et al.*, 1995). Up to 10% of Non-Hodgkin's Lymphoma (NHL) patients may develop t-AML within 10 years of primary therapy (Armitage *et al.*, 2003), while an even higher incidence of t-AML has been reported in cases where radiotherapy was followed by alkylating agents treatment, suggesting an additive effect (Travis *et al.*, 1996). The mechanisms of malignant transformation following exposure to ionising radiation and alkylating agents appear to be similar, while at the same time there are distinct differences between these cases and cases of *de novo* AMLs (Travis *et al.*, 1996).

The LSS has provided great insight into the mechanisms of radiation-induced carcinogenesis as well as other radiation-induced effects, such as cardiovascular disease. Cancer risks, cancer and non-cancer mortality have been well-characterised in this large cohort population that includes both sexes and a wide range of ages, and the available data cover almost 50 years. These studies identified the radiosensitive bone marrow (see section 1.3.2; **Figure 1.3**) as one of the most susceptible tissues to malignant transformation (Pierce *et al.*, 1996; Shimizu *et al.*, 1999) and constitute this tissue an ideal system to investigate both cancer susceptibility and radiosensitivity *in vivo*.

1.4 Considering DNA methylation as a factor in radiation-induced genomic instability.

Most of the inheritable chromosomal instability syndromes (**Table 1.1**) are characterised by genomic instability and cancer predisposition, and are a result of germline mutations in DNA repair-related genes (Little, 2003). Moreover, these genetic syndromes suggest that a relationship may exist between cellular radiosensitivity, genomic instability and cancer susceptibility. This is expected, as failure to repair radiation-induced DNA damage will result in increased cell death. At the same time, inefficient DNA damage response pathways can increase the incidence of mutations and/or deleterious genetic rearrangements, which could, in the long term, give rise to cancer.

Immunodeficiency, centromeric instability and facial anomalies (ICF) patients also show hypersensitivity to ionising radiation and exhibit chromosomal instability (**Table 1.1**) (Ehrlich *et al.*, 2001). The ICF syndrome (later discussed in **Chapter 4**) is caused by mutations in the *DNMT3B* gene which is involved in DNA methylation (see section 1.5). The low numbers of identified ICF patients (<40), as well as their reduced life expectancy, might account for the fact that no association has been established between ICF and cancer (Narayan *et al.*, 2000). However, aberrant DNA methylation is often seen in cancer (see sections 1.5.4 and 1.5.5), which raises the hypothesis that DNA methylation may also be part of the radiosensitivity, chromosomal instability, and carcinogenesis equation.

Further supportive evidence for this hypothesis comes from mouse *in vivo* studies investigating genomic instability in the progeny of irradiated parents. As previously discussed (see section 1.3.3), the presence of non-clonal genomic alterations in the progeny of irradiated cells suggested that radiation-induced genomic instability is not the result of stable radiation-induced mutations. Radiation-induced ROS can result in ongoing apoptotic death and persistent oxidative stress, but can not explain trans-generational genomic instability. Dubrova *et al.* (2000) have shown that increased mutation rates at expanded simple-tandem repeat (ESTR) loci can be observed in the F_2 progeny of male irradiated mice. (CBA/H x CBA/H) F_1 mice also exhibited increased mutation rates and more than 50% of mutations detected in the F_2 mice were shared by two or more litter-mates (Dubrova *et al.*, 2000). However, *de novo* mutations seen in only one member of a litter (termed singleton mutations by the authors) were also more frequent in the F_2 mice, suggesting that the progeny of an irradiated sperm cell can inherit and transmit a radiation-induced genetic effect other than a stable mutation, which may significantly affect genomic stability and mutation rates. DNA methylation is an ideal candidate as it is faithfully transmitted through cell divisions and it can affect both genome stability and gene function. DNA methylation and its involvement in gene regulation, genome stability, and cancer will be discussed in the following sections.

1.5 DNA methylation.

DNA methylation is an epigenetic heritable DNA modification. The term epigenetic is used to describe mechanisms that affect gene activity by means other than altering DNA sequence (Paulsen *et al.*, 2008). Epigenetic events also include histone modifications, such as methylation, acetylation and phosphorylation, which will not be considered in this thesis (for further details see: Sims *et al.*, 2008).

DNA methylation is seen in many organisms, including bacteriophages, fungi and plants. In mammals, DNA methylation involves the addition of a methyl group to the 5-carbon of cytosine in a CpG dinucleotide. Methylated cytosines account for 0.75-1% of all DNA bases in the human genome, with at least 70% of all CpG dinucleotides being methylated (Bestor, 2000). Methylated cytosine (5-^{Me}C) is in itself mutagenic, as it can undergo spontaneous hydrolytic deamination, resulting in a cytosine-to-thymine transition. Moreover, methylated CpG dinucleotides are more prone to ultraviolet (UV) light-induced mutations and carcinogen-induced guanine-to-thymine transversions (reviewed in Jones and Baylin, 2002). This inherent susceptibility to mutation events has resulted in a low frequency of CpG dinucleotides in the genome. However, ~1% of the DNA contains CpG dinucleotides at the expected or higher frequency and these short (~0.2-4Kb) regions are called CpG islands. Despite covering only a small proportion of the human genome, CpG islands contain a relatively large fraction (~5.5%) of all CpGs (Rollins *et al.*, 2006). Many CpG islands overlap with gene promoters (sometimes extending into the first exon). A prominent feature of these CpG islands is that they remain largely unmethylated, resulting in a transcription-ready gene state. Conversely, promoter CpG methylation is associated with gene silencing (Robertson and Wolffe, 2000; Plass, 2002). A large fraction (~50%) of all CpG dinucleotides are found in DNA repetitive sequences (see section 1.5.1).

1.5.1 The importance of DNA methylation.

It is generally accepted that methylation of promoter CpGs can control gene expression (at least in ubiquitously expressed genes), by blocking the access of transcription factors or by recruiting protein complexes that suppress transcription (reviewed in Jones and Baylin, 2002). CpG methylation is tightly regulated during development (Monk *et al.*, 1987; Ehrlich *et al.*, 2003), whilst mouse studies have demonstrated that complete loss

of DNA methylation results in embryonic lethality during organ development (reviewed in Goll and Bestor, 2005). DNA methylation is tissue-specific in adults, suggesting that it is either a determinant or a by-product of mammalian differentiation (Ehrlich *et al.*, 1982; Gama-Sosa *et al.*, 1983; Walsh and Bestor, 1999).

DNA methylation is a critical signal in mammalian genomic imprinting. Imprinting occurs at a small subset of genes (to date, at least 80 mouse and human genes) and results in a state of monoallelic expression of a biallelic gene, in a parent of origin-dependant fashion (Morison *et al.*, 2005). Thus, one of the two copies of these genes is silenced by means of DNA methylation. Genomic imprinting is established during embryogenesis and the resulting monoallelic expression is faithfully transmitted throughout cell divisions. The importance of genomic imprinting has been demonstrated in mouse studies in which gynogenetic embryos (carrying two maternal genomes, but no paternal one) and androgenetic embryos (carrying two paternal genomes, but no maternal one) displayed gross developmental abnormalities and failed to develop to term (reviewed in Herman and Feil, 2008). The pseudohemizygosity imposed by genomic imprinting confers a genetic vulnerability as exemplified by the Prader-Willi (PWS) and Angelman (AS) syndromes. Loss of the paternal *SNRPN* and *necdin* genes in the PWS/AS region results in the Prader-Willi syndrome (as the maternal copies are silenced), whereas loss of the maternal *UBE3A* gene in the same region results in the AS syndrome (as the paternal copy is silenced) (Connor and Ferguson-Smith, 1997). It has been hypothesised that this genomic vulnerability could possibly constitute imprinted genes as targets for genomic instability-inducing changes (Schofield, 1998).

In order to compensate for the dosage difference of X chromosomal genes between XX females and XY males, female mammals inactivate one X chromosome. The process, known as X-inactivation, occurs early in development and is mediated by the X inactivation centre (*Xic*). Along with the long-non-protein-coding *Xist* RNA and chromatin modifications, DNA methylation plays a crucial role in the process of X inactivation. CpG islands become hypermethylated (increased levels of CpG methylation) on the inactive X chromosome but, unlike genomic imprinting, X inactivation is independent of parental origin (reviewed in Sengupta *et al.*, 2008).

Approximately 50% of all CpG dinucleotides are located within repetitive DNA elements (Paulsen *et al.*, 2008). In contrast to CpG islands, repetitive DNA elements are heavily methylated, giving rise to the hypothesis that DNA methylation evolved as a defence mechanism, designed to prevent integration of foreign DNA into the host genome (Yoder *et al.*, 1997; Paulsen *et al.*, 2008). Local DNA hypermethylation is associated with transcriptional inactivation of endogenous retrotransposons (Robertson and Wolffe, 2000; Ehrlich, 2002). Inversely, hypomethylation (reduced levels of CpG methylation) of repetitive DNA elements is a common feature of cancer cells in many rodent and human cancers (Chen *et al.*, 1998; Chalitchagorn *et al.*, 2004; Gaudet *et al.*, 2004).

Intracisternal A Particles (IAP) and Long Interspersed Nucleotide Elements-1 (LINE-1) are such repetitive DNA elements (**Figure 1.6**). IAP is rodent-DNA specific whereas LINE-1 is seen in both human and mouse DNA. Both IAP and LINE-1 are able to retrotranspose following reverse transcription of their RNA and reintegration into the genome (reviewed in Kazazian, 2004). Most copies of these repeat elements produce truncated proteins, but some are still active and normally silenced by DNA methylation (Bourc'his and Bestor, 2004). Hypomethylation can lead to transcription and subsequent random integration into DNA (insertional mutagenesis). Elevated rates of insertional mutagenesis might result in gene function modifications (e.g. activation/inactivation of a gene located on the site of integration) (Robertson and Wolffe, 2000; Ehrlich, 2002).

Due to their high CpG content and hypermethylated state, LINE-1 and IAP elements have been used as surrogates for global DNA methylation (Bourc'his and Bestor, 2004). Pericentromeric tandem repeats have also been used as such surrogates (Bourc'his and Bestor, 2004). These repeats are thought to play a structural role in the genome and are usually methylated in adults. Hypomethylation of these repeats is seen in ICF patients (Tuck-Muller *et al.*, 2000; Ehrlich *et al.*, 2001), which exhibit increased chromosomal instability (later discussed in **Chapter 4**) and increased radiosensitivity (**Table 1.1**). Most importantly, hypomethylation of pericentromeric regions has been found in a number of cancers and has been associated with increased chromosomal instability at specific sites (Narayan *et al.*, 1998; Qu *et al.*, 1999), emphasising the importance of DNA methylation in maintaining genome stability.

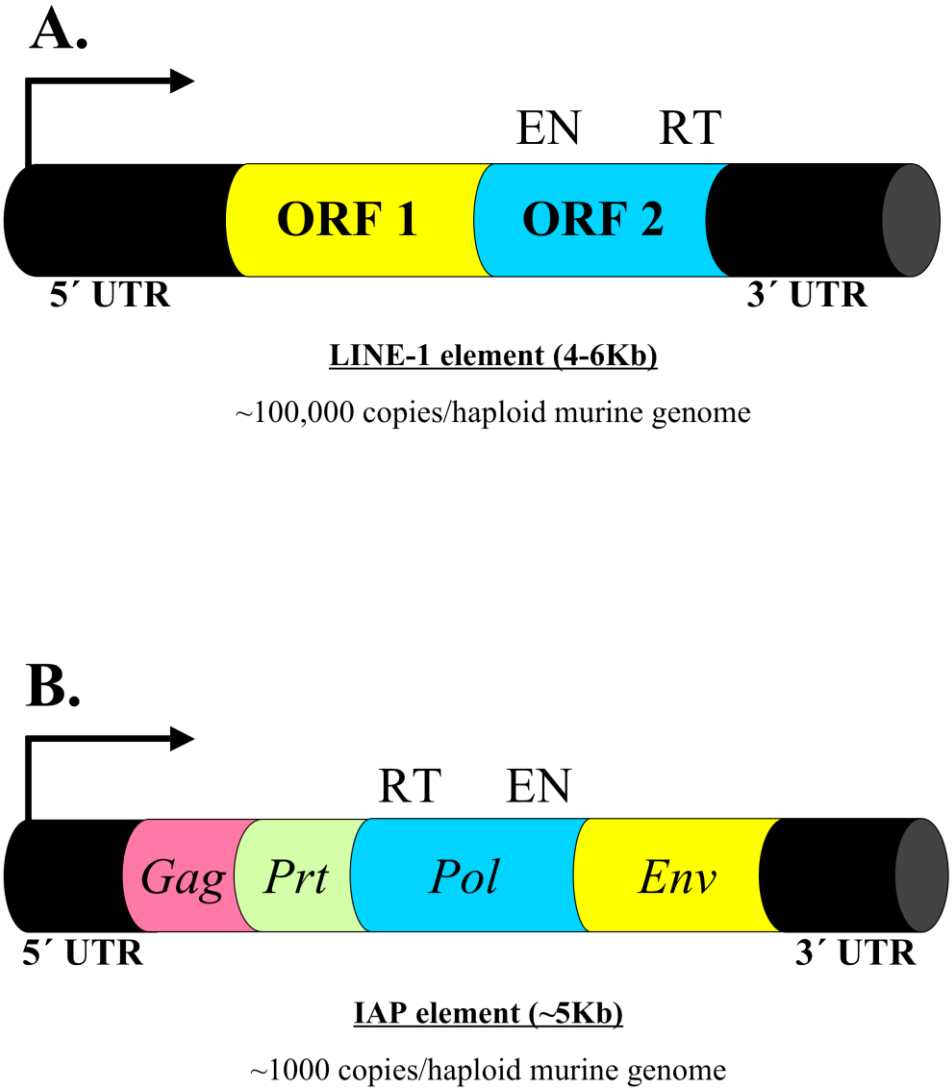

Figure 1.6: LINE-1 (A) and IAP (B) retrotransposons. LINE-1 elements consist of a 5′-untranslated region (UTR), two open reading frames (ORF) and a 3′UTR. An internal promoter is located within the 5′UTR. ORF-1 encodes a nucleic acid binding protein, whereas ORF-2 encodes reverse transcriptase (RT) and an endonuclease (EN). IAP repetitive elements consist of a 5′UTR, slightly overlapping ORFs and a 3′UTR. The ORFs encode for group-specific antigen (*gag*), protease (*prt*), RT and EN (*pol*), and envelope (*env*) genes (adapted from Kazazian, 2004).

1.5.2 DNA methyltransferases.

DNA methylation is established and maintained through the action of at least three independent DNA methyltransferases (DNMTs). These enzymes catalyse the transfer of the methyl group to the CpG cytosine and exhibit functional specificity (reviewed in Robertson and Wolffe, 2000).

DNMT1 is the most abundant DNA methyltransferase in somatic cells and was the first to be discovered (Bestor *et al.*, 1988). It is ubiquitously expressed both in adult and embryonic tissues, has a preference for hemi-methylated DNA and is required for proper embryonic development, genomic imprinting and X-inactivation (Robertson and Wolffe, 2000). It is a 'maintenance methyltransferase', responsible for copying DNA methylation patterns following DNA replication, although *in vitro* studies have shown that it is also capable of *de novo* methylation (Jair *et al.*, 2006).

DNMT3A and *DNMT3B* are '*de novo* methyltransferases', responsible for the establishment of methylation patterns following embryo implantation and/or the integration of retroviral elements in mouse embryonic stem cells (Robertson and Wolffe, 2000). They are both expressed in most adult tissues, but show higher expression levels in embryonic stem cells (Robertson *et al.*, 1999; Xie *et al.*, 1999). These two methyltransferases show overlapping functions in their *de novo* methylation of DNA, but also exhibit some functional specificity. Okano *et al.* (1999) investigated developmental defects in *Dnmt3a*$^{-/-}$ and *Dnmt3b*$^{-/-}$ mouse embryos and reported that *Dnmt3b* is specifically required for methylation of a subset of centromeric minor satellite repeats. The observation that ICF patients show hypomethylation at those regions similar to that seen in *Dnmt3b*$^{-/-}$ mouse embryos, together with genetic linkage data raised the possibility (later confirmed) that this rare autosomal syndrome may be caused by dysfunction of DNMT3B (Okano *et al.*, 1999).

An additional methyltransferase, coding for a DNMT3-like protein has also been identified. DNMT3L lacks DNA methyltransferase activity, but is involved in the regulation of methylation patterns in early development through interactions with DNMT3A and DNMT3B (Van Emburgh and Robertson, 2008).

Finally, DNMT2 exhibits weak methyltransferase activity and functions as an RNA methyltransferase, specifically methylating $tRNA^{Asp}$; but the exact function of this enzyme remains unknown (Goll *et al.*, 2006).

1.5.3 The one-carbon transfer pathway.

Figure 1.7 is a schematic representation of the one-carbon transfer pathway which is involved in DNA synthesis, DNA repair and DNA methylation. Folate is a water-soluble vitamin B that holds a crucial role in the one-carbon transfer pathway. Folate deficiency can result in reduced levels of S-adenosyl methionine (SAM) and therefore impaired DNA methylation. Aberrant DNA methylation, as well as the effects of ionising radiation on the one-carbon transfer pathway will be discussed later (see sections 1.5.4, 1.5.5 and 1.5.6).

Folate deficiency can also result in uracil incorporation in the DNA as the conversion of dUMP to dTMP will also be affected due to reduced N^5N^{10}-methylenetetrahydrofolate levels (**Figure 1.7**; Fenech, 2001; Zhang *et al.*, 2003). The presence of uracil in the DNA may lead to mutations and genomic instability through the disruption of DNA repair and the induction of chromosome breaks (Blount *et al.*, 1997; Ames, 2001; Zhang *et al.*, 2003).

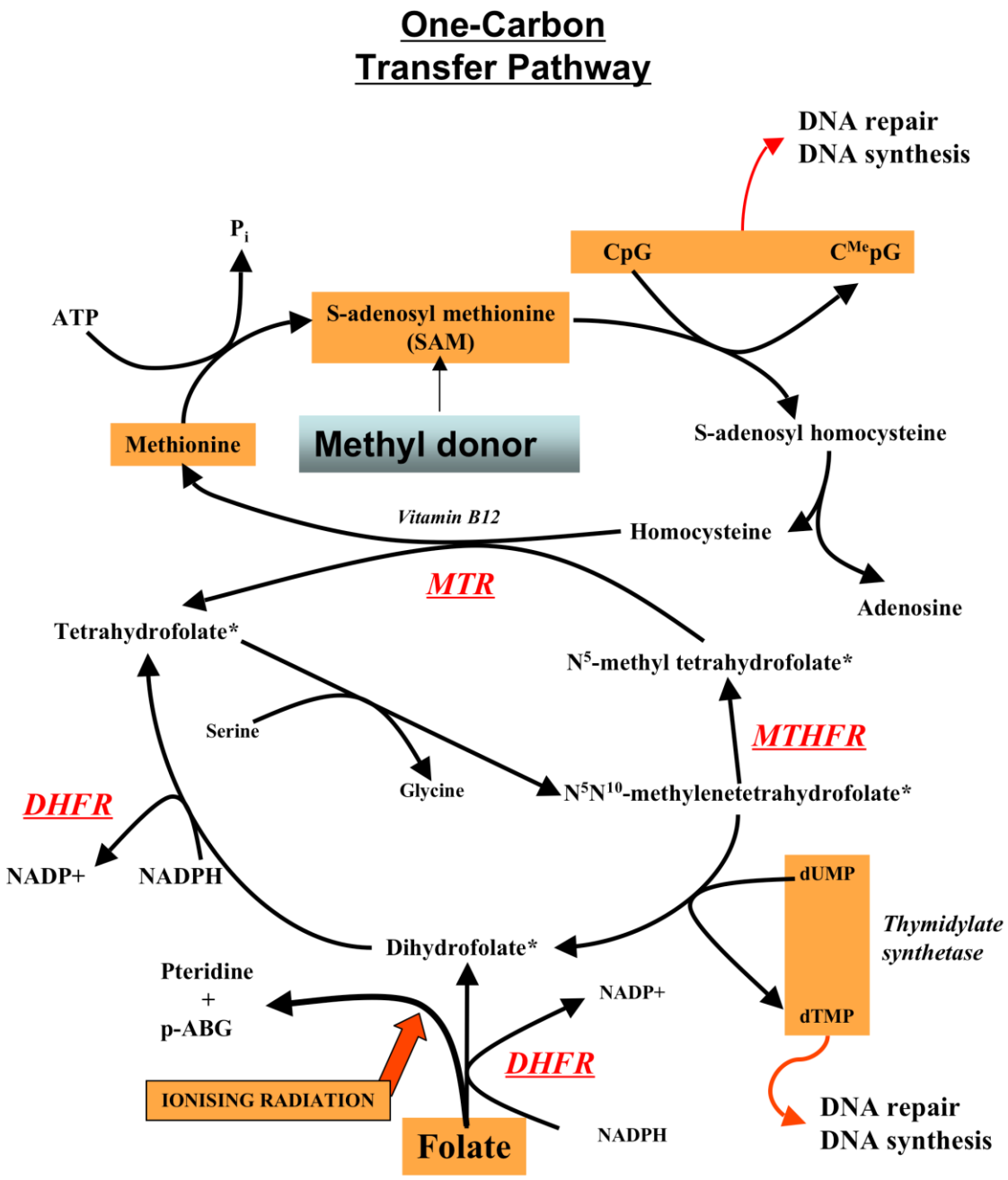

Figure 1.7: Dependant on dietary uptake, folate enters the one-carbon transfer pathway and is initially converted to dihydrofolate by dihydrofolate reductase (*DHFR*). The same enzyme will then convert dihydrofolate to tetrahydrofolate, which will be later converted to N^5N^{10}-methylenetetrahydrofolate. This molecule is involved in the synthesis of dMTP and N^5-methyl tetrahydrofolate which are catalysed by thymidylate synthetase and methylenetetrahydrofolate reductase (*MTHFR*) respectively. A methyl group is then transferred from N^5-methyl tetrahydrofolate to homocysteine. The process is catalysed by methionine synthase (*MTR*) and results in the production of methionine. Finally S-adenosyl methionine (SAM) acts as a final carbon donor for DNA methylation. The addition of the final methyl group is catalysed by DNA methyltransferases (adapted from Kim, 2004).

1.5.4 Aberrant DNA methylation in cancer.

Aberrant DNA methylation is seen in most cancers. The effect of local hypermethylation has been defined: hypermethylation of the promoter regions of tumour suppressor genes can result in gene inactivation (loss of function) and generate malignant potential (reviewed in Esteller, 2002; Jones and Baylin, 2007). For example, specific sub-types of leukaemia exhibit characteristic gene-specific hypermethylation (Esteller, 2003).

In contrast to the hypermethylation of tumour suppressor genes, an overall reduction of global DNA methylation levels is seen in many cancers (Gama-Sosa *et al.*, 1983; Chen *et al.*, 1998; Chalitchagorn *et al.*, 2004; Gaudet *et al.*, 2004). The proposed mechanisms of hypomethylation-related carcinogenesis include transcriptional activation of oncogenes and loss of imprinting. However, since most of this hypomethylation is seen in repetitive DNA elements such as retrotransposable elements (e.g. LINE-1) and pericentromeric satellite repeats, it has also been suggested that global DNA hypomethylation results in an increased karyotypic instability via transcriptional activation of retrotransposable elements and unmasking of repetitive structural elements, which are normally heavily methylated (Ehrlich, 2002; Feinberg *et al.*, 2006).

As previously discussed (see section 1.5.1), hypomethylation of pericentromeric tandem repeats is seen in a wide range of cancers and has been associated with increased chromosomal instability (Narayan *et al.*, 1998; Qu *et al.*, 1999). Transgenic mice, expressing a hypomorphic *Dnmt1* allele (10% of the wild-type expression levels) show genome-wide hypomethylation of all tissues and are prone to T cell lymphomas (Gaudet *et al.*, 2003), which suggests that DNA methylation may have an important role in cancer susceptibility.

1.5.5 Hypomethylation as a risk factor in cancer.

A number of different studies have associated global genomic hypomethylation with cancer predisposition. Rodents that were fed folate-deficient diets showed an increased cancer risk (reviewed in Duthie, 1999; Kim, 2004) supporting the involvement of DNA hypomethylation in the multistage carcinogenic process. Either as a result of a poor diet or due to inherited defects in genes encoding for enzymes involved in folate metabolism

(Ames, 2001), similar studies have identified folate deficiency as a risk factor in human cancer (Heijmans *et al.*, 2003; Zhang *et al.*, 2003; Sharp and Little, 2004). Notably, an increased maternal intake of folate has been associated with decreased childhood leukaemia risk (reviewed in Tower and Spector, 2007).

Defects in enzymes involved in DNA methylation have also been found to increase mutation rates and predispose to cancer (Heijmans *et al.*, 2003; Zhang *et al.*, 2003; Sharp and Little, 2004). In mouse embryonic stem cells, inactivation of *Dnmt1* has been associated with increased mutation rates, genome-wide hypomethylation and increased chromosomal instability (Chen *et al.*, 1998).

Table 1.1 shows a number of genetic syndromes in which chromosomal instability and radiosensitivity are seen. With the exception of ICF, patients affected by these syndromes are also cancer-prone (Little, 2003). However, irradiated ICF cell lines show increased cell death and permanent cell cycle arrest, as well as increased genomic instability, possibly suggesting that hypomethylation increases the risk of exaggerated responses to the direct and delayed effects of ionising radiation (Narayan *et al.*, 2000).

1.5.6 Ionising radiation and hypomethylation.

Radiation-induced global DNA hypomethylation is well established both *in vivo* and *in vitro* (Tawa *et al.*, 1998; Kovalchuk *et al.*, 2004; Pogribny *et al.*, 2004; Raiche *et al.*, 2004; Koturbash *et al.*, 2005). The proposed mechanisms include uracil misincorporation, incorporation of unmethylated cytosines into DNA during the repair of double strand breaks, or activation of unknown demethylases (Sandovici *et al.*, 2008).

Oxidative stress increases the risk of a number of cancers (see section 1.3.3). Whole-body exposure to ionising radiation has been found to induce oxidative stress that persists *in vivo* and may be involved in the delayed effects of ionising radiation (Lorimore *et al.*, 2003). Mouse *in vivo* studies have shown that exposure to ionising radiation results in cleavage of folate into pteridine and *p*-aminobenzoglutamic acid (*p*-ABG) (**Figure 1.7**), inducing a transient folate deficiency and possibly disrupting the one-carbon transfer pathway. Kesavan *et al.* (2003) reported a ~47% decrease in folate

levels in rodent liver tissue within 5 days following whole-body exposure to 5Gy γ-rays. This was accompanied by a 15% increase in *p*-ABG levels in liver tissue within 24 hours post-irradiation, which later increased to ~300% of control levels over the five-day period (Kesavan *et al.*, 2003). The mice were given free access to food over the course of the aforementioned study and folate levels could have thus been replenished. However, the increase of *p*-ABG levels over the 5 day period suggested that cleavage of the folate molecule persisted, possibly due to the radiation-induced oxidative stress (Kesavan *et al.*, 2003).

1.5.7 DNA methylation in this study.

Aberrant DNA methylation has thus been associated with genomic instability, radiosensitivity and cancer. Most importantly, ionising radiation has been shown to have a direct, as well as an indirect effect on the folate pathway and the levels of DNA methylation.

A number of studies have investigated the effects of aberrant DNA methylation in transgenic mouse models and the effects of ionising radiation on mouse DNA methylation (see section 1.5). Radiation-induced genomic instability has been well characterised in the mouse haemopoietic system (see section 1.3.3). The murine haemopoietic system was therefore used as a model in this thesis, to investigate the combined effects of ionising radiation and DNA methylation on carcinogenesis and radiosensitivity, as bone marrow is a very good *in vivo* model of a radiosensitive (see section 1.2.3; **Figure 1.3**), cancer-prone (see section 1.3.4), hierarchical tissue. The haemopoietic system will be discussed in the following sections.

1.6 Haemopoiesis.

The term haemopoiesis refers to the continuous production of blood cells. The sites of blood cell production vary throughout development. The foetal liver sustains haemopoiesis throughout gestation (McGrath and Palis, 2008). Shortly before birth and throughout life, haemopoiesis is maintained in the bone marrow (reviewed in Greaves, 1996).

In normal BM haemopoiesis, a population of multipotent stem cells is responsible for the production of more mature haemopoietic cells as well as maintaining a constant number of stem cells in the BM (i.e. self-renewal) (Greaves, 1996). As seen in **Figure 1.8**, all haemopoietic cells will arise following differentiation of a population of multipotent stem cells that account for ~0.02% of total BM and are known as haemopoietic stem cells (HSC). These cells show no maturation or lineage commitment, but can differentiate into progenitor cells. These progenitor cells can differentiate into two different types of blood cells: myeloid (including red blood cells which carry oxygen to the various tissues and platelets which are responsible for blood clotting) and/or lymphoid blood cells (B- and T-cells which are part of the immune system) (**Figure 1.8**) (Greaves, 1996). Given the fact that haemopoiesis is a dynamic process ($1x10^{10}$ red blood cells per hour) the self-renewal and differentiation processes have to be tightly regulated (Cheshier *et al.*, 1999).

1.6.1 Defining the Haemopoietic Stem Cell (HSC).

HSC have been functionally and phenotypically defined using a number of *in vivo* and *in vitro* techniques. These assays measure both cell proliferation (by the number of cells produced) and the ability to differentiate into more mature haemopoietic cells (estimated by the number of different lineages represented in progeny). Each assay has identified specific subpopulations of BM cells such as the immature HSC or the more mature progenitor cells (**Figure 1.8**).

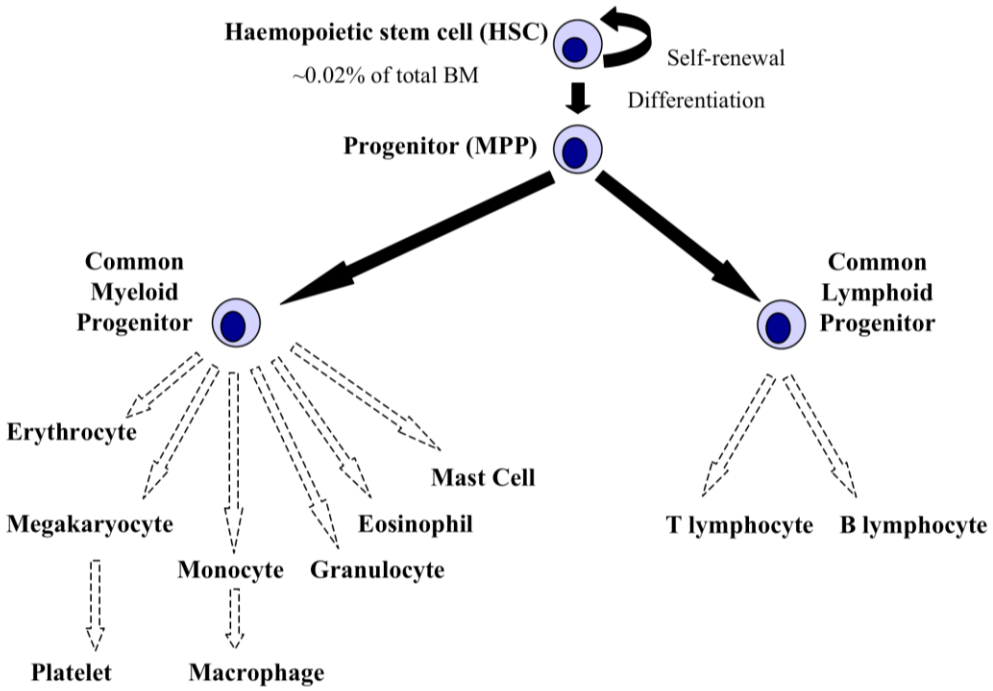

Figure 1.8: Simple schematic representation of adult haemopoiesis. All mature blood cells are formed following proliferation and differentiation of the haemopoietic stem cells.

The HSC compartment is heterogeneous and can be divided into two major groups of cells. The long term self-renewing HSC (LT-HSC) and the transiently/short term self-renewing HSC (ST-HSC) (Jones *et al.*, 1989). LT-HSC show greater self-renewal and differentiation capacity compared to ST-HSC. These are classified as HSC as they fulfil three functional requirements. First, they have the ability to self-renew. Second, they can differentiate into all haemopoietic blood cell lineages (i.e. they are multipotent), and third, they can reconstitute long term haemopoiesis in ablated recipients (Kondo *et al.*, 2003). Non-self-renewing multipotent progenitor cells (MPP) are also immature BM cells that are able to differentiate into either the lymphoid or myeloid lineage. MPP cells are not classified as HSCs as they have lost their ability to self-renew (Cheshier *et al.*, 1999) and cannot sustain long term haemopoiesis (Jones *et al.*, 1989).

1.6.1.1 *In vivo* assays.

In vivo transplantation techniques allow the assessment of the stem cells' repopulating capacity. Following lethal irradiation (~100% bone marrow cell killing) and subsequent transplantation, some of the donor cells form macroscopic colonies of differentiated

cells in the spleen, known as spleen colony forming units (CFU-S). These can be counted at approximately 7-12 days post-irradiation. CFU-S Day 8 and CFU-S Day 12 assays can select for the lineage restricted progenitor cells and primitive progenitor cells respectively (Coulombel, 2004) (**Figure 1.9**). Identifying the LT-HSC cells requires long term repopulating (LTR) assays. In these assays, lethally irradiated female mice receive male donor-derived BM cells, engraftment is investigated >10 weeks post-irradiation and confirmed by the presence of the Y chromosome in various haemopoietic lineages (Szilvassy *et al.*, 1990) (**Figure 1.9**).

1.6.1.2 *In vitro* assays.

A number of *in vitro* clonogenic assays have also been devised in order to identify and study specific subpopulations of immature bone marrow cells. These assays can be divided into short term (ST) and long term (LT), depending on the relative maturity of the cells they study. Similar to the *in vivo* CFU-S assays, ST semi solid colony assays investigate the primitive progenitor cells by measuring the numbers of agar colony forming units (CFU-A) (Lorimore *et al.*, 1990). The CFU-A clones are indistinguishable from the CFU-S Day 12 clones, whereas progenitor cells showing different levels of maturation can also be identified based on their sensitivity to cytokines, the size of the colonies, and the time required to generate differentiated cells [e.g. the most immature progenitors are the lympho-myeloid progenitors (CFU-Ly-My) progressing to blast formation (CFU-B), whereas colony forming unit erythroid (CFU-E) are amongst the most mature progenitors] (Coulombel, 2004) (**Figure 1.9**).

Due to the limited lifespan of the medium they use (~3 weeks), ST *in vitro* assays can not detect more immature BM cells (Kondo *et al.*, 2003). Long term (LT) *in vitro* assays have identified two different cell types: the Long Term Culture Initiating Cell (LTC-IC) and the Cobblestone Area Forming Cell (CAFC). LTC-IC cells are cultured for a long period (5-8 weeks) on an irradiated stroma layer. During this time only the most primitive cells will survive (Müller-Sieburg and Riblet, 1996). In the CAFC assay the seeded cells integrate in an adherent layer of feeder cells and form a cobblestone area. Cells of various developmental stages require different times to form these cobblestone areas (de Haan and Van Zant, 1997). The relative maturity of the cell in question can thus be directly assessed (e.g. colonies that appear by day 7 are generated by mature

progenitor cells, which correspond to CFU-S Day 8). CAFC Day 28 and 35 assays can identify the more immature LT-HSC (equivalent to the stem cells identified by the *in vivo* LTR assay). A summary of the *in vivo* and *in vitro* assays, as well as the immature BM cells they identify can be found in **Figure 1.9**.

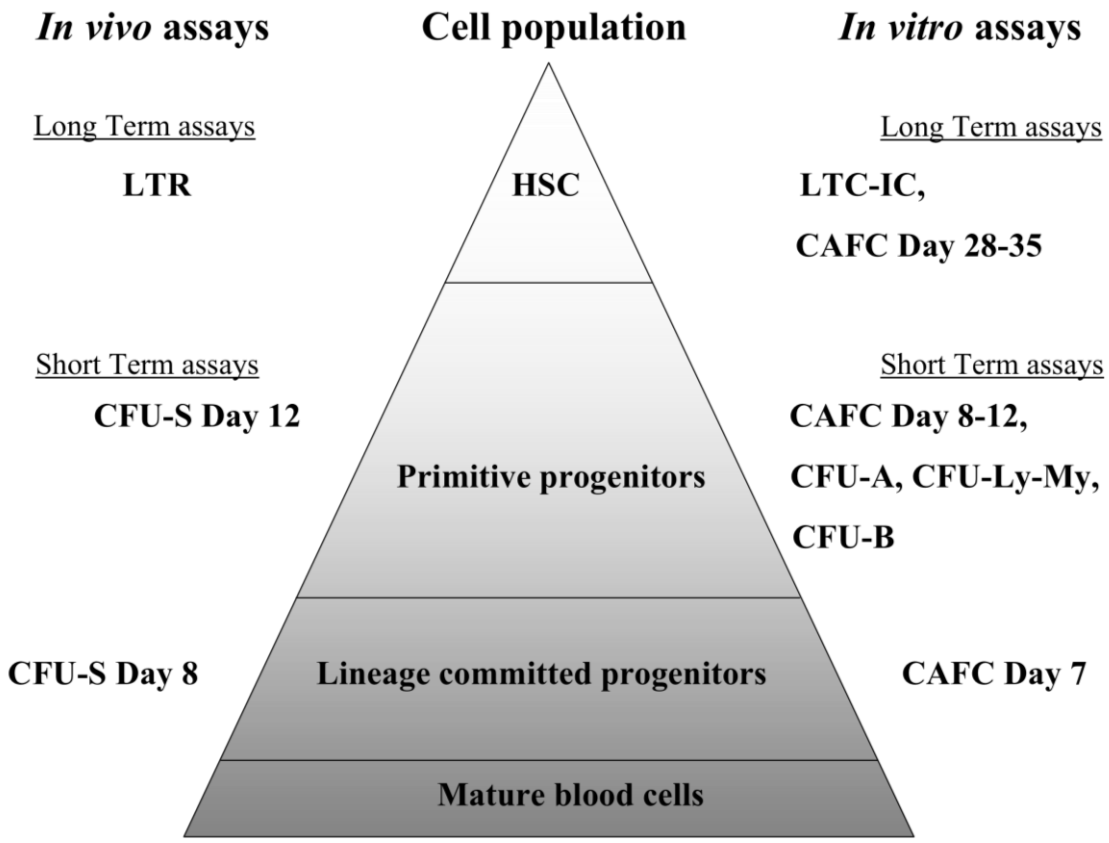

Figure 1.9: *In vivo* and *in vitro* assays investigating immature bone marrow cells at different stages of maturation. The frequency of the specific cell populations increases with differentiation reflecting the hierarchical motif of haemopoiesis.

1.6.1.3 Flow cytometry-based assays.

The realisation that different lineages of haemopoietic cells express cell-specific surface markers has revolutionised the isolation and characterisation of HSC. Spangrude *et al.* (1988) were the first to use a combination of monoclonal antibodies against cell surface markers in order to isolate and characterise murine HSC by fluorescence activated cell sorting (FACS). In contrast to the aforementioned *in vivo* and *in vitro* techniques (**Figure 1.9**), flow cytometry allows identification and separate analysis of both HSC

(LT- and ST-HSC) and progenitor cells, as well as mature cells, and can be used both under *in vivo* or *in vitro* experimental settings. Well-characterised cell surface markers can be used to distinguish between the various cell types, whereas immunomagnetic depletion of more mature cells allows for HSC enrichment and subsequent Fluorescent Activating Cell Sorting (FACS) analysis (**Table 1.2**; **Figure 1.10**). **Table 1.2** shows important cell surface markers of murine HSC and progenitor cells.

Table 1.2

Cell type	Cell surface marker
LT-HSC	Lin^-, $Sca\text{-}1^+$, $c\text{-}Kit^+$, $Thy\text{-}1.1^{lo}$, $FLK\text{-}2^-$, $CD34^{lo/-}$
ST-HSC	Lin^-, $Sca\text{-}1^+$, $c\text{-}Kit^+$, $Thy\text{-}1.1^{lo}$, $FLK\text{-}2^+$, $CD34^+$
MPP	Lin^-, $Sca\text{-}1^+$, $c\text{-}Kit^+$, $Thy\text{-}1.1^-$, $FLK\text{-}2^+$, $CD34^+$
Common Lymphoid Progenitor	Lin^-, $Sca\text{-}1^{lo}$, $c\text{-}Kit^{lo}$, $Thy\text{-}1.1^-$, $FLK\text{-}2^+$, $CD34^+$, $CD43^+$
Common Myeloid Progenitor	Lin^-, $Sca\text{-}1^-$, $c\text{-}Kit^+$, $Thy\text{-}1.1^-$, $CD34^+$

Table 1.2: Cell surface markers of murine HSC and progenitor cells (Kondo *et al.*, 2003). FACS analysis employs the different expression profiles to identify specific subpopulations.

Murine HSC do not express any lineage-specific cell markers (Lin^-), show low or negative expression of the differentiation marker Thy-1 and express the stem cell antigen-1 ($Sca\text{-}1^+$) (Uchida and Weissman, 1992). Additional cell surface markers such as c-Kit, can further enrich for immature HSC. Hence, the Lin^- $Sca\text{-}1^+$ $c\text{-}Kit^+$ $Thy^{lo/-}$ ($L^-S^+K^+$ $Thy^{lo/-}$) population represents the most immature HSC. Single $L^-S^+K^+$ $Thy^{lo/-}$ cells can sustain long term haemopoiesis and self-renewal in ablated recipient mice (Smith *et al.*, 1991; Wagers *et al.*, 2002). In contrast, transplantation studies with Lin^- $c\text{-}Kit^-$ or Lin^- $Sca\text{-}1^-$ $c\text{-}Kit^+$ cells did not restore long term repopulation of haemopoietic lineages suggesting that expression of both $Sca\text{-}1^+$ and $c\text{-}Kit^+$ is a valid HSC marker (Okada *et al.*, 1991 and 1992; Ikuta and Weissman, 1992). Additional markers include combinations of cell surface receptors of the SLAM family (Kiel *et al.*, 2005). SLAM family members regulate the proliferation and activation of lymphocytes (Wang *et al.*, 2004) and are differentially expressed among functionally distinct immature BM cells. Combinatorial expression of these cell surface receptors can precisely distinguish

between HSC, MPP and lineage committed progenitor cells (Kiel *et al.*, 2005; Yilmaz *et al.*, 2006).

There is increasing evidence that the frequency of HSC and progenitor BM cells is controlled by genetic factors, whereas a number of haemopoietic malignancies arise following transformation of specific HSC or progenitor cells (see **Chapter 3**). Inter-strain variation of HSC frequency and flow cytometry have been utilised in **Chapter 3** in order to identify the genetic factors that control HSC frequency and, possibly, susceptibility to malignant transformation *in vivo*.

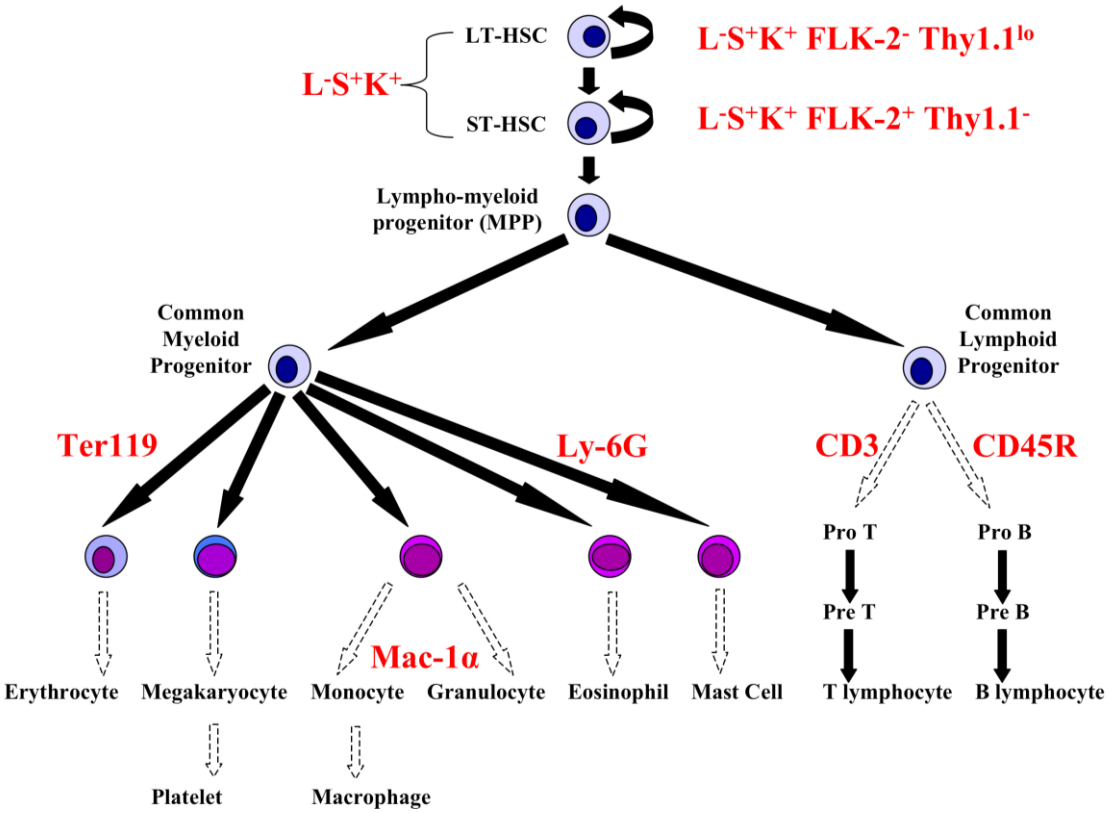

Figure 1.10: Cell type specific markers (red font). The Lin^- cells (HSC and lympho-myeloid progenitors) can be analysed by flow cytometry following immunomagnetic depletion of Lin^+ cells through the use of Ter119, Mac-1α, Ly-6G, CD3, and CD45R antibodies. FLK-2 and Thy1.1 can be used to distinguish between LT-HSC, ST-HSC and lympho-myeloid progenitors.

1.7 Bone marrow and cancer.

Most cancers are of clonal origin (i.e. always arise from a single cell). The uncontrolled proliferation of this cell and its offspring will result in a cluster of cells that is called a neoplasm/tumour. The neoplasm can be malignant or benign (Franks and Teich, 1997). Malignant and benign tumours display characteristic cell and tissue architecture. Their main difference however is the ability of malignant growths to invade surrounding tissues (invasion) and spread to other parts of the body (metastasis) by entering the bloodstream or the lymphatic system. Clinically a cancer is defined as a malignant growth which is invasive and able to metastasise (King, 2000).

Genes involved in cancer formation can be divided into two main classes: tumour suppressor genes and proto-oncogenes. As the name implies tumour suppressor genes (e.g. *p53*) carry out functions which suppress cancer formation. Mutations in these genes may result in "loss of function" and therefore generate malignant potential. The accumulation of errors in the DNA sequence might eventually lead to cancer formation. "Loss of function" of DNA repair genes (e.g. *MSH2*, *MLH1*) might lead to subsequent accumulation of replicative errors and eventually cancer formation.

Unlike the above class, mutations in proto-oncogenes might result in "gain of function" and produce malignant potential. A classic example is the Philadelphia chromosome which results from a reciprocal translocation between chromosomes 9 and 22. As seen in 90-95% of Chronic Myeloid Leukaemia (CML) cases, the translocation of the oncogene *abl* (located on chromosome 9) to chromosome 22 brings it under the regulatory influence of the *bcr* oncogene and eventually leads to CML (Connor and Ferguson-Smith, 1997; King, 2000).

Cancers originating in epithelium tissue are classified as carcinomas whereas cancers in the mesenchyme (cartilage, fat, blood vessels or other connective and supportive tissue) are classified as sarcomas (King, 2000).

1.7.1 Leukaemias.

Cancers that begin in the blood-forming tissue such as BM are classified as leukaemias or lymphomas (since metastasis is not exactly applicable in such tissues the use of the term 'malignancy' is preferred to that of 'cancer' with regards to blood-forming tissue). The two main classes of leukaemia are myelocytic leukaemias and lymphocytic leukaemias, whereas lymphomas are solid tumours derived from B- or T-lymphocytes. Leukaemias can be further subdivided depending on the speed that they develop. In contrast to the rapidly progressing acute myeloid and lymphoblastic leukaemias (AML and ALL respectively) chronic myeloid or lymphoid leukaemias (CML and CLL respectively) show slow progression rates. Lymphoid leukaemias generally arise from the relatively mature lymphoid progenitor cells, whilst myeloid leukaemias arise following transformation and clonal expansion of an immature multipotent stem cell (Warner *et al.*, 2004). Lymphomas originate from B- and/or T-lymphocytes, but unlike the other two forms of leukaemia in which malignant cells enter the bloodstream, lymphomas remain as solid cell aggregates in the lymph nodes (King, 2000). This thesis will focus specifically on AML.

1.7.2 Acute Myeloid Leukaemia (AML).

AML is a HSC malignancy. Also known as acute nonlymphocytic leukaemia and acute myelogenous leukaemia, AML is the most common form of acute leukaemia in adults. The HSC compartment is believed to be the major target for AML (**Figure 1.11**; Warner *et al.*, 2004). This means that AML will develop following malignant transformation of cells belonging to this heterogeneous population of multipotent stem cells. Upon transformation, overproduction of immature blast cells will disrupt haemopoiesis. The inadequate production of blood cells and platelets can lead to symptoms such as anaemia and bruising. Moreover, as white blood cells fail to mature, patients are prone to infection due to the absence of an effective immune system (Souhami *et al.*, 2001).

Similarly to most cancers, leukaemia risk increases with age (Balducci, 2000) suggesting that it is a multistage process. In AML, the HSC accumulates mutations over time, which might eventually lead to transformation, clonal expansion and progression to leukaemia (Warner *et al.*, 2004; Bonnet, 2005). The clonality of leukaemia (i.e. all

leukaemic cells are descendants of a single transformed cell) is demonstrated by a number of genomic rearrangements which are present in the majority of leukaemic cells. For example, most of r-AML cells exhibit characteristic large chromosomal deletions (e.g. long arm of chromosomes 5 and 7 in human) (Pedersen-Bjergaard *et al.*, 1995). Similarly, specific immunoglobulin and T-cell receptor rearrangements are seen in the leukaemic cells of murine B- and T-cell leukaemias (Boulton *et al.*, 2002).

As previously discussed (see section 1.3.4), whole-body exposure to ionising radiation results in a high excess relative risk of r-AML. Different mouse strains show different susceptibility to r-AML suggesting that a strong genetic component is involved in radiation-induced leukaemogenesis. The mouse strains used in this thesis will be discussed in section 1.8.

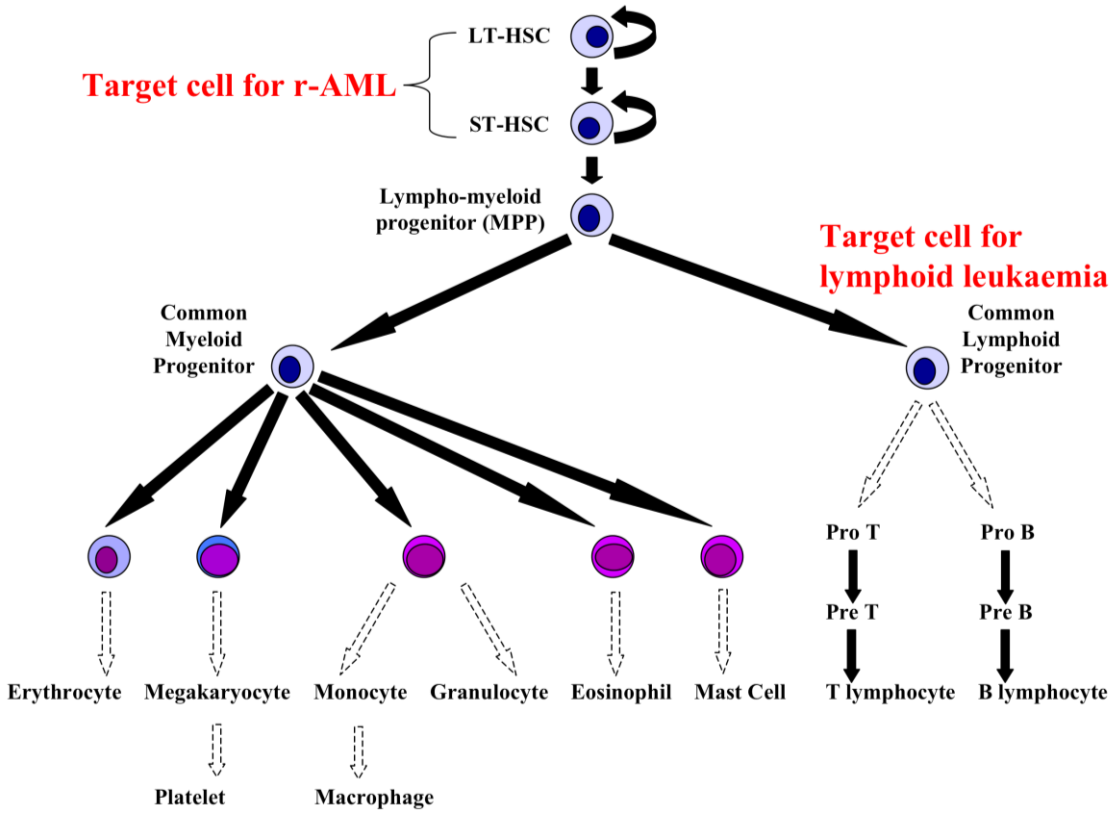

Figure 1.11: Different haemopoietic malignancies arise following transformation of specific BM cells. Radiation-induced AML results following transformation and clonal expansion of a HSC whereas B-cell leukaemia and T-cell lymphomas arise from more mature progenitor cells.

1.8 The mouse model.

The CBA/H mouse strain has been used in this project. This mouse model has been described as the most appropriate animal model for the study of human r-AML (Plumb *et al.*, 1998; Rithidech *et al.*, 1999). CBA/H mice have a low spontaneous leukaemia incidence (0.1-1%), but a large proportion (~25%) will develop AML following acute whole-body exposure to 3Gy X-rays (Plumb *et al.*, 1998). Additionally, leukaemic CBA/H mice show cytogenetic, molecular and histopathological characteristics (e.g. splenomegaly, accumulation of megakaryocytes in the BM and spleen) which are comparable to those seen in human AML (Rithidech *et al.*, 1999).

The C57BL/6 mouse strain has also been used. C57BL/6 mice are resistant to r-AML, but develop thymic lymphomas (a T-cell malignancy) following exposure to ionising radiation (Plumb *et al.*, 1998). Both mouse strains develop leukaemias between 6 to 24 months post-irradiation (mean latency of 18 months), consistent with the paradigm of cancer being a multi-stage process (Plumb *et al.*, 1998).

In addition to their different susceptibility to specific haematological malignancies, the two mouse strains show different sensitivity to radiation-induced genomic instability. Watson *et al.* (1997) demonstrated that irradiated CBA/H bone marrow cells show a higher frequency of aberrant cells, compared to irradiated C57BL/6 bone marrow cells. Similar genotype-specific differences in radiation-induced genomic instability have been reported in other mouse studies (Ponnaiya *et al.*, 1997) and human studies (Kadhim *et al.*, 1994), suggesting that there may be a strong genetic component influencing responses to ionising radiation. Differences in the frequency of HSC have also been reported for the two mouse strains (see **Chapter 3**; Müller-Sieburg and Riblet, 1996).

1.9 Factors influencing normal tissue reactions.

Radiotherapy patients show considerable variation with regards to their acute or long term reactions to ionising radiation, even when treated with identical treatment schedules (Bentzen, 2006). This clinical observation implies that radiosensitivity may be under genetic control.

Unarguably, many factors could contribute to this variable radiosensitivity (e.g. age, nutrition, coexisting morbidity such as collagen vascular disease or diabetes mellitus, anatomical differences) (Bentzen and Overgaard, 1994). There is however, substantial evidence that a genetic basis may also contribute to radiosensitivity. First-degree relatives of patients showing high levels of radiosensitivity *in vitro* also exhibit increased *in vitro* radiosensitivity (Roberts *et al.*, 1999; Burrill *et al.*, 2000). Most importantly, patients affected by rare genetic syndromes such as ataxia telangiectasia, Nijmegen breakage syndrome, Bloom's syndrome, and Fanconi anaemia, exhibit enhanced cellular as well as clinical radiosensitivity (Rogers *et al.*, 2000; Alter, 2002). Severe combined immunodeficiency (SCID) mice are also characterised by hypersensitivity to ionising radiation due to their inability to repair double strand breaks (Biedermann *et al.*, 1991; Kobayashi *et al.*, 1997). Sproston *et al.* (1997) reported an increased *in vitro* radiosensitivity in human SCID syndromes which was comparable to that seen in ataxia telangiectasia patients.

Chromosome instability syndromes (**Table 1.1**) provide strong evidence that radiosensitivity can be influenced by genetic factors. However, these syndromes are rare and are usually of little relevance when investigating radiosensitivity in unselected cancer patients. It is now accepted that clinical radiosensitivity is a complex phenotype that is probably determined by numerous genetic factors (Andreassen *et al.*, 2002). The proposed model is similar to that of multifactorial diseases such as cancer or cardiovascular disease. Mutations found in chromosome instability syndromes (e.g. *ATM* mutations) represent the high penetrance gene mutations found in familial cancer susceptibility syndromes (e.g. *BRAC1* and *BRCA2* mutations) and account for a relatively small percentage of radiosensitive cancer patients (Meyn, 1999). The majority of the variable clinical radiosensitivity of radiotherapy patients is therefore probably due to genetic polymorphisms that do not result in deleterious or inactivating mutations, but have subtle effects on protein activity (or protein expression levels), which in turn has a small but significant effect on clinical radiosensitivity (Andreassen *et al.*, 2002); especially when the effects of several polymorphisms are combined.

To date, all genetic association studies investigating the genetic determinants of clinical radiosensitivity have followed the so-called candidate gene approach. The candidate genes are primarily involved in biological pathways that are thought/or have been found

to be implicated in normal tissue damage. The major disadvantage of this approach is however, the fact that it is subject to investigator bias and restricted to the most obvious candidates. Candidate genes include DNA repair genes, genes coding for pro-fibrotic and inflammatory cytokines, and genes coding for free radical scavengers (reviewed in Andreassen *et al.*, 2002). A genetic association study has been performed in this thesis and included such candidate genes (see **Chapter 5**).

1.10 Project aims.

As part of a collaborative effort within the group, a whole-genome screen was performed to map Quantitative Trait Loci (QTL) influencing strain-specific (CBA/H and C57BL/6) differences in stem cell frequency, bone marrow cellularity, peripheral blood cellularity, and spleen size (**Chapter 3**). The long term aim of this project was to identify possible candidate genes that regulate these traits and investigate possible polymorphisms/differences between the two mouse strains.

The effects of ionising radiation on global DNA methylation levels of haemopoietic tissues in the CBA/H and C57BL/6 mice were investigated (**Chapter 4**). Post-irradiation DNA methylation levels were compared to those of control tissues and radiation-induced leukaemias. Additionally, this project investigated the relationship between global DNA methylation levels and relative radiosensitivity in irradiated bone marrow and spleen *in vivo*.

Finally, the acute and long term tissue effects (normal tissue damage) of ionising radiation were investigated in a group of breast cancer patients treated with radiotherapy (**Chapter 5**). A genetic association study was performed, in order to identify functional gene polymorphisms that might predispose to radiation-induced normal tissue damage.

Chapter 2:

Materials and methods

2.1 Materials.

2.1.1 Chemicals/reagents.

Chemicals were obtained from Bio Wittaker Molecular Applications (BMA) (Rockland, USA), Fisher Scientific (Loughborough, UK), Flowgen (Ashby de la Zouch, UK) and Sigma-Aldrich Company Ltd (Poole, UK).

Molecular biology reagents were obtained from ABgene (Epsom, UK), Ambion, Inc. (Austin, USA), Amersham Biosciences (Little Chalfont, UK), Applied Biosystems (Warrington, UK), Biogenesis (Poole, UK), Bio-Rad (Hemel Hempstead, UK), Bio Wittaker Molecular Applications (BMA) (Rockland, USA), Dynal Ltd (Merseyside, UK), Invitrogen UK (Paisley, UK), Millipore (Watford, UK), New England Biolabs (NEB) (Hitchin, UK), Perkin Elmer LAS Ltd (Bucks, UK), Promega (Southampton, UK), Qiagen Ltd (Crawley, UK), Raymond A Lamb Ltd (East Sussex, UK), ResGen (Division of Invitrogen Ltd, Paisley, UK), Roche Molecular Biochemicals (Mannheim, Germany), Sigma-Aldrich Company Ltd (Poole, UK), and Stratagene (Amsterdam, The Netherlands).

Specialised equipment was obtained from Applied Biosystems (Warrington, UK), Becton Dickinson-Pharmingen (Oxford, UK), Bio-Rad (Hemel Hempstead, UK), Cecil Instruments (Cambridge, UK), Eppendorf (Hamburg, Germany), Fisher Scientific (Loughborough, UK), Genetic Research Instrumentation (GRI) (Braintree, UK), Helena Biosciences (Sunderland, UK), Heraeus Instruments (Hanau, Germany), Labtech International Ltd (East Sussex), Life Sciences (Cambridge, UK), MJ Research (Waltham, USA), ThermoHybaid (Ashford, UK), Thermo Shandon (Pittsburgh, USA) and Ultra Violet Products (UVP).

2.1.2 Kits.

The following kits were used: ABI Prism Big Dye Terminator Cycle Sequencing Ready Reaction kit [ABI Prism (Warrington, UK)], One Step RT-PCR kit, QIAprep Maxiprep kit, QIAprep Miniprep kit, QIAquick Gel extraction kit, QIAamp DNA mini kit [Qiagen Ltd (Crawley, UK)], Random Primer DNA Labelling System and TOPO TA cloning kit with One Shot Competent *E.Coli* [Invitrogen UK (Paisley, UK)].

2.1.3 Solutions.

Table 2.1 shows all solutions used. Any additional solutions have been described at the relevant sections. Unless indicated, solutions were stored at room temperature**.**

Table 2.1

Solution	Preparation
10xKinase Mix	700mM Tris-HCl [pH 7.5], 100mM $MgCl_2$, 50mM spermidine trichloride, 20mM dithiothreitol. **Stored at -20°C**.
10xMOPS	0.2M MOPS, 0.05M NaAc, 0.01M EDTA. Adjusted to pH 7 with 10M NaOH.
10xTAE	0.4M Tris-Ac, 0.05M NaAc, 0.001M EDTA. Adjusted to pH 7.8 with acetic acid.
10xTE	100mM Tris-HCl [pH 8.0], 10mM EDTA.
10xTBE	44.5mM Tris-borate [pH 8.3], 1mM EDTA.
20xSSC	3M NaCl, 0.3M Tri-Sodium Citrate.
Ampicillin	10mg/ml (dissolved in distilled water). **Stored at -20°C**.
Church Buffer	5g BSA, 250ml 14% SDS, 250ml Na_2HPO_4, 1ml 0.5M EDTA [pH 8.0]. Preheated to 65°C, filtered [0.45µm]. **Stored at -20°C.**
Column Wash	1xTE, 0.1% SDS.
Denaturing mix	0.5M NaOH, 2M NaCl, 25mM EDTA, 0.1g bromophenol blue.
DEPC water	10µl Diethyl Pyrocarbonate in 200ml sterile water. Autoclaved.
DNA loading Dye	10ml 50xTAE, 12.48g Ficoll, 0.1g bromophenol blue. Final volume 100ml with sterile water.
Ethidium bromide	10mg/ml (dissolved in distilled water)
Dot-Blot hybridisation solution	5M TMAC, 10% (w/v) SDS, 0.5M disodium EDTA, 0.1M sodium phosphate [pH 6.8], 50xDenhardt's solution, 10mg/ml yeast RNA. **Stored at 4°C.**
Kinase stop solution	25mM disodium EDTA, 0.1%SDS, 10mM ATP. **Stored at -20°C**.

Table 2.1 (continued)	
Solution	**Preparation**
Luria Agarose (LUA) plates	Solid LA agar (media Kitchen, University of Leicester) was melted and cooled to 50°C before 0.1mg/ml ampicillin was added and poured into Petri dishes to set. 40µl of 40mg/ml X-galactoside (dissolved in dimethylforamide) were spread onto the plates using sterile procedures.
Lysis buffer	50mM Tris-HCl [pH 8], 100mM EDTA [pH 8], 100mM NaCl, 1% (w/v) SDS.
NDS	93g Na2EDTA2H_2O, 0,605g Tris, bring up to 400ml, adjust to pH>8 with NaOH, dissolve 5g sodium-N-lauroyl sarcosine in 50ml water and add. Adjust the pH to 9.5 with NaOH. Make up final volume to 500ml with water.
PBS/BSA Buffer	0.2% (w/v) fraction PBS in BSA, 65°C overnight, filtered (0.2µm). **Stored at 4°C**.
PBS	1 tablet of Phosphate buffered saline dissolved in 100ml of dH_2O.
Proteinase K	10mg/ml (dissolved in distilled water). **Stored at -20°C**.
RNA loading dye	40mM MOPS, 10mM NaOAc [pH7], 1mM EDTA, 50% (v/v) formamide, 7.4% (v/v) formaldehyde, xylene cyanol and 0.1g bromophenol blue. **Stored at -20°C**.
RNase A	10mg/ml (dissolved in distilled water). **Stored at -20°C**.
Sequencing stop buffer	98% (v/v) formamide, 0.01M EDTA [pH 8], 300µg/ml blue dextran.
0.5M Sodium phosphate [pH 7.2]	342ml of 1M Na_2HPO_4 and 158ml of 1M NaH_2PO_4. Make up to a final 1lt volume with dH_2O.
Southern Denaturing solution	0.5M NaOH, 1M NaCl.
Southern Depurinating solution	0.25M HCl.
Southern Neutralising solution	0.5M Tris-HCl [pH 7.5], 3M NaCl.
Southern wash Solutions	2x-, 0.2x-, or 0.1x-SSC, 0.1% SDS.
TMAC wash solution	5M TMAC, 10% (w/v) SDS, 0.5M disodium EDTA, 0.1M sodium phosphate [pH6.8]. **Stored at 4°C**.

Table 2.1: List of solutions used in this thesis.

2.1.4 Oligonucleotides.

DNA sequences were obtained from the NCBI database (found at: http://www.ncbi.nlm.nih.gov). These were used to design primer pairs, Allele Specific Oligonucleotides (ASOs) and confirm sequencing results. Unless obtained from published studies, primers were designed using http://www-genome.wi.mit.edu/cgi-

bin/primer/primer3.cgi. Primers (**Table 2.2**) and ASOs (**Table 2.3**) were obtained from Amersham Biosciences (Little Chalfont, UK) and/or Invitrogen UK (Paisley, UK).

Mouse microsatellite primer sequences were chosen from: the Chromosome Committee Report from MGI (http://www.informatics.jax.org/) or the Whitehead Institute for Biomedical Research/MIT Centre for Genome Research (http://www-genome.wi.mit.edu). These mouse microsatellite primers (**Appendix I**) were obtained from Research Genetics (Division of Invitrogen Ltd, Paisley, UK).

Table 2.2

Gene	Primer Sequence (5′-3′)	Size (bp)	NCBI Acc. No. / Reference.
APEX1 D148E	F: CTG TTT CAT TTC TAT AGG CTA R: AGG AAC TTG CGA AAG GCT TC	164	Hu *et al.*, 2001
CX3CR1 V249I	F: AGA ATC ATC CAG ACG CTG TTT TCC R: CAC AGG ACA GCC AGG CAT TTC C	311	McDermott *et al.*, 2001
DHFR deletion	F1: CCA CGG TCG GGG TAC CTG GG F2: ACG GTC GGG GTG GCC GAC TC R: AAA AGG GGA ATC CAG TCG G	113	Johnson *et al.*, 2004
EPHX1 Y113H	F: GAT CGA TAA GTT CCG TTT CAC C R: ATC TTA GTC TTG AAG TGA GGA T	162	Lebailly *et al.*, 2002
EPHX1 H139R	F: ACA TCC ACT TCA TCC ACG T R: ATG CCT CTG AGA AGC CAT	210	Lebailly *et al.*, 2002
HFE C282Y	F: TGG CAA GGG TAA ACA GAT CC R: CCA TCC CCT AAC AAA GAG CA	446	NG_001335
IAP	F: GTT ACA AGA TGG CGC TGA CA R: TCT CCC CGC TTT ACT TCT GA	721	M17551
LINE-1	F: GCC CTG ACC ACA GTG ATC TT R: AGT GCT GCG TTC TGA TGA TG	1443	M13002
MTHFR C677T	F: TGA AGG AGA AGG TGT CTG CGG GA R: AGG ACG GTG CGG TGA GAG TG	198	Kara *et al.*, 2003
MTHFR A1298C	F: CAA GGA GGA GCT GCT GAA GA R: CCA CTC CAG CAT CAC TCA CT	128	Kara *et al.*, 2003
MTR D919G	F: GGT GTG TTC CCA GCT GTT AGA TG R: GAC ACT GAA GAC CTC TGA TTT GAA C	265	Lincz *et al.*, 2003
TGFβ-1 C-509T	F: CAG ACT CTA GAG ACT GTC AG R: GTC ACC AGA GAA AGA GGA C	419	Quarmby *et al.*, 2003
XRCC1 R194W	F: GCC CCG TCC CAG GTA R: AGC CCC AAG ACC CTT TCA CT	490	Hu *et al.*, 2001
XRCC1 R399Q	F: TCT CCC TTG GTC TCC AAC CT R: AGT AGT CTG CTG GCT CTG G	402	Hu *et al.*, 2001
XRCC2 R188H	F: CTG AGG AAA TGT TCT CAG TGC TTA GA R: TGA TGA GCT CGA GGC TTT CTG	102	Rafii *et al.*, 2002

Table 2.2: Primer sequences used in this thesis.

Table 2.3		
Gene/SNP	**Allele**	**ASO Sequence (5′-3′)**
HFE C282Y	G	TAT ACG T**G**C CAG GTG GAG
	A	TAT ACG T**A**C CAG GTG GAG
TGFβ-1 C-509T	C	TCC ATC C**C**T CAG GTG TCC
	T	TCC ATC C**T**T CAG GTG TCC
XRCC2 R188H	G	GAC TAT C**G**C CTG GTT CTT
	A	GAC TAT C**A**C CTG GTT CTT
Minor satellite	-	AAC AGT GTA TAT CAA TGA GTT ACA ATG AG

Table 2.3: Allele Specific Oligonucleotides (ASOs) used in this thesis.

2.1.5 Enzymes and radiolabelled reagents.

Restriction enzymes were supplied by New England Biolabs (NEB) (Hitchin, UK). *Taq* polymerase was supplied by ABgene (Epsom, UK). *Pfu* polymerase was supplied by Stratagene (Amsterdam, The Netherlands). Proteinase K and RNase A were supplied by Sigma-Aldrich Company Ltd (Poole, UK). γ-^{32}P-ATP (10mCi/ml) and α-^{32}P-dCTP (3000Ci/mmol) were supplied by Amersham Pharmacia Biotech (Amersham, UK).

2.1.6 Mouse Strains.

CBA/H mice from the Harwell colony were bred at the Biochemical Services department (Leicester Royal Infirmary). C57BL/6 mice (originally maint. by JN Ola) were purchased from Harlan UK Limited (Bicester, UK). (CBA/H x C57BL/6) F_1 and F_2 mice were bred at the Biochemical Services department (Leicester Royal Infirmary). The animal studies were carried out under guidance issued by the MRC in 'Responsibility in the use of animals for medical research' (July 1993) and Home Office Project licences No PPL 80\1565, 80\1564 and 40/2605.

2.1.6.1 Mouse irradiation.

Mice which were at least 8 weeks old were exposed to a single acute dose of 3Gy X-rays (0.5 Gy/minute, constant potential, 250 kV) using a Pantak industrial X-ray machine (Connecticut, USA). Animals were then killed at specific time-points using a Home Office Schedule 1 approved method [Appropriate methods of humane killing (Appendix 1 – Schedule 1), 1990].

2.1.6.2 Diagnosis of mouse haemopoietic malignancies.

DNA and RNA stocks of mouse leukaemias were available in the lab. Diagnosis of all malignancies was as previously described (Cleary *et al.*, 2001; Boulton *et al.*, 2002). Leukaemic spleens were snap frozen in dry ice followed by DNA and/or RNA extraction.

2.1.7 Human buccal swab samples.

The study in **Chapter 5** was undertaken with the participation of 167 patients attending the oncology departments of Leicester Royal Infirmary, Glenfield Hospital, Leicester and Nottingham City Hospital, UK. Full ethical and local trust approval was obtained from the relevant ethics committees and trust Research and Development departments. DNA was collected from patients by means of a buccal swab stored in NDS solution (**Table 2.1**). Drs Paul Symonds, Karen Foweraker, Matt Griffin and Irene Peat were responsible for sample collection. DNA extraction procedure is described in section 2.6.

2.2 Mouse tissue extraction.

Mice were killed at specific time-points by cervical dislocation inside a room designated for surgical procedures under relatively sterile conditions. Organs were removed, snap frozen on dry ice and stored at -80^{o}C unless immediately used. Blood was collected by cardiac puncture using a 25 gauge needle and transferred into an eppendorf containing heparin anticoagulant.

Bone marrow (BM) was collected by flushing both mouse femurs using PBS/BSA (or PBS only) solution and a 25 gauge syringe. Samples were then pelleted (5 minutes, 2000rpm at 4^{o}C) and stored at -80^{o}C unless immediately used.

2.3 Mouse tissue DNA extraction.

A number of different tissues were used in this thesis. Mouse whole tails were cut into small pieces and transferred into 15ml polypropylene tubes containing 2ml PBS. Bone marrow samples were transferred into 15ml polypropylene tubes containing 1ml PBS. All other solid tissues used were placed in liquid nitrogen, pulverised using a mortar and

pestle before being placed into 15ml polypropylene tubes containing at least 2ml of PBS (4ml of PBS were used in the case of larger organs such as liver and intestine).

2.3.1 Lysis/Proteinase K digestion.

As soon as samples were transferred into the 15ml polypropylene tubes, equal volumes of lysis buffer and 1/10th volume of Proteinase K (10mg/ml) were added to the re-suspended sample. Samples were shaken and incubated overnight at 55^{o}C. Lysis buffer enabled cell lysis whilst Proteinase K digested proteins and prevented nuclease activity. Following overnight incubation, 1/20th volume of RNase A was added to the mix to cleave single stranded RNA, the samples were gently shaken and incubated for a further 60 minutes at 37^{o}C. Genomic DNA was then purified with phenol/chloroform (see section 2.3.2).

2.3.2 Phenol/chloroform extraction.

DNA was purified following incubation with Lysis buffer, Proteinase K and RNase A by phenol/chloroform. One volume of phenol [Fisher Scientific (Loughborough, UK)] was added to the sample. To minimise DNA shearing, samples were gently inverted in order to emulsify the mixture. The mix was then centrifuged at 3000rpm for 5 minutes at room temperature. DNA remained in the aqueous (upper) phase whilst proteins and phenol partitioned into the organic (lower) phase. The aqueous layer was removed and transferred into a new 15ml polypropylene tube. The same procedure was repeated with 1 volume of phenol/chloroform (1/2 volume each) followed by a final 1 volume of chloroform. The chloroform step was added to remove any traces of phenol from the aqueous phase. In cases where the aqueous phase was cloudy, an additional phenol step was included prior to the phenol/chloroform step. Samples were then ethanol precipitated (see section 2.3.3).

2.3.3 Ethanol precipitation.

Following the chloroform step, the aqueous phase was transferred into a new 15ml polypropylene tube containing 1 volume of isopropanol and 1/10th volume of 3M NaAc [pH 5.5]. Tubes were inverted to precipitate the DNA which was then transferred into

1.5ml of 70% (v/v) ethanol (EtOH). DNA was pelleted by centrifugation for 10 minutes at 3000rpm (room temperature). EtOH was removed, the pellet was air dried, DNA was re-suspended in appropriate (0.05-1.5ml depending on pellet size) quantity of 1xTE buffer (or nuclease free water depending on the downstream processes) and stored at 4^{o}C. This protocol was used for all DNA precipitations in this thesis. In cases where isopropanol was not used, DNA was precipitated in 3 volumes of 100% EtOH.

2.4 Mouse tissue RNA extraction.

To minimise chances of contamination or RNA degradation, RNA extractions were performed on ice using sterile tubes and DEPC-treated water, eppendorfs and tips. Similar to the DNA extraction protocol, RNA extraction involves separation of RNA from DNA and proteins followed by removal of phenol traces by a chloroform step. Mouse tissues were placed in liquid nitrogen and pulverised as previously described (section 2.3), transferred into sterile 15ml polypropylene tubes containing 6-8ml of RNAzol (Biogenesis, UK) and mixed vigorously. In cases of large solid tissues such as liver and intestine, 10ml of RNAzol were used. One-tenth volume of chloroform was added; the mix was shaken well and placed on ice for 20 minutes. The sample was centrifuged at 6000rpm for 20 minutes at 4^{o}C and the aqueous phase was transferred into a new 15ml polypropylene tube. One volume of isopropanol was added to the sample which was then left on ice for 15 minutes to enable RNA precipitation. RNA was pelleted by centrifugation at 6000rpm for 20 minutes at 4^{o}C. The sample was washed in 70% (v/v) EtOH and centrifuged at 6000rpm for 20 minutes at room temperature. EtOH was carefully removed, the tube was inverted and the pellet was air-dried at room temperature. The RNA sample was dissolved in 50% (v/v) EtOH in a 1.5ml DEPC-treated eppendorf and stored at -20^{o}C. RNA degradation was checked by running some of the sample on a 1% (w/v) formaldehyde agarose/1xMOPS gel (see section 2.14).

2.5 Staining cytospin preparations.

Bone marrow cytospin slides were prepared using positively charged Histobond microscope slides (75 x 25 x 1mm) (Raymond A Lamb Ltd). Approximately 50,000

bone marrow cells were diluted in 200µl PBS and transferred onto the cytospin slides (centrifuged at 400rpm for 5 minutes at room temperature).

Cytospin preparations were air-dried and fixed in 100% EtOH for 15 minutes at room temperature. Slides were stained with either 56% (v/v) Jenners stain [pH 6.4] followed by 15% (v/v) Giemsa stain [pH 6.4] (5-10 minutes each) or with 1% Eosin (2-5 minutes) followed by Haematoxylin (2-5 minutes) (**Figure 2.1**). Stained slides were air-dried and mounted using DePex and a coverslip.

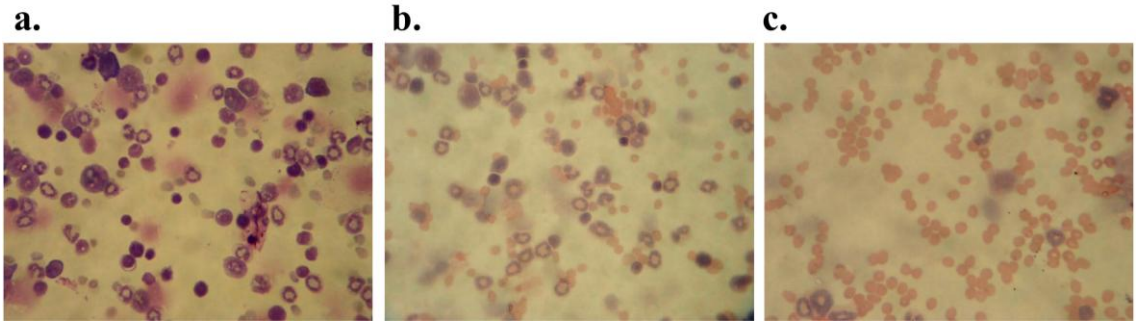

Figure 2.1: Typical cytospin slides of total BM stained with Jenners/Giemsa stain (a) and Haematoxylin/Eosin (b and c). As seen from slide c, exposure to 3Gy X-rays kills 80-90% of enucleated BM cells.

2.6 Human DNA extraction from buccal swabs.

DNA was extracted from buccal swabs using the QIAamp DNA mini kit [QIAGEN Ltd (Crawley, UK)] according to the manufacturer's protocol. Lysis of cells in the presence of Proteinase K is followed by the binding of DNA onto the QIAamp silica-gel membrane. Salt and pH conditions ensure that protein or other contaminants are not retained on the membrane. DNA is then washed and purified. Following the removal of residual contaminants DNA was eluted and stored at 4^{o}C.

2.7 PCR reactions.

DNA was amplified by Polymerase Chain Reaction using an MJ Peltier Thermal Cycler (PCT)-200 and 0.2ml sterile tubes. Genomic DNA (10-100ng) was amplified in a 10µl

reaction containing: 0.9µl (~1x) of reaction buffer type 11.1x (see section 2.7.1), 0.3µM of each primer, 12mM 2M Tris and 0.5U of *Taq* polymerase [ABgene (Epsom, UK)]. *Taq* polymerase was 'spiked' with *Pfu* polymerase [1:20 (U/U)] in order to increase PCR fidelity. PCR conditions were primer/fragment-size specific and unless specified were: 5 minutes of denaturing at 96^{o}C, followed by 35 cycles of: 1 minute of denaturing at 96^{o}C, 1 minute at the appropriate annealing temperature, 1 minute of elongation at 72^{o}C, followed by a final 7 minutes elongation at 72^{o}C. Primer sequences can be found on **Table 2.2**).

2.7.1 11.1x buffer.

Stocks of 11.1x reaction buffer were prepared in the lab and used in all PCR reactions. The 11.1x buffer contained: Tris-HCl [pH 8.8], ammonium sulphate, magnesium chloride, 2-mercaptoethanol, EDTA [pH 8.8], equal volumes of all 4 dNTPs, and BSA. Addition of 0.9µl of 11.1x buffer gave the following final concentrations in a 10µl total volume PCR reaction mix: 45mM Tris-HCl [pH 8.8], 11mM ammonium sulphate, 4.5mM magnesium chloride, 0.045% 2-mercaptoethanol, 4.4µM EDTA [pH 8.8], 1mM of each dNTP, and 13µg/ml BSA.

2.8 Agarose gel electrophoresis.

DNA fragments were separated by horizontal agarose gel electrophoresis. Agarose gels [0.8-4.5% (w/v)] were prepared by boiling agarose in 1xTBE (which contained Ethidium Bromide) and cast in sealed gel trays. Gel combs were used to generate wells of desired volume and gels were left to solidify inside a fume hood at room temperature. DNA samples were mixed with DNA loading dye (**Table 2.1**) and loaded in the wells next to the appropriate DNA size markers. The 1Kb, 100bp [supplied by New England Biolabs (NEB) (Hitchin, UK)], φX174/*Hae*III or λDNA/*Hind*III [supplied by ABgene (Epsom, UK)] DNA ladders were used. Ethidium bromide-stained DNA was visualised under UV light using a Gene Genius Bioimaging system and Gene SNAP computer package [Syngene Ltd (Cambridge, UK].

RNA samples were run on a 1xMOPS gel (see section 2.14) and DNA fragments were isolated from 1xTAE gels (see section 2.8.1).

2.8.1 Isolation of DNA from gel.

PCR purification/DNA fragment isolation was carried out using the QIAquick gel extraction kit [Qiagen Ltd (Crawley, UK)]. Resolved DNA fragments were excised from a 1-1.5% (w/v) low melting point agarose [Invitrogen (Paisley UK)] gel prepared with 1xTAE and stained with Ethidium bromide. Low melting point agarose gels melt at 50^{o}C, which is well below the DNA melting point. DNA was extracted using the QIAquick gel extraction kit according to the manufacturer's protocol. Essentially, excised gel fragments were melted at 50^{o}C and the solution was passed through a column. DNA was bound on the QIAquick silica membrane, washed and purified. Following the removal of residual contaminants DNA was eluted and fragment size was confirmed by agarose gel electrophoresis.

2.9 RFLP analysis and restriction digestion.

DNA (genomic, plasmid, or PCR amplified) was digested using enzymes supplied from New England Biolabs (NEB) (Hitchin, UK). Digestion conditions, buffer and addition of BSA were as recommended by the supplier. All reactions contained 1x of the appropriate NEB buffer and incubation time varied from 1 hour to an overnight period. To avoid possible star activity, glycerol concentration (<5%), enzyme concentration and pH (>8) were kept at recommended levels.

2.10 Cloning/Transformation.

Cloning and transformation were performed using the TOPO TA cloning kit with One Shot Competent *E.Coli* [Invitrogen (Paisley, UK)] according to the manufacturer's protocol. Essentially the desired fragment is *Taq* polymerase-amplified which adds a single deoxyadenosine (A) to the 3′ end of the PCR product. The linearized pCR®2.1-TOPO® vector has single overhanging 3′ deoxythymidine (T) residues. The PCR fragment is thus ligated with the vector which is then used to transform chemically competent *E.Coli*. Transformants are streaked on ampicillin supplemented/X-gal coated LUA plates. Successful transformation results in the disruption of the plasmid's *β*-galactosidase gene (*lacZ*) and colonies appear as white due to their inability to metabolise X-gal.

2.10.1 Ligation.

Fresh PCR product (2-3µl) was incubated with 1µl salt solution and 1µl of the vector. PCR-clean water was used to adjust the reaction volume to 6µl which resulted in a final salt concentration of 200mM NaCl and 10mM $MgCl_2$. This is the optimum salt concentration recommend by the manufacturer to ensure efficient transformation of chemically competent *E.coli* in the downstream process. The reaction mix was left at room temperature for 5 minutes to ensure ligation.

2.10.2 Transformation of chemically competent *E.Coli.*

Two µl of the ligated vector were transferred into a vial of One Shot® Chemically Competent *E.Coli* and gently mixed. The reaction was incubated on ice for 30 minutes and the cells were heat-shocked for 30 seconds at 42^{o}C without shaking. Samples were immediately transferred on ice and 250µl of SOC medium (2% Tryptone, 0.5% Yeast Extract, NaCl, KCl, $MgCl_2$, $MgSO_4$, 20mM Glucose) was added. Cultures were shaken horizontally (~200rpm) at 37^{o}C for 1 hour.

Aliquots of each culture (50µl and 150µl) were streaked onto pre-warmed (37^{o}C) ampicillin supplemented (10mg/ml)/X-gal coated (40µl from a 40µg/µl stock)-LUA plates (**Table 2.1**) and incubated overnight at 37^{o}C. Upon successful transformation white colonies were formed. These ampicillin resistant colonies were unable to metabolise X-gal. Colonies that contained the vector, but not the fragment, were still ampicillin resistant, but were able to metabolise X-gal and appeared as blue. White colonies were picked and plasmid DNA was purified (see section 2.11).

2.11 Plasmid DNA purification.

Plasmid DNA was isolated from bacteria and purified using the QIAprep Miniprep and QIAprep Maxiprep kits [Qiagen Ltd (Crawley, UK)] according to the manufacturer's protocol. Essentially, bacteria cells are cultured overnight and lysed in alkaline solution. Denatured proteins, RNA and other impurities are removed in subsequent washes and DNA is bound onto the QIAprep silica-gel membrane. Purified plasmid DNA is finally eluted.

2.11.1 Small-scale cultures for Qiagen Miniprep.

Single white colonies were picked and cultured (shaken) overnight at 37^{o}C in 5ml LB medium containing ampicillin (10mg/ml). An aliquot (1.5ml) of the expanded culture was used to isolate/purify plasmid DNA using the QIAprep Miniprep kit according to the manufacturer's protocol.

2.11.2 Size/sequence verification of inserted PCR fragment.

The PCR fragment was isolated from the vector by means of restriction enzyme digestion (see section 2.11.4). Band size was confirmed by agarose gel electrophoresis (see section 2.8); the band was excised from the gel (see section 2.8.1) and sequenced (see section 2.16). Upon confirmation, 1.5ml of the cultured colonies was used for large-scale plasmid DNA extraction using the QIAprep Maxiprep kit (see section 2.11.3).

2.11.3 Large-scale cultures for Qiagen Maxiprep.

One aliquot (1.5ml) of the cultured mix (section 2.11.1) was cultured (shaken) overnight at 37^{o}C in 400ml LB medium containing ampicillin (10mg/ml). Cells were pelleted by centrifugation (2000rpm for 20 minutes at 4^{o}C) and plasmid DNA was isolated/purified using the QIAprep Maxiprep kit according to the manufacturer's protocol. Plasmid DNA was precipitated using isopropanol (see section 2.3.3) and re-suspended in appropriate amounts of 1xTE to a final concentration of 1mg/ml.

2.11.4 Isolation of probes used in this study.

Plasmid stocks containing the desired fragments were stored at 4^{o}C. The IAP 5′LTR genomic probe was isolated from the transformed plasmid by a double (*Eco*RV/*Bam*HI) digestion. The L1 LINE insert was extracted from the transformed plasmid by an *Eco*RI digestion. Plasmid DNA (~20µg) was digested at 37^{o}C for at least 2 hours with 60 units of enzyme(s) and the appropriate buffer in a 50µl reaction. Fragment size was confirmed by agarose gel electrophoresis; DNA was isolated from a 1xTAE gel (see section 2.8.1), eluted with 50µl of EB buffer and the probe was stored at 4^{o}C until needed (see section 2.13).

2.12 Microsatellite genotyping.

(CBA/H x C57BL/6) F_1 x F_1 hybrid mice (F_2) were genotyped using polymorphic microsatellite markers. These are randomly repeated sequences found in the mouse genome and their sizes may differ between different mouse strains. Microsatellite repeats were PCR-amplified using unique primer sequences that flank each repeat (see section 2.1.4; **Appendix I**). Markers that gave the greatest allelic size variation between DBA/2 and C57BL/6 mice were chosen, as CBA/H inbred mice had not been assessed in the MGI database and DBA/2 mice are close relatives. Microsatellite repeats were PCR-amplified and fragments were resolved by agarose gel electrophoresis (see sections 2.7 and 2.8). CBA/H, C57BL/6 and (CBA/H x C57BL/6) F_1 samples were run alongside the F_2 samples and acted as genotype markers (**Figure 2.2**).

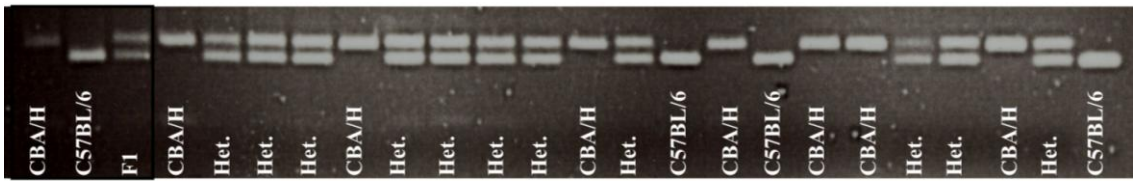

Figure 2.2: Agarose gel of PCR-amplified microsatellite markers. CBA/H, C57BL/6 and (CBA/H x C57BL/6) F_1 samples (Lanes 1, 2 and 3) were used as markers to genotype DNA from F_2 mice (Lane 4 – end).

2.13 Southern blotting.

Southern blotting was employed in order to assess the methylation status of 5′-CCGG-3′ sites in 3 different CpG-rich genomic repeat elements. Essentially, genomic DNA was digested with the methylation-sensitive *Hpa*II and methylation status-independent *Msp*I enzymes, resolved on an agarose gel, denatured, neutralised and transferred onto a magna nylon membrane. Genomic probes (see sections 2.10 and 2.11) were radiolabelled, denatured and hybridised with the membrane. Following hybridisation and washing, the sites of hybridisation were visualised by autoradiographic exposure.

2.13.1 DNA digestion and transfer onto a Magna nylon membrane.

Two aliquots of the same sample (2-3µg of genomic DNA) were digested with *Hpa*II and *Msp*I respectively overnight at 37^{o}C using the manufacturer's recommended conditions. Digested DNA was loaded onto a 1.5% (w/v) agarose gel and run overnight at a constant current of 30 Volts. The gel was photographed and subsequently washed/shaken as follows: 2 washes (10 minutes each) in depurinating buffer, 2 washes (20 minutes each) in denaturing buffer, and 2 washes (20 minutes each) in neutralising buffer.

The southern apparatus was set up as follows: The gel was placed top-side down on a strip of Whatman 3MM paper which acted as a wick on top of a tank filled with 10xSSC. The membrane was placed on top of the gel, followed by 3 Whatman 3MM strips of paper (membrane and paper were cut to the exact gel dimensions). Air-bubbles and excess liquid were carefully removed as they can disrupt the DNA transfer process. Paper towels and a weight were placed on top of the paper strips and DNA was transferred overnight by capillary action. The membrane was then baked at 80^{o}C for 1 hour and the DNA was covalently linked to the membrane by exposure to $7x10^{4}$ J/cm^{2} of UV light in a RPN 2500 ultraviolet crosslinker [Amersham Biosciences (Little Chalfont, UK)]. Membranes were stored at room temperature unless immediately used.

2.13.2 Pre-hybridisation of the membrane.

The membrane was soaked in 2xSSC, transferred into hybridisation bottles containing 12ml of hybridisation solution (Church buffer pre-heated to 65^{o}C) and pre-hybridised for at least 5 hours at 65^{o}C in a Mini 10 Hybridisation oven [Thermohybaid (Ashford, UK)].

2.13.3 Radiolabelling the probe.

Genomic probes were labelled with α-^{32}P-dCTP (3000Ci/mmol) using the Random Primer DNA Labelling System [Invitrogen UK (Paisley, UK)]. Genomic probes (20-50ng diluted in 22µl PCR-clean water) were denatured by boiling (6 minutes) and transferred on ice. The labelling reaction contained: 15µl of Random primer buffer, 6µl of dNTPs (excluding dCTP), 5µl α-^{32}P-dCTP (3000Ci/mmol) and 1µl of Klenow

Fragment. The reaction mix was left at room temperature for 1 hour, after which the reaction was stopped with 30µl of column wash. G50Nic columns [Amersham Biosciences (Little Chalfont, UK)] were used to remove unincorporated dNTPs. Columns were equilibrated twice with column wash and the probe was added. Unincorporated dNTPS were removed by adding 400µl of column wash. Probes were eluted and collected from the column by adding a further 400µl of column wash, denatured by boiling (6 minutes), snap-chilled on ice (6 minutes) and added to pre-hybridising membranes.

2.13.4 Hybridisation and washing.

The denatured probe was added to pre-hybridising membranes and hybridised overnight at 65^{o}C. Excess probe was removed by: 2 washes of 2xSSC (30 minutes each), 2 washes of 0.2xSSC (30 minutes each) and a final wash of 0.1xSSC (20 minutes) (All washes at 65^{o}C).

After washing, the membrane was blotted with Whatman 3MM paper to remove any excess liquid and wrapped in cling film to prevent drying. Hybridisation patterns were visualised by autoradiography using Fuji RX 100 or Kodak BIOMAX XAR film and Hypercassette autoradiographic cassettes [Autorads (Lutterworth, UK)] with intensifying screens. Films were exposed for 1 to 5 days at -80^{o}C depending on the strength of the signal.

To enable re-hybridisation membranes were stripped by immersing in boiling 0.1xSSC, 0.1% (w/v) SDS for 10-20 minutes. The procedure was repeated if the radioactivity detected with a Geiger counter exceeded 5counts/second. Stripped membranes were placed against film to check for any remaining radioactivity. When no background signal was produced membranes were re-used or stored at 4^{o}C wrapped in cling film.

2.14 Northern blotting.

RNA samples were run on 1% (w/v) 1xMOPS/formaldehyde agarose gels. Appropriate amounts of agarose were boiled in 1xMOPS, left at room temperature to cool down

(~50^{o}C) and formaldehyde was added to a final concentration of 7.4% (v/v). Ethidium bromide was added to the solution (0.04µg/ml) and the gel was cast in a sealed gel tray.

RNA (10-20µg) was denatured for 5 minutes at 65^{o}C in 20µl of RNA loading dye (**Table 2.1**) and snap-chilled on ice before being loaded on a 1% (w/v) 1xMOPS/formaldehyde agarose gel. Gels were run in 1xMOPS buffer overnight at a constant current of 30 Volts. Gels were then photographed, washed in 10xSSC to remove excess formaldehyde and used to set up the Northern apparatus. All downstream procedures were the same as for Southern blotting and have been described in section 2.13.

2.15 Dot blotting.

The tetramethylammonium (TMAC) hybridisation protocol was used [as instructed by Professor Sir Alec Jeffreys, University of Leicester (Leicester, UK)]. Two Allele Specific Oligonucleotides (ASOs), each specific to the version of the allele, were designed for each Single Nucleotide Polymorphisms (SNP). ASOs were 18bp in length with the polymorphic site located 8 nucleotides from the 5′ end (see section 2.1.4; **Table 2.3**). Essentially, PCR products were denatured in alkaline solution, loaded onto the membrane and neutralised with 2xSSC. The single-stranded DNA was then covalently linked to the membrane and hybridised with a radiolabelled ASO. The membrane was washed and placed against film.

2.15.1 Denaturing the PCR product.

Following successful PCR amplification of the desired fragments (checked by running a small volume on an agarose gel), 5 volumes (45µl) of denaturing mix (**Table 2.1**) were transferred into each 9µl PCR sample. Samples were left at room temperature for 15 minutes to ensure denaturing of DNA.

2.15.2 Dot blot membrane.

Two wet 12cm x 8.5cm Whatman 3MM [Whatman's International Ltd (Maidstone, UK)] paper strips were placed on-top of the dot blot manifold, followed by the 12cm x

8.5cm Hybond N-Fp membrane which had been soaked in 2xSSC. The dot blot apparatus was set up and attached to a 96 well vacuum manifold. Vacuum was applied, 26µl of the denaturing mix/PCR product were transferred onto the wells and neutralised with 150µl 2xSSC. The apparatus was dismantled and the same procedure was repeated using fresh paper strips/membrane and the remaining quantity of denaturing mix/PCR product. Thus, each PCR reaction was used to prepare 2 membranes. The membranes were baked at 80^{o}C for 10 minutes and the DNA was covalently linked to the membrane by exposure to $7x10^{4}$ J/cm^{2} of UV light using a RPN 2500 ultraviolet crosslinker (Amersham Biosciences). Unless immediately used, membranes were stored at room temperature.

2.15.3 Kinase labelling.

γ-^{32}P-ATP was incorporated in the ASO in a labelling reaction containing: 1µl 10x kinase mix, 0.35µl T4 Polynucleotide Kinase (stock: 10U/µl), 0.12µl γ-^{32}P-ATP (stock: 10mCi/ml), 1µl of the appropriate ASO (stock: 8ng/µl) and 7.8µl of dH_2O. T4 kinase catalyses the transfer of a phosphate group from the γ position of the ATP molecule to the 5′ hydroxyl terminus of the ASO. The reaction was incubated at 37^{o}C for at least 45 minutes (45 minutes-5 hours) and stored at -20^{o}C unless immediately used for hybridisation. Prior to hybridisation, 20µl of Kinase stop solution were added to inactivate the enzyme.

2.15.4 Dot blot membrane hybridisation.

Under appropriate conditions, a radiolabelled single stranded ASO will bind to its homologous single stranded DNA sequence that has been fixed onto a membrane. The membrane can then be washed to remove unbound DNA and placed against film. Incorporation of radioactivity can thus be detected and visualised.

Membranes were soaked in 3xSSC, transferred into hybridisation bottles containing 3ml of hybridisation solution (**Table 2.1**) (pre-heated to 58^{o}C) and pre-hybridised for 5 minutes at 58^{o}C in a Mini 10 Hybridisation oven [Thermohybaid (Ashford, UK)]. The hybridisation solution was discarded, an additional 3ml of fresh solution and 20µl (20-fold excess) of unlabelled competitor ASO were added and the bottle was placed back

in the oven for an additional 5 minutes. Following the addition of the labelled ASO (see section 2.15.3) hybridisation was carried out at 53^{o}C for at least 2 hours (2 hours–overnight). Membrane was washed twice with 3ml of TMAC wash solution (**Table 2.1**) for 5 minutes at 56^{o}C followed by a final 10 minutes wash with 4ml of TMAC wash solution. Membranes were rinsed with 3xSSC and washed in a tray containing 3xSSC. To remove any excess liquid, membranes were blotted with Whatman 3MM paper and placed against film. To prevent drying, membranes were sealed in cling film. Hybridisation patterns were visualised by autoradiography using Fuji RX 100 or Kodak BIOMAX XAR film and Hypercassette autoradiographic cassettes [Autorads (Lutterworth, UK)] with intensifying screens. Films were exposed for 1 to 2 days at -80^{o}C depending on the strength of the signal.

To enable re-hybridisation with the other ASO, membranes were stripped by immersing in boiling 0.1xSSC, 0.1% (w/v) SDS for 5-10 minutes. The procedure was repeated if the radioactivity detected with a Geiger counter exceeded 5counts/second. Stripped membranes were placed against film to check for any remaining radioactivity. When no background signal was produced membranes were re-used or stored at 4^{o}C wrapped in cling film.

2.16 Sequencing.

DNA fragments were sequenced using an ABI PRISM BigDye^{TM} Terminator Cycle Sequencing Ready Reaction kit and an Applied Biosystems Model 377 DNA Sequencing System. Essentially, DNA fragments were PCR-amplified/fluorescently labelled in the forward or reverse direction, run vertically on a 5.35% (w/v) Longranger acrylamide gel followed by specialised sequence analysis computer software.

The sequencing reaction was prepared according to the manufacturer's protocol and included 20-40ng of PCR product, 3.2µM primer, 3µl Big Dye Terminator Ready reaction Mix in a total volume of 10µl. PCR conditions were: 5 minutes of denaturing at 96^{o}C, followed by 25 cycles of: 10 seconds of denaturing at 96^{o}C, 10 seconds of annealing at 50^{o}C and 4 minutes of elongation at 60^{o}C.

PCR products were purified by ethanol precipitation, dissolved in 3µl of 83% (v/v) de-ionised formamide in 8.3mM EDTA and denatured at 96^{o}C for 2 minutes before being loaded onto the sequencing gel. Fluorescently labelled DNA fragments were run on a 5.35% (w/v) Longranger acrylamide gel [10.8g Urea, 15.6ml distilled ultra-pure water, 3ml of 10xTBE, 3ml Longranger acrylamide, 21µl N′-Tetramethylethylene diamine (TEMED) and 150µl of 10xAPS (Ammonium persulfate)] for 7 hours at 1300Volts in an ABI Prism 377 DNA Sequencer.

Sequence data were analysed using Factura^{TM} Release 1.2.0 [Applied Biosystems, Warrington, UK)] and Autoassembler Release 1.4.0 on Apple Macintosh computers. Sequences were authenticated and confirmed by comparing against the appropriate DNA sequence found at http://www.ncbi.nlm.nih.gov/. **Figure 2.3** shows typical sequencing results.

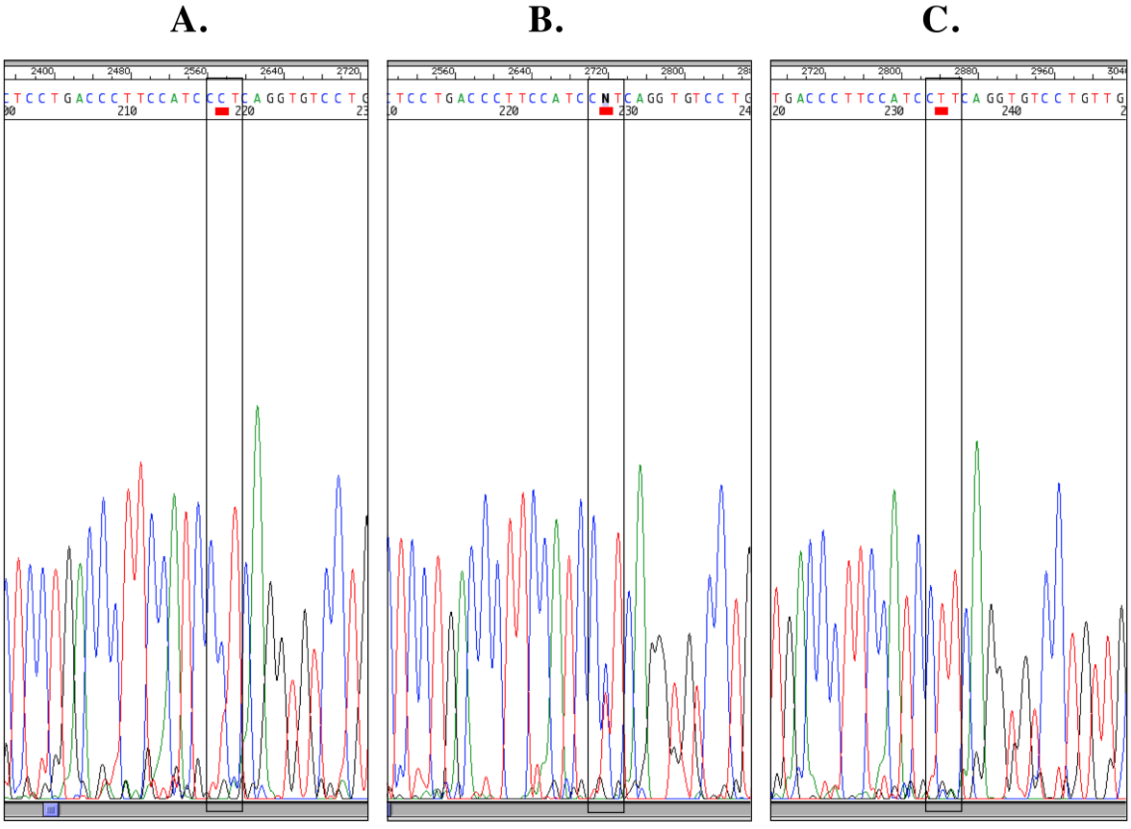

Figure 2.3: Typical sequencing results. DNA sequencing was performed to verify insertion of the correct PCR product (see section 2.10; probes in **Chapters 3** and **4**) and confirm RFLP/ASO results (**Chapter 5**). The figure shows the 3 possible genotypes (CC, TT, CT) for the TGFβ-1 C-509T polymorphism. Patient 'A' is homozygous for the C allele and patient 'C' is homozygous for the T allele. Patient 'B' is carrying one C allele and one T allele.

2.17 Total bone marrow and peripheral blood cell counts.

Bone marrow and peripheral blood (see section 2.2) were diluted in Isotone II and quantified using a Scharfe system Casy® 1 cell coulter counter. The system distinguishes different cell types on the basis of their size (µM in diameter). As seen in **Figure 2.4** cells with diameter greater than 6µM are classified as white bone marrow cells (WBMC) whereas cells with diameter less than 6µM are classified as mature (no nucleus) red bone marrow cells (RBMC).

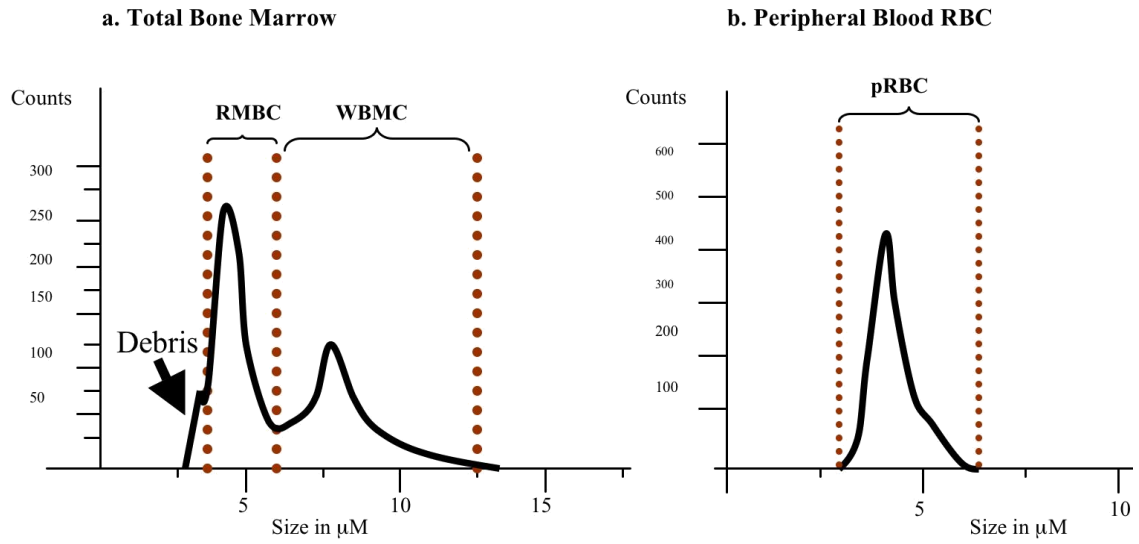

Figure 2.4: Total bone marrow and peripheral blood cell counter profiles. a) Two distinct peaks of: red bone marrow cells (3-6µM in diameter) and white bone marrow cells (>6µM in diameter), are seen in total bone marrow (anything smaller than 3µM was classified as debris and was not included in the counts). b) Peripheral blood profile showing a single peak of mature peripheral red blood cells (pRBC) (Figure obtained from Dr Jawad thesis, with permission).

2.18 Mouse flow cytometry analysis.

Biotinylated monoclonal antibodies and streptavidin coated magnetic beads were used to deplete mature (Lin^+) cells from total bone marrow. Lin^- bone marrow cells were then fluorescently labelled and analysed by Fluorescence Activated Cell Scanning (FACS). Biotinylated antibodies were purchased from BD Pharmingen (Oxford, UK) [foetal liver

kinase 2 (FLK-2) was purchased from eBiosciences (San Diego, USA)]. Streptavidin coated magnetic beads were purchased from Qiagen Ltd (Crawley, UK).

2.18.1 Preparation of magnetic beads.

BioMag® particles coated with streptavidin (5mg/ml) came stored in phosphate-buffered saline containing EDTA and 0.08% (w/v) sodium azide. According to the manufacture's notes, 1ml (5mg) of Streptavidin binds to >2μg of biotin/mg of particles. Beads were washed 3 times in PBS/BSA buffer by magnetic separation.

2.18.2 Immunomagnetic depletion of Lin^+ total bone marrow cells.

A cocktail of biotin-conjugated hamster/rat anti-mouse monoclonal antibodies was used in order to deplete lineage committed (Lin^+) mature bone marrow cells (**Table 2.4**). Following addition of total bone marrow to the cocktail, lineage committed (Lin^+) cells bind to the appropriated biotinylated antibodies which then subsequently bind to streptavidin coated magnetic beads. The complex can then be removed by the use of a magnet.

Table 2.4

Antibody	Conjugates to
CD3	Thymocytes, T lymphocytes, NK T-cells
CD45	B-Lymphocytes
Ter119	Erythrocytes
Ly-6G (and Ly-6C)	Monocytes
Cd11b (Mac-1α)	Macrophage, granulocytes and NK cells

Table 2.4: List of antibodies used to deplete mature Lin^+ bone marrow cells. In order to deplete progenitor cells the FLK-2 antibody was used.

Approximately 5-7 million of white bone marrow cells (see section 2.17 for quantification) were incubated at 4°C for 40 minutes whilst mixing in a polypropylene tube containing a cocktail of antibodies [6μg of all biotinylated antibodies (except for

Ter119 and FLK-2 in which 10μg and 7μg were used respectively) were diluted to a total of 5ml in PBS/BSA buffer]. Samples were pelleted (centrifuged at 1200rpm for 10 minutes at 4^{o}C) and re-suspended in fresh buffer to remove any excess of antibody.

Pre-washed streptavidin coated beads (0.3mg/million of WBMC) were added and the mix was incubated at 4^{o}C for 30 minutes whilst mixing gently. Tubes were placed against a magnet for 10 minutes and the supernatant was collected. Cells were pelleted (centrifuged at 1500rpm for 10 minutes at 4^{o}C), re-suspended in fresh buffer and placed against the magnet to ensure that all conjugated beads were removed. Lin^{-} cells were pelleted and analysed (see section 2.18.3).

2.18.3 Fluorescence activated cell scanning (FACS) analysis.

Lin^{-} cells were fluorescently labelled with either Fluroscein Isothiocyanate (FITC) or R-phycoerythrin (PE) rat anti-mouse monoclonal antibody conjugated to Sca-1, c-Kit, FLK-2 or MAC-1α. Lin^{-} cells were suspended in 200μl PBS/BSA and incubated for 30 minutes at 4^{o}C after addition of lμl of the appropriate isothiocyanate (FITC) anti-mouse (0.5μg/μl) and lμl of R-Phycoerythrin (R-PE) anti-mouse (0.2μg/μl) antibodies. Samples were pelleted (2000rpm for 5 minutes at 4^{o}C), re-suspended in 200μl of fresh PBS/BSA buffer and re-pelleted. The final pellet was re-suspended in 500μl of fresh PBS/BSA buffer and quantified by FACS using a Becton Dickson Facscan in conjunction with the Cell Quest pro computer package.

Chapter 3:

Haemopoietic stem cell frequency, and bone marrow and peripheral blood cellularity in (CBA/H x C57BL/6) F_2 intercross mice

3.1 Introduction.

As previously discussed (see section 1.6) haemopoiesis is tightly regulated. The continuous production of at least 8 separate mature blood lineages is reliant on the haemopoietic stem cell (HSC) compartment. A number of *in vitro* and *in vivo* studies have characterised and defined specific subpopulations within the HSC compartment that show different levels of maturation (e.g. stem cells and progenitor cells). The assays as well as the immature bone marrow cells they investigate have been reviewed in section 1.6.1.

Mouse models can provide the statistical power needed to identify the complex genetic determinants that influence the frequency of haemopoietic cells. A number of inbred strains show differences in their numbers of HSC or mature blood cells (Jawad *et al.*, 2007a). Quantitative Trait Loci (QTL) mapping can be employed to associate specific genomic regions (genotype) with specific cell frequencies (phenotype). This is made possible as inbred strains may differ in the sizes of polymorphic microsatellite markers, randomly repeated sequences found in the mouse genome. PCR-amplification of these regions can therefore reveal a strain-specific genetic signature. Analysis of F_2 intercross mice is ideal for QTL mapping as recombination events result in a relatively heterogeneous population. Thus, a phenotype can be linked to a specific genotype or to separate genomic regions that may act synergistically. Linkage of a phenotype to a QTL suggests that the gene(s) responsible for the specific trait lie within that genomic region and that inter-strain differences in those genes are responsible for the cell frequency variation. The approach allows mapping to relatively large intervals of 10-30cM, but the QTL region can be further refined using additional markers.

3.1.1 Haemopoietic stem cell (HSC) frequency QTL.

Müller-Sieburg and Riblet (1996) demonstrated differences in the HSC numbers of C57BL/6, BALB/c and DBA/2 recombinant mouse strains and identified three QTL influencing HSC frequency (Chromosome 1, *Scfr1* – 100cM; Chromosome 1, *Scfr2* – 50cM; Chromosome 18 – 32cM). De Haan and Van Zant (1997) made use of the same recombinant mouse strains and reported a similar QTL (Chromosome 18 – 19cM). The chromosome 1 (100cM) QTL was also reported by another independent study (Geiger *et al.*, 2001) which also identified additional QTL involved in HSC numbers (Chromosome 1 – 38cM; Chromosome 2 – 72cM; Chromosome 3 – 24cM; Chromosome 5 – 20cM; Chromosome 18 – 27cM; X chromosome – 51cM). Morrison *et al.* (2002) reported an additional QTL (Chromosome 17 – 20cM) and the list was further expanded by other studies (Chromosome 4 – 66-78.5cM; Chromosome 7 – 51-53cM; Henckaerts *et al.*, 2002 and 2004) (Chromosome 1 – 86.6cM; Chromosome 10 – 51-70cM; van Os *et al.*, 2006). There is little overlap between the QTL identified by the different studies which can be partly attributed to the different mouse strains and assays used. A list of QTL reported by those studies can be found in **Table 3.1**.

Table 3.1

Mouse Strain	Assay	Chromosome	Reference
(BXD)R1*	LTC-IC	1 (50cM) **1 (100cM)** 11 (32cM)	Müller-Sieburg and Riblet, 1996
(BXD)R1*	CAFC Day 35	**18 (19cM)**	de Haan and Van Zant 1997
(BXD)R1*	CAFC Day 35	1 (38cM) **1 (100cM)** **2 (72cM)** 3 (24cM) 5 (20cM) **18 (27cM)** X (51cM)	Geiger *et al.*, 2001
(AKR/JxC57BL/Thy-1.1) F_2	$L^-S^+K^+$ Thy-1.1^{lo}	17 (20cM)	Morrison *et al.*, 2002
(BXD)R1*	$L^-S^+K^+$	**2 (72.1-73cM)** 4 (66-78.5cM) 7 (51-53cM)	Henckaerts *et al.*, 2004
(C57BL/6xAKR) F_2	$L^-S^+K^+$	6 (51cM) 10 (51-70cM)	van Os *et al.*, 2006
(C57BL/6xAKR) F_2	CAFC Day 35	1 (86.6cM)	van Os *et al.*, 2006

Table 3.1: Reported haemopoietic stem cell (HSC) frequency QTL. QTL confirmed by different studies are given in bold. The assays used have been previously described (see section 1.6.1). *refers to (C57BL/6 x DBA) recombinant mice.

3.1.2 Target cell frequency QTL and haemopoietic malignancy susceptibility loci.

Interestingly, cell frequency QTL have been found to co-localise with haemopoietic malignancy susceptibility loci. The chromosome 1 QTL that determines the frequency of LTC-IC cells (~50cM; Müller-Sieburg and Riblet, 1996) (see section 1.6.1) (**Table 3.1**) is mapped to a very similar position with a susceptibility to pristane-induced plasmacytoma QTL (54cM; Mock *et al.*, 1993). Similarly, our group had previously mapped an r-AML susceptibility locus to distal chromosome 1 (~100cM) (Boulton *et al.*, 2003), a position previously reported to regulate the numbers of LTC-IC and CACF Day 35 cells (see section 1.6.1.2) (Müller-Sieburg and Riblet, 1996; Geiger *et al.*, 2001) (**Table 3.1**).

Combined, these studies suggest that increased numbers of specific haemopoietic cells might predispose to specific haemopoietic malignancies. For example r-AML develops following malignant transformation of immature bone marrow HSC (Warner *et al.*, 2004). The numbers of HSC are regulated by the chromosome 1 (100cM) QTL which was also identified as an r-AML susceptibility QTL (Boulton *et al.*, 2003). Higher numbers of those cells increase r-AML risk 2-3fold thus constituting target cell size as a risk factor in radiation-induced leukaemia (Boulton *et al.*, 2003). Identifying QTL that regulate the frequency of specific subpopulations within the immature HSC compartment and comparing them against malignancy-specific susceptibility loci might therefore improve the current understanding of the multistage process of radiation-induced leukaemogenesis.

3.1.3 Peripheral blood and bone marrow cell frequency QTL.

Similar to the HSC frequency, differences in the numbers of mature blood cells between various mouse strains have been exploited to identify possible QTL involved in the frequency of specific mature blood cells.

Chen and Harrison (2002) analysed the concentrations of circulating white bone marrow cells in a number of inbred strains and identified QTL involved in circulating levels of B lymphocytes B220 (Chromosome 1 – 63.1cM; Chromosome 1 – 48.4cM), T lymphocytes CD4 (Chromosome 8 – 73cM) and T lymphocytes CD8 (Chromosome 19 – 12cM). Other studies have investigated QTL in bone derived macrophages (Fijneman

et al., 2004) and platelet counts (Cheung *et al.*, 2004) confirming that such inter-strain variant phenotypes can be exploited to elucidate the genetic mechanisms of haemopoiesis.

3.1.4 Erythropoiesis.

The term erythropoiesis refers to the production of red blood cells, which are responsible for tissue oxygenation. Derived from pluripotent haemopoietic stem cells, the red blood cells (RBC) content of whole-blood (haematocrit) is tightly regulated. A reduction in RBC numbers will compromise oxygen carrying capacity resulting in anaemia, whereas increased RBC levels result in increased blood viscosity and have been associated with a wide range of diseases, including cardiovascular disease and hypertension (Lin *et al.*, 2005).

The process of erythropoiesis involves many genes with erythropoietin (*EPO*), erythropoietin receptor (*EPO-R*) and Janus Kinase 2 (*JAK2*) playing crucial roles in RBC production and maturation. EPO is released in the blood stream in response to tissue hypoxia and binds to EPO-R, expressed by the BM erythroid progenitors. This enables phosphorylation of JAK2 and activates further transduction signals, essential for erythrocyte cell proliferation, differentiation and viability (Tilbrook and Klinken, 1999).

The content of peripheral red blood cells (pRBC) has been used as a phenotype in a human study (Lin *et al.*, 2005) which identified a haematocrit QTL on chromosome 6q23-24. Similarly, haematocrit was used as a phenotype in a rat study and identified a QTL on chromosome 4 (Pravenec *et al.*, 1997). To this point, no mouse studies have investigated strain-specific variations in erythropoiesis which comes as a surprise, given the differences observed in the frequency of BM and peripheral blood cells in inbred mouse strains (Jawad *et al.*, 2007a).

3.1.5 Aims of the study.

This study was a collaborative effort within Dr Mark Plumb's group. The project was primarily driven by Dr Mays Jawad and also involved the participation of Dr Chris Talbot, Mrs Abigail Zanker, Dr Clare Cole, and Mr Simon Fitch. Erythroid/non-

erythroid (E/NE) bone marrow ratio data were available for 234 (CBA/H x C57BL/6) F_2 mice. E/NE bone marrow ratio and peripheral red blood cell (pRBC) counts were also available for CBA/H (n=37), C57BL/6 (n=19) and F_2 (n=22) mice.

At the beginning of this PhD, these numbers were supplemented with an additional group of 124 F_2 mice. This included tissue extraction (peripheral blood, bone marrow, spleen, and tail), DNA extraction, whole-genome genotyping using 133 polymorphic markers, and immunodepletion of Lin^+ bone marrow cells and subsequent FACS analysis of Lin^- cells labelled with Sca-1 and c-Kit. The QTL analysis included the following phenotypes: erythroid/non erythroid (E/NE) bone marrow ratio, peripheral red blood cell (pRBC) counts, spleen weight and Lin^- bone marrow cells according to expression of Sca-1 and c-Kit. The results and discussion will be presented in that order.

The aims of this study were to combine the genotype data with the aforementioned phenotypes in order to identify QTL that regulate them. The long term aim of this *in vivo* study is to identify possible candidate genes within those QTL and investigate possible differences between the two mouse strains.

3.2 Materials and methods.

3.2.1 Mice, irradiation and tissue extraction.

Adult (2-5 month old) CBA/H, C57BL/6, (CBA/H x C57BL/6) F_1 and (CBA/H x C57BL/6) F_2 (see section 2.1.6) mice were used in this study. Irradiated mice were exposed to 3Gy X-rays (0.5Gy/min) (see section 2.1.6.1) and sacrificed at 48 hours post-irradiation by cervical dislocation.

Total BM was flushed from mouse femurs; blood was taken by cardiac puncture; spleen and tail were also collected (see section 2.2). Tail DNA was used for the genetic analyses (see section 2.3).

3.2.2 Peripheral red blood cell (pRBC) and white bone marrow cell (WBMC) counts.

Peripheral blood was diluted with isotone II (dilution factor: 1 in 800,000), total bone marrow was diluted in PBS/BSA (**Table 2.1**) and isotone II (dilution factor: 1 in 2,000). Both were quantified using a Scharfe system Casy® 1 cell coulter counter (see section 2.17). Total bone marrow samples were also manually quantified by Haematoxylin/Eosin stained BM cytospin preparations (see section 2.5).

3.2.3 Genetic analysis.

Tail DNA from the 124 (CBA/H x C57BL/6) F_2 mice was genotyped using 133 polymorphic microsatellite markers (**Appendix 1**) spanning the whole mouse genome at 15-20cM intervals. Genotyping was as previously described (sections 2.1.4 and 2.12; Boulton *et al.*, 2003).

Lin^- BM cells from the 124 F_2 mice were analysed by flow cytometry for Sca-1 and c-Kit expression. The procedures for immunomagnetic depletion of Lin^+ BM cells and the downstream labelling of Lin^- cells, as well as mature red blood cell depletion have been described (see section 2.18).

The genotype/phenotype data for each of the F_2 mice were analysed by composite interval mapping using Windows QTL cartographer Version 2.5 (Wang *et al.*, 2001-2004). Significance linkage levels were calculated by permuting the data 10,000 times and interpreted as determined by Lander and Kruglyak (1995) according to whom: suggestive linkage: LOD>2.5, significant linkage: LOD>3.5, and highly significant linkage: LOD>5.8 (QTL analysis was performed by Drs Mays Jawad and Chris Talbot).

The 713bp fragment of the *EPO* promoter region (-613 to +100 nucleotides from the ATG start site) was sequenced using primers 5′- GAG CAC AAG GCA GGA GAG AG -3′ (forward primer) and 5′- ATG CAG CCC TAG CTT CAG G -3′ (reverse primer). Southern blot analysis of *EPO* and *EPO-R* genes was performed using cDNA probes available in the lab and restriction digests of genomic CBA/H and C57BL/6 mice.

3.3 Results.

3.3.1 pRBC and WBMC counts.

Peripheral blood and total bone marrow were initially analysed using a Scharfe system Casy® 1 cell coulter counter. As previously discussed (see section 2.17), the system distinguishes different cell types on the basis of their size (μM in diameter). As seen in **Figure 3.1**, cells with diameter greater than 6μM are classified as white bone marrow cells (WBMC) whereas cells with diameter less than 6μM are classified as mature (no nucleus) red bone marrow cells (RBMC). The efficiency of this method is illustrated in **Figure 3.1**. The profile of peripheral blood reveals a single peak of red blood cells (<6μM in diameter, **Figure 3.1a**). Total BM reveals two discreet peaks (**Figure 3.1b**); white bone marrow cells (WBMC) with a diameter >6μM and red bone marrow blood cells (RBMC) with a diameter <6μM. Immunomagnetic depletion of red blood cells (i.e. terminally differentiated erythrocytes and normoblasts) was achieved through the use of biotinylated anti-Ter119 antibody (see section 2.18) and resulted in a single peak (>6μM in diameter, **Figure 3.1c**) of WBMC. A small proportion of cells remained in the <6 μM peak which was however less that 1% of the total. In contrast, exposure of mice to an acute dose of 3Gy X-rays resulted in depletion of WBMC and a single peak of RBMC (<6μM in diameter, **Figure 3.1d**). Exposure to such doses kills 80-90% of enucleated BM cells but has no effect on red blood cell counts (**Figure 2.1c**). These suggested that this method could sufficiently discriminate between most red and white blood cells.

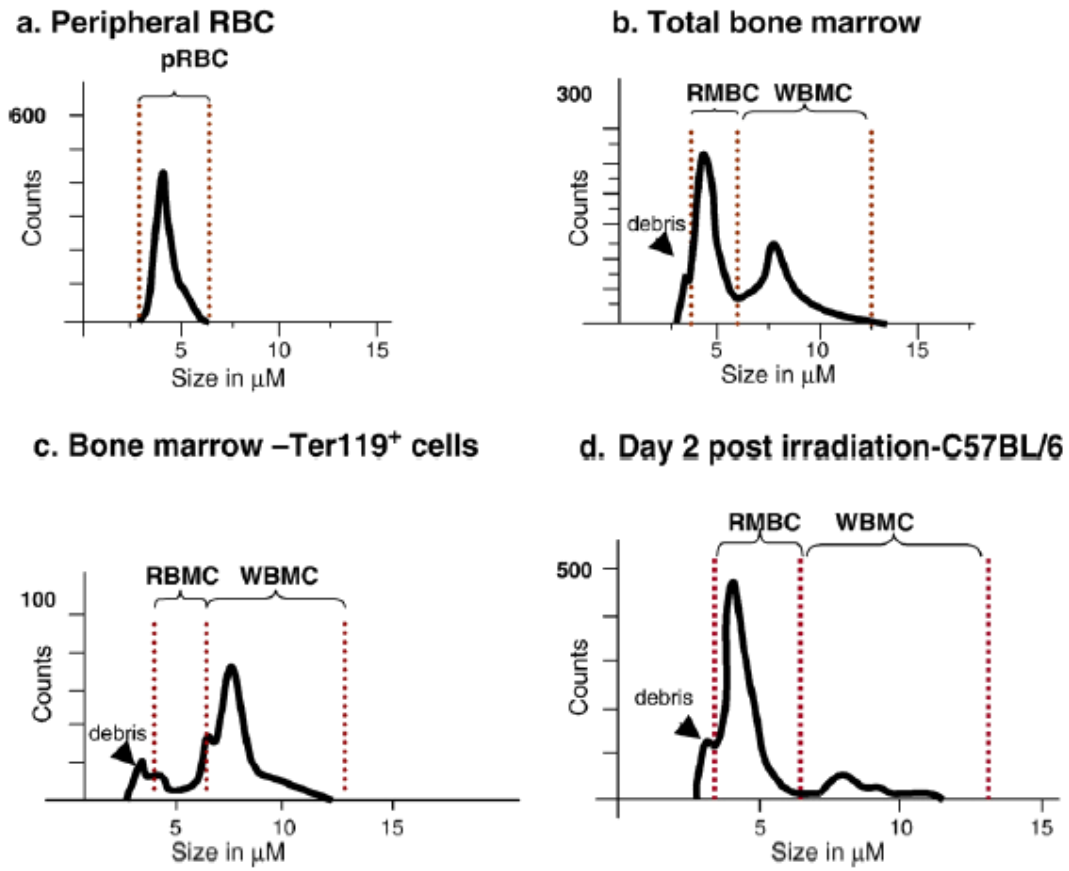

Figure 3.1: Casy coulter counter profiles of: (a) peripheral blood showing a single peak or red blood cells (3-6µM in diameter) and (b) total bone marrow showing two distinct peaks of red blood cells and white bone marrow cells (3-6µM and >6µM in diameter, respectively). The efficiency of this method was validated by (c) immunomagnetic depletion of RBMC and (d) depletion of WBMC by means of acute irradiation with 3Gy X-rays. Anything smaller that 3µM was considered debris and was not included in the analysis.

Differences in the number of normoblasts between the two mouse strains were investigated by cytospin analysis (see section 2.5) of Haematoxylin/Eosin stained bone marrow. Normoblasts are the immediate precursors of erythrocytes and can sometimes be found in the >6µM peak. There was no difference between the numbers of those small enucleated cells suggesting that any inter-strain variation was a result of differences in the numbers of either the WBMC or the erythrocytes.

3.3.2 Statistical analysis.

The following phenotypes were considered: White bone marrow cell counts (WBMC), red bone marrow cell counts (RBMC), peripheral red blood cells (pRBC) and spleen weight.

Table 3.2 summarises the results. There was no statistically significant difference in the number of white (non-erythroid) bone marrow cells between the two mouse strains (p=0.47, t-test). There was however a statistically significant difference in the numbers of RBMC (p=0.0002, Kruskal-Wallis test), peripheral RBC (p=0.0009, Kruskal-Wallis test) and spleen weight (p=0.018, Kruskal-Wallis test). C57BL/6 mice have lower numbers of red bone marrow cells but higher numbers of peripheral red blood cells, compared to the CBA/H mice. Total bone marrow cellularity was also expressed as the ratio of erythroid/non-erythroid (E/NE) cells to correct for possible day-to-day variations in the efficiency of bone marrow harvesting. The E/NE ratio was also different between the two mouse strains (p=0.0001, Kruskal-Wallis test).

Table 3.2

Mouse strain	Non-Erythroid (x 10^6/2 femurs)	Erythroid (x 10^6/2 femurs)	E/NE ratio	pRBC (x 10^6/μl)	Spleen weight (mg)
CBA/H (n=37)	30.85±0.36	24.5±0.86	0.79±0.03	6.63±0.22	85.3±2.2
C57BL/6 (n=19)	32.29±0.33	19.4±0.65	0.61±0.02	7.89±0.23	94.2±2.8
F_1 (n=22)	N/A	N/A	0.77±0.03	6.72±0.63	N/A
F_2	N/A	N/A	0.74±0.22 (n=348)	7.31±0.12 (n=144)	100.3±1.9 (n=113)
Female F_2	N/A	N/A	0.82±0.24 (n=156)	7.53±0.11 (n=65)	102.4±3.2 (n=56)
Male F_2	N/A	N/A	0.69±0.2 (n=192)	7.13±0.12 (n=79)	98.2±2.1 (n=57)

Table 3.2: Phenotypes of parental, F_1 and F_2 mice with SEM for non-erythroid and erythroid bone marrow cells, peripheral red blood cells and spleen weight. The table contains data pooled from the lab.

Previous F_1 data suggested that higher red bone marrow cell counts is a dominant CBA/H trait, as the E/NE ratio of F_1 mice was not statistically different to that of

CBA/H but statistically different to that of C57BL/6 (p=0.92 and p=0.0075 respectively, Kruskal-Wallis test). The E/NE ratio was strongly influenced by sex (p=4 x 10^{-8}, t-test) with females showing higher numbers of RBMC (also reflected in their E/NE ratio), whereas pRBC counts and spleen weight were not (p=0.064 and p=0.29 respectively, t-test). There were no age-dependent effects noted for either the spleen weight or the E/NE ratio. Peripheral red blood cells declined with age (r=-0.41, p<0.01).

3.3.3 QTL mapping of E/NE ratio.

A total of 358 F_2 adult mice were included in this analysis. These included previous data from the lab, along with the new group of 124 F_2 mice. Composite interval mapping for the E/NE ratio of all F_2 mice revealed two QTL with LOD Scores of 4.5 (Chromosome 5 - >75cM) and 6.3 (Chromosome X - >65cM). These showed higher than the significant linkage LOD>3.5 as determined by Lander and Kruglyak (1995). Three additional QTL (Chromosome 10 - 14-43cM, LOD 2.7; Chromosome 15 - >47cM, LOD 2.8; Chromosome X - 0-27cM, LOD 2.8) showed suggestive linkage (LOD>2.5).

Along with the observation that female F_2 mice show higher numbers of red bone marrow cells, the identification of two chromosome X loci provided evidence that sex is influencing the E/NE ratio. QTL analysis was therefore restricted to either male (n=192) or female F_2 (n=156) mice. Additional QTL were identified, presumably masked by sex effects in the first (n=358) QTL mapping. The female F_2 analysis revealed a single significant QTL (Chromosome 11 - 25-31cM, LOD 4.4). Analysis of the F_2 males identified an additional significant QTL (Chromosome 5 - 44-61cM, LOD 3.5) and a suggestive QTL (Chromosome 9 - 0-9cM, LOD 2.7). As expected, separate analysis of the F_2 males and females revealed QTL that influenced RBMC counts within the male and/or female populations.

Further analysis was performed in all F_2 mice, using sex as a covariate. This removed the sex effect and revealed a new significant QTL (Chromosome 19 - >31cM, LOD 4.3). As expected, the significant X chromosome QTL was abolished. The suggestive QTL on chromosomes 10 and 15 were also abolished. However, the chromosome 5 QTL (LOD 4.5) was still present and in agreement with the previous (all mice,

unadjusted for sex) analysis. **Table 3.3** summarises all significant QTL that were identified. **Figure 3.2** shows the linkage plots of the significant E/NE bone marrow ratio QTL.

Table 3.3

Group	QTL peak	Peak LOD	Human orthology	Increaser allele	Dominant allele
F_2 (n=361)	Chromosome 5, 78cM (75-Telomere)	4.5	7q22.1	C57BL/6	CBA/H
	Chromosome X, 69cM (69-Telomere)	6.3	Xp22.2	CBA/H	C57BL/6
F_2 male (n=192)	Chromosome 5, 57cM (44-61cM)	3.5	4q21.2	C57BL/6	C57BL/6
F_2 female (n=156)	Chromosome 11, 30cM (25-32cM)	4.4	5q33	CBA/H	CBA/H
F_2 – sex (n=361)	Chromosome 5, 78cM (75-Telomere)	4.5	7q22.1	C57BL/6	CBA/H
	Chromosome 19, 42cM (42-Telomere)	4.3	10q24	C57BL/6	C57BL/6

Table 3.3: Significant QTL influencing the E/NE bone marrow ratio in the F_2 mice. 'F_2 - sex' refers to the analysis in which sex was used as covariate. Human chromosome orthology, and the dominant and increaser alleles (i.e. strain allele that increases the phenotype) are also shown.

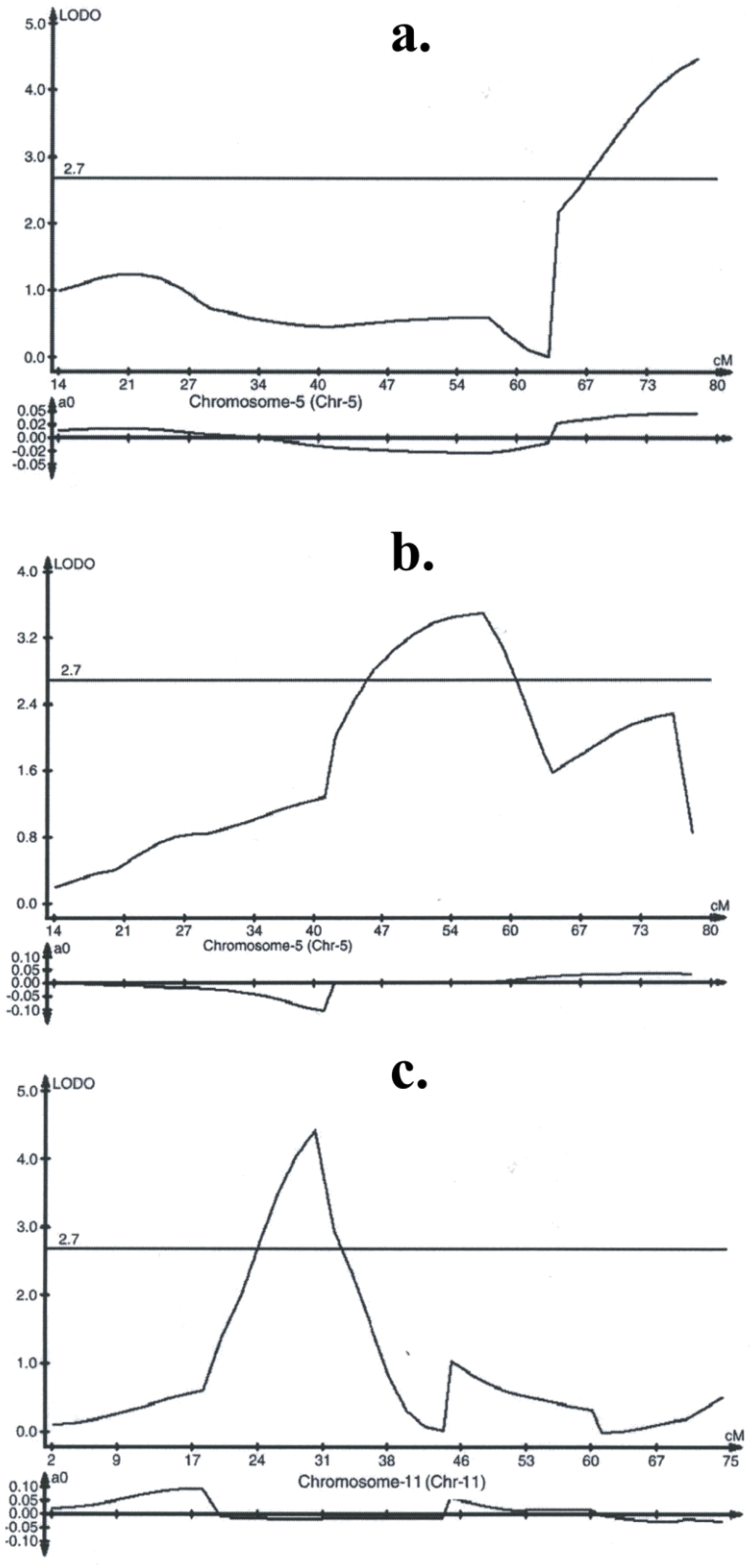

Figure 3.2: Linkage plots of significant E/NE bone marrow ratio QTL: (a) Chromosome 5 (78cM, LOD 4.5), (b) Chromosome 5 (57cM, LOD 3.5), and (c) Chromosome 11 (30cM, LOD 4.4). The LOD Score is seen on the Y axis and the Chromosomal distance (cM) on the X axis. Bottom graphs determine the increaser allele where: >0 then increaser allele is C57BL/6 and <0 increaser allele is CBA/H.

3.3.3.1 E/NE bone marrow ratio candidate genes.

Erythropoietin (*EPO*) and its receptor (*EPO-R*) are important genes involved in erythropoiesis (see section 3.1.4). Significantly, *EPO* lies within one of the E/NE bone marrow ratio QTL (peak of chromosome 5 QTL, LOD 4.5). Although the locus contains 325 known genes erythropoietin was the most obvious candidate gene. Similarly, the erythropoietic receptor gene lies within the suggestive male specific E/NE bone marrow ratio QTL (Chromosome 9 QTL, LOD 2.7). Any strain-specific variation in either of these genes could account for the observed differences in the E/NE bone marrow ratio between the parental strains.

The genomic DNA and cDNA of both genes was sequenced (Dr Mays Jawad) but no strain-specific polymorphisms were found between the CBA/H and C57BL/6 parental strains. Analysis was further expanded to include the promoter regions of both genes, but failed to identify any sequence variation between the two mouse strains. Southern blot analysis of restricted genomic DNA did not reveal any copy number variation between the CBA/H and C57BL/6 stains in either gene (data not shown).

3.3.4 QTL mapping of peripheral red blood cell (pRBC) counts.

This analysis included the 124 F_2 mice group. Peripheral red blood counts were used as the phenotype to map the corresponding QTL. As seen from **Table 3.2** C57BL/6 mice showed increased numbers of peripheral RBC (p=0.0009, Kruskal-Wallis test) compared to the CBA/H mice. pRBC counts were not found to be influenced by sex (p=0.064, t-test) but declined with age (r=-0.41, p<0.01). Additionally, there was no statistically significant correlation between pRBC counts and the E/NE bone marrow ratio (r=0.08). As pRBC counts are dependant on both spleen and BM this suggested that erythrocyte production is regulated by different loci in the two haemopoietic tissues.

QTL analysis of pRBC revealed one significant QTL (Chromosome 4 - 32.2-48.2cM, LOD 4.0) and one suggestive QTL (Chromosome X - >57cM, LOD 3.3). The chromosome 4 QTL was also identified in another mouse strain by QTL analysis of the genotype data of the AXA/BXA recombinant inbred strains (Williams *et al.*, 2001). The analysis revealed two highly significant QTL (Chromosome 4 - 38-44.6cM, LOD 7.5;

Chromosome 16 - 57-66cM, LOD 6.0) and one significant QTL (Chromosome 1 - 56-59.5cM, LOD 4.9). The chromosome 1 and 16 QTL might not segregate in the CBA/H x C57BL/6 cross and this could explain why they were not identified in the analysis of the 124 F_2 mice. The results of both analyses are summarised in **Table 3.4** and the linkage plots of significant QTL are shown in **Figure 3.3**.

Table 3.4

Cross	QTL peak	Peak LOD	Human orthology	Increaser allele	Dominant allele
CBA/H x C57BL/6 (n=124)	Chromosome 4, 31.9cM (32.2-48.2cM)	4.0	9p22	CBA/H	C57BL/6
	Chromosome X, 69cM (57-Telomere)	3.3	Xp22	C57BL/6	C57BL/6
A/J x C57BL/6 29 RI lines (~8 mice/line)	Chromosome 4, 40cM (38.0-44.6cM)	7.5	9p22	C57BL/6	N/A
	Chromosome 1, 58.5cM (56-59.5cM)	4.9	2q37	A/J	N/A
	Chromosome 16, 59.9cM (57-66cM)	6.0	21q21	C57BL/6	N/A

Table 3.4: Significant QTL influencing the peripheral red blood cell counts in the 124 (CBA/H x C57BL/6) and (A/J x C57BL/6) mice. Human chromosome orthology, and the dominant and increaser alleles (i.e. strain allele that increases the phenotype) are also shown.

There was only one overlapping QTL for the pRBC and E/NE bone marrow ratio suggesting that the underlying genetic differences in the two phenotypes are largely independent and emphasising the role of spleen in peripheral blood erythropoiesis. A subsequent QTL analysis using sex as a covariate abolished the chromosome X QTL but not the chromosome 4 QTL and revealed no additional QTL. The common chromosome X QTL may represent a common sex-specific genetic effect. Interestingly, the pRBC and the E/NE are not correlated (r=0.08) and there is no statistically significant sex influence on the pRBC counts (p=0.064). The increaser alleles are different for the two traits (E/NE bone marrow ratio increaser allele: CBA.H, **Table 3.3**; pRBC increaser allele C57BL/6, **Table 3.4**) which raises the possibility of a sex-specific pleiotropic locus (i.e. a single locus producing different phenotypes in BM and spleen).

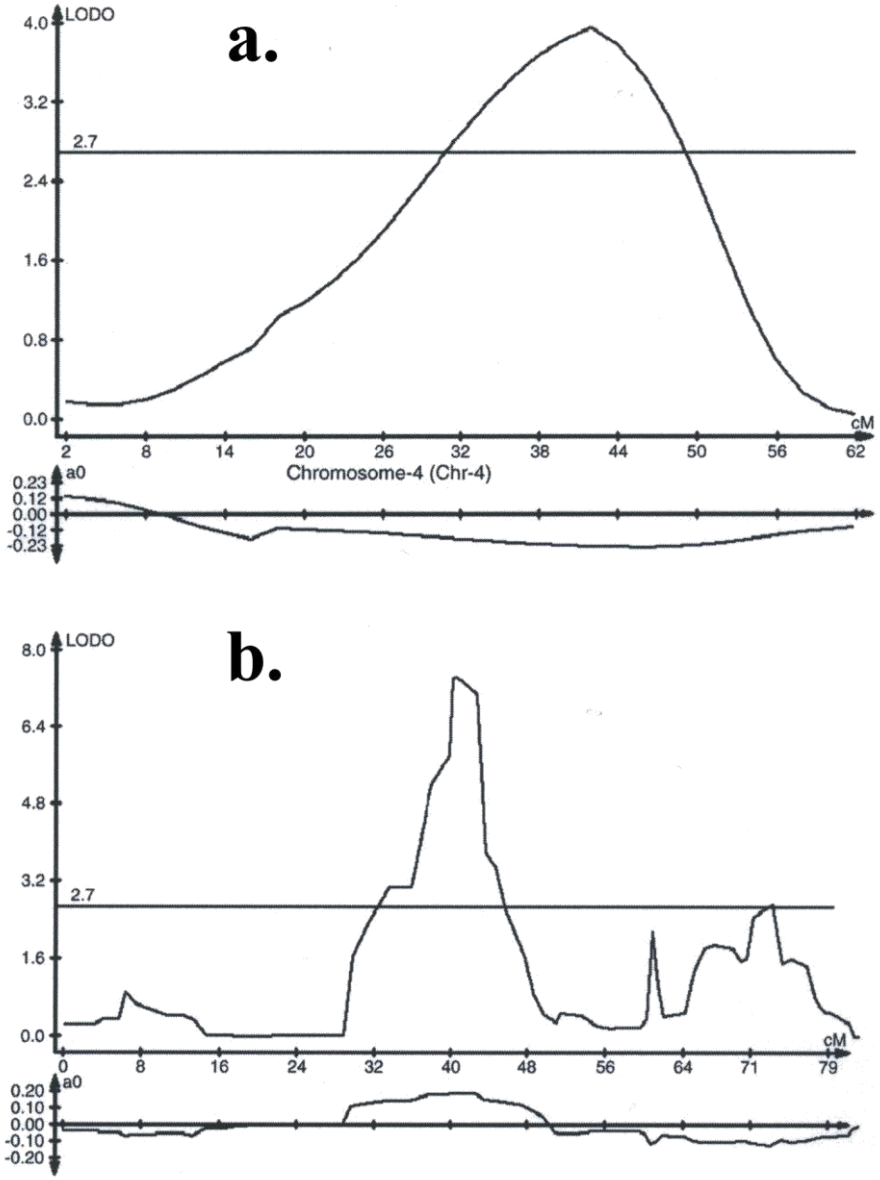

Figure 3.3: Linkage plots of significant pRBC QTL: (a) Chromosome 4 (LOD 4) QTL in the group of 124 (CBA/H x C57BL/6) F_2 mice, and (b) Chromosome 4 (LOD 7.5) in AXB/BXA mice. The LOD Score is seen on the Y axis and the Chromosomal distance (cM) on the X axis. Bottom graphs determine the increaser allele where: >0 then increaser allele is C57BL/6 and <0 increaser allele is CBA/H.

3.3.5 QTL mapping of spleen weight.

The E/NE bone marrow ratio and pRBC QTL analyses emphasised the role of spleen in peripheral erythropoiesis. Spleen weight was therefore used as a possible surrogate for

peripheral red blood cell production in the 124 F_2 mice. QTL analysis using spleen weight as the phenotype revealed three suggestive QTL (Chromosome 3 - 27-44cM, LOD 3.0; Chromosome 15 - 20-38cM, LOD 3.1; Chromosome 17 - 15-34cM, LOD 3.5) (**Figure 3.4**). The chromosome 17 QTL overlaps with a reported spleen weight QTL (Rocha *et al.*, 2004) but none of the three spleen weight QTL overlapped with any pRBC QTL, suggesting that spleen weight is not an appropriate surrogate for peripheral red blood cell production.

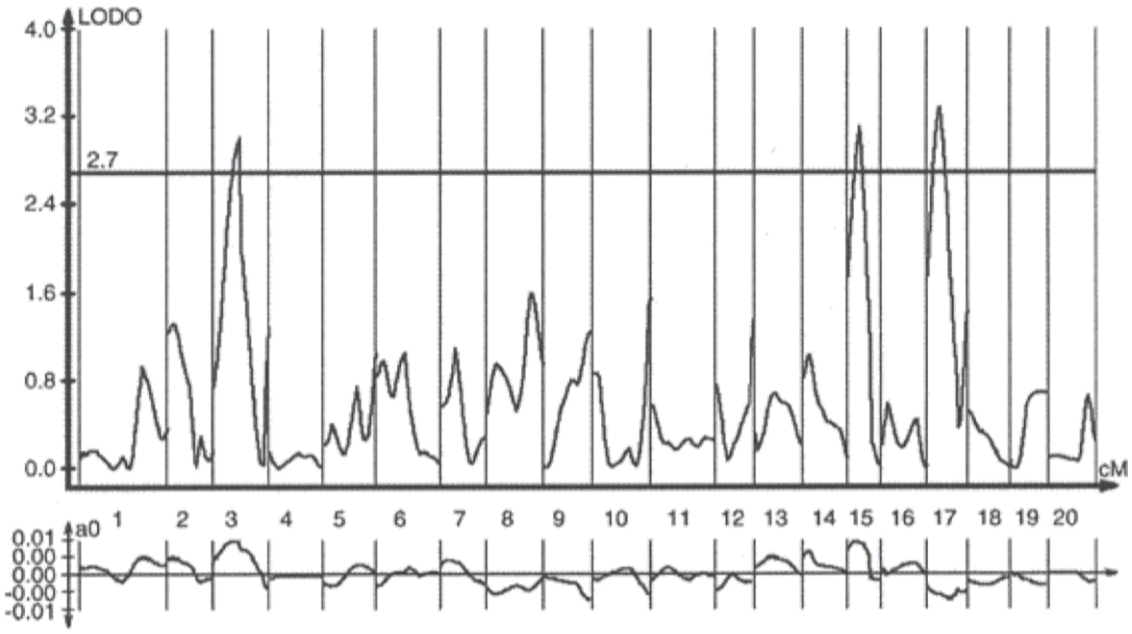

Figure 3.4: Linkage plots of suggestive spleen weight QTL. The LOD Score is seen on the Y axis and the chromosome on the X axis. Bottom graphs determine the increaser allele where: >0 then increaser allele is C57BL/6 and <0 increaser allele is CBA/H. A higher spleen weight was identified as a C57BL/6 dominant trait.

3.3.6 QTL mapping of Lin^- $Sca\text{-}1^+$ $c\text{-}Kit^+$ bone marrow cells.

As previously discussed (see section 1.6) the haemopoietic stem cell (HSC) compartment is comprised of immature cells defined as Lin^-. This contains both the stem and progenitor cells that give rise to all lineages of mature blood types. The expression of specific cell surface antigens such as Sca-1 and c-Kit has been used to phenotypically define these cell populations (see section 1.6.1.3). Previous work in the

lab had revealed a statistically significant difference in the frequency of $L^-S^+K^+$ cells between the two mouse strains with the CBA/H mice having an approximately four-fold-higher frequency of $L^-S^+K^+$ cells (**Figure 3.5**).

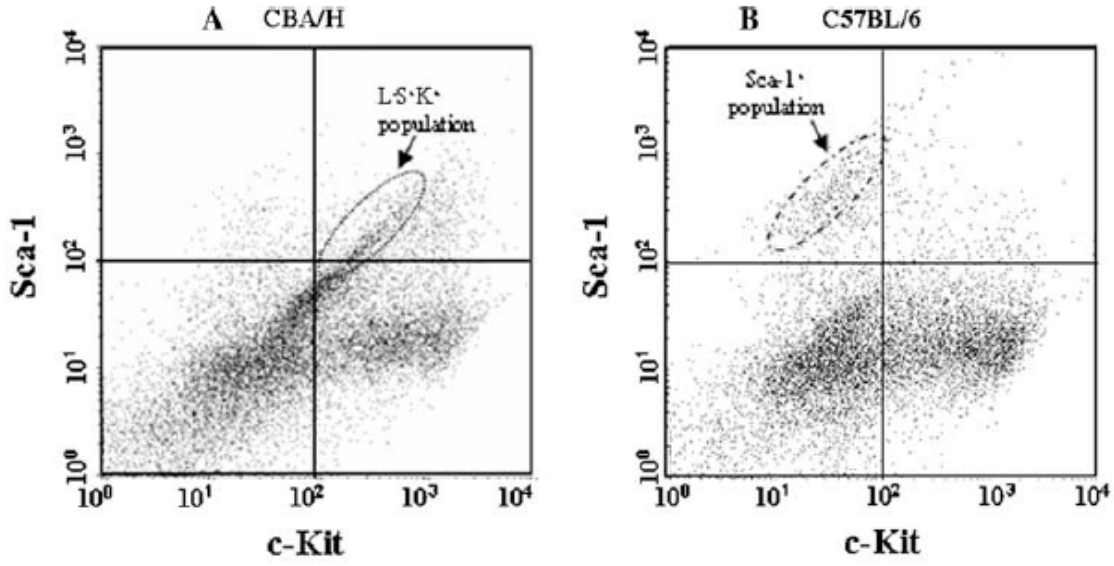

Figure 3.5: Flow cytogram of Lin^- bone marrow cells labelled with anti Sca-1 (S) and anti-c-Kit (K) antibodies in the CBA/H (A) and C57BL/6 (B) mouse strains. The population of $L^-S^+K^+$ cells that distinguish CBA/H from C57BL/6 mice is seen in the R1 (A) region ($L^-S^+K^+$ population).

In order to map QTL that influence the frequency of these Lin^- subpopulations of cells, Lin^- cells were quantified according to their intensity of Sca-1 and c-Kit labelling in the 124 F_2 mice group. Total BM was depleted of Lin^+ cells, the remaining Lin^- cells (~3% of total bone marrow) were labelled with the appropriate antibodies and visualised by flow cytometry (see section 2.18). Tail DNA from the F_2 group was genotyped using 133 polymorphic microsatellite markers (see section 3.2.3) spanning the whole mouse genome at 15-20cM intervals. The cell frequency (phenotype) and DNA genotypes were analysed by composite interval mapping using Windows QTL cartographer Version 2.5 (see section 3.2.3).

In the analysis of the flow cytograms, and as seen from **Figure 3.6 (A)**, unlabelled Lin^- cells were constrained within the 30x30 lower left region. In order to estimate background fluorescence outside this region, Lin^- cells were single labelled with R-PE anti-mouse c-Kit and FITC anti-Sca-1 antibodies (**Figure 3.6 B** and **C** respectively). This showed that background fluorescence outside the 30x30 region was less that 3%.

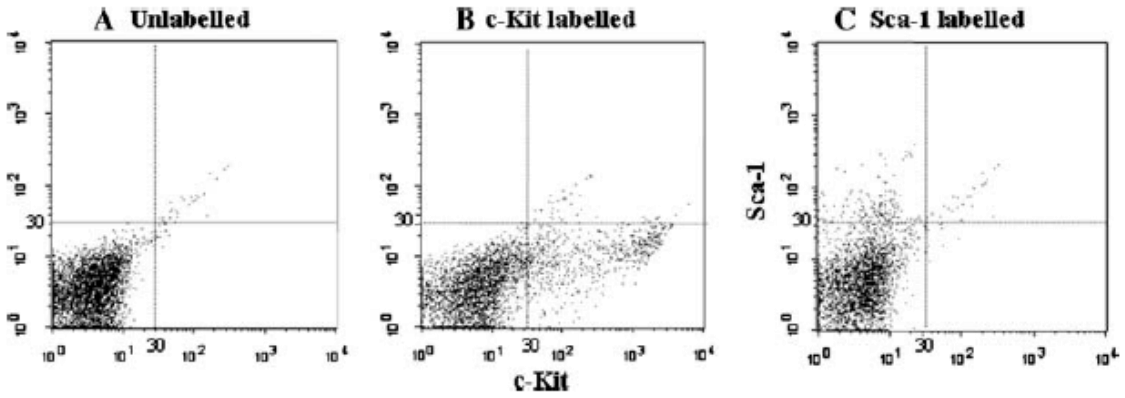

Figure 3.6: Flow cytograms of unlabelled Lin^- cells (A), single c-Kit labelled Lin^- cells (B), and single labelled Sca-1 Lin^- cells (C). Background fluorescence and autofluorescence events outside the 30x30 region were less that 3%.

For convenience, the flow cytograms were split into 9 areas defined by the relative fluorescence intensity (- for negative or unlabelled cells, + for intermediate labelling, or ++ for high labelling) (**Figure 3.7**). This enabled quantification of Lin^- $Sca\text{-}1^+$ $c\text{-}Kit^+$ cells (found in the R1 region).

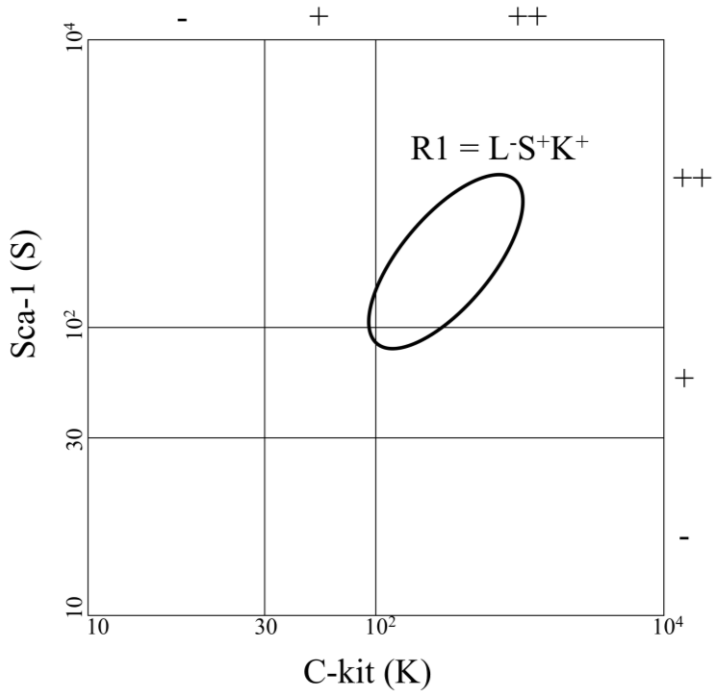

Figure 3.7: Defining the $L^-S^+K^+$ cells on the flow cytogram.

Different areas of the flow cytograms were investigated in order to map QTL that control the frequency of specific subpopulations of Lin^- cells (e.g. $L^-S^-K^-$ cells are found in the 30 x 30 region whereas $L^-S^+K^+$ R1 are within the R1 region in **Figure 3.7** (also in **Figure 3.5** and **Figure 3.6**).

One significant QTL (Chromosome 17 - 11-22.6cM, LOD 4.6) and one suggestive (Chromosome 19 - 22-Telomere, LOD 2.7) that influence the frequency of $L^-S^-K^-$ cells were found. A significant QTL (Chromosome 15 - 23.2-42.9cM, LOD 3.7) and a suggestive QTL (Chromosome 17 - 10.7-22.9cM, LOD 3.1) were found for the intensely (++) labelled L^-S^{++} cells ($y>10^2$ in **Figure 3.7**) whereas no QTL were identified for the L^-K^+ ($x>30$ in **Figure 3.7**).

Four suggestive and one significant QTL were found to determine the frequency of the $L^-S^+K^+$ R1 cells (Chromosome 6 - 25.6-31.1, LOD 3.0; Chromosome 6 - 45.9-56, LOD 2.6; Chromosome 10 - 32.4-50.4cM, LOD 3.5; Chromosome 17 - Telomere-16.5, LOD 3.2; Chromosome 18 - 7-21cM, LOD 2.8). Further QTL (multiple-interval mapping; Dr Chris Talbot) analysis revealed an additional suggestive QTL on chromosome 1 at 62cM (epistatic effect with the chromosome 17 QTL). The results are summarised in **Table 3.5** and LOD plots can be found in **Figure 3.8**.

Table 3.5				
FACS area	**QTL peak**	**Peak LOD**	**Increaser allele**	**Dominant allele**
	Chromosome 17, 18.4cM (11-26.6cM)	4.6	CBA/H	Additive effect
	Chromosome 19, 46cM (22-Telomere)	2.7	CBA/H	C57BL/6
	Chromosome 15, 37.6cM (23.2-42.9cM)	3.7	C57BL/6	C57BL/6
	Chromosome 17, 16.5cM (10.7-22.9cM)	3.1	CBA/H	Additive effect
	Chromosome 6, 29.9cM (25.6-31.1cM)	3.0	CBA/H	CBA/H
	Chromosome 6, 48cM (45.9-56cM)	2.6	C57BL/6	Additive effect
	Chromosome 10, 41.5cM (32.4-50.4)	3.5	CBA/H	CBA/H
	Chromosome 17, 6.4cM (Telomere-16.5cM)	3.2	CBA/H	Additive effect
	Chromosome 18, 13.1cM (7-21cM)	2.8	CBA/H	C57BL/6

Table 3.5: Summary of suggestive (LOD>2.5) and significant (LOD>3.5) QTL influencing the frequency of $L^{-}S^{-}K^{-}$, $L^{-}S^{++}$ and $L^{-}S^{+}K^{+}$ R1 cells. Dominant and increaser (i.e. strain allele that increases the phenotype) alleles are also shown.

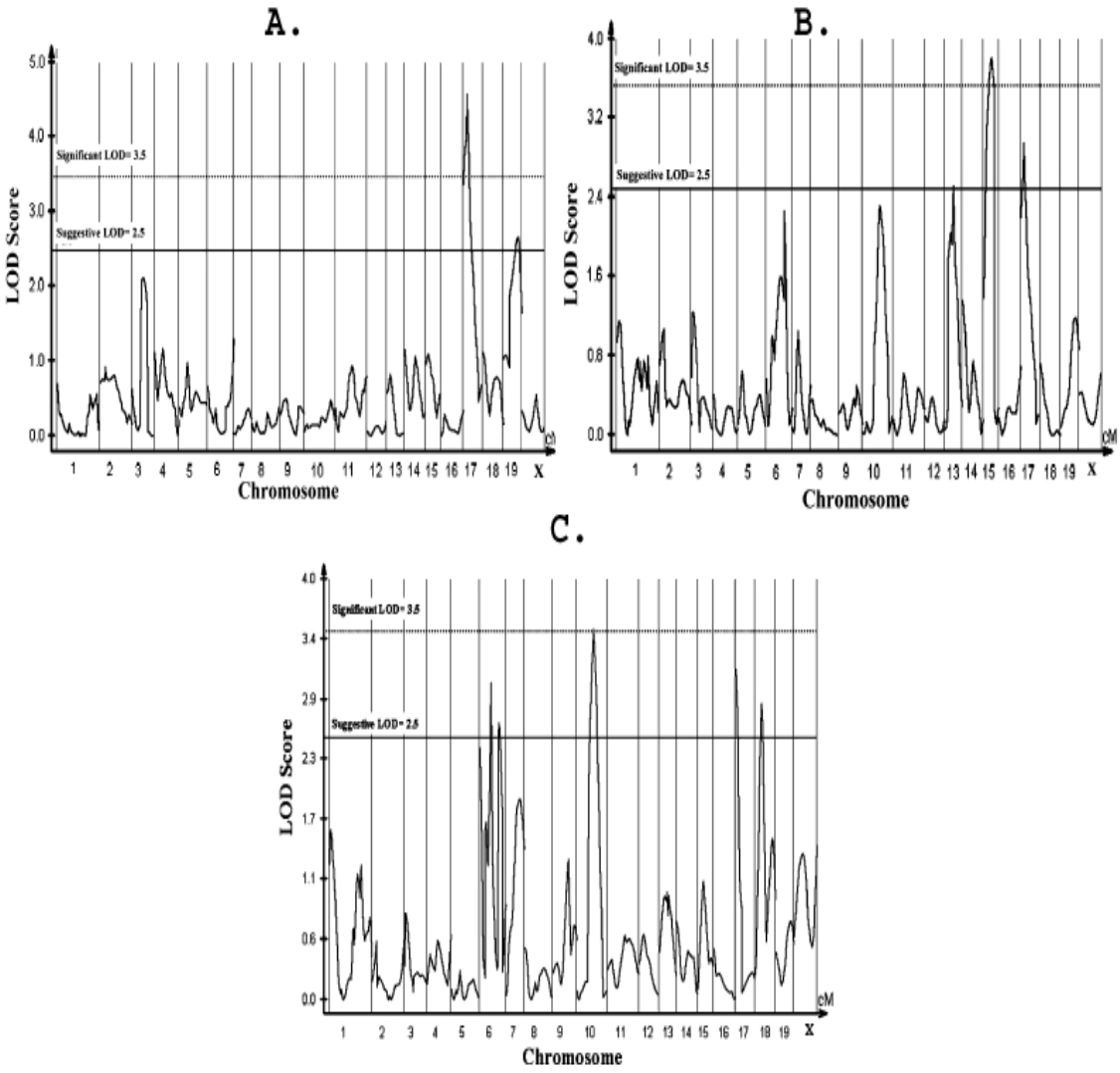

Figure 3.8: Linkage plots of suggestive (LOD>2.5) and significant (LOD>3.5) QTL influencing the frequency of $L^-S^-K^-$ (A), L^-S^{++} (B) and $L^-S^+K^+$ R1 (C) cells. The LOD Score is seen on the Y axis and the chromosome on the X axis.

3.3.7 Summary of results.

This chapter involved a series of analyses using a range of haemopoietic phenotypes in CBA/H, C57BL/6 and (CBA/H x C57BL/6) F_1 and F_2 mice. Data were already available in the lab and supplemented with data from an additional group of 124 F_2 mice. The study revealed that:

- There is no statistically significant difference in the number of white (non-erythroid) bone marrow cells between the two mouse strains or the numbers of normoblasts (immediate erythrocyte precursors) (**Table 3.2**).

- There is a statistically significant difference in the numbers of red bone marrow cells [also expressed as the erythroid/non erythroid (E/NE) bone marrow ratio], peripheral red blood cells (pRBC) and spleen weight between the two mouse strains. CBA/H showed higher numbers of RBMC but lower pRBC counts compared to C57BL/6 mice (**Table 3.2**).
- The E/NE ratio is strongly influenced by sex with females showing higher numbers of RBMC (also reflected in their E/NE ratio) whereas pRBC counts and spleen weight are not (**Table 3.2**).
- QTL analysis revealed one highly significant QTL, one significant QTL and three suggestive QTL influencing the E/NE ratio (**Table 3.3**; **Figure 3.2**).
- As females show higher numbers of RBMC, males and females were also separately analysed. One significant QTL was found for the female F_2 mice, one significant and one suggestive QTL were found for the male F_2 mice. These QTL presumably determine RBMC within the male or female populations (**Table 3.3**).
- When sex was used a covariate in the analysis, two significant QTL were found, which determine RBCM counts in a genotype-dependant/sex-independent fashion (**Table 3.3**).
- No sequence variation was found between the two strains in the Erythropoietin gene and its receptor (intronic regions, cDNA and promoter regions). Similarly no copy number variation was found. Both genes are located within QTL that were revealed by QTL analysis and were strong candidates for the differences in the E/NE ratio between the two mouse strains.
- One significant and one suggestive QTL were found to influence peripheral red blood cell (pRBC) counts. Three suggestive QTL were found to determine spleen weight but there was no overlap between the pRBC and spleen weight QTL suggesting that spleen weight is not informative as a surrogate for spleen erythropoiesis (**Table 3.4**; **Figures 3.3** and **3.4**).
- One significant QTL was found to influence the frequency of $L^-S^-K^-$ cells. One significant QTL was found to determine the frequency of intensely labelled L^-S^{++} cells whereas no QTL were identified for the L^-K^+ bone marrow cells. Four suggestive and one significant QTL were found to determine the frequency of the $L^-S^+K^+$ R1 cells. Further QTL analysis revealed an additional suggestive

QTL on chromosome 1 at 62cM (epistatic effect with the chromosome 17 QTL). (**Table 3.5**; **Figure 3.8**).

3.4 Discussion.

3.4.1 E/NE bone marrow ratio QTL.

Consistent with the observation that the E/NE bone marrow ratio is strongly influenced by sex (**Table 3.2**), linkage analysis revealed a highly significant QTL (LOD: 3.5) on chromosome X. Additionally, a significant QTL was mapped to chromosome 5 (LOD: 4.5) and a suggestive male-specific on chromosome 9 (LOD: 2.7), suggesting that variations within those regions may result in the different E/NE ratio between the two mouse strains. Erythropoietin and its receptor are located within those QTL and were the most obvious candidates, as they hold important roles in erythropoiesis. Possible sequence variations in those genes were therefore investigated in the parental CBA/H and C57BL/6 mouse strains.

No sequence variations were detected between the two mouse strains. The intronic regions, coding and promoter DNA sequences were investigated by direct sequencing whereas Southern blotting excluded gene copy variations. However, the possibility of sequence variations in other upstream or downstream gene regulatory regions can not be excluded and further work is needed in order to conclusively exclude these two genes as variation-causing candidates.

Other potential candidates include Janus Kinase 2 (see section 3.1.4) which maps close to the significant chromosome 19 QTL (T**able 3.3**) and possibly genes in the suggestive chromosome 10 QTL. This region is syntenic to the human chromosome region 6q23-24 in which a haematocrit (i.e. the percentage of red cells in blood) QTL has been previously mapped (Lin *et al.,* 2005). Additionally, the possible involvement of other candidates needs to be investigated and the QTL regions further refined.

The significant QTL have been registered with the Mouse Genomic Nomenclature Committee as locus symbols: bmRBC1 (chromosome 5), bmRBC2 (Chromosome 11), bmRBC3 (chromosome 19), and bmRBC4 (Chromosome X).

3.4.2 Peripheral red blood cell (pRBC) QTL.

Two significant QTL (**Table 3.4**) were identified which harbour possible genes influencing the pRBC counts. Significantly, the Chromosome 4 QTL was replicated in two independent studies (**Table 3.4**), strong evidence of its possible implication.

Other QTL that map close to the chromosome 4 region include loci that control splenomegaly (Sbw2, Orgwg6, Spm1) and anti-red-blood cell IgG antibodies. Elevated serum levels of anti-red blood IgG antibodies and spontaneous overproduction of anti-erythrocyte auto-antibodies in response to splenomegaly lead to autoimmune haemolytic anaemia (Ochiai *et al.*, 2000; Lee *et al.*, 2005).

There was little overlap between the E/NE bone marrow ratio and the pRBC QTL. As pRBC represent contributions from both spleen and BM, this suggests that erythropoiesis is regulated by different loci in the two haemopoietic tissues. The chromosome X QTL was identified in both the E/NE and pRBC analyses. This could represent a common sex-specific genetic effect in the two phenotypes. However, the increaser alleles are different for the two traits (**Tables 3.2** and **3.4**) suggesting that the specific locus might result in a variable phenotype that is strain/tissue-specific (pleiotropic effect).

The chromosome 4 QTL has been registered with the Mouse Genomic Nomenclature Committee as locus symbol pRBC1.

3.4.3 Spleen weight QTL.

Spleen weight was used as surrogate for peripheral red blood cell production. In humans, erythropoiesis takes place in the bone marrow. However, in many small mammals, including mice, erythropoiesis also occurs in the spleen. Peripheral red blood cell numbers therefore reflect contributions by both spleen and BM.

QTL analysis revealed three suggestive QTL, one of which overlaps with a known spleen weight QTL (Splq9) (Rocha *et al.*, 2004). However, none of the three QTL overlaps with any of the pRBC or E/NE bone marrow ratio QTL. This might suggest

that spleen weight is not an appropriate surrogate for peripheral red blood cell production and a more quantitative measure of erythropoiesis in the spleen is required.

3.4.4 Lin^- $Sca\text{-}1^+$ $c\text{-}Kit^+$ bone marrow cells QTL.

Flow cytometry allowed quantification of specific subpopulations of immature bone marrow cells and revealed differences between the two mouse strains. Following immunomagnetic depletion of Lin^+ cells, Lin^- bone marrow cells were analysed for expression of Sca-1 and c-Kit. Subsequent QTL analysis of 124 F_2 mice identified QTL influencing the frequency of specific Lin^- subpopulations.

The strain-specific expression levels of Sca-1 complicate the characterisation of murine HSC when the specific marker is used. In mice, Sca-1 is encoded by strain-specific alleles Ly-6A and Ly-6E. Expression levels of the Sca-1 protein are dependant on the haplotype of the Ly-6 locus. The $Ly\text{-}6^b$ haplotype is associated with high levels of Sca-1 expression. C57BL/6, AKR/J, DBA/J, and SJK/L mice have the $Ly\text{-}6^b$ haplotype and therefore show high levels of Sca-1 expression. In contrast, mouse strains which carry the $Ly\text{-}6^a$ haplotype (CBA/J, Balb/c, CeH/J, and A/J) show lower levels of Sca-1 expression (Spangrude and Brooks, 1993).

Previous FACS analysis in the lab had revealed a 4-fold difference in the number of $L^-S^+K^+$ cells between CBA/H and C57BL/6, with CBA/H mice showing higher numbers of the specific subpopulation. Moreover, C57BL/6 mice have higher numbers of $Sca\text{-}1^{++}$ (intensely labelled) cells (see **Figure 3.5**), which is consistent with their $Ly\text{-}6^b$ haplotype and suggests that the $L^-S^+K^+$ cells can be directly visualised by flow cytometry, irrespective of the parental Ly-6 haplotype.

Interestingly, the QTL on chromosome 1 and 18 ($L^-S^+K^+$ R1) overlap with the QTL influencing the frequency of LTC-IC (**Table 3.1**; Müller-Sieburg and Riblet, 1996) and CAFC Day 35 (**Table 3.1**; de Haan and Van Zant, 1997) respectively. As previously discussed (see section 1.6.1; **Figure 1.9**), the LTC-IC, $L^-S^+K^+$ and CAFC Day 35 bone marrow cells contain the long term repopulating haemopoietic stem cells. The overlap between these independent *in vitro* studies and this *in vivo* study strongly supports the

presence of the LTC-IC and CAFC Day 35 cells in the $L^-S^+K^+$ R1 population of this study.

The chromosome 17 QTL has also been previously implicated in the frequency of $L^-S^+K^+$ Thy^{lo} cells (Morrison *et al.*, 2002). Higher expression of Thy-1 can be used to further classify L^-S^+ cells in terms of long-term repopulating capacity. However, the specific QTL was identified in the analysis of $L^-S^+K^+$ R1, $L^-S^+K^+$, and $L^-S^-K^-$ (**Table 3.5**), suggesting that it might be involved in determining the frequency of most Lin^- bone marrow cells. The specific QTL contains the mouse H-2 complex, including the class I MHC alleles. The H-2 complex contains many histocompatibilty genes and immune response regulators. The class I MHC alleles are targets for natural killer cells which inhibit haemopoietic stem cell engraftment (Morrison *et al.*, 2002).

Finally, the chromosome 10 and chromosome 6 QTL map to very similar positions with suggestive $L^-S^+K^+$ QTL identified by another study (van Os *et al.*, 2006). The number of QTL identified by this and other studies highlight the genetic complexity of haemopoietic development and necessitate further studies in order to refine the QTL regions, identify and exclude possible false positives as well as identify genes determining the frequency of specific Lin^- subpopulations.

3.5 Conclusion and future work.

CBA/H and C56BL/6 mice are two inbred mouse strains that show susceptibility to different haemopoietic malignancies. Moreover, they differ in a number of haemopoietic traits (**Table 3.2**) which constitutes them an ideal experimental model to investigate the genetic regulation of haemopoiesis and cancer susceptibility. In this study, (CBA/H x C57BL/6) F_1 mice were intercrossed and their progeny (F_2) phenotypes were linked to QTL possibly harbouring the genes that regulate them.

To our knowledge, this is the first study to report strain-specific differences in normal erythropoiesis (E/NE bone marrow ratio and pRBC counts). Analysis of the E/NE bone marrow ratio identified QTL that are specific to bone marrow erythropoiesis, whereas pRBC production reflects the overall contribution made by both spleen and bone marrow. Interestingly a human study employed haematocrit and haemoglobin levels as

the phenotype (Lin *et al.*, 2005) and identified a QTL similar to the E/NE bone marrow ratio QTL in this study. The little overlap between the pRBC counts and E/NE bone marrow ratio suggests that erythropoiesis is regulated by different autosomal loci in the bone marrow and spleen. Additionally, spleen weight is not an appropriate surrogate for peripheral red blood cell production.

No sequence variation was detected in the strongest E/NE bone marrow ratio candidate genes (*EPO* and *EPO-R*) but neither gene can be conclusively excluded as possible upstream or downstream sequence variations could result in the different phenotypes in the two mouse strains. As altered erythropoiesis can result in a wide range of conditions (e.g. autoimmune haemolytic anaemia and thalassaemia), sequence variations altering the frequency and/or stability of red blood cells are of significant clinical importance.

Analysis of the Lin^- bone marrow cells identified a number of QTL some of which have been reported by independent *in vitro* studies. As previously discussed (see section 3.1.2) a number of independent *in vitro* studies have reported distinct strain-specific QTL. As previously discussed (see section 1.6.1) the LTC-IC and CAFC Day 35 cells contain the LT-HSC and ST-HSC populations. The apparent conflict in the QTL identified by those assays (**Table 3.1**) could suggest that they measure different haemopoietic stem cells. Alternatively, the reported differences can be attributed to the artificial environment of the *in vitro* stem cells studies, emphasising the need for *in vivo* BM analysis.

The QTL identified by this study, overlap with QTL identified by both LTC-IC and CAFC Day 35 *in vitro* assays, strong genetic evidence that flow cytometry can be employed to identify BM HSC *in vivo*. The overlap between the two different *in vitro* and this *in vivo* assay also suggests that $L^-S^+K^+$ cells (as defined by flow cytometry) are enriched for both LTC-IC and CAFC Day 35 cells.

In order to support the link between target cell size and r-AML susceptibility (see section 3.1.2) the $L^-S^+K^+$ QTL should co-localise with the r-AML susceptibility QTL identified by other studies (Chromosome 1 - 100cM, Müller-Sieburg and Riblet, 1996; Geiger *et al.*, 2001; Boulton *et al.*, 2003) (Chromosome 6 – 27.5cM, Boulton *et al.*, 2003). The chromosome 1 QTL was not identified in this study, possibly reflecting the

heterogeneity of the $L^-S^+K^+$ cells or simply due to the relatively low suggestive significance of the specific QTL, as reported by the original studies (Müller-Sieburg and Riblet, 1996; Geiger *et al.*, 2001; Boulton *et al.*, 2003). However, the suggestive Chromosome 6 (**Table 3.5**) $L^-S^+K^+$ QTL maps remarkably close to a reported r-AML susceptibility locus (Chromosome 6 – 27.5cM, Boulton *et al.*, 2003).

Similarly with other *in vivo* or *in vitro* techniques, this mouse genetic study has some limitations. The approach allows mapping to relatively large intervals of 10-30cM and the QTL identified contain many genes. However, many of those genes can be excluded and the regions can be further refined using additional markers. The co-localisation of at least one stem cell frequency QTL with an r-AML susceptibility locus, suggests that quantitative BM differences may also explain the different predisposition to haemopoietic malignancies seen in the CBA/H and C57BL/6 mice. Many genetic studies investigating radiation-induced cancer susceptibility have focused on candidate genes involved in protecting cellular genomes from exposure to DNA damaging agents. However, the number of genomes at risk from these DNA damaging agents should also be considered. CBA/H mice show increased numbers of $L^-S^+K^+$ BM cells compared to C57BL/6 mice which could account for their increased susceptibility to r-AML (the target cell is the HSC) but not B-cell leukaemia or T-cell lymphoma (the target cell is the more mature progenitor cell).

The contents of this chapter have been published (Jawad *et al.*, 2007b and 2008). Future work should focus on identifying candidate genes within the mapped QTL and investigate possible sequence variations. Factors such as gene expression levels in the BM or known mutations which cause a haemopoietic phenotype can be employed to identify and focus on the strongest candidates.

Chapter 4:

DNA methylation during mouse haemopoietic differentiation and radiation-induced leukaemia (r-AML)

4.1 Introduction.

Studies on A-bomb survivors have associated acute whole-body exposure to ionising radiation with an excess relative risk of r-AML, a clonal haemopoietic stem cell malignancy (see sections 1.3.4 and 1.7.2). Similarly, cancer patients who have received whole-body radiotherapy also run the risk of developing AML as a secondary cancer following treatment (Pedersen-Bjergaard *et al.*, 1995; Armitage *et al.*, 2003; Plumb *et al.*, 2003). Despite having had their whole body exposed, a higher incidence of radiation/therapy-induced AML is found in these groups compared to the general population, suggesting that bone marrow cells might be more susceptible to radiation-induced cancer than other cell types. Bone marrow (BM) cells are also very radiosensitive compared to most other adult somatic tissues (Van der Kogel, 1993). As seen from radiotherapy treatment schedules, BM is the main limiting factor in whole-body dose, as an acute dose of 7Gy will kill ~100% of bone marrow cells (**Figure 1.3**). All the above might suggest that exposure of the relatively radiosensitive BM cells to ionising radiation might trigger events that will eventually lead to r-AML development and raise the possibility of a relationship between cellular radiosensitivity and r-AML susceptibility *in vivo*.

The levels of radiation-induced apoptosis vary between different tissues (relative tissue radiosensitivity) and are usually higher in hierarchical adult tissues such as BM, spleen, skin, and the intestinal epithelia (Van der Kogel, 1993; Midgley *et al.*, 1995; MacCallum *et al.*, 1996; Coates *et al.*, 2003). Similarly, the degree of cell radiosensitivity within the same tissue (relative cell radiosensitivity) may vary. In mice for example, p53 induction and apoptosis following exposure to ionising radiation is mainly confined to cells at the base of the crypts in the intestinal track, whereas those

effects are seen in most spleen cell populations, including proliferating and non-proliferating cells (MacCallum *et al.*, 1996; Coates *et al.*, 2003).

Ionising radiation has been found to result in genomic instability (see section 1.3.3). Irradiated BM stem cells show radiation-induced persistent genomic instability in a genotype-dependant fashion (see section 1.8; Kadhim *et al.*, 1994; Watson *et al.*, 1997; Lorimore *et al.*, 2003). There is evidence that exposure to ionising radiation can lead to persistent global DNA hypomethylation in a dose-dependant manner *in vivo* (Kovalchuk *et al.*, 2004; Pogribny *et al.*, 2004; Koturbash *et al.*, 2005) and induces cleavage and increased catabolism of folate *in vivo* (Kesavan *et al.*, 2003) (see section 1.5.6). The importance of folate in regulating the levels of DNA methylation and genome stability has been demonstrated by a large number of studies (see sections 1.5.3, 1.5.4 and 1.5.5; Everson *et al.*, 1988; Libbus *et al.*, 1990; MacGregor *et al.*, 1990). Global DNA hypomethylation is often seen in a wide range of cancers (reviewed in Ehrlich, 2002) and folate deficiency has been associated with increased risk of cancer (Eichholzer *et al.*, 2001; Giovannucci, 2002; Zhang *et al.*, 2003) and genomic instability both *in vivo* and *in vitro* (Duthie and Hawdon, 1998; Fenech, 2001; Zijno *et al.*, 2003; Basten *et al.*, 2006).

DNA hypomethylation can also lead to transcriptional activation of endogenous retrotransposable elements which might result in increased levels of insertional mutagenesis and affect genome stability (see section 1.5.1). LINE 1 is a highly repeated and widely dispersed human/murine retrotransposon (L1 repeats constitute ~17% of the human genome), found to be highly methylated in normal tissues. Chalitchagorn *et al.* (2004) found significantly greater L1 hypomethylation in a wide range of cancers (urinary bladder, head and neck, lung, prostate gland, stomach, colon, breast, and oesophagus) compared to their untransformed tissues. Increased levels of IAP RNA (a mouse retroviral-like retrotransposon) were found in radiation-induced AML tumour cell lines derived from C3H/He mice suggesting that retrotransposons may have a significant impact during or after radiation leukaemogenesis (Ishihara *et al.*, 2004).

Local DNA hypomethylation is also seen in ICF (immunodeficiency, centromeric region instability and facial anomalies) patients (reviewed in Ehrlich, 2002). Patients affected by this rare autosomal recessive chromosome instability syndrome show

specific chromosomal anomalies whilst the syndrome itself results from mutations in the *DNMT3B* methyltransferase gene (Ehrlich *et al.*, 2001). A number of different cell lines from ICF patients (fibroblasts, lymphoblastoid, and mitogen-stimulated lymphocytes) showed significant hypomethylation at the centromeric region of chromosome 1 (satellite α) and/or the juxtacentromeric regions of chromosomes 1 and 16 (satellite 2) which was associated with centromeric decondensation and chromosomal rearrangements (Tuch-Muller *et al.*, 2000; Ehrlich *et al.*, 2001). Hypomethylation of the same regions has been found in a significant proportion of human breast adenocarcinomas, ovarian epithelial carcinomas, and Wilms tumour samples (Narayan *et al.*, 1998; Qu *et al.*, 1999). This suggests that these satellite repeat regions, which are normally hypermethylated in adults, may have an important role in genome stability. Interestingly, ICF cell lines are also hypersensitive to ionising radiation, exhibiting increased cell death and permanent cell cycle arrest following exposure (Narayan *et al.*, 2000).

Global DNA methylation levels are tissue-specific in adult humans and mice, and overall, highly proliferating tissues tend to be hypomethylated compared to low turnover tissues, although there are some exceptions (Ehrlich *et al.*, 1982; Gama-Sosa *et al.*, 1983). Moreover, as seen from radiotherapy in cancer patients, highly proliferating (usually hypomethylated) tissues show increased radiosensitivity (**Figure 1.3**; Van der Kogel, 1993).

Ionising radiation induces hypomethylation and persistent genomic instability. As hypomethylation has been implicated in both increased genomic instability and cancer predisposition and given the fact that the effects of ionising radiation are non-targeted, radiation-induced effects on DNA methylation status are likely to be involved in the process of genomic instability and cancer predisposition. Moreover, the increased radiosensitivity seen in ICF patients and folate deficiencies raise the possibility of an association between DNA methylation status and relative radiosensitivity.

4.1.1 CBA/H and C57BL/6 mouse strains.

The CBA/H inbred mouse strain is an ideal experimental system to assess the role of DNA methylation in both radiosensitivity and radiation leukaemogenesis *in vivo* (see

section 1.8). A number of r-AML (leukaemic spleen DNA), lymphoid B-cell leukaemias (BL) (leukaemic spleen DNA) and thymic lymphomas (TL) (thymus DNA) mouse samples were available in the lab. This made it possible to compare the methylation status of control bone marrow and spleen (haemopoietic tissues that show different levels of maturation) to that of the stem cell-derived AML and the progenitor cell-derived BL and TL (haemopoietic malignancies that resulted following transformation of haemopoietic cells at different stages of maturation).

CBA/H (r-AML susceptible) and C57BL/6 (r-AML resistant) inbred mouse strains were also compared. Additionally, it was possible to assess the proposed relationship between DNA methylation and relative radiosensitivity of spleen and BM *in vivo*, as increased levels of apoptosis are seen in both tissues following exposure to ionising radiation (MacCallum *et al.*, 1996).

4.1.2 Aims of the study.

The aim of this study was to investigate the effects of acute whole-body exposure to ionising radiation on global DNA methylation levels of haemopoietic tissues (BM and spleen) in the CBA/H and C57BL/6 mouse strains.

Additionally, to assess global DNA methylation levels in murine leukaemias and investigate the relationship between global DNA methylation levels and relative radiosensitivity in irradiated spleen and BM *in vivo*.

4.2 Materials and methods.

4.2.1 Mouse irradiation.

Adult (8-12 weeks of age) CBA/H and C56BL/6 mice (see section 2.1.6) were irradiated with an acute whole-body dose of 3Gy X-rays (see section 2.1.6.1). Irradiated mice were sacrificed at specific time-points post-irradiation, their levels of BM and spleen cell death/recovery were recorded and tissues extracted (see section 2.2). Spleen weight was used to monitor levels of cell death and recovery in the spleen, as in this tissue the levels of apoptosis induction and loss of spleen weight have previously been

found to correlate (Midgley *et al.*, 1995). White bone marrow cellularity (WBMC) was determined using a Scharfe system Casy® 1 cell coulter counter (see section 2.17). Both spleen weight and WBMC were compared against age-matched un-irradiated mice. DNA and/or RNA were prepared from snap-frozen tissues (see sections 2.3 and 2.4). Radiation-induced AML (leukaemic spleen), BL (leukaemic spleen) and TL (thymus) DNA and/or RNA were available in the lab.

4.2.2 Genomic 5-methyldeoxycytosine (5-^{Me}C) content.

The genomic 5-methyldeoxycytosine (5-^{Me}C) content of control, irradiated and leukaemic samples was analysed using High Performance Liquid Chromatography (HPLC) as previously described (Plumb *et al.*, 2000). HPLC analysis was performed by collaborators Prof. Robert Brown and Mrs. Carol McCormick (then located at: Centre for Oncology and Applied Pharmacology, CRUK Beatson Laboratories, Glasgow University, Glasgow, UK). Essentially, DNA samples were denatured and digested with P1 nuclease, proteins were removed, and the deoxynucleotides were separated and quantified by HPLC. In HPLC, deoxynucleotides are eluted from a column at different times (known as retention time) according to their physical/chemical properties. The size difference between methylated and unmethylated cytosine enables quantifying the genomic 5-methyldeoxycytosine content.

4.2.3 Southern blot analysis.

Genomic DNA (3-5μg) from control, irradiated, and leukaemic samples was digested overnight at 37^{o}C with *Hpa*II or *Msp*I in a total reaction volume of 300μl according to the manufacturer's recommendations (see sections 2.9 and 2.13). Samples were resolved by 1.5% (w/v) agarose gel electrophoresis, transferred to Magna nylon membranes and probed with α-^{32}P-dCTP-labelled (IAP, L1 LINE) or γ-^{32}P-ATP-end-labelled (Minor satellite) probes (see sections 2.10, 2.11, 2.13 and 2.15). The L1 LINE promoter sequence probe was from nucleotides 370-1812 of the consensus L1 LINE sequence (NCBI accession number: M13002). PCR conditions were: 5 minutes of denaturing at 96^{o}C, followed by 35 cycles of: 45 seconds of denaturing at 96^{o}C, 45 seconds of annealing at 59^{o}C, 45 seconds of elongation at 72^{o}C, followed by a final 7 minutes elongation at 72^{o}C. The IAP 5′LTR genomic probe was from nucleotides 22 to

721 of the consensus IAP sequence (NCBI accession number: M17551). PCR conditions were the same as for the L1 LINE probe with an annealing temperature of 58^{o}C. Primer sequences for both probes can be found in **Table 2.2** and in both cases the 11.1x buffer was used (see section 2.7) in a reaction of a total volume of 10µl. The mitochondrial probe was as previously described (Walsh and Bestor, 1999). The minor satellite probe was a γ-^{32}P-ATP-end-labelled oligonucleotide (**Table 2.3**) (Bourc'his and Bestor, 2004).

4.2.4 Northern blot analysis.

Total cellular RNA (10µg) from control, irradiated, and leukaemic samples was resolved by denaturing agarose gel electrophoresis, transferred to nylon membranes (see section 2.14) and probed with α-^{32}P-dCTP-labelled probes (see section 2.13). The Intracisternal A particle (IAP) probe was available in the lab and was a PCR-amplified 1800bp *gag* gene (NCBI accession number: M17551).

4.3 Results.

4.3.1 DNA methylation of mouse bone marrow and spleen samples.

Two different methods were employed in order to assess DNA methylation in control un-irradiated BM and spleen samples: High Performance Liquid Chromatography (HPLC) and methylation-sensitive restriction digestion followed by Southern blotting.

The genomic 5-methyldeoxycytosine (5-^{Me}C) content of adult CBA/H and C57BL/6 mouse bone marrow, spleen and kidney samples was determined by HPLC (collaborators, Prof. Robert Brown and Mrs. Carol McCormick). Human placenta DNA was used as internal control. Results were reproducible and highly consistent with the previously reported values for human placenta (0.76 mol % 5-^{Me}C) (Ehrlich *et al.*, 1982). Similarly, adult mouse spleen 5-^{Me}C values (0.93 ± 0.03 mol %) were comparable to those reported for mouse (0.89 ± 0.04 mol %) and human (0.93 ± 0.03 mol %) spleens (Ehrlich *et al.*, 1982; Gama-Sosa *et al.*, 1983). The genomic 5-^{Me}C content of adult mouse bone marrow had not been previously reported but very little inter-individual variation was seen in the BM control tissues. Additionally, no mouse

genotype-dependent differences were seen, so the data for both control mouse strains were pooled and the average 5-^{Me}C content of spleen (n=22) was used as a standard (**Figure 4.1**) for convenience (where 5-^{Me}C: 1.00). Bone marrow DNA samples were found to be hypomethylated (5-^{Me}C: 0.84 ± 0.005, n=4) compared to spleen DNA (5-^{Me}C: 1.00 ± 0.006, n=22) (**Figure 4.1**).

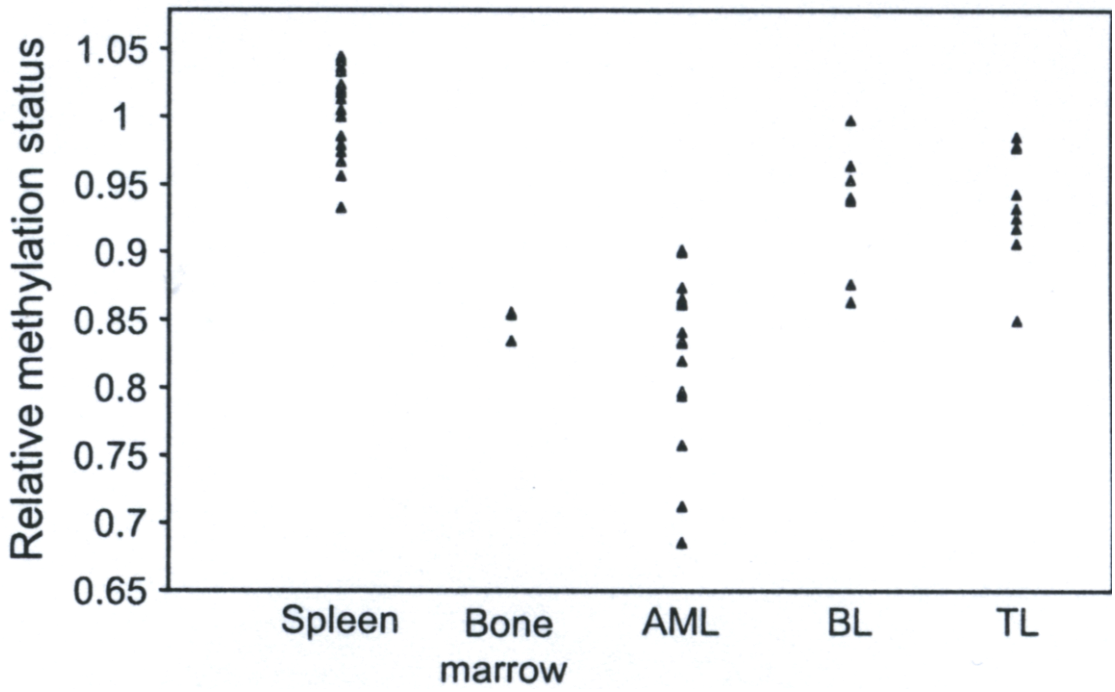

Figure 4.1: DNA 5-methyldeoxycytosine (5-^{Me}C) content in normal and malignant haemopoiesis as determined by HPLC. Results are expressed relative to the average of un-irradiated control spleens. Spleen (n=22): 4CBA/H, 3 C57BL/6, 3 (CBA/H x C57BL/6) F_1 and 12 F_1 x F_1 mice. Bone marrow (n=4): 2 CBA/H and 2 C57BL/6 mice. AML (leukaemic spleen) (n=17): 9 CBA/H and 8 (CBA/H x C57BL/6) F_1 x CBA/H mice. BL (B-cell leukaemia, leukaemic spleen) (n=7): (CBA/H x C57BL/6) F_1 x CBA/H mice. TL (Thymic lymphomas, thymus) (n=8): (CBA/H x C57BL/6) F_1 x CBA/H mice. AML, BL, and TL malignancies arose in 3Gy X-irradiated mice.

Table 4.1				
Tissue	**Human**	**Rat**	**Mouse**	**Mouse (this study)**
Placenta	0.82	-	-	0.81
Bone marrow	-	-	-	0.85
Sperm	0.9	-	0.93	-
Heart	0.96	0.94	0.94	-
Lungs	0.98	0.95	0.94	-
Spleen	1.00	1.00	1.00	1.00
Kidney	-	0.92	1.01	1.00
Liver	0.94	1.0	1.07	-
Brain	1.05	1.02	1.08	-
Thymus	1.07	1.08	1.08	-

Table 4.1: Relative methylation status of adult human (Ehrlich *et al.*, 1982), rat and mouse (Gama-Sosa *et al.*, 1983) tissues compared to mouse data obtained from this study. All data was normalised according to spleen (5-^{Me}C: 1) for convenience.

Table 4.1 shows the relative methylation status of adult tissues in previous studies and in this one. Liver was reported to be hypomethylated compared to spleen in humans (Ehrlich *et al.*, 1982) but hypermethylated compared to spleen in rats and mice (Gama-Sosa *et al.*, 1983). Apart from human liver and as seen from **Table 4.1**, methylation data are consistent between species and across studies indicating that bone marrow is one of the most hypomethylated adult somatic tissues.

The methylation status of 5′-CCGG-3′ sites in 3 different CpG-rich genomic repeat elements was also assessed by Southern blotting to confirm the relative hypomethylation of mouse bone marrow as suggested by HPLC. Adult mouse genomic DNA was digested using methylation-sensitive restriction (*Hpa*II and *Msp*I enzymes) followed by Southern blot analysis. *Hpa*II is methylation-sensitive (i.e. will only cut if the cytosine in the CpG dinucleotide is not methylated in a 5′-CCGG-3′ site) while the endonuclease activity of the *Msp*I (a *Hpa*II isoschisomer) is not affected by the methylation status of the cytosine residue (i.e. methylation-insensitive). Decreased levels of methylation will therefore result in increased levels of *Hpa*II digestion which

can be visualised by hybridisation with appropriate radiolabelled probes and subsequent autoradiographic exposure.

Although this method is semi-quantitative, Southern blotting confirmed that bone marrow is one of the most hypomethylated adult tissues. **Figure 4.2** shows the southern blot analyses of the L1 LINE repeat promoter region (A), the minor satellite repeat sequence (B) and the 5′LTR of the IAP repeat element region (C) in various mouse control tissues. Membranes were stripped and re-probed with a mitochondrial probe (D) to confirm complete *Hpa*II digestion.

The great difference between IAP and LINE-1 repeat copy numbers in the murine genome [IAP: ~1000 copies/haploid genome, LINE-1 ~100,000copies/haploid genome (Kuff *et al.,* 1983; Loeb *et al.,* 1986)] resulted in significant differences in signal intensity between the two probes. The IAP probe revealed increased *Hpa*II digestion in bone marrow samples which was less marked than that revealed by the LINE-1 and Minor satellite probes (**Figure 4.2**). There was significant variation across tissues but the overall pattern agreed with the HPLC results and the previously reported trend of DNA methylation across tissues. For example, testes, BM, heart, and gut tissues showed the greatest relative hypomethylation which is consistent with the previous data in the literature and in the lab (**Figure 4.2** and **Table 4.1**).

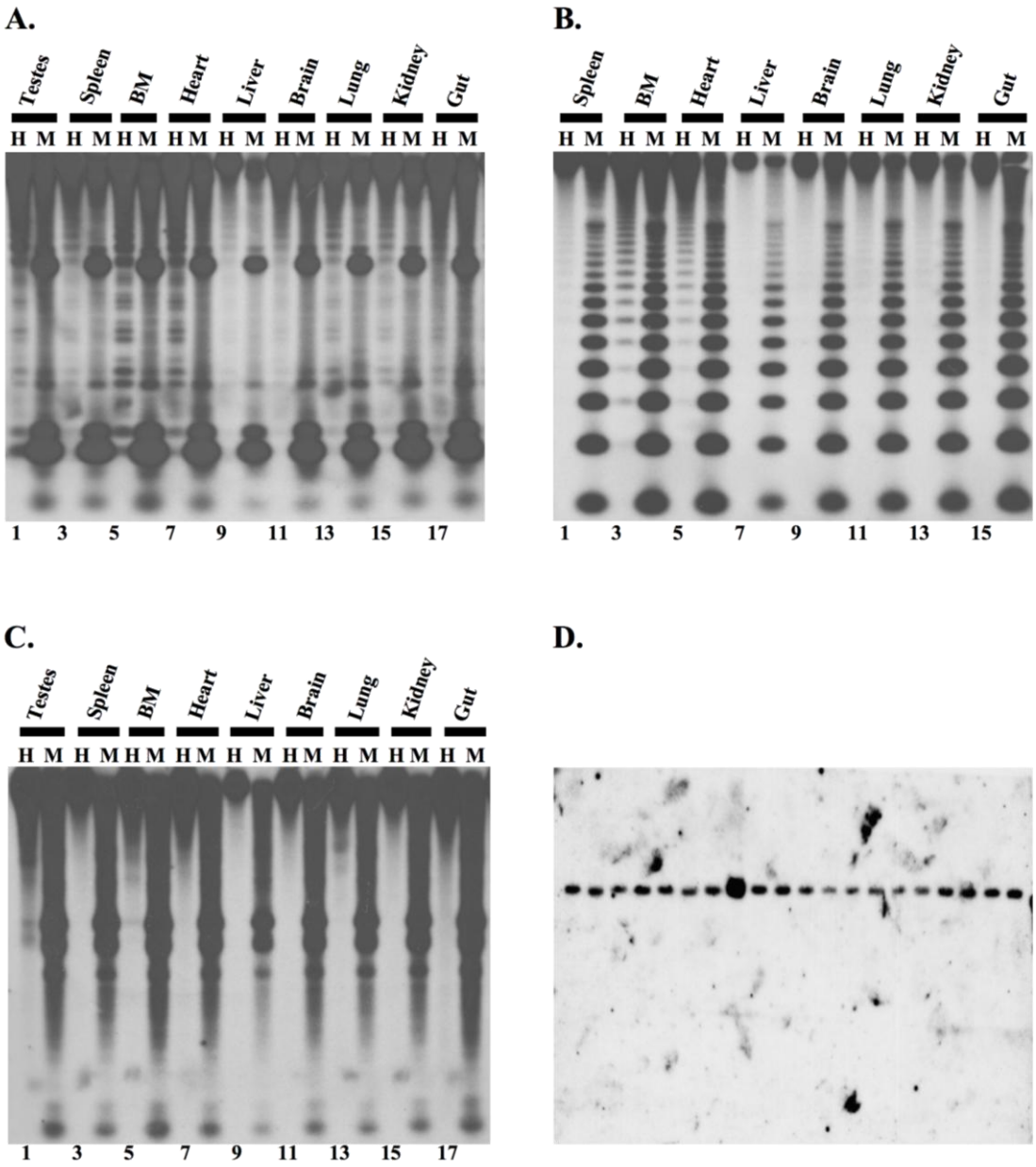

Figure 4.2: Southern blot analysis of (H) *Hpa*II- or (M) *Msp*I-digested mouse genomic DNA. 2-5µg of mouse DNA were digested with either the methylation-sensitive *Hpa*II or the methylation-insensitive *Msp*I and probed against the LINE-1 repeat promoter region (A), the minor satellite repeat sequence (B) and the 5'LTR of the IAP repeat element region (C). Membranes were stripped and re-probed with a mitochondrial probe (D) to confirm complete (*Hpa*II and *Msp*I) digestion. In agreement with the literature and the previous HPLC data (**Table 4.1**), increased levels of *Hpa*II digestion (indicative of hypomethylation) were seen in the case of BM, testes, heart and gut.

4.3.2 DNA methylation of mouse radiation-induced leukaemias.

Similarly to control tissues, the methylation status of radiation-induced mouse leukaemias was analysed by HPLC and Southern blotting. Radiation-induced AML (leukaemic spleen), BL (leukaemic spleen) and TL (thymus) DNA samples were available in the lab. These represent malignancies that arose following transformation and clonal expansion of haemopoietic cells at different stages of maturation. BL and TL arose from mature progenitor cells compared to the more immature stem cells that gave rise to AML (Cleary *et al.*, 2001; Boulton *et al.*, 2002).

HPLC analysis (**Figure 4.1**) revealed that r-AML (5-^{Me}C: 0.824 ± 0.015, n=17) samples were less methylated (on average) than the progenitor cell BL (5-^{Me}C: 0.934 ± 0.018, n=7) and TL (5-^{Me}C: 0.946 ± 0.011, n=8) (p<0.0001; Kruskal-Wallis test). No statistically significant differences were seen between the methylation status of the BL and TL malignancies. Although variation was seen in the methylation status of individual malignancies, there was very little overlap between r-AML and the two progenitor cell malignancies whilst all leukaemia/lymphoma samples were significantly hypomethylated compared to control spleen (p<0.0001; Kruskal-Wallis test).

Analysis of r-AML leukaemic spleens (5-^{Me}C: 0.824 ± 0.015) revealed that their methylation levels are similar to control bone marrow (5-^{Me}C: 0.849 ± 0.05). This was expected as r-AML leukaemias arose from the immature BM stem cell compartment. Consistent with immunogenotype evidence that BL and TL arose from a more mature lymphoid progenitor cell, these malignancies (average 5-^{Me}C: 0.94) were found to be hypermethylated compared to control BM (5-^{Me}C: 0.849) but hypomethylated compared to control spleen (5-^{Me}C: 1.00).

The methylation status of control spleen, bone marrow and mouse radiation-induced malignancies was also analysed by southern blotting and yielded similar results (**Figure 4.3**). As in the control tissue Southern blot analysis, leukaemic genomic DNA was digested with *Hpa*II or *Msp*I and probed with 3 different CpG-rich genomic repeat elements. Despite *Hpa*II cleavage of repeat elements being a semi-quantitative reflection of overall genomic DNA methylation, and although high inter-sample variation was seen, the increased cleavage of *Hpa*II in the BM and r-AML (and to a

lesser extent in BL and TL) samples was highly reproducible and confirmed the previous HPLC results (**Figure 4.1** and **Figure 4.3**).

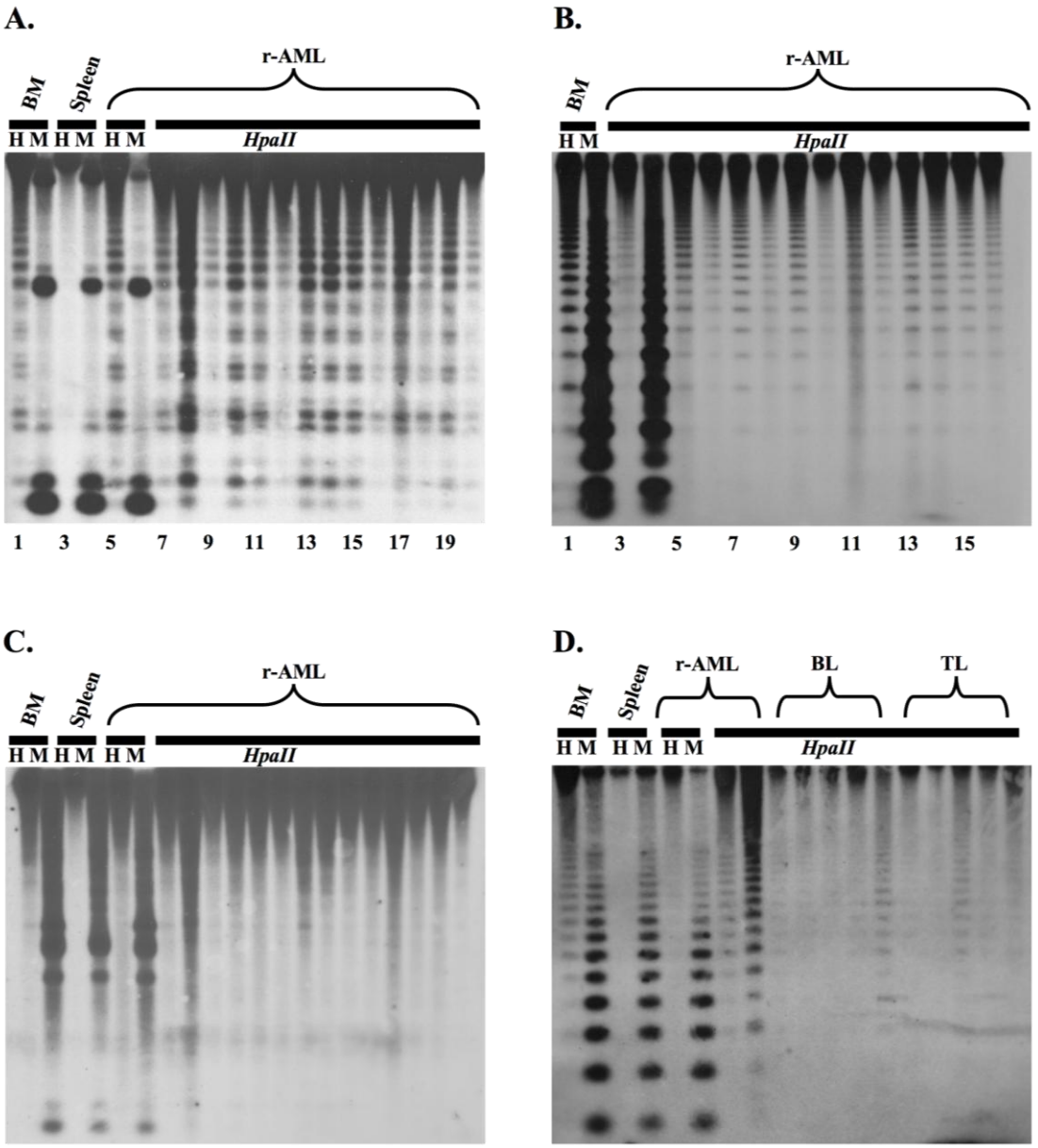

Figure 4.3: Southern blot analysis of (H) *Hpa*II- or (M) *Msp*I-digested genomic mouse DNA. 2-5µg of mouse genomic control DNA and r-AML leukaemic spleen DNA were digested with either the methylation-sensitive *Hpa*II or the methylation-insensitive *Msp*I and probed against the L1 LINE repeat promoter region (A), the minor satellite repeat sequence (B) and the 5'LTR of the IAP repeat element region (C). Increased cleavage of *Hpa*II was seen to a lesser extent in BL (leukaemic spleen) and TL (thymus) malignancies (D) probed with the minor satellite repeat sequence. Membranes were stripped and re-probed with a mitochondrial probe to confirm complete (*Hpa*II and *Msp*I) digestion (**Figure 4.2** and data not shown).

Compared to control spleen genomic DNA, r-AML samples (n=57) were found to be hypomethylated, supporting the previous HPLC data. Similar results were obtained in the case of the BL (n=28) and TL (n=5) samples analysed. Not unexpectedly inter-individual variation was recorded. However, compared to spleen, all r-AML samples as well as all the lymphoid leukaemias and lymphomas that were analysed were hypomethylated (**Figure 4.3** and data not shown).

The global DNA methylation status of the mouse leukaemias, spleen and BM was compared to the reported methylation status of other adult mouse, rat and human haemopoietic cells (Ehrlich *et al.*, 1982; Gama-Sosa *et al.*, 1983) using spleen as a standard. As seen from **Figure 4.4**, DNA methylation tends to increase with relative haemopoietic cell differentiation. Moreover, the methylation status of different mouse malignancies reflects the global DNA methylation levels of their normal untransformed target haemopoietic stem cell (r-AML) or progenitor cell (BL and TL).

Both in the case of control tissues and radiation-induced malignancies, Southern blot results were in agreement with the HPLC results thus confirming that *Hpa*II cleavage of DNA repeat elements is a semi-quantitative reflection of relative DNA 5-^{Me}C content.

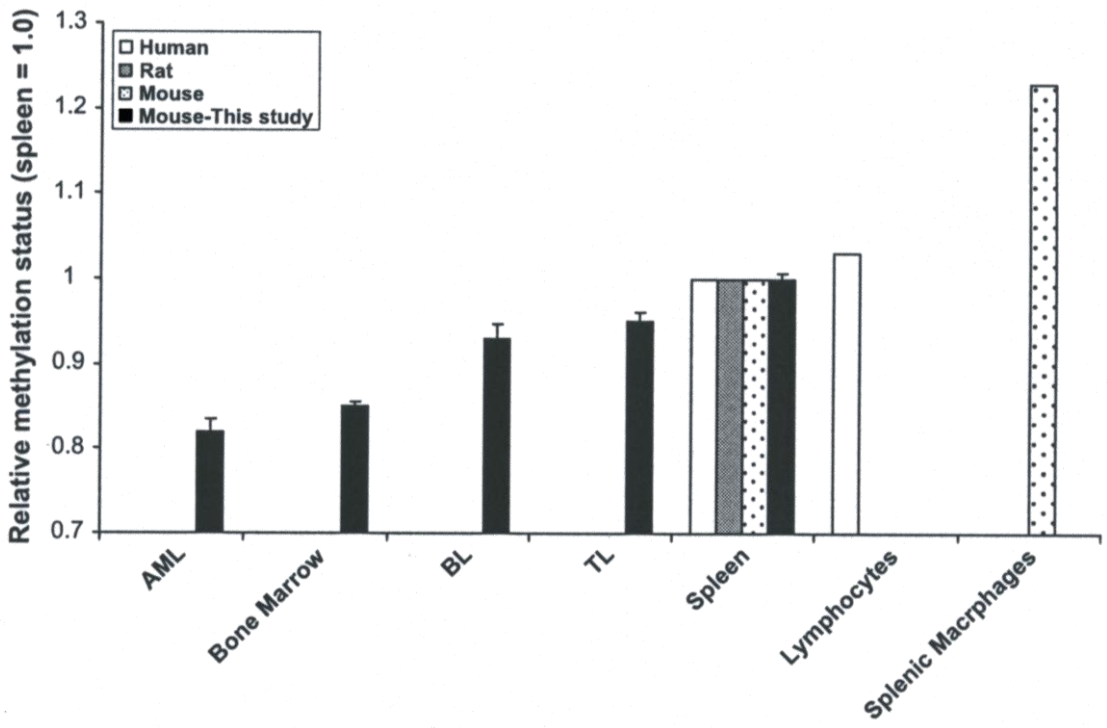

Figure 4.4: The average relative methylation status of normal haemopoietic tissues and radiation-induced malignancies was compared to reported rat/mouse (Gama-Sosa *et al.*, 1983) and human (Ehrlich *et al.*, 1982) global DNA methylation levels using normal spleen as a standard. DNA methylation tends to increase with haemopoietic differentiation whilst the DNA methylation status of mouse haemopoietic malignancies tends to reflect the global DNA methylation of their normal untransformed target haemopoietic stem cell (r-AML) of more mature progenitor cell (BL and TL).

4.3.3 Genomic DNA methylation status and haemopoietic tissue relative *in vivo* radiosensitivity.

To investigate any possible correlation between relative radiosensitivity and global DNA methylation, mice were exposed to an acute whole-body dose of 3Gy X-rays and their levels of spleen and BM cell death/rates of recovery were monitored (see section 4.2.1). Adult CBA/H (n=71) and C57BL/6 (n=86) were exposed to 3Gy X-rays and sacrificed at various time-points post-irradiation (pooled lab data). White bone marrow cell counts (see section 2.17 for quantification) and spleen weight values were compared against control un-irradiated CBA/H (n=17) and C57BL/6 (n=18) mice. There were no genotype-dependent differences in cell death and recovery so the data for both mouse strains were pooled (**Figure 4.5**).

On average, exposure to an acute whole-body dose of 3Gy X-rays resulted in ~80% (white bone marrow cells) and ~50% cell loss in BM and spleen respectively (**Figure 4.5**). Tissue recovery commenced at day 3-4 in the case of bone marrow. Consistent with a previous study (Midgley *et al.*, 1995) a significant increase in spleen weight was not detected until day 5-6. Cellularity reached control (100%) levels in both tissues at day 10 and remained at relatively constant levels at least 42 days post-irradiation. This three-phase pattern of expansion (initial lag phase, rapid expansion, stationary phase) is also seen in haemopoietic multipotent stem cell cultures *in vitro* (Colter *et al.*, 2001; Dazzi *et al.*, 2006) and agrees with the notion that tissue reconstitution is driven by these immature stem cells.

BM cellularity levels exceeded those of the un-irradiated controls (~20% increase), which reflects age-dependant changes in both femur size and bone marrow cellularity. This increase was consistent with changes previously observed in un-irradiated controls (Dr Clare Cole thesis) and was not radiation-induced. The *in vivo* BM and spleen radiosensitivity data support the proposed correlation between methylation status and relative radiosensitivity.

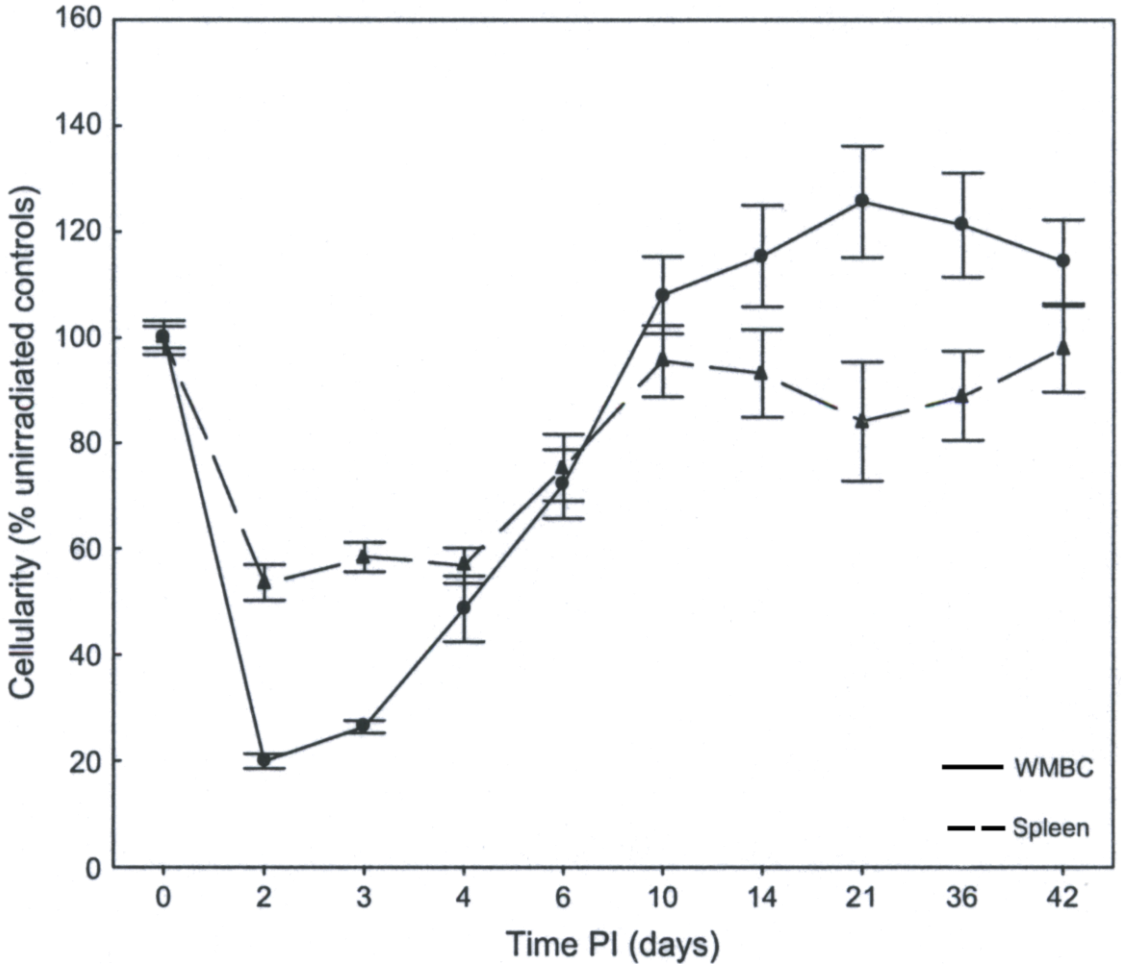

Figure 4.5: Cell death (%) and recovery rates in the spleen and bone marrow of CBA/H (n=71) and C57BL/6 (n=86) mice irradiated with an acute whole-body dose of 3Gy X-rays. Data for the two mouse strains was pooled as no genotype-dependant differences were observed. WBMC counts as measured by a Scharfe system Casy® 1 cell coulter counter (see section 2.17) and spleen weight (Midgley *et al.*, 1995) were used to determine cell death/recovery in the irradiated mice compared to un-irradiated CBA/H (n=17) and C57BL/6 (n=18) control mice (100% cellularity). The graph is based on pooled data from the lab and includes mice irradiated by Dr Clare Cole and Mrs Abigail Zanker.

4.3.4 Genotype- and tissue-specific radiation-induced DNA hypomethylation in CBA/H and C57BL/6 mice following exposure to 3Gy X-rays.

As seen in **Figure 4.5** exposure to a dose of 3Gy X-rays results in high levels of cell death both in the bone marrow and spleen. Both tissues are then forced to proliferate rapidly in order to restore tissue cellularity. There is increasing evidence that exposure to ionising radiation can lead to DNA hypomethylation both *in vitro* and *in vivo*

(Kalinich *et al.*, 1989; Kovalchuk *et al.*, 2004; Pogribny *et al.*, 2004; Koturbash *et al.*, 2005). Global DNA methylation levels were therefore assessed in recovered BM and spleen tissues following exposure of adult mice to 3Gy X-rays.

HPLC analysis revealed no difference in spleen DNA methylation levels between un-irradiated CBA/H (5-^{Me}C: 1.00, n=22) and irradiated CBA/H (5-^{Me}C: 0.994 ± 0.015, n=4). Considerably greater inter-individual variation was observed in the BM 5-^{Me}C content of irradiated CBA/H (5-^{Me}C range: 0.859-0.977, n=15) and C57BL/6 (5-^{Me}C range: 0.806-1.05, n=15) mice compared to un-irradiated controls [5-^{Me}C range: 0.976-1.024, n=12 (9 CBA/H and 3 C57BL/6 mice)]. Moreover, bone marrow strain-specific differences were observed following irradiation (**Figure 4.6**), despite the fact that control (CBA/H and C57BL/6) bone marrow 5-^{Me}C content was not found to be statistically different and no differences were noted in the levels of radiosensitivity and the kinetics of bone marrow recovery between the two mouse strains.

The average 5-^{Me}C content of irradiated CBA/H bone marrow (5-^{Me}C: 0.924 ± 0.01, n=15) was significantly lower than the un-irradiated control bone marrow (5-^{Me}C: 1.00 ± 0.005, n=12) (p<0.0001; Mann-Whitney *U*-test). No statistically significant differences were noted in the case of irradiated C57BL/6 bone marrow (5-^{Me}C: 0.982 ± 0.012, n=15) when compared against control un-irradiated bone marrow (p=0.494; Mann-Whitney *U*-test). There was a statistically significant difference between the exposed CBA/H and C57BL/6 bone marrow samples (p=0.0008; Mann-Whitney *U*-test) suggesting a genotype-dependant effect. This hypomethylation can be detected 10-14 days post-irradiation when BM cellularity and proliferation rates have returned to normal levels (**Figure 4.5**). Moreover, radiation-induced hypomethylation was also detected 2 years following exposure in two (CBA/H x C57BL/6) F_1 x CBA/H mice (5-^{Me}C: 0.93 and 0.849) that showed no evidence of a radiation-induced malignancy. This suggested that radiation-induced hypomethylation is persistent.

The methylation status of pre- and post-X-ray irradiated bone marrow samples was also assessed by Southern blotting (data not shown), but this semi-quantitative technique proved to be uninformative in this type of investigation and no firm conclusions could be drawn.

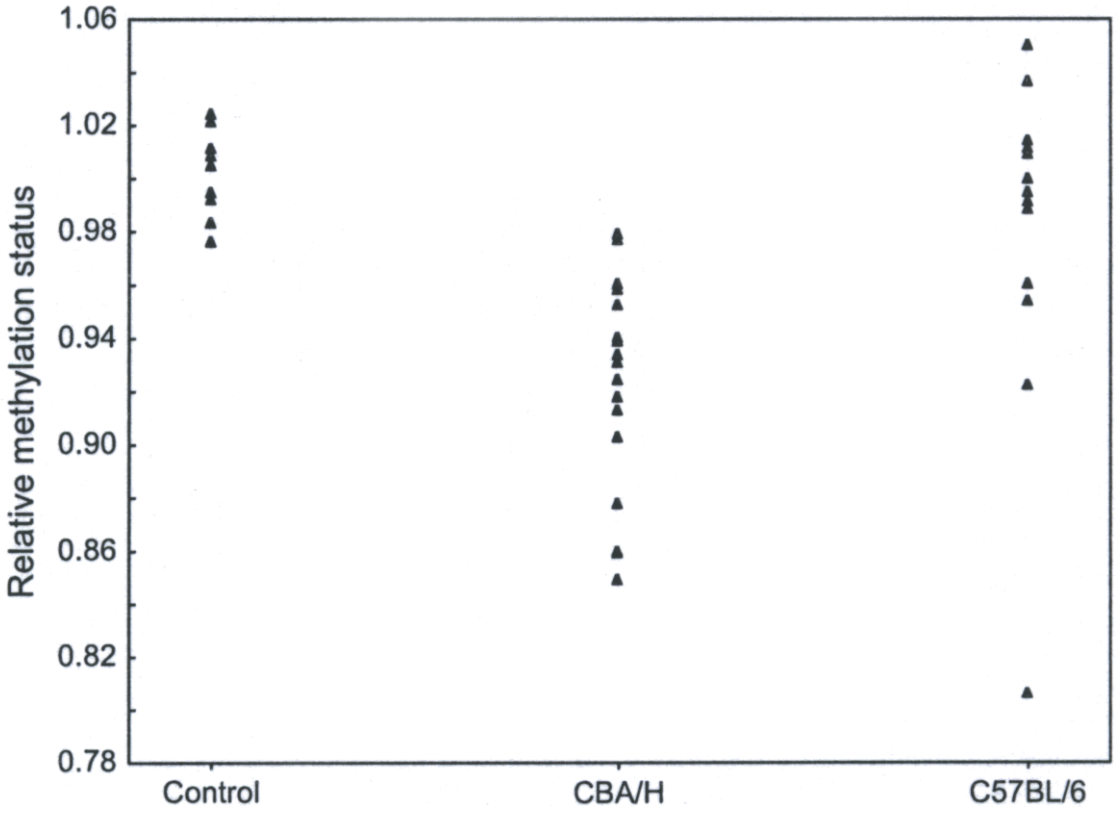

Figure 4.6: Un-irradiated 5-^{Me}C bone marrow content from both mouse strains was used as standard 5-^{Me}C: 1.00 (9 CBA/H and 3 C57BL/6 mice). On average bone marrow 5-^{Me}C content was found to be significantly lower in irradiated CBA/H (5-^{Me}C: 0.924 ± 0.01, n=15) (p<0.0001; Mann-Whitney *U*-test) but not in C57BL/6 (5-^{Me}C: 0.982 ± 0.012, n=15) mice, compared to un-irradiated controls (5-^{Me}C: 1.00 ± 0.005, n=12). Additionally, the irradiated CBA/H bone marrow 5-^{Me}C content was on average significantly lower compared to that of irradiated C57BL/6 mice (p=0.0008; Mann-Whitney *U*-test).

4.3.5 Northern blot analysis.

Southern blotting revealed the presence of hypomethylated genomes in a number of control tissues (e.g. testes and BM). As hypomethylation may lead to activation of endogenous retrotransposable elements and since their transcriptional activation is often seen in aberrant DNA hypomethylation, Northern blot analysis was performed on control and leukaemic samples. Negligible levels of IAP RNA were seen in the control tissues analysed (adult BM, spleen, testes, heart, liver, brain, lung, kidney and small intestine) despite the fact that some were previously found to be relatively hypomethylated (**Figure 4.7** and data not shown). In contrast, significant levels of IAP RNA were detected in r-AML (n=38) (**Figure 4.7**) and BL (n=18) (data not shown).

Leukaemic spleens showed high levels of inter-sample variation and strongly supported an aberrant DNA hypomethylation status in the haemopoietic malignancies. GAPDH was initially used as a loading control but showed variance in expression and proved to be unsuitable (as also reported in the literature: Savonet *et al.*, 1997; Mayer *et al.*, 2002). The ethidium bromide stain of the original gels was also used to crudely monitor sample loading and intensity (**Figure 4.7**).

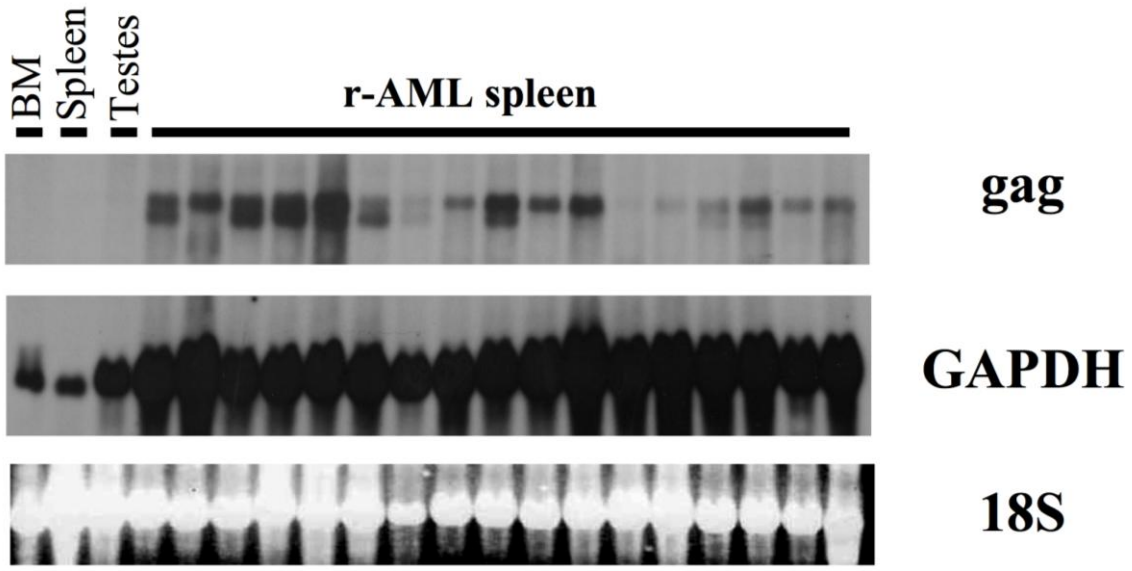

Figure 4.7: Northern blot analysis of control (BM, Spleen, Testes) and r-AML (leukaemic spleens). Approximately 10µg of total cellular RNA were probed with an 1800bp IAP *gag* gene genomic clone. Negligible levels of IAP RNA were detected in the control tissues whereas high variation was seen in IAP RNA levels of r-AML samples, evidence of aberrant DNA methylation. The ethidium bromide staining of the 18S r-RNA molecules was used to monitor sample loading.

4.3.6 Summary of results.

Global DNA methylation levels in control, irradiated and leukaemic samples were assayed using two independent methods (HPLC and Southern blotting) and the radiosensitivity of different haemopoietic tissues (BM and spleen) was compared *in vivo*:

- Based on results from both techniques, and given that the reported tissue-specific methylation data are consistent between mouse and human, bone marrow is one of the most hypomethylated tissues in adults.
- Highly proliferating tissues that have also been reported as radiosensitive showed the greatest degree of hypomethylation.
- DNA methylation increases with haemopoietic differentiation. Moreover, haemopoietic malignancies were found to be hypomethylated, compared to their appropriate controls. Their methylation status reflects that of their untransformed stem cell (for r-AML) and/or progenitor cell (for BL and TL).
- The relatively hypomethylated bone marrow showed increased levels of cell death (~80% cell death) compared to spleen (~50% cell death) following acute whole-body exposure to 3Gy X-rays.
- Exposure to the same dose resulted in a persistent genotype-dependent decrease of global DNA methylation levels in the BM, but not the spleen of CBA/H mice. No decrease in the average 5-^{Me}C content of BM was seen in the C57BL/6 mice.
- Northern blot analysis revealed little, if no IAP transcription in control tissues, despite the fact that some were found/reported to be relatively hypomethylated. In contrast, increased levels of IAP transcription were seen in the three haemopoietic malignancies, evidence of aberrant DNA hypomethylation.

4.4 Discussion.

The methylation status of normal and malignant haemopoietic tissues was assessed using two independent methods, HPLC and Southern blotting. Southern blot analysis was in agreement with the HPLC and the literature data (**Table 4.1** and **Figure 4.2**), confirming that *Hpa*II cleavage of genomic repeat elements can be used as a surrogate for relative DNA methylation levels, as previously suggested (Bourc'his and Bestor, 2004; Yang *et al.*, 2004).

Both techniques showed that bone marrow is one of the most hypomethylated tissues in adult mice. Moreover, there is a trend of increasing methylation during haemopoietic differentiation seen in human, mice and rats (**Figure 4.4**; Ehrlich *et al.*, 1982; Gama-Sosa *et al.*, 1983; Giotopoulos *et al.*, 2006; Tadokoro *et al.*, 2007).

BM is also one of the most radiosensitive adult tissues (Van der Kogel, 1993). The proposed correlation between relative DNA hypomethylation and radiosensitivity was supported by the *in vivo* radiosensitivity of BM and spleen (**Figure 4.5**). Unarguably, cell proliferation rate is a factor in radiosensitivity, as highly proliferating tissues are more prone to radiation-induced cell death (Van der Kogel, 1993; Midgley *et al.*, 1995). However, apoptosis is seen in both proliferating and non-proliferating spleen cells as in most BM cells (MacCallum *et al.*, 1996; Coates *et al.*, 2003) suggesting that additional factors may also be involved; and DNA methylation is a good candidate. This is further supported by the increased radiosensitivity recorded in ICF patients' cell line studies. As previously discussed, ICF patients show increased radiosensitivity and hypomethylation at specific sites (reviewed in Ehrlich, 2002). Narayan *et al.* (2000) reported an increased radiosensitivity of ICF lymphoblastoid cell lines compared to analogous normal cell lines. Radiation-induced cytotoxicity in those cell lines was even higher than that of ataxia telangiectasia (AT) cell lines, a chromosome instability syndrome also characterised by hypersensitivity to ionising radiation.

BM, testes and gut (hierarchical highly proliferating tissues) were found to be hypomethylated compared to liver, kidney and brain (low turnover tissues in which there is no clearly defined stem cell compartment) (**Figure 4.2**). Those highly proliferating tissues also show the greatest degree of radiosensitivity under clinical settings (**Figure 1.3**; Van der Kogel, 1993). Accidental or therapy related over-exposure to ionising radiation results in acute radiation sickness (ARS). Major manifestations include bone marrow failure, gastrointestinal syndrome and impaired fertility (Mettler *et al.*, 2007) which reflect stem/progenitor cell death and are seen in highly proliferating tissues enriched for hypomethylated genomes (**Figure 4.2**).

Heart appears to be an exception, as it is a low turnover tissue but was also found to be hypomethylated. However, the presence of heart stem cell-like cell populations has been demonstrated (Beltrami *et al.*, 2003; Matsuura *et al.*, 2004) whilst skeletal muscle regeneration studies have shown that ionising radiation can disrupt proliferation of satellite cells with little or no apparent damage to the mature muscle fibre (Quinlan *et al.*, 1995 and 1997; Hodgetts and Grounds, 2003). If the same is true for cardiac muscle this could suggest that the initial radiation-induced damage may not be easily detectable and would further support the correlation between radiosensitivity and DNA

methylation status as this would constitute heart as a radiosensitive hypomethylated but low turnover tissue. Additionally, an increased long-term risk of cardiovascular disease has been associated with exposure to ionising radiation (Kodama *et al.*, 1996; Preston *et al.*, 2003; Trivedi and Hannan, 2004).

The methylation status of r-AML and BL and TL was also assessed using both HPLC and Southern blotting. All radiation-induced malignancies (DNA extracted from leukaemic spleens and thymus) arose in mice following exposure to 3Gy X-rays and were found to be hypomethylated compared to control spleen (**Figures 4.1** and **4.3**). Moreover, their methylation status reflected that of their un-transformed target cells. As expected for a BM stem cell malignancy (Greaves, 1996) r-AML samples showed a 5-^{Me}C content similar to that of BM. Similarly, the overall methylation levels of progenitor cell BL and TL (Cleary *et al.*, 2001; Boulton *et al.*, 2002) were intermediate between spleen and bone marrow and reflected the 5-^{Me}C content of the more mature progenitor cell they arose from.

A similar correlation between malignancy/untransformed cell relative LINE-1 methylation status has been reported in a wide range of human cancers (including lung, prostate gland, stomach, colon and breast cancer) (Chalitchagorn *et al.*, 2004) highlighting the importance of choosing the appropriate control when reporting the relative methylation of various types of cancer.

Hypomethylation can lead to transcriptional activation of endogenous retrotransposable elements. Radiation-induced malignancies showed increased levels of IAP RNA which was not seen in any of the control tissues analysed (**Figure 4.7**). BM and testes were found to be relatively hypomethylated but showed negligible levels of IAP RNA. Moreover the high variation in the levels of IAP RNA seen in the three malignancies, provide strong evidence of aberrant DNA methylation patterns in the process of radiation-induced leukaemogenesis. Retrotransposon related disease is a rare event seen more often in mice than human (Kazazian and Moran, 1998). There have been however, some reports implicating LINE-1 retrotransposition-like insertions in human cancer. Disruption of the *APC* gene, following insertion of a LINE-1 has been reported in a colon cancer patient (Miki *et al.*, 1998) and a similar event disrupting the proto-oncogene c-*myc* has been found in breast cancer (Morse *et al.*, 1988). Decreased

methylation of LINE-1 sequences has been documented in a large number of human cancers (Chalitchagorn *et al.*, 2004; Schulz, 2006) including chronic lymphocytic leukaemia (Dante *et al.*, 1992). It has not been determined if these events can trigger leukaemogenesis but they can be considered a phenotype of increased genomic instability and aberrant DNA methylation, possibly predisposing cells to malignant transformation.

Exposure of C57BL/6 and CBA/H mice to 3Gy X-rays revealed a genotype- and tissue-dependant radiation-induced hypomethylation. Both strains had shown similar radiosensitivity levels and rates of recovery (**Figure 4.5**) for both spleen and BM. No decrease in the overall DNA methylation levels was seen in the CBA/H spleen and C57BL/6 bone marrow, which is in agreement with previous studies (Tawa *et al.*, 1998).

A persistent decrease in DNA methylation levels was seen in irradiated CBA/H bone marrow, suggestive of radiation-induced tissue hypomethylation. Total BM was used for the analyses so it was not possible to deduce whether this hypomethylation was ubiquitous or restricted to specific subpopulations of BM cells. Moreover, the overall decrease in BM methylation could actually reflect changes in the numbers of specific BM cell populations, given the expected differences in the global DNA 5-^{Me}C content of different populations of cells (as also seen in **Figure 4.4**). A Scharfe system Casy® 1 cell coulter counter was used to monitor BM recovery post-irradiation (see section 2.17). This method was reliable in quantifying the percentage of white bone marrow cell loss but could not distinguish between different subpopulations of WBMC. A 4-fold difference in the number of Lin^- $Sca\text{-}1^+$ $c\text{-}Kit^+$ cells was found between the r-AML susceptible CBA/H and the r-AML resistant C57BL/6 mouse strains (see **Chapter 3**; Jawad *et al.*, 2008) using flow cytometry. As haemopoiesis appears to be driven by different cell populations in the two mouse strains, it is possible that exposure to ionising radiation will have different effects on their BM proliferating compartments. Further analysis using cell fractionation and a more sensitive DNA methylation assay might reveal further differences in the reconstituted BM in terms of cell numbers and DNA methylation levels.

4.5 Conclusion and future work.

Ionising radiation has been found to induce genotype-dependant genomic instability in bone marrow cells (Kadhim *et al.*, 1994; Watson *et al.*, 1997; Lorimore *et al.*, 2003). CBA/H (r-AML susceptible) BM cells are more susceptible to radiation-induced chromosomal instability compared to the r-AML resistant C57BL/6 mouse strain. CBA/H total BM showed decreased levels of DNA methylation following exposure to 3Gy X-rays (**Figure 4.6**) whereas no decrease was seen in the BM of irradiated C57BL/6 mice. DNA hypomethylation is often seen in cancer and has been associated with genomic instability both *in vivo* and *in vitro* (Duthie and Hawdon, 1998; reviewed in Fenech, 2001; Zijno *et al.*, 2003; Basten *et al.*, 2006). Additionally, ionising radiation induces cleavage and increased catabolism of folate *in vivo* (Kesavan *et al.*, 2003) possibly disrupting DNA synthesis/repair and DNA methylation. This raises the possibility of a relationship between relative hypomethylated status and susceptibility to r-AML.

The role of ionising radiation as the sole causative agent in the process of leukaemogenesis can not be conclusively supported. However, cleavage of folate as a direct result of ionising radiation exposure (Kesavan *et al.*, 2003), radiation-induced bystander effects, radiation-induced genomic instability and the role of oxidative stress in a wide range of health implications (see sections 1.3.2, 1.3.3, 1.5.3 and 1.5.5) suggest that exposure to ionising radiation might predispose the surviving BM stem cell compartment to malignant transformation by promoting the development of genotoxic conditions within the tissue microenvironment. Irrespective of its exact role, ionising radiation exposure is involved in the multistage process of r-AML and as the effects of ionising radiation are non-targeted, aberrant DNA methylation could also be implicated.

If ionising radiation induces further DNA hypomethylation and if aberrant DNA hypomethylation can lead to increased chromosomal instability and activation of retrotransposable elements, then, already hypomethylated genomes will be at a higher risk of radiation-induced effects. Ionising radiation might thus induce epigenetic changes in the already hypomethylated bone marrow that predispose the radiosensitive bone marrow cells to malignant transformation following exposure. This could explain the higher incidence of r-AML in A-bomb survivors and whole-body-radiotherapy

patients. Moreover the relatively long r-AML latency period (1 ½ years in mice) and the aberrant hypomethylation seen in the haemopoietic malignancies (**Figure 4.7**) support the hypothesis that this initial decrease in global methylation could result in increased genomic instability and the accumulation of genetic and epigenetic changes that might trigger malignant transformation (i.e. hypomethylation could be the initiating event in radiation leukaemogenesis).

Similarly, highly proliferating hypomethylated genomes might show increased rates of cell death following exposure to ionising radiation as they are at a higher risk of radiation-induced deleterious effects. This study investigated the radiosensitivity of two different haemopoietic tissues *in vivo* (spleen and BM). The relatively hypomethylated BM showed increased radiosensitivity compared to the relatively hypermethylated spleen. The radiosensitivity and kinetics of recovery support the correlation between hypomethylation and radiosensitivity and are in agreement with previous findings (Midgley *et al.*, 1995; Colter *et al.*, 2001; Dazzi *et al.*, 2006). This is best seen when considering the increased radiosensitivity of ICF patients. ICF patients' lymphoblastoid cell lines show increased levels of radiation-induced cytotoxicity when compared to control and AT cell lines (Narayan *et al.*, 2000). Although differences in proliferation rates might partly account for differences in cell death between different tissues, the *in vitro* experimental data suggest that other factors might also be involved (since proliferation rates was not a factor in these clonogenic assays). Hypomethylation of specific centromeric and juxtacentromeric genomic regions has been shown to increase chromosomal rearrangement events and affect genome stability (Tuch-Muller *et al.*, 2000; Ehrlich *et al.*, 2001). BM cells were found to be hypomethylated in those repeats which could exasperate the effects of ionising radiation exposure and result in increased levels of cell death.

This published study (Giotopoulos *et al.*, 2006) has produced interesting results and has generated preliminary data to support further investigations. BM is comprised of a highly heterogeneous population of cells. Cell fractionation assays could enable the isolation and assessment of specific cell populations (e.g. in terms of cell numbers and DNA methylation levels), particularly the immature haemopoietic stem cell compartment, before and after irradiation *in vivo*. It is possible that the radiation-induced hypomethylation seen in CBA/H mice is a reflection of changes in the numbers

of cell subpopulations in the reconstituted BM, rather than an actual decrease in DNA methylation levels. The kinetics of BM recovery could also be analysed in a similar fashion to enable identification of possible differences between the r-AML resistant and r-AML susceptible mouse strains that could elucidate their different predisposition to specific haemopoietic malignancies. The cell coulter counter profiles did not reveal any obvious differences in the kinetics of BM recovery between the two strains but could not distinguish between the different types of white bone marrow cells during the reconstitution process as seen between the two mouse strains using flow cytometry (**Chapter 3**; Jawad *et al.*, 2007b and 2008). Flow cytometry techniques could therefore, provide the required sensitivity to detect subtle changes in WBMC composition between the two strains and characterise the reconstituted BM following exposure to ionising radiation in greater detail. Finally, if radiation-induced hypomethylation is a by-product of the folate cycle disruption, other possible implications should also be investigated. Disruption of the folate pathway can also result in uracil incorporation, increasing mutation rates and genomic instability (see section 1.5.3). The folate availability in the BM and serum can be assessed and possibly linked to both the levels of resulting hypomethylation and incidence of uracil incorporation in post-irradiated tissues from both mouse strains.

Chapter 5:

Radiotherapy and normal tissue damage in breast cancer patients

5.1 Introduction.

As previously discussed (see section 1.4), radiotherapy patients show considerable variation with regards to their acute or long term normal tissue reactions to ionising radiation. The increased cellular and clinical radiosensitivity of patients affected by genetic syndromes such as AT (Rogers *et al.*, 2000), as well as the increased *in vitro* radiosensitivity of first-degree relatives of radiosensitive patients (Roberts *et al.*, 1999; Burrill *et al.*, 2000) suggest that these reactions might be under genetic control. Identifying such modifying genetic factors could lead to the development of a clinically useful genetic test.

5.1.1 Radiotherapy and breast cancer.

With ~44,000 new cases diagnosed in 2004, breast cancer is the most common female cancer in the UK. It is estimated that the lifetime risk of women in the UK developing breast cancer is 1:9 (Toms, 2004).

Radiotherapy is one of the most effective treatments for cancer as it offers high probability of local tumour control in a variety of malignancies, including breast cancer. The prevalence of radiotherapy treatment in breast cancer is high since it substantially reduces the risk of local recurrence after surgery. Patients with high risk factors for local recurrence after mastectomy and all patients treated by breast conservation (combination of chemotherapy, radiotherapy and lumpectomy) will be offered radiotherapy as part of their treatment (Bentzen, 2006).

Despite its benefits radiotherapy has however been associated with a variety of normal tissue reactions (see section 1.3.1) ranging from asymptomatic changes in tissue

structure and function to cosmetic disfiguration, or even significant (and in rare cases life threatening) changes in organ function (Bentzen *et al*., 2003; O'Sullivan and Levin, 2003). These normal tissue reactions mainly affect the patient's quality of life and as the life expectancy of cancer patients increases, normal tissue effects are of growing clinical importance.

5.1.2 Normal tissue reactions in breast cancer patients treated with radiotherapy.

As previously discussed (see section 1.3.1), normal tissue reactions can be divided into early/acute reactions, which occur within 90 days of treatment, and late/long term reactions, that occur more than 90 days after treatment (Bentzen and Overgaard, 1993). Breast cancer patients may present with acute and/or late reactions to radiotherapy. Many studies support the involvement of genetic factors in radiosensitivity and predisposition to long term normal tissue damage (reviewed in Andreassen *et al.*, 2002; discussed in section 1.4).

5.1.3 Scoring of normal tissue injury.

It is not clear whether late tissue effects such as fibrosis, telangiectasia and atrophy are biologically or radiologically related. The fact that patients may present with one or different combinations of these phenotypes suggests that their underlying causes may not necessarily be the same. The power of genetic studies seeking to associate a genotype with a phenotype is therefore absolutely dependent on the precise definition of the injury phenotype.

Several normal tissue damage scoring systems have been developed but many failed to gain general acceptance due to their limitations. For example, the French/Italian Glossary scale records the maximum grade of any reaction, therefore merging various endpoints for each organ. Shakespeare *et al.* (1998) reported failure to score 56.5% of toxicities in a study of 47 patients treated for cervical cancer using this scale. In addition to its specificity to gynaecological cancers the French Italian glossary fails to distinguish between acute and late reactions, thus excluding important radiological parameters such as large dose per fraction or high dose rate (Christie *et al.*, 1995; Shakespeare *et al*., 1998). A commonly used scoring system is the Radiation Therapy

Oncology Group (RTOG) and European Organization for Research and Treatment of Cancer (EORTC) scales. The RTOG/EORTC system covers all major tissues that might be injured following radiotherapy and does separate early from late reactions. The site treated is scored on a scale from 0–5 according to the degree of injury incurred, with an extreme score of 5 indicating patient death (Cox *et al.*, 1995). A major limitation of this scoring system is however the fact that it does not allow scoring of specific phenotypes as the patient is given a single overall score.

In order to improve the efficiency of normal tissue damage scoring, as well as enable uniform reporting of toxicity, the Late Effects of Normal Tissue-Subjective Objective Management Analytical (LENT-SOMA) system was introduced, based on recommendations from both the RTOG and EORTC groups (Pavy *et al.*, 1995). As in the case of the RTOG/EORTC scales, the LENT-SOMA scales can be used to score normal tissue damage in all major cancers and distinguish between acute and late reactions. The inclusion of the SOMA (**S**ubjective-**O**bjective-**M**anagement-**A**nalytic) scales allows a more detailed and specific description of the nature (phenotype) and severity of the injury/ies. Each treatment site can be assessed using a combination of organ-specific scales with each scale given a score of 0–4 (5 indicating death or loss of organ). The system employs the following scales (according to: Pavy *et al.*, 1995; Rubin *et al.*, 1995):

- Subjective: Relying on questionnaires, diaries, or interviews, the subjective scales are used to record treatment toxicity from the patients' point of view (e.g. pain).
- Objective: Various phenotypes of normal tissue damage are scored separately during a physical examination by a clinician. This section includes separate scores for telangiectasia, atrophy and fibrosis. As well as improving the recording of treatment toxicity, this separation of phenotypes is extremely useful in genetic association studies as it allows for separate analysis of different phenotypes.
- Management: Records any medical intervention (e.g. drugs) in order to palliate or ameliorate radiation-induced symptoms.
- Analytic: This subcategory is an extension of the objective/management scales, indicating whether even more specialised techniques have been employed to asses tissue function (e.g. MRI).

A final summary section is often included in order to combine the various SOMA scales into a final clinical assignment of grade (Rubin *et al.*, 1995).

5.1.4 Selecting candidate genes.

To identify any functional SNPs associated with normal tissue injury, a retrospective genetic association study was conducted. This was a pilot study in which a candidate gene approach was adopted. Breast cancer patients that had been offered radiotherapy as part of their treatment were scored using the LENT-SOMA scale and genotyped for a number of known functional SNPs in genes that may be involved in normal tissue damage (**Table 5.1**).

Table 5.1

Polymorphism	Function	Locus	SNP	NCBI rs number
APEX1 D148E	DNA repair	14q11.2-q12	T → G	rs1130409
CX3CR1 V249I	Inflammation response	3p21.3	G → A	rs3732379
DHFR deletion	Folate metabolism	5q11.2-q13.2	19bp deletion	not available
EPHX1 Y113H	Carcinogen metabolism	1q42.1	T → C	rs1051740
EPHX1 H139R	Carcinogen metabolism	1q42.1	A → G	rs2234922
HFE C282Y	Iron metabolism	6p21.3	G → A	rs1800562
MTHFR A226V	Folate metabolism	1p36.3	C → T	rs1801133
MTHFR E433A	Folate metabolism	1p36.3	A → C	rs1801131
MTR D919G	Folate metabolism	1q43	A → G	rs45445801
TGFβ-1 C-509T	Inflammation response	19q13.1	C → T	rs1800469
XRCC1 R194W	DNA repair	19q13.2	C → T	rs1799782
XRCC1 R399Q	DNA repair	19q13.2	G → A	rs25487
XRCC2 R188H	DNA repair	7q36	G → A	rs3218536

Table 5.1: Gene polymorphisms investigated in this study.

For the purposes of this thesis, the definition of 'homozygotes for a specific polymorphism' refers to the individuals carrying the rare/less common allele. Unless otherwise stated, any effects reported (e.g. enzymatic activity, cancer risk,

radiosensitivity) correspond to the less common allele. When discussing the polymorphism, the position of the polymorphism is preceded by the common allele version and followed by the rare (e.g. in the XRCC1 R194W polymorphism, R has been substituted with W in the amino acid position 194).

5.1.4.1 DNA repair genes.

The importance of DNA repair mechanisms in response to ionising radiation has been previously discussed (see section 1.3.2). X-ray Repair Cross Complementing genes (XRCC)-1 and -2 play major roles in different DNA repair pathways and were thus included in the study.

XRCC1 is involved in base excision repair (BER) of single strand breaks. *XRCC1*$^{-/-}$ mice exhibit an embryonic lethal phenotype whilst mutant embryo-derived cells show a 1.4-fold hypersensitivity to X-rays compared to control cell lines in which the gene is normally expressed (Tebbs *et al.*, 1999). In humans, breast cancer cell lines expressing different levels of XRCC1 protein showed increased radiosensitivity which correlated with reduced levels of XRCC1 expression (Brem and Hall, 2005). A number of studies have investigated the role of at least two *XRCC1* functional SNPs in IR hypersensitivity and risk of long term normal tissue damage in breast cancer patients (Hu *et al.*, 2001 and 2002; Andreassen *et al.*, 2003 and 2006). XRCC1 R194W and R399Q are frequently found polymorphisms in the general population and have also been included in a number of cancer association studies (reviewed in Ladiges, 2006).

A large number of studies have reported a reduced cancer risk in the presence of the XRCC1 194W allele (reviewed in Goode *et al.*, 2002; Hu *et al.*, 2005; Hung *et al.*, 2005). It has been suggested that the amino acid change in the XRCC1 194W allele could enhance protein binding (Ladiges, 2006) but this has not been verified by any functional studies.

The XRCC1 R399Q SNP has also been extensively studied. In a review by Goode *et al.* (2002) the XRCC1 399Q allele was associated with a decreased risk for bladder and oesophageal cancer but an increased risk for lung and stomach cancer. There was however no association found between cancer risk and the specific genotype in a meta-

analysis (Hu *et al.*, 2005) and a later study (Hung *et al.*, 2005). Au *et al.* (2003) reported an increase in chromosomal deletions in whole-blood cells from individuals carrying the 399Q polymorphism following exposure to X-rays or UV light.

XRCC2 is involved in the repair of double strand breaks by homologous recombination repair (HRR). The gene encodes a Rad51-like protein and was shown to be an essential part of the HRR repair pathway by promoting the activity of Rad51 (Liu, 2002; Thacker and Zdzienicka, 2004). XRCC2 cDNA can significantly complement the phenotype of the irs1 hamster cell line which shows hypersensitivity to ionising radiation (Cartwright *et al.*, 1998). Rafii *et al.* (2002) demonstrated that the naturally occurring XRCC2 R188H polymorphism has a weak increasing effect on protein function and is weakly associated with breast cancer risk [OR=1.3 (95%CI 1.0-1.8)]. In contrast, Danoy *et al.* (2007) have shown that the XRCC2 188H allele confers increased resistance to cisplatin-induced DNA damage *in vitro*.

APEX1 (also found as *APE1*) is involved in the base excision repair (BER) pathway. In humans, it is the major protein responsible for the removal of abasic sites in the DNA. A number of APEX1 polymorphisms exhibit reduced nuclease function (Hadi *et al.*, 2000). The APEX1 D148E polymorphism has been shown to induce prolonged cell cycle arrest in irradiated (3Gy) human lymphocytes (Hu *et al.*, 2001 and 2002) and could possibly impair the DNA repair efficiency of its carriers.

5.1.4.2 Folate metabolism genes.

A number of genes involved in folate metabolism were included in this study. These enzymes are essential for DNA methylation, homocysteine metabolism and the conversion of Uracil to Thymine (see section 1.5.3; **Figure 1.7**). Ionising radiation induces cleavage of folate (Kesavan *et al.*, 2003) possibly affecting the pathway. Any aberrations in enzymatic activity could therefore have an effect on both radiosensitivity and risk of long term normal tissue damage.

Two Methylenetetrahydrofolate Reductase (*MTHFR*) polymorphisms have well characterised effects on MTHFR enzymatic activity. Homozygotes for the T allele of the MTHFR C677T polymorphism have ~30% of the *in vitro* MTHFR enzyme activity

of those who are homozygous for the common C allele, whereas individuals carrying the 677CT genotype show ~65% of the *in vitro* normal MTHFR enzyme activity (Sarbia *et al.*, 2006). The specific polymorphism has been associated with increased risk for coronary artery disease (Morita *et al.*, 1997) and neural tube defects (van der Put *et al.*, 1995). Homozygotes for the MTHFR A1298C polymorphism do not appear to have an altered biochemical profile to the individuals carrying the common allele. However, individuals who are heterozygotes for both the C677T and A1298C show an increase in serum homocysteine levels and have decreased serum folate levels (Kara *et al.*, 2003).

Homozygotes for the 5-Methyltetrahydrofolate-homocysteine methyltransferase (*MTR*) (also found as *MS*, methionine synthase) A2756G polymorphism present with lower serum homocysteine levels, indicative of increased enzymatic activity (Sarbia *et al.*, 2006). The MTR 2756GG genotype has been associated with an increased risk of lymphoma (Matsuo *et al.*, 2001) and coronary heart disease (Klerk *et al.*, 2003).

The only non-single nucleotide polymorphism in this study was a 19bp deletion in the intron-1 of the Dihydrofolate Reductase (*DHFR*) gene. Homozygosity for the specific polymorphism was significantly more frequent in mothers of patients affected with spina bifida (a condition strongly influenced by folate levels during pregnancy), possibly suggesting decreased enzymatic activity (Johnson *et al.*, 2004).

5.1.4.3 Inflammation genes.

Oxidative stress induced by ionising radiation (see sections 1.3.2 and 1.3.3) can lead to local and persistent inflammation. Genes that are involved in inflammatory responses are therefore ideal candidates for this study.

CX3CR1 encodes for a chemokine receptor specific for the chemokine fractaline (CX3CL1) which is upregulated on inflamed endothelium (McDermott *et al.*, 2001). Chemokines act as chemoattractants, directing migration of leukocytes from the blood to sites of inflammation, and have been implicated in a wide range of conditions such as cancer, atherosclerosis, autoimmune diseases and graft rejection (reviewed in Dong *et al.*, 2003). The CX3CR1 V249I polymorphism (I allele) has been associated with a

reduced risk of acute coronary events and a reduced number of fractaline binding sites (McDermott *et al.*, 2001 and 2003).

Transforming Growth Factor beta-1 (TGF*β*-1) is a cytokine responsible for regulation of fibroblast proliferation and differentiation (Randall and Coggle, 1995; Gauldie *et al.*, 2003). Development of fibrosis involves the replacement of normal cells with mesenchymal cells, which then overproduce extracellular matrix resulting in the fibrotic phenotype (see section 1.3.1; Li *et al.*, 1999). TGF*β*-1 is actively involved in the formation of fibrosis by means of stimulating fibroblast growth and inducing deposition of extracellular matrix (Davis *et al.*, 2003). Randall and Coggle (1995 and 1996) reported a radiation-induced over-expression of TGF*β*-1 which was persistent for the duration of these studies (55 days and 9 months post-irradiation respectively). Radiation-induced over-expression of TGF*β*-1 has been reported by a number of studies (Ehrhart *et al.*, 1997; Martin *et al.*, 1997 and 2000; O'Sullivan and Levin, 2003) whereas increased plasma levels of TGF*β*-1 correlated with radiation-induced fibrosis in lung and breast cancer patients (Anscher *et al.*, 1997; Awad *et al.*, 1998; Grainger *et al.*, 1999; Li *et al.*, 1999). The TGF*β*-1 C-509T promoter polymorphism (T allele) results in higher plasma TGF*β*-1 levels and has been associated with an increased risk of fibrosis in breast cancer patients (Quarmby *et al.*, 2003). All the above constituted TGF*β*-1 as the strongest candidate in this study as this was the only gene for which data reported in the literature were at least suggestive of its implication in radiation-induced long term normal tissue damage.

5.1.4.4 General metabolism and carcinogen detoxification genes.

The Microsomal Epoxide Hydrolase gene (*EPHX1*) was also included in the study. The EPHX1 (also found as HYL1) enzyme plays an important role in the hydrolysis of various environmental carcinogens and is involved in benzene metabolism (Lebailly *et al.*, 2002). The relatively common functional polymorphisms EPHX1 Y113H and H139R result in a 40-50% decrease and a 25% increase in enzymatic activity (*in vitro*) respectively (Gresner *et al.*, 2007). Combinations of these two polymorphisms resulting in high enzymatic activity have been associated with increased risk of t-AML (Lebailly *et al.*, 2002) and increased lung cancer risk in Caucasians (Gresner *et al.*, 2007).

Iron is known to cause oxidative stress via the production of Reactive Oxygen Species (ROS) and is probably the most abundant pro-oxidant in the organism (Andreassen, 2002). Iron metabolism is impaired in individuals affected with haemochromatosis which is a very common single-gene hereditary disorder. Heterozygotes for mutations n the *HFE* gene show elevated levels of iron in their blood due to defective iron metabolism (Bulaj, 1996) which could possibly exacerbate the effects of exposure to ionising radiation. A common mutation in the *HFE* gene (C282Y) was therefore included in the study.

5.1.5 Aims of the study.

The aim of this study was to investigate any possible association between selected known functional gene polymorphisms (**Table 5.1**) and normal tissue damage in breast cancer patients treated with radiotherapy.

5.2 Materials and Methods.

5.2.1 Patients.

This study has been undertaken with the participation of 167 patients attending the oncology departments of Leicester Royal Infirmary, Glenfield Hospital, Leicester and Nottingham City Hospital, UK. Drs Paul Symonds, Karen Foweraker, Matt Griffin and Irene Peat were responsible for patient recruitment, scoring of radiation-induced normal tissue damage and sample collection. Full ethical and local trust approval was obtained from the relevant ethics committees and trust Research and Development departments. Seven patients refused to take part in the study whilst all remaining (n=167) patients gave written informed consent before entry into the study.

Clinicians performed a physical examination during follow-up clinics and scored signs (or absence) of normal tissue damage using both the LENT/SOMA and RTOG scales. Patients' records indicated whether they had suffered from an acute reaction.

All patients were tumour-free and had received radiotherapy as part of their treatment for breast cancer. The majority (155/167) were treated more than 4 years previously

(median=6.1 years), but 12 additional patients who were known to have late effects were examined at the City Hospital, Nottingham (n=5), and the Leicester Royal Infirmary (n=7), UK between 2.3 and 3.6 years after treatment. The mean age at treatment was 56.92 (range 30–78). The majority of patients (157/167) were Caucasians, with nine patients being of Asian descent and one patient of African Caribbean descent.

All patients were asked about potential radiosensitising co-morbid diseases such as diabetes or collagen vascular disorders and a family history of abnormal reactions to radiotherapy.

One hundred and sixteen patients had a lumpectomy, forty-seven patients had a mastectomy plus auxiliary dissection, two patients had a lumpectomy but then went on to have a mastectomy and two had no surgery. Radiotherapy (6MV X-rays) was given either after mastectomy or lumpectomy using tangential fields, and all patients received similar field sizes. All patients also had a 1.5 cm thick strip of wax 4 cm in width applied to either the lumpectomy or mastectomy scar to reduce 'skin sparing' during every second fraction. **Table 5.2** shows the details of radiotherapy, chemotherapy and hormonal treatment schedules.

Table 5.2				Number of patients			
No. of patients	Total dose	No. of fractions	2Gy/fraction equivalent dose	Chemotherapy	Tamoxifen	No boost	Boost
1*****	15.75	7	16.73	-	1	1	-
1*****	34	17	34	-	-	-	1
1*****	38	17	40.64	-	1	-	1
10	40	15	46.6	2	10	9	1
119	45	20	47.81	33	109	48	71
2	48	24	48	1	1	1	-
33	50	25	50	9	29	33	1

Table 5.2: Summary of radiotherapy, chemotherapy and hormonal treatment schedules. In cases where the patient also received a 15Gy electron boost, an additional 18.57Gy (2Gy/fraction equivalent isoeffective dose) should be added to their total dose. The isoeffective dose (column 4) takes into account factors (e.g. dose per fraction, number of fractions, exposed tissue) that can influence clinical effects. This value was used in all statistical analyses.

***** refers to patients that did not complete radiotherapy due to a severe acute reaction.

One hundred and nineteen patients received 45 Gy (20 fractions in 4 weeks) which was the standard departmental protocol at the time. Ten patients received 40 Gy in 15 fractions as part of the START B trial (NCRN Trial Standardisation of Breast Radiotherapy, 1998). Thirty-three patients were treated with a whole-breast dose of 50 Gy in 25 fractions either as part of the START trial or following the publication of the European Organisation of Cancer Radiotherapy and Breast Cancer Groups study (EORTC) (Bartelink *et al.*, 2001), which identified a group of patients (node negative, complete excision, aged <50) who did not require a local boost. In addition to X-rays, 71 of these patients treated by local excision also received a boost of 15 Gy in 5 fractions in 1 week using 8–12 MeV electrons to the site of the lumpectomy. Boost area sizes were between 6x6 and 8x10 cm. Twenty-seven patients received anthracycline based chemotherapy (two of whom also received CMF), eighteen patients received non-anthracycline-based chemotherapy (CMF) before radiotherapy, and one hundred and fifty-one patients were further treated with tamoxifen. Twenty-five patients were positive for an acute reaction within 90 days of treatment and three patients did not complete the radiotherapy schedule due to a severe acute reaction to radiotherapy.

5.2.2 Sample collection and preparation.

DNA was collected from patients by means of a buccal swab, stored in NDS solution and extracted using the QIAamp DNA mini kit (QIAGEN Ltd, Crawley, UK) using the manufacturer's standard protocol (see section 2.6).

5.2.3 PCR amplification.

PCR primer sequences were designed or obtained from published studies (see section 2.1.4; **Table 2.2**) and PCR conditions optimised for each gene polymorphism. In all cases the 11.1x PCR buffer was used (see sections 2.7 and 2.7.1). PCR conditions can be found in **Table 5.3**.

In order to genotype patients' DNA for the *DHFR* deletion three primers were used in the reaction mix· one reverse and two forward primers. Primer F1 rests within the 19bp deletion region whilst primer F2 bridges the gap caused by the deletion. This results in

fragments of 113bp and 92bp respectively, depending on the absence or presence of the deleted region.

Patients' DNA genotyping was performed by either RFLP analysis or dot blotting. In cases where a conclusive genotype could not be assigned, patient samples were sequenced. Additionally, ~5% of patients were randomly selected and sequenced for each polymorphism.

Table 5.3

Gene	PCR conditions
APEX1 D148E	5mins. at 96°C, followed by 40 cycles of: 1min. at 96°C, 1min. at 61°C, 1min. at 72°C, followed by a final 7mins. at 72°C.
CX3CR1 V249I	5mins. at 96°C, followed by 35 cycles of: 1min. at 96°C, 1min. at 69°C, 1min. at 72°C, followed by a final 7mins. at 72°C.
DHFR deletion	5mins. at 96°C, followed by 35 cycles of: 1min. at 96°C, 1min. at 60°C, 1min. at 72°C, followed by a final 7mins. at 72°C.
EPHX1 Y113H	5mins. at 96°C, followed by 35 cycles of: 1min. at 96°C, 1min. at 55°C, 1min. at 72°C, followed by a final 7mins. at 72°C.
EPHX1 H139R	5mins. at 96°C, followed by 35 cycles of: 1min. at 96°C, 1min. at 58°C, 1min. at 72°C, followed by a final 7mins. at 72°C.
HFE C282Y	5mins. at 96°C, followed by 35 cycles of: 1min. at 96°C, 1min. at 55°C, 1min. at 72°C, followed by a final 7mins. at 72°C.
MTHFR C677T	5mins. at 96°C, followed by 35 cycles of: 1min. at 96°C, 1min. at 65°C, 1min. at 72°C, followed by a final 7mins. at 72°C.
MTHFR A1298C	5mins. at 96°C, followed by 40 cycles of: 1min. at 96°C, 1min. at 62°C, 1min. at 72°C, followed by a final 7mins. at 72°C.
MTR D919G	5mins. at 96°C, followed by 35 cycles of: 1min. at 96°C, 1min. at 54°C, 1min. at 72°C, followed by a final 7mins. at 72°C.
TGFβ-1 C-509T	5mins. at 96°C, followed by 35 cycles of: 1min. at 96°C, 1min. at 58°C, 1min. at 72°C, followed by a final 7mins. at 72°C.
XRCC1 R194W	5mins. at 96°C, followed by 40 cycles of: 1min. at 96°C, 1min. at 62°C, 1min. at 72°C, followed by a final 7mins. at 72°C.
XRCC1 R399Q	5mins. at 96°C, followed by 40 cycles of: 1min. at 96°C, 1min. at 63°C, 1min. at 72°C, followed by a final 7mins. at 72°C.
XRCC2 R188H	5mins. at 96°C, followed by 40 cycles of: 30secs. at 96°C, 30secs. at 63°C, 30secs. at 72°C, followed by a final 7mins. at 72°C.

Table 5.3: Optimised PCR conditions for the candidate SNPs.

5.2.4 Restriction length fragment polymorphism (RFLP) genotyping.

In cases where the gene polymorphism was located within an enzyme restriction site, RFLP analysis (see section 2.9) was employed to genotype patients' DNA. The appropriate enzymes and resulting fragments are shown in **Table 5.4** and **Figure 5.1**. In all cases 5µl of PCR product were digested in a total reaction volume of 20µl containing: 1µl of the appropriate enzyme, 2µl of the appropriate NEB buffer and 12µl of dH_2O. The reactions were incubated overnight at 37^oC. All samples were genotyped blind and in duplicate.

In most cases digested DNA confirmed the presence of the polymorphic allele whereas undigested fragments denoted homozygosity for the common allele (except for: XRCC1 R399Q, MTHFR E433A, CX3CR1 V249I, and EPHX1 Y113H, for which the opposite applied). An additional *Mbo*II restriction site, located within the MTHFR E433A amplified fragment, created a digested fragment that was present in all patient samples and acted as internal control for complete digestion. Both the undigested and digested bands were present in heterozygotes. **Figure 5.1** shows examples of digested PCR products.

Table 5.4				
Gene/SNP	**Polymorphism**	**Restriction enzyme**	**Undigested fragment size (bp)**	**Digested fragment size (bp)**
APEX1 D148E	T → G	*Bfa*I	164	144 + 20 (G allele)
CX3CR1 V249I	G → A	*Acl*I	311	107 + 204 (G allele)
EPHX1 Y113H	T → C	*Eco*RV	162	140 + 22 (T allele)
EPHX1 H139R	A → G	*Rsa*I	210	163 + 47 (G allele)
MTHFR A226V	C → T	*Hinf*I	198	175 + 23 (T allele)
MTHFR E433A	A → C	*Mbo*II	128	28 + (28 + 72)***** (A allele)
MTR D919G	A → G	*Hae*III	265	180 + 85 (G allele)
TGF*β*-1 C-509T	C → T	*Bsu36*I	419	190 + 229 (T allele)
XRCC1 R194W	C → T	*Pvu*II	490	294 + 196 (T allele)
XRCC1 R399Q	G → A	*Msp*I	402	269 + 133 (G allele)

Table 5.4: Restriction enzymes and resulting fragments (in bp). All reactions were incubated overnight at 37^{o}C.

*****The amplified fragment contained an additional *Mbo*II restriction site.

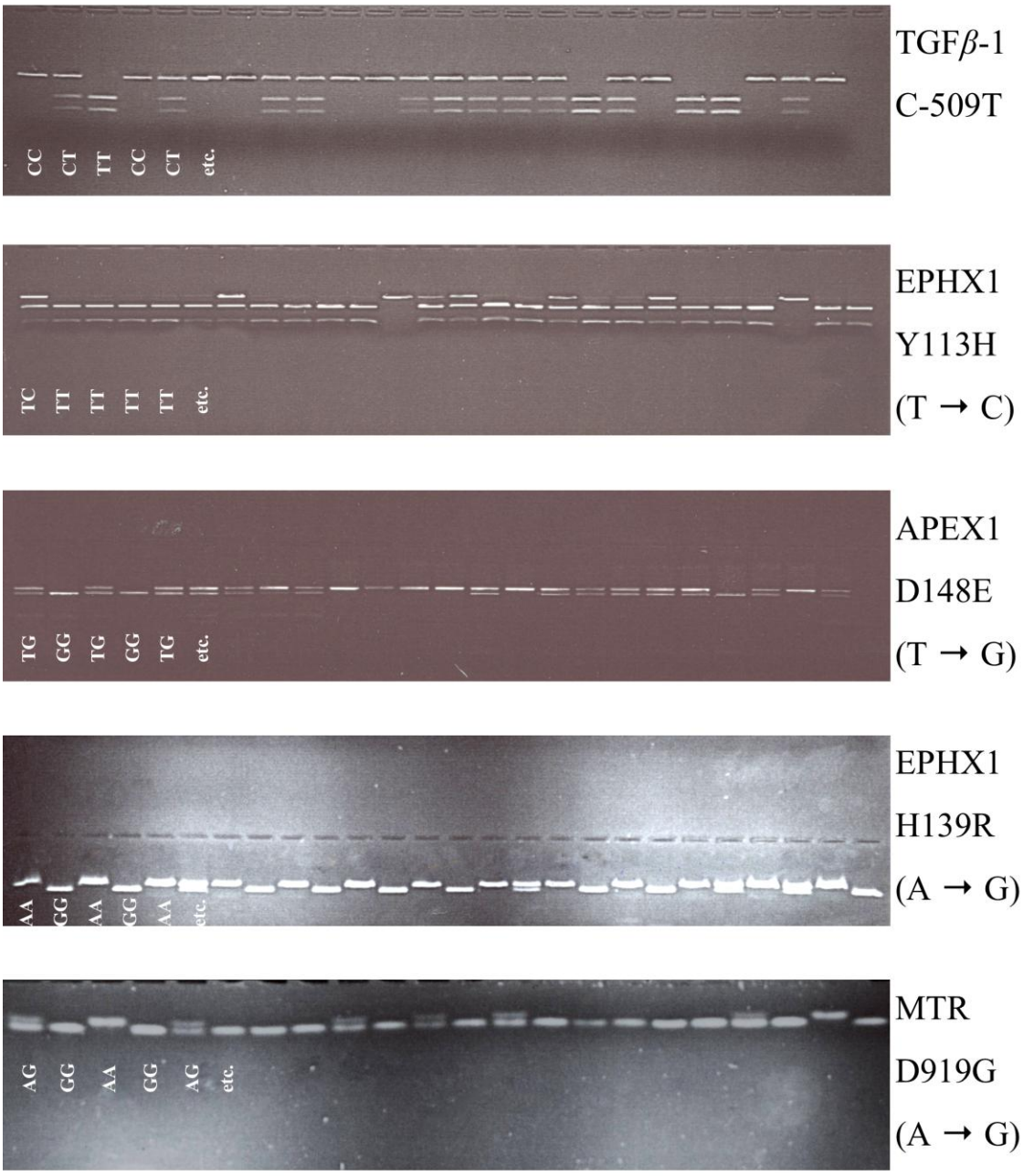

Figure 5.1: Digested PCR products were resolved by agarose gel electrophoresis and patients' genotypes were deduced from the resulting fragments.

5.2.5 Dot blot genotyping.

In cases where RFLP analysis was not applicable, Allele Specific Oligonucleotides (ASOs) were designed (see section 2.1.4; **Tables 2.2** and **2.3**). Following PCR amplification of the region of interest (see sections 2.7 and 2.7.1), a small volume ($1/10^{th}$ of the total PCR reaction volume) was run on a 1.5% agarose gel to confirm both the fragment size and DNA content across samples. Samples were then transferred onto a Hybond N-Fp membrane, hybridised with the appropriate common allele α-^{32}P-ATP labelled ASO probe and placed against film (see section 2.15 for the complete protocol). The membrane was then stripped and re-probed with the ASO for the rare polymorphism. All samples were genotyped blind and in duplicate.

Upon hybridisation a dot will appear on the exposed film indicating the presence of the corresponding allele. By combining the results of both ASO hybridisations a genotype can be assigned to each patient. **Figure 5.2** shows examples of hybridised membranes following autoradiographic exposure.

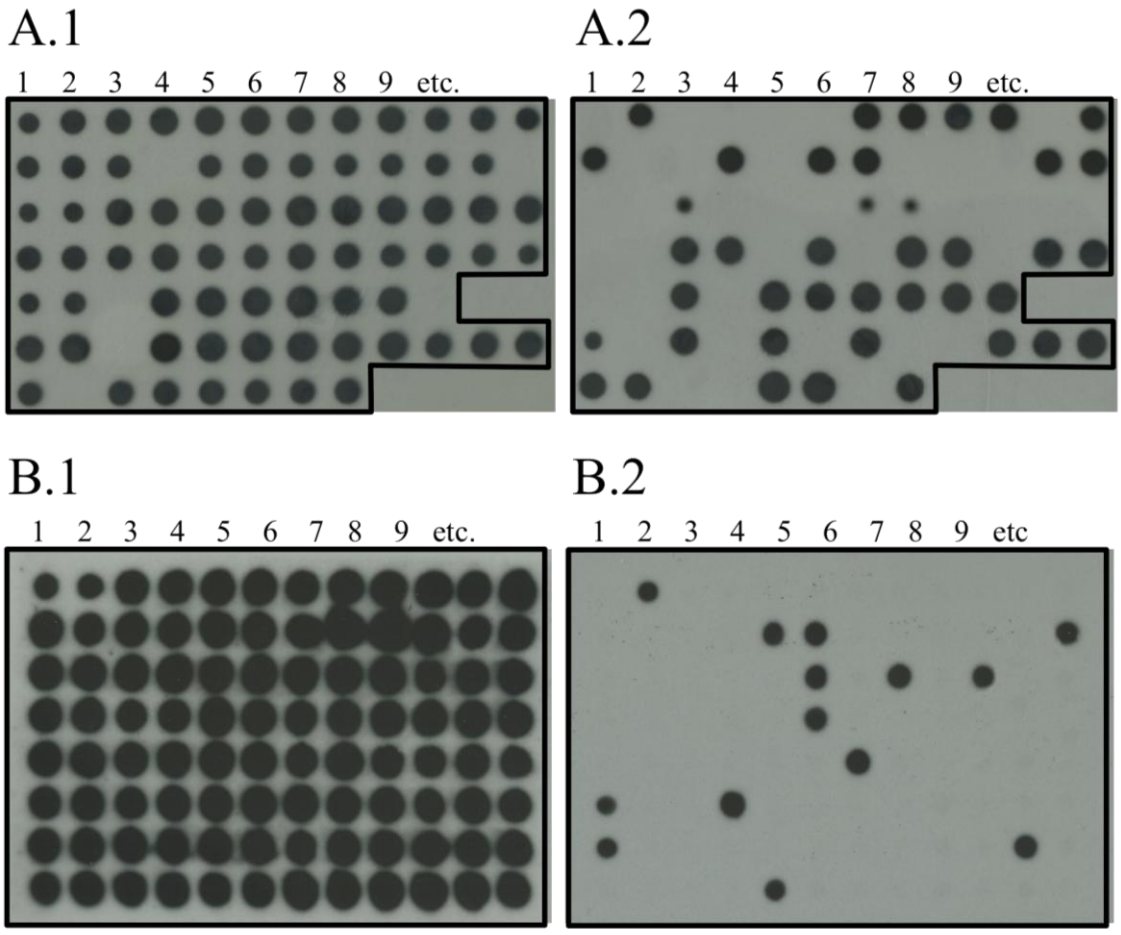

C.

A											
1:CC	2:CT	3:CC	4:CC	5:CC	6:CC	7:CT	8:CT	9:CT	10:CT	11:CC	12:CT
13:CT	14:CC	15:CC	16:TT	17:CC	18:CT	19:CT	20:CC	21:CC	22:CC	23:CT	etc.
B											
1:GG	2:GA	3:GG	4:GG	5:GG	6:GG	7:GG	8:GG	9:GG	10:GG	11:GG	12:GG
13:GG	14:GG	15:GG	16:GG	17:GA	18:GA	19:GG	20:GG	21:GG	22:GG	23:GG	etc.

Figure 5.2: Dot blot results for TGFβ-1 (A) and HFE (B) polymorphisms. Membranes were hybridised with oligonucleotides specific for one allele version (A1 and B1), stripped, and re-hybridised with oligonucleotides specific for the other (polymorphic) allele version (A2 and B2). Upon successful hybridisation a dot will appear on the exposed film, indicating the presence of the specific allele. A genotype can then be assigned to each sample by scoring both membranes for the presence/absence of hybridisation (C).

5.2.6 Statistical analysis.

All patients who participated in this study had been treated with radiotherapy for breast cancer and scored for any signs of radiation-induced normal tissue damage. This genetic association study was performed in order to associate a phenotype of normal tissue damage with a specific genotype, which should be in excess amongst the patients who presented with more severe reactions. A great advantage of this study was the fact that it required no additional group of controls (i.e. non-breast cancer patients) since patients who did not respond badly to radiotherapy acted as controls. The allele frequencies of all genotypes investigated were initially compared with those previously reported in the literature and assessed to be in Hardy-Weinberg equilibrium using the χ^2 test of independence (Sokal and Rohlf, 1995). According to the Hardy-Weinberg principle, allele frequencies (p and q) tend to remain constant within a model population, unless a certain genotype (p^2 or $2pq$ or q^2) confers a selective advantage (or disadvantage). In this study, any deviation from the reported frequencies might suggest a genotype predisposing to breast cancer or raise the question of incorrect genotyping.

The G-test was employed in order to investigate any possible associations between a specific genotype and phenotypes of radiation-induced damage. Due to the relative small sample size in this study, the G-test was preferred to the χ^2 test. The G-tests are maximum likelihood statistical significance tests (log-likelihood ratio) using the William's correction for small sample size (Sokal and Rohlf, 1995). Allele frequencies were also examined by calculating the odds ratios (OR), with 95% confidence intervals (95% CI), for the frequency of the polymorphic allele in one group relative to another.

5.3 Results.

A total of 167 breast cancer patients that had been treated with radiotherapy were recruited and examined for late normal tissue damage. With the exception of three patients, all patients received doses of ~45-50Gy X-rays. In some cases, an additional 15Gy electron boost was administered raising the highest dose to ~65Gy. Two out of the three patients who did not complete their radiotherapy schedules also received an electron boost which meant that only one out of 167 patients did not receive at least 45Gy as part of their treatment (**Table 5.2**).

Both the RTOG and the LENT-SOMA scales were used in order to score for signs of normal tissue damage. As expected, the comparatively non-specific RTOG scoring system, as well as the overall (sum of scores) LENT-SOMA values, proved to be non-informative in all association tests performed (data not shown). These approaches mix various endpoints (i.e. do not separate different phenotypes of normal tissue damage) therefore possibly masking any association with a specific genotype.

The separate objective LENT-SOMA (0-4) scales were used to perform the association study (Pavy *et al.*, 1995; Rubin *et al.*, 1995). These allow for separate scoring of fibrosis, atrophy and telangiectasia, which represent separate phenotypic measures of late normal tissue damage. Patients were divided into two groups: A group which showed no signs of a particular injury phenotype (LENT-SOMA score of 0) and a group in which patients showed unambiguous evidence of late tissue injury (LENT-SOMA score of 2-4). The SOMA scores of 1 represent subtle examiner-dependent changes that are inconclusive and in this study are either excluded or included in the group of patients that show no signs (SOMA 0) of a particular injury phenotype. Unless stated otherwise, comparisons in this study included patients with scores of 0 *vs.* patients with scores of 2-4.

In addition to genetic predisposition, factors such as anatomical differences between individuals, radiation dose, chemotherapy and an early acute reaction might influence the risk and severity of late normal tissue damage. A number of studies have reported an increased risk of late effects due to anthracycline containing regimens (Fiets *et al.*, 2003; Shanley *et al.*, 2006) but the number of patients who received anthracycline and non-anthracycline-based chemotherapy in this study was too small for any meaningful statistical analysis (**Table 5.2**).

5.3.1 Radiation dose and normal tissue damage.

Most patients included in this study received similar treatment doses (~45-50Gy). In addition to standard treatment some patients also received a 15Gy (2Gy/fraction isoeffective dose of 18.57Gy) which accounts for any major differences in dose received. As previously discussed, the boost area was similar in all patients. When taking the electron boost into account, only one patient out of the 167 received

significantly less than 45Gy (**Table 5.2**). This patient received only 15.75 Gy and was excluded from this analysis.

Table 5.5 shows the severity of atrophy, fibrosis and telangiectasia in patients who received a boost and in those who did not. No association was found between boost and acute reaction (p=0.34; data not shown).

Table 5.5	**Number of patients**					
	Fibrosis		Telangiectasia		Atrophy	
SOMA score	No boost	Boost	No boost	Boost	No Boost	Boost
0	67	47	66	44	69	43
1	14	18	10	7	15	24
2	8	8	11	14	6	6
3	2	2	4	10	1	2
p value (G-test)	0.47		0.03		0.28	

Table 5.5: Incidence and severity of normal tissue damage phenotypes in patients analysed, when divided into boost/no boost groups.

Patients who received the 15Gy boost (n=75) were compared with those who did not (n=91). The objective LENT-SOMA scales for atrophy, fibrosis and telangiectasia were employed and each phenotype was analysed separately. When comparing clearly affected patients (SOMA score: 2-4) with clearly unaffected (SOMA score: 0) no association was found between fibrosis and the 15Gy electron boost (p=0.47). Similarly no association was found between boost and atrophy (p=0.28).

Within the dose range of 45-65Gy, a 15Gy electron boost was weakly associated with an increased risk of telangiectasia (SOMA scores: 0 *vs.* 2-4, n=149) (OR 2.4; 95%CI 1.1-5.4; p=0.033). This was consistent with empirical clinical evidence as telangiectasia is usually confined to the area of the breast exposed to the boost.

5.3.2 Acute reaction and normal tissue damage.

To investigate whether an acute reaction (such as erythema and moist desquamation) predisposes patients (or can act as a predictive marker) to long term normal tissue

injury, presence/absence of an acute reaction was compared with the objective SOMA scales. There was no association between an early acute reaction and telangiectasia (p=0.67).

An increased incidence of both fibrosis and atrophy was seen in patients who presented with an acute reaction to radiotherapy. An acute reaction increased the risk of long term fibrosis (SOMA scores: 0 *vs.* 2-4, n=135) (OR 8.5; 95%CI 2.6-28.5; p=0.00004) and long term atrophy (SOMA scores: 0 *vs.* 2-4, n=128) (OR 4.7; 95%CI 1.2-17.6; p=0.02). **Table 5.6** shows the severity of atrophy, fibrosis and telangiectasia in patients who showed an acute reaction and in those who did not.

Table 5.6	**Number of patients**					
	Fibrosis		Telangiectasia		Atrophy	
SOMA score	Not Acute	Acute	Not Acute	Acute	Not Acute	Acute
0	103	12	97	14	99	14
1	29	3	12	5	34	5
2	8	8	22	3	8	4
3	2	2	11	3	1	2
p value (G-test)	0.00004		0.67		0.02	

Table 5.6: Incidence and severity of normal tissue damage phenotypes in patients stratified by acute response.

5.3.3 Genetic association between genotype and phenotype.

A total of 13 polymorphisms were analysed (12 single nucleotide polymorphisms and a 19bp deletion). All samples were genotyped blind and (at least) in duplicate. Approximately 5% of genotypes were also confirmed by direct sequencing. The TGFβ-1 C-509T polymorphism was analysed using both RFLP and ASO dot blotting due to its highly significant result. Additionally, ~10% of patients were randomly selected and sequenced for the specific polymorphism. In all cases the frequency of the variant allele was comparable with those reported in the literature. All SNPs were found to be in Hardy-Weinberg equilibrium (**Table 5.7**). G-test p values can be found in **Table 5.8**. Only polymorphisms that showed an association with a normal tissue injury phenotype will be discussed in the following sections.

Table 5.7		
Gene/SNP	**Variant allele frequency**	**Hardy Weinberg (*p*)**
APEX1 D148E	0.34	0.39
CX3CR1 V249I	0.28	0.88
DHFR deletion	0.46	0.35
EPHX1 Y113H	0.33	0.25
EPHX1 H139R	0.21	0.17
HFE C282Y	0.07	0.88
MTHFR C677T	0.33	0.61
MTHFR A1298C	0.29	0.34
MTR D919G	0.23	0.09
TGFβ-1 C-509T	0.33	0.22
XRCC1 R194W	0.06	0.42
XRCC1 R399Q	0.37	0.51
XRCC2 R188H	0.05	0.45

Table 5.7: Variant allele frequencies and Hardy-Weinberg Equilibrium (χ^2 test *p* values).

Table 5.8				
Polymorphism/ risk factor	**G-test *p* value**			
	Fibrosis	**Telangiectasia**	**Atrophy**	**Acute reaction**
APEX1 D148E	0.77	0.12	0.78	0.80
CX3CR1 V249I	0.78	0.86	0.99	0.78
DHFR deletion	0.60	0.27	0.16	0.06
EPHX1 Y113H	0.06	0.8	0.32	0.10
EPHX1 H139R	0.63	0.86	0.44	0.94
HFE C282Y	0.81	0.54	0.99	0.93
MTHFR C677T	0.86	0.18	0.79	0.94
MTHFR A1298C	0.75	0.70	0.54	0.28
MTR D919G	0.53	0.47	0.98	0.29
TGFβ-1 C-509T	**0.004**	0.39	0.14	0.72
XRCC1 R194W	0.56	0.98	0.91	0.39
XRCC1 R399Q	0.73	**0.01**	0.54	0.48
XRCC2 R188H	0.62	0.98	0.91	0.25
Boost	0.47	**0.03**	0.28	0.34
Acute reaction	**0.00004**	0.67	**0.02**	-

Table 5.8: G-test *p* values comparing patients with scores of 0 *vs.* patients with scores 2-4.

As previously discussed, patients were divided into clearly affected (SOMA score: 2-4) and clearly unaffected (SOMA score: 0) and their genotype distributions were compared using the objective SOMA scales for telangiectasia, fibrosis, and atrophy separately. TGFβ-1 C-509T and XRCC1 R399Q were the only polymorphisms that showed an

association with late normal tissue damage in this study (fibrosis and telangiectasia respectively). There was no statistically significant association between any of the polymorphisms investigated and the development of atrophy.

5.3.3.1 XRCC1 R399Q and telangiectasia risk.

The XRCC1 R399Q polymorphism showed a weak but statistically significant association with the development of telangiectasia. The presence of the Q allele was significantly associated with an increased risk of telangiectasia (SOMA scores: 0 *vs.* 2-4, n=150) (*p*=0.01) (**Table 5.9**).

As an increased risk of telangiectasia was also found in patients who received the additional 15Gy electron boost, analysis for the specific polymorphism was repeated excluding those patients (n=75). The XRCC1 399Q allele was still associated with an increased risk of telangiectasia (p=0.03) in the remaining (n=82) group, suggesting that the two risk factors (the 15Gy electron boost and the XRCC1 R399Q polymorphism) are distinct. (Note: The specific polymorphism was still significantly associated with the development of telangiectasia (*p*=0.01) in the group of patients (n=75) who had received an electron boost as part of their treatment).

Table 5.9

Gene/SNP	G-test *p* value	Scores compared	Number of patients
Including patients who received a 15Gy boost.			
XRCC1 R399Q	0.01	0 *vs.* 2-4	111 *vs.* 39
	0.006	0-1 *vs.* 2-4	128 *vs.* 39
Excluding patients who received a 15Gy boost.			
XRCC1 R399Q	0.03	0 *vs.* 2-4	67 *vs.* 15

Table 5.9: G-test *p* values when comparing telangiectasia scores with the XRCC1 R399Q genotype distribution. Analysis was repeated excluding those who had received a 15Gy boost as boost was associated with an increased risk of telangiectasia.

5.3.3.2 TGF*β*-1 C-509T and fibrosis risk.

Development of long term fibrosis was significantly associated with the TGF*β*-1 C-509T polymorphism (SOMA scores: 0 *vs.* 2-4, n=135) (*p*=0.0041) (**Table 5.9**). Since an acute response was significantly associated with fibrosis, patients who presented with an acute response (n=25) were excluded and the analysis repeated. The results were still significant (*p*=0.0034) for the group of remaining patients (n=113) (**Table 5.10**) suggesting that the gene polymorphism and an acute reaction to radiotherapy are separate fibrosis risk factors. (Note: On its own, the group of patients who developed an acute reaction (n=25) was too small for any meaningful statistical analysis).

Table 5.10

Gene/SNP	G-test *p* value	Scores compared	Number of patients
Including acute responders.			
TGF*β*-1 C-509T	0.0041	0 *vs.* 2-4	115 *vs.* 20
	0.0032	0-1 *vs.* 2-4	147 *vs.* 20
Excluding patients who showed an acute reaction to radiotherapy.			
TGF*β*-1 C-509T	0.0034	0 *vs.* 2-4	103 *vs.* 10

Table 5.10: G-test *p* values when comparing fibrosis scores with the TGF*β*-1 C-509T genotype distribution. Analysis was repeated excluding those who presented with an acute reaction to radiotherapy as an acute reaction was found to be associated with development of fibrosis.

Table 5.11

Acute reaction /genotype	Number of patients	
	Fibrosis Score: 0	Fibrosis Score: 2-4
No acute / CC	49	-
No acute / CT	47	7
No acute / TT	7	3
Acute / CC	4	2
Acute / CT	7	7
Acute / TT	1	1

Groups Compared	*p* value (one-tailed χ^2 test with Yates' correction)
No acute/CC *vs.* Acute/TT	0.0083

Table 5.11: Summary of combined genotype status/acute reaction distribution.

Given the suggestive evidence that fibrosis and an acute reaction each make independent contributions to the risk of long term fibrosis patients were analysed according to their genotype status/presence of an acute reaction and their fibrosis score. As expected, analysis revealed a statistically significant association between patient status for both risk factors and fibrosis risk (p=0.0083, one tailed χ^2 test of independence with Yates' correction for small sample size). **Table 5.11** summarises the results.

There were no patients with fibrosis in the 'no acute reaction-CC genotype' group (false negative) and only one patient in the 'yes acute-TT genotype group' who had not developed fibrosis (false positive), suggesting that when combined these two risk factors can significantly increase the predictive power of such a test. This needs however to be independently confirmed using a larger sample size.

5.3.4 Combined TGFβ-1 C-509T analysis.

Quarmby *et al.* (2003) had previously reported an association between development of fibrosis and the TGFβ-1 C-509T polymorphism in breast cancer patients (OR=3.4; 95%CI 1.38-8.40; p=0.0036). Fibrosis was scored using the LENT/SOMA scales and patients had received similar doses with the patients in this study (40Gy in 15 fractions). Additionally, Quarmby *et al.* (2003) had compared patients with fibrosis scores of 2-4 (n=14) with patients who had shown no signs of fibrosis (scores of 0, n=87). Both studies were quite similar in their design and the reported TGFβ-1 C-509T genotype frequencies. The two sets of data were therefore combined in order to increase the total number of patients analysed (n=236). **Table 5.12** shows the reported TGFβ-1 C-509T genotype frequencies in both studies. Genotype distributions between the two studies were not found to be statistically different (p=0.48).

Table 5.12						
	Quarmby *et al.*, 2003 (number of patients)		**This study (number of patients)**		**Combined (number of patients)**	
Genotype	**No fibrosis**	**Fibrosis**	**No fibrosis**	**Fibrosis**	**No fibrosis**	**Fibrosis**
CC	45	4	53	2	98	6
CT	40	5	54	14	94	19
TT	2	5	8	4	10	9

Table 5.12: TGFβ-1 C-509T genotype distributions reported by both studies and combined number of patients. The two groups were not found to be statistically different (p=0.48).

The results (summarised in **Table 5.13**) show an increased risk of fibrosis (OR=3.06; 95%CI 1.7-5.3; p=0.00006) in patients carrying at least one variant allele (CT or TT) compared with the homozygous CC patients. The risk is significantly higher for TT homozygotes (OR=14.7; 95%CI 3.8-60.3; p=0.000003) compared with CC homozygotes suggesting an additive allele effect. This was also supported by an increased risk of TT homozygotes (OR=4.45; 95%CI 1.4-14; p=0.007) compared with CT heterozygotes and an increased risk of CT heterozygotes (OR=3.3; 95%CI 1.2-9.7; p=0.002) compared with CC homozygotes. Approximately 56% of all patients were carriers of at least on variant allele whilst 8% of all patients were homozygous for the T allele which demonstrates that these highly significant risks apply to a large number of patients.

Table 5.13			
Genotypes compared	**Odds Ratio**	**95% Confidence intervals**	***p* value**
CC *vs.* (CT + TT)	3.06	1.7-5.3	0.00006
(CC + CT) *vs.* TT	7.27	2.4-21.8	0.00005
CC *vs.* TT	14.7	3.8-60.3	0.000003
CT *vs.* TT	4.45	1.4-14	0.007
CC *vs.* CT	3.3	1.2-9.7	0.002

Table 5.13: Risk of fibrosis according to TGFβ-1 C-509T genotype between different groups. The increased risk of T allele homozygotes compared with CT and CC genotypes suggests an additive effect of the increase T allele.

5.3.5 Summary of results.

This pilot study investigated possible risk factors for long term normal tissue damage in breast cancer patients who had received radiotherapy as part of their treatment. G-test *p* values can be found in **Table 5.8**.

Within the range of 45-50Gy in 10-25 fractions the following were found:

- An additional 15Gy electron boost (p=0.033) and the XRCC1 R399Q polymorphism (p=0.01) seem to make independent contributions to the overall risk of telangiectasia.
- An acute reaction was associated with the development of long term fibrosis (p=0.00004) and long term atrophy (p=0.02).
- Development of atrophy was not associated with any of the polymorphisms investigated.
- Irrespective of an acute reaction, the TGFβ-1 C-509T polymorphism is associated with an increased risk of fibrosis (p=0.0041).
- The TGFβ-1 C-509T fibrosis risk was significantly raised (p=0.00006) after combining data obtained from a very similar study (Quarmby *et al.*, 2003) thus confirming previously reported results and minimising chances of a false positive.

5.4 Discussion.

The results obtained from this study suggest that both genetic and radiological factors make independent contributions to the overall risk of fibrosis, telangiectasia and atrophy. These may act synergistically, increasing the severity of normal tissue damage. For example, an increased risk of telangiectasia was associated with the XRCC1 R399Q polymorphism, but was also seen in patients who had received an additional 15Gy electron boost. However, the effects of the specific polymorphism on telangiectasia risk were still statistically significant even when patients who had received a boost were excluded from the study.

In a similar fashion, the risk of fibrosis was influenced separately by the TGFβ-1 C-509T polymorphism status and the development of an acute reaction. Atrophy was not

associated with any of the SNPs analysed in this study but an acute reaction was found to increase the risk of long term atrophy.

A number of studies have produced inconclusive results for the XRCC1 R399Q polymorphism and the risk for normal tissue damage following radiotherapy. In a study published by Moullan *et al.* (2003) the XRCC1 399Q allele was found more frequently in radiosensitive breast cancer patients. The study was very similar to this one with an average dose of 50Gy (in dose fractions of 2.5Gy) followed by a 10Gy boost. However, the study employed the EORTC scales in order to score for adverse reactions to radiotherapy and could not associate the polymorphism with increased risk for a specific injury phenotype. De Ruyck *et al.* (2005a and 2005b) reported an increased risk of normal tissue reactions in cervical or endometrial cancer patients carrying the XRCC2 399Q allele, but did not associate the polymorphism with a specific type of injury. Andreassen *et al.* (2003) found an association between the XRCC1 399Q allele and an increased risk for fibrosis in breast cancer patients but failed to reproduce this finding in consequent studies (Andreassen *et al.*, 2005 and 2006). Despite some of the data being different to those produced by this study, all the above suggest that XRCC1 is possibly involved in the process of long term normal tissue damage but further studies are needed in order to determine its nature and exact effects.

The connections between fibrosis, over-expression of TGFβ-1 and ionising radiation have been reported in a large number of studies (Randall and Coggle 1995 and 1996; Anscher *et al.*, 1997; Ehrhart *et al.*, 1997; Martin *et al.*, 1997 and 2000; Awad *et al.*, 1998; Grainger *et al.*, 1999; Li *et al.*, 1999; O'Sullivan and Levin, 2003; Quarmby *et al.* 2003). Ionising radiation induces long term over-expression of TGFβ-1 which is a major cytokine involved in inflammation response and fibrosis development. Increased TGFβ-1 plasma levels have been associated with radiation-induced fibrosis in lung and breast cancer patients and the TGFβ-1 C-509T polymorphism has been found to increase the risk of long term fibrosis in breast cancer patients.

Quarmby *et al.* (2003) were the first to report an association between the specific promoter polymorphism and increased risk of fibrosis in breast cancer patients. That study involved breast cancer patients who had been treated with radiotherapy doses similar to this study, made use of the LENT/SOMA scales to score for long term

fibrosis and produced genotype distributions that were not found to be statistically different. By combining that data with those obtained from this study, the total number of patients was significantly increased thus increasing the statistical power of the association study. The combined analysis revealed an even higher association of the TGF*β*-1 C-509T polymorphism with fibrosis, raising fibrosis risk of TT homozygotes 15-fold (p=0.000003) and risk of carriers of at least one T allele 3-fold (p=0.00006) compared to the CC group. This also suggested an additive effect which is in agreement with previous reports. The -509T allele was associated with higher TGF*β*-1 plasma concentrations and these were associated with development of severe radiation-induced fibrosis (Anscher *et al.*, 1997; Awad *et al.*, 1998; Grainger *et al.*, 1999; Li *et al.*, 1999). This could explain the higher frequency of the T allele in patients with higher fibrosis scores.

Andreassen *et al.* (2003 and 2005) had also reported an association between the TGF*β*-1 -509T allele and an increased risk of radiation-induced fibrosis in breast cancer patients but failed to reproduce their findings in a later study (Andreassen *et al.*, 2006). Despite the similar experimental design, data from the Danish (Andreassen *et al.*, 2005) study could not be combined with the UK (Quarmby *et al.*, 2003; Giotopoulos *et al.*, 2007) studies as the precise patient genotype frequencies are not given in the publication (Andreassen *et al.*, 2005).

Differences between the UK (Quarmby *et al.*, 2003; Giotopoulos *et al.*, 2007) and the later Danish study (Andreassen *et al.* 2006) could account for the contrasting results. All patients included in the latter Danish (Andreassen *et al.* 2006) study had been treated with higher radiation doses per fraction and were specifically selected retrospectively because they had developed fibrosis. Thirteen percent of the Danish (Andreassen *et al.*, 2005) breast cancer patients were homozygous for the T allele as opposed to 7-9% of the combined UK studies (Quarmby *et al.*, 2003; Giotopoulos *et al.*, 2007) and this was also lower than the 26% of the UK patients that were positive for both the TT genotype and fibrosis (**Table 5.11**). The higher doses might be masking any genetic contribution to the risk of fibrosis. Genotype distributions from that study (Andreassen *et al.* 2006) could not be combined with the UK (2003 and 2007) studies due to differences in experimental design.

There are presumably additional gene polymorphisms implicated in the process of adverse radiotherapy reactions. In this study for example ~2% of patients developed fibrosis despite being homozygous for the common (reduced risk) TGF*β*-1 -509C allele and ~6% did not develop fibrosis despite being homozygous for the increased risk (T) rare allele. Similarly, ~6% of patients developed severe telangiectasia despite carrying the common XRCC1 399R allele and ~10% did not show any signs of telangiectasia despite being homozygous for the increaser (H) allele. A number of low penetrance genes may act synergistically to increase (or decrease) the risk of abnormal cell and tissue radiosensitivity. Apart from the TGF*β*-1 C-509T and the XRCC1 R399Q polymorphisms, none of the SNPs analysed in this study were significantly associated with an acute response or any phenotype of radiotherapy-induced normal tissue damage. However, it is possible that the small sample size could not allow for any low penetrance genes to be identified and their possible implication can not be positively ruled out.

With the exception of the association between fibrosis and the TGF*β*-1 C-509T polymorphism which was a confirmation of previous independent studies (Quarmby *et al.*, 2003; Andreassen *et al.*, 2005) all results from this study should be considered as suggestive and need to be independently reproduced. The underlying mechanisms of radiation-induced normal tissue damage are not entirely understood and various studies have so far produced contrasting results. As in this study, a major limitation in genetic association studies seeking to associate a genotype with a specific normal tissue damage phenotype is sample size. Additionally, treatment regimes and radiobiological factors such as treatment dose, fraction size and whether the patient received chemotherapy, might mask any genetic contributions and need to be taken under consideration. The number of patients in this study who received anthracycline based chemotherapy (reported to increase the risk of late effects: Fiets *et al.*, 2003; Shanley *et al.*, 2006) was too small for any meaningful statistical analysis but will need to be addressed in a future larger sample study. Similarly, ethnic background, anatomical differences between individuals, lifestyle and dietary habits might influence genotype distributions and the severity of adverse responses to radiotherapy (for example, possible negative effects of polymorphisms involved in folate metabolism enzymes may be exacerbated in individuals who have a low folate diet). Standard radiotherapy protocols and uniform scoring of late normal tissue damage by using a common efficient scoring system will

enable future comparisons between different studies which can increase statistical power and reveal low penetrance genes involved in the process of long term normal tissue damage. Multiple testing has been performed on the same patient samples so false positive results are likely. Additionally, all results are based on the specific dose range and on a relatively small sample size so further analysis using an independent cohort of breast cancer patients is required to validate the data obtained from this study.

5.5 Conclusion and future work.

Breast cancer is the most common female cancer in the UK. Radiotherapy is an essential part of breast cancer treatment and can substantially increase chances of local tumour control whilst reducing the risk of local recurrence. Additionally, the risk of secondary non-breast cancers and heart disease associated with older radiotherapy regimes has decreased (EBCTCG, 2005) which has resulted in an increase in patients' life expectancy.

A significant number of patients (~5%) will develop some form of radiation-induced normal tissue damage which implies that relatively high numbers of patients are affected and raises the clinical significance of studies seeking to identify the underlying genetic and radiobiological causes. These effects are rarely life-threatening but can substantially affect the patient's quality of life. For example, as evidenced by the Subjective SOMA scales, fibrosis is often associated with painful tender breasts. This was evident in this study as a significant association was found between fibrosis scores and pain (p=0.003; data not shown). Late normal tissue damage is rarely reversible and its effect on quality of life is in most cases life-long. Identifying patients that are at a higher risk of developing late radiation effects could substantially improve treatment by either dose adjustments or by seeking alternative forms of therapy. To this point no clinical test exists to identify patients who are at high risk of developing late effects whereas *in vitro* studies seeking to associate peripheral blood lymphocyte radiosensitivity with acute or late tissue reactions have produced contrasting results (Hoeller *et al.*, 2003; Popanda *et al.*, 2003; Lopez *et al.*, 2005; Pinar *et al.*, 2007). Additionally, such *in vitro* tests involve blood irradiation, lymphocyte culture and cytogenetic screening which is a laborious and expensive process. Identifying

combinations of genes that significantly alter normal tissue damage risk could lead to a PCR-based predictive test that requires less time and is less laborious.

This study included 167 breast cancer patients that had been offered standard radiotherapy treatment (40-50Gy) with or without an additional 15Gy electron boost and identified: an acute response as a risk factor for long term fibrosis (p=0.0004) and atrophy (p=0.02), the additional 15Gy boost and the presence of the XRCC1 R399H polymorphism as risk factors for long term telangiectasia (p=0.033 and p=0.01 respectively) and the TGFβ-1 C-509T polymorphism as a major risk factor for long term fibrosis [p=0.0041 and p=0.00006 in the combined analysis (Quarmby *et al.*, 2003; Giotopoulos *et al.*, 2007)]. It is worth noting that when both the acute reaction and the TGFβ-1 TT genotype were considered, there were no false negatives (patients who were homozygous for the C allele and did not have an acute reaction to radiotherapy but did develop fibrosis) and only one false positive (one patient showed an acute reaction and carried the TGFβ-1 TT genotype but did not develop fibrosis). If these findings are reproduced on a larger scale, they could be employed in the clinic as a simple predictive test in order to identify patients which have a higher risk of developing fibrosis.

Future work should aim to increase the sample size and the list of gene polymorphisms that might be involved in the process of radiation-induced damage. Genes that might predispose to an acute reaction should also be included as an acute reaction might act as a predictive marker (or increase risk) of long term tissue fibrosis.

This pilot study has been quite successful and has produced promising preliminary data that could in the long term be used in the clinic as part of a predictive test. These results have been published (Giotopoulos *et al.*, 2007) and funding has been secured (Breast Cancer Campaign) in order to establish a larger independent cohort of breast cancer radiotherapy patients.

Chapter 6:

Final conclusion and future work

6.1 Thesis summary.

Ionising radiation is one of the most extensively studied environmental carcinogens. A large number of studies have shown that exposure to moderate-to-high levels can cause most forms of cancer (Pierce *et al.*, 1996; Ron, 1998). Notably, studies on A-bomb survivors have associated acute whole-body exposure to ionising radiation with an excess relative risk of r-AML, suggesting that BM is one of the most susceptible tissues to malignant transformation following exposure to ionising radiation (see section 1.3.4). Additionally, radiotherapy treatment schedules have identified BM as one of the most radiosensitive tissues (**Figure 1.3**). Combined with data from chromosome instability syndromes (see section 1.3.3), these findings reveal an apparent connection between tissue radiosensitivity and cancer predisposition; particularly cancers of haemopoietic tissues (**Table 1.1**). The haemopoietic system was thus employed to investigate the biological effects of ionising radiation and identify factors that may be implicated in radiosensitivity and cancer susceptibility.

This thesis investigated genetic (QTL influencing HSC frequency, gene polymorphisms) and epigenetic (global DNA methylation levels) factors that may be involved in biological responses to ionising radiation exposure. The study in **Chapter 3** identified genetic factors possibly involved in radiation leukaemogenesis and haemopoiesis. The study in **Chapter 4** assessed the global DNA methylation levels of control haemopoietic tissues and radiation-induced leukaemias and compared the relative radiosensitivity of BM and spleen. Finally, the study in **Chapter 5** investigated genetic factors influencing radiosensitivity in a group of breast cancer patients that had received local radiotherapy as part of their cancer treatment.

6.2 BM cellularity and pRBC counts.

A number of haemopoietic phenotypes were investigated in **Chapter 3**. F_2 mice were genotyped and QTL influencing the frequency of BM red blood cells, pRBC and spleen weight were mapped. To our knowledge, strain-specific differences in BM erythropoiesis had not been previously reported.

The two mouse strains show differences in BM red blood cell numbers (E/NE bone marrow ratio), with CBA/H mice having higher numbers of RBMC compared to C57BL/6 mice (**Table 3.2**). Inversely, C57BL/6 mice have higher numbers of pRBC compared to the CBA/H mice (**Table 3.2**). In contrast to the E/NE bone marrow ratio, which mainly reflects BM erythropoiesis, pRBC counts represent the overall contributions made from both BM and spleen. A number of QTL were identified, which were specific to BM (**Table 3.3**) or peripheral blood (**Table 3.4**), suggesting that murine erythropoiesis is controlled by different autosomal loci in the BM and spleen.

Spleen weight was used as a potential surrogate to investigate the relative contribution of spleen in erythropoiesis. Three suggestive QTL were identified (**Figure 3.4**), one of which overlaps with a reported spleen weight QTL (Chromosome 17 - 15-34cM; Rocha *et al.*, 2004). However, none of these spleen weight QTL overlapped with any pRBC QTL, suggesting that spleen weight is not an appropriate surrogate for peripheral red blood cell production.

The study identified novel QTL possibly responsible for differences in BM erythropoiesis for the first time. Most importantly, the little overlap between E/NE bone marrow ratio and pRBC QTL highlights the complex genetics of haemopoiesis and emphasises the need for *in vivo* studies, as *in vitro* techniques can not assess the combined BM and spleen contributions in erythropoiesis.

6.2.1 Future work.

The QTL identified in this study harbour many genes that could be implicated in mouse erythropoiesis. As previously discussed (see **Chapter 3**), *EPO* and *EPO-R* are the most obvious candidates as they are both directly involved in erythropoiesis and are located within QTL influencing E/NE bone marrow ratio. No sequence variation between the

two mouse strains was detected in either of these genes, but neither can be conclusively excluded, as possible upstream or downstream sequence variations in regulatory regions could result in the different phenotypes in the two mouse strains. EPO and EPO-R both interact with a number of regulatory genes and sequence variations in those regulatory regions could affect downstream processes. For example, thrombopoietin is responsible for megakaryocyte growth and development and shows strong sequence homology with erythropoietin (Wada *et al.*, 1995). Rouleau *et al.* (2004) demonstrated that in combination with EPO and its receptor (EPO-R), thrombopoietin can affect growth and development of red blood cells even in the absence of its own receptor.

Other genes within the QTL identified are potential candidates (e.g. Janus Kinase 2) and have been discussed in **Chapter 3**. Identifying polymorphisms that have an effect of erythropoiesis could lead to a better understanding of diseases like erythroleukaemias or other myeloproliferative disorders.

6.3 HSC numbers as a risk factor in r-AML.

AML is a clonal malignancy that arises following malignant transformation of a HSC (Warner *et al.*, 2004). The mean latency of t-AML is 5 years and it is often preceded by a pre-leukaemic stage (MDS) in which altered BM cellularity is seen (e.g. symptomatic anaemia and thrombocytopenia) (Leone *et al.*, 1999; Armitage *et al.*, 2003). Thus, similar to other cancers, radiation-induced leukaemogenesis is a multistage process, involving the accumulation of gene mutations, malignant transformation and clonal expansion of a single cell (Warner *et al.*, 2004). The risk factors therefore include the rates of mutations and the number of mutations required to transform the HSC, the efficiency in repairing these mutations or triggering apoptosis. Most of the genetic association studies investigating cancer risk have focussed on genes involved in DNA repair and cell cycle checkpoints and have identified a large number of polymorphic variations that alter cancer risk (Taramelli and Acquati, 2004). However, the actual number of genomes at risk (i.e. the number of cells that have the potential to transform and give rise to cancer) should also be part of the equation that defines cancer risk.

Human genetic association studies aiming to identify t-AML susceptibility genes are constrained by relatively low number of patients. Additional confounding factors (e.g.

lifestyle, differences in treatment, age of onset, and site of primary malignancy) might necessitate dividing patients into subgroups, thus reducing the statistical power needed to reveal low penetrance cancer susceptibility genes.

Mouse studies provide the necessary statistical power to identify the complex genetic determinants of cancer susceptibility. The process of cancer development is remarkably similar between mouse and human (Balmain and Harris, 2000), whilst the presence of inbred mouse strains that are highly resistant/susceptible to a particular cancer and the possibility of generating crosses between these strains, has led to mapping of many mouse tumour susceptibility QTL (Taramelli and Acquati, 2004).

This thesis used the r-AML susceptible CBA/H and the r-AML resistant C57BL/6 mouse strains. CBA/H mice have four times more $L^-S^+K^+$ cells than the r-AML resistant C57BL/6 mice (see **Chapter 3**; Jawad *et al.*, 2008) which is consistent with their increased r-AML risk (2-3fold increased risk compared to C57BL/6 mice) (Boulton *et al.*, 2003) and supports the hypothesis that HSC frequency is a risk factor in r-AML.

A whole-genome screen was thus performed in F_2 mice, to map QTL influencing strain-specific (CBA/H and C57BL/6) differences in stem cell frequency. The study identified novel and previously reported QTL influencing the frequency of $L^-S^-K^-$, L^-S^{++} and $L^-S^+K^+$ cells. The overlapping QTL between this *in vivo* study and previous *in vitro* studies provide strong evidence that the $L^-S^+K^+$ (as selected by flow cytometry) are enriched for both LTC-IC and CAFC Day 35 cells and thus contain the target cell for r-AML (see **Chapter 3**). Most importantly, at least one suggestive QTL overlaps with a previously reported r-AML susceptibility locus (Chromosome 6 – 27.5cM, Boulton *et al.*, 2003), further supporting the hypothesis that HSC frequency is a risk factor in r-AML.

As previously discussed (see **Chapter 3**) traditional mouse genetic studies have limitations. The relatively large mapping intervals (10-30cM), the limited locus variability between different inbred mouse strains and the fact that cancer susceptibility is determined by multiple loci (or multiple genes within the same locus) complicate the process of identifying candidate genes (Taramelli and Acquati, 2004). However, a

number of candidate genes have been found using this approach and mutations conferring altered cancer risk have been identified (Mao and Balmain, 2003; Jawad *et al.*, 2006).

Inter-individual variation in the numbers of specific BM cell types has been demonstrated in humans (Humpe *et al.*, 1997; Chapple *et al.*, 1998; Marley *et al.*, 1999). Together with previously reported cell type specific QTL that co-localise with leukaemia/lymphoma susceptibility loci (reviewed in Jawad *et al.*, 2007a), the data obtained by this study provided evidence that target cell frequency may also be a risk factor in r-AML.

6.3.1 Future work.

Future work should concentrate on identifying candidate genes within the QTL and investigate possible sequence variations between the two mouse strains. A strong candidate is the *CXCR4* gene, which is located within the suggestive chromosome 1 QTL (62cM). CXCR4 is an essential chemokine receptor for homing and maintenance of HSC in the vascular BM niche (Burger and Bürkle, 2007). Deregulated CXCR4 signalling has been demonstrated in CML patients (Ptasznik *et al.*, 2002), whereas the protein was found to be important for AML cell homing in the BM of NOD/SCID mice (Tavor *et al.*, 2004). CXCR4 is the receptor for the chemokine SDF1, which is critical for murine BM engraftment by human SCID stem cells (Peled *et al.*, 1999). Interestingly, SDF1 is located within another QTL identified by this study (Chromosome 10 - 32.4-50.4cM). It is likely that variation in a common HSC homing pathway may have an actual impact on stem cell numbers and further work is needed to test this hypothesis.

6.4 DNA methylation in r-AML and relative radiosensitivity.

It is well established that exposure to ionising radiation results in genomic instability (see section 1.3.3). In addition to susceptibility to specific malignancies, different mouse strains also show variable sensitivity to radiation-induced genomic instability (see section 1.8). This suggests that there is a strong genetic component influencing responses to ionising radiation. However, the exact mechanism by which genomic

instability propagates is not understood and can not be explained by genetic factors alone.

In this thesis, we hypothesised that DNA hypomethylation might be involved in the process of radiation-induced genomic instability and cancer predisposition. Aberrant DNA methylation and genomic instability are hallmarks of cancer (see sections 1.3.3, 1.5.4 and 1.5.5). Global DNA hypomethylation increases the risk of cancer and affects genome stability (see section 1.5). The effects of ionising radiation are non-targeted and given the fact that genomic instability can be passed on to offspring of irradiated parents by means other than a stable mutation (Dubrova *et al.*, 2000; Barber *et al.*, 2002; Barber *et al.*, 2006), DNA hypomethylation is a good candidate.

To test this hypothesis, the global DNA methylation status of control and irradiated haemopoietic tissues was assessed and compared to that of radiation-induced haemopoietic malignancies. If hypomethylation contributes to radiation leukaemogenesis, irradiated BM cells and the r-AMLs that arise as a consequence should be hypomethylated. Leukaemic samples were found to be hypomethylated but it is not clear if this hypomethylation is directly involved in leukaemogenesis or is simply a by-product of malignant transformation, as many cancers are hypomethylated (Ehrlich, 2002; Chalitchagorn *et al.*, 2004). There is however, suggestive evidence that changes in DNA methylation precede malignant transformation and are not necessarily a consequence of it. For example, Nakagawa *et al.* (2001) showed an age-related progressive methylation of the *MLH1* promoter in the normal colonic mucosa of individuals that in many cases correlated with the development of colorectal cancer. Mouse studies have shown that global DNA hypomethylation increases the risk for cancer (Chen *et al.*, 1998; Gaudet *et al.*, 2003), whilst ICF patients provide a direct link between pericentromeric repeat hypomethylation and chromosomal instability (Narayan *et al.*, 1998; Qu *et al.*, 1999; Narayan *et al.*, 2000).

This study identified BM as one of the most hypomethylated murine tissues. The 5-^{Me}C content of total BM had not been previously reported but previous studies had assessed the global DNA methylation levels in other haemopoietic tissues/cells (spleen, lymphocytes and splenic macrophages) (Ehrlich *et al.*, 1982; Gama-Sosa *et al.*, 1983). Combined, these data suggested that DNA methylation increases with haemopoietic

differentiation. This was later confirmed by an independent study (Tadokoro *et al.*, 2007) which reported that $L^-S^+K^+$ BM cells were significantly hypomethylated compared to more mature haemopoietic cells.

Interestingly, DNA hypomethylation correlated with relative radiosensitivity. BM was particularly susceptible to radiation-induced killing, as an acute whole-body exposure to 3Gy X-rays resulted in loss of ~80% of white bone marrow cells. BM reconstitution over the next 5-14 days was preceded (0-4 days) by the amplification and differentiation of surviving haemopoietic stem cells that drive BM recovery (Colter *et al.*, 2001; Dazzi *et al.*, 2006). This necessary HSC proliferation occurs under conditions of a radiation-induced transient folate deficiency and genotoxic stress, which could result in further hypomethylation and/or uracil incorporation. This could explain the radiation-induced genetic instability observed experimentally in irradiated HSC and the specific risk of r-AML following whole-body exposure.

A persistent radiation-induced hypomethylation was seen the in the BM of CBA/H, but not C57BL/6 mice. In addition to radiation-induced hypomethylation, this overall decrease in BM methylation could also reflect changes in the numbers of specific BM cell populations in the reconstituted tissue. Such changes in BM cellularity could, in the long term, result in a pre-leukaemic stage (MDS) and eventually give rise to r-AML. As previously discussed (**Chapter 3**), CBA/H mice have four times more $L^-S^+K^+$ cells than the r-AML resistant C57BL/6 mice and a 2-3fold increased risk of r-AML. DNA methylation increases with differentiation (see **Chapter 4**) and as the $L^-S^+K^+$ cells are hypomethylated compared to other more mature haemopoietic stem cells (**Figure 4.4**; Ehrlich *et al.*, 1982; Gama-Sosa *et al.*, 1983; Giotopoulos *et al.*, 2006; Tadokoro *et al.*, 2007), this could suggest that CBA/H mice are more susceptible to r-AML because they have higher numbers of HSC cells that are more hypomethylated and, as a result, more prone to radiation-induced genomic instability.

6.4.1 Future work.

Future studies could further characterise the reconstituted BM in both mouse strains following exposure to ionising radiation. As seen in **Chapter 3**, flow cytometry can be employed to quantify different BM cell types and possibly reveal subtle radiation-

induced cellularity changes in the two strains that might account for their different levels of r-AML susceptibility. The effects of a methyl donor deficient diet on BM cellularity and radiosensitivity could also be investigated. Folate deficiency can also result in uracil incorporation in the DNA leading to mutations and genomic instability (Blount *et al.*, 1997; Ames, 2001; Zhang *et al.*, 2003). Thus, the levels of uracil incorporation under conditions of methyl donor deficiency and/or following exposure to ionising radiation should also be assessed. If our hypothesis is correct, then folate depletion should result in an increased radiosensitivity and cancer predisposition.

6.5 Normal tissue damage.

The data obtained in **Chapter 4** suggested that DNA methylation may be involved in relative radiosensitivity following acute whole-body exposure. A number of genes involved in the one-carbon transfer pathway, were investigated as potential candidates influencing responses to ionising radiation and altering the risk for normal tissue damage in a group of breast cancer patients in **Chapter 5**.

None of these genes was found to be associated with any phenotype of normal tissue damage (**Table 5.8**), which could imply that polymorphisms in folate metabolism genes do not have an effect on normal tissue damage. However, these results could have been affected by lifestyle factors such as smoking or dietary habits. Moreover, in contrast to whole-body radiotherapy, these patients received local irradiation, which might not have a significant effect on the availability of folate. In addition to the above, the relatively small sample size might also account for these negative results. Perhaps a better surrogate, such as plasma folate levels before and after irradiation would be a better predictor of normal tissue damage.

Irrespective of the results for the folate genes, the study identified factors that have an effect on adverse reactions. Within the standard breast cancer radiotherapy treatment dose range (45-60Gy), dose and the presence of the XRCC1 399Q allele appeared to make independent contributions to the risk of telangiectasia (**Table 5.8**). Additionally, the development of an acute reaction severely affected the risk for both atrophy and fibrosis (**Table 5.8**). The risk of fibrosis was severely altered by the presence of the TGFβ-1 509T allele (**Table 5.8**), irrespective of an acute reaction. All the above suggest

that these biological reactions have distinct genotype- and radiological-dependent causes.

6.5.1 Future work.

The study in **Chapter 5** was a pilot study, as it was constrained by the relatively low number of patients. Funding has been secured (Breast Cancer Campaign) in order to establish a larger independent cohort (~1,000 new patients) of breast cancer patients. This will allow validation of previous findings as well as investigation of other potential candidates. As previously discussed (**Chapter 5**), combining the development of an acute reaction with the presence of the TGFβ-1 TT genotype in the Leicester cohort, results in 100% specificity for the development of fibrosis. Identifying genes that are implicated in acute response to radiotherapy could therefore significantly increase the power to predict the risk of fibrosis. Theoretically, genes involved in cell cycle checkpoints, apoptosis and DNA repair are the best candidates as inability to repair DNA damage and increased levels of apoptosis will lead to the development of acute responses. Additionally, chemokines or cytokines involved in inflammatory responses could be implicated and should thus be included in the list of potential candidates.

6.6 Final conclusion.

This thesis has produced many interesting findings and generated further questions that need to be investigated. The mechanisms of radiation leukaemogenesis and radiation-induced genomic instability are still not clear. The *in vivo* data obtained from this thesis suggest that the biological responses to exposure to ionising radiation may involve both genetic and epigenetic factors that had not been previously considered to be risk factors in radiosensitivity and/or cancer susceptibility. While most genetic association studies seeking to identify cancer susceptibility genes have focussed on DNA repair or apoptosis related genes, the data presented in **Chapter 3** (published as Jawad *et al.*, 2007b; Jawad *et al.*, 2008) suggest that the number of genomes at risk should also be part of the equation. Similarly, the study in **Chapter 4** (published as Giotopoulos *et al.*, 2006) showed genotype-dependant epigenetic alterations in response to ionising radiation. Our proposed model suggests that already hypomethylated genomes are at a higher risk of radiation-induced genomic instability and malignant transformation

following exposure. The HSC are hypomethylated compared to more mature haemopoietic cells and are also the target for r-AML. In agreement with this model, CBA/H mice are at a higher risk of r-AML due to their higher numbers of HSC, compared to the r-AML resistant mouse strain. Thus, r-AML susceptibility appears to be a combination of epigenetic (DNA methylation status of the HSC) and genetic (HSC frequency) factors. This is a compelling hypothesis, but needs to be further investigated before any firm conclusions can be drawn. Similarly, the study in **Chapter 5** (published as Giotopoulos *et al.*, 2007) demonstrated that the risk of long term normal tissue damage is a combination of biological (e.g. gene polymorphism) and radiological (e.g. dose) factors. Increasing the sample size will enable validation of these results and help towards developing a clinically useful predictive test.

Appendix I

Mouse microsatellite primers

Chromosome 1		Chromosome 2		Chromosome 3		Chromosome 4	
D1mit231	8.7	D2mit365	17.0	D3mit93	12.0	D4mit235	3.3.0
D1mit527	17.5	D2mit237	27.0	D3mit151	13.1	D4mit192	10.9
D1mit435	36.9	D2mit241	28.5	D3mit49	30.6	D4mit214	21.9
D1mit136	59.6	D2mit433	31.7	D3mit199	33.7	D4mit288	28.4
D1mit105	80.0	D2mit249	50.5	D3mit257	49.0	D4mitMP15	42.7
D1mit315	101.6	D2mit397	56.8	D3mit116	64.5	D4mit332	52.3
D1mit17	110.0	D2mit423	68.9			D4mit204	61.2
		D2mit51	79.8				
		D2mit265	92.0				
Chromosome 5		**Chromosome 6**		**Chromosome 7**		**Chromosome 8**	
D5mit75	0.0	D6mit1	3.3	D7mit178	0.0	D8mit95	6.6
D5mit386	9.8	D6mit74	10.9	D7mit25	13.1	D8mit64	16.0
D5mit233	19.7	D6mit384	15.3	D7mit145	24.0	D8mit69	31.0
D5mit135	28.0	D6mit188	21.9	D7mit40	43.0	D8mit208	41.5
D5mit157	39.3	D6mit146	31.7			D8mit320	61.5
D5mit188	51.4	D6mit55	45.9			D8mit156	73.0
D5mit168	66.7	D6mit198	57.0				
D5mit247	73.2	D6mit201	65.5				
Chromosome 9		**Chromosome 10**		**Chromosome 11**		**Chromosome 12**	
D9mit224	13.1	D10mit80	2.2	D11mit78	4.4	D12mit270	9.8
D9mit227	23.0	D10mit213	11.0	D11mit296	14.2	D12mit52	27.0
D9mit48	31.7	D10mit194	29.0	D11mit349	28.0	D12mit101	45.0
D9mit355	49.2	D10mit42	41.5	D11mit245	40.4	D12mit20	56.8
D9mit115	54.6	D10mit233	63.4	D11mit327	49.0		
D9mit18	68.9	D10mit271	75.4	D11mit198	61.0		
				D11mit301	72.1		
				D11mit61	74.3		
				D11mit203	78.7		
Chromosome 13		**Chromosome 14**		**Chromosome 15**		**Chromosome 16**	
D13mit303	2.2	D14mit10	3.0	D15mit111	17.8	D16mit131	4.3
D13mit17	9.0	D14mit62	18.5	D15mit123	30.6	D16mit165	10.3
D13mit94	17.5	D14mit203	28.3	D15mit28	43.7	D16mit59	27.8
D13mit248	19.7	D14mit225	42.5	D15mit108	55.6	D16mit76	43.0
D13mit13	21.9	D14mit165	52.0			D16mit189	55.2
D13mit256	25.0						
D13mit76	43.0						
Chromosome 17		**Chromosome 18**		**Chromosome 19**		**X Chromosome**	
D17mit46	10.0	D18mit64	2.0	D19mit61	9.0	DXmit166	15.5
D17mit101	16.4	D18mit225	16.0	D19mit106	22.0	DXmit172	48.7
D17mit28	18.4	D18mit53	27.0	D19mit65	37.0	DXmit186	69.0
D17mit178	24.5	D18mit184	41.0	D19mit152	52.0		
D17mit39	45.3	D18mit142	47.0				
D17mit123	56.7	D18mit80	50.0				

Microsatellite name and chromosomal location (cM). Primers were chosen from the 2001 Chromosome Committee Report at MGI (http://www.informatics.jax.org/). (Jawad, 2006)

Appendix II

Publications

References

Alter BP. (2002) Radiosensitivity in Fanconi's anaemia patients. *Radiother Oncol.* **62:**345-7.

Ames BN. (2001) DNA damage from micronutrient deficiencies is likely to be a major cause of cancer. *Mutat Res.* **475:**7-20.

Andreassen CN, Alsner J, Overgaard M, Sørensen FB, Overgaard J. (2006) Risk of radiation-induced subcutaneous fibrosis in relation to single nucleotide polymorphisms in TGFB1, SOD2, XRCC1, XRCC3, APEX and ATM--a study based on DNA from formalin fixed paraffin embedded tissue samples. *Int J Radiat Biol.* **82:**577-86.

Andreassen CN, Alsner J, Overgaard J, Herskind C, Haviland J, Owen R, Homewood J, Bliss J, Yarnold J. (2005) TGFB1 polymorphisms are associated with risk of late normal tissue complications in the breast after radiotherapy for early breast cancer. *Radiother Oncol.* **75:**18-21.

Andreassen CN, Alsner J, Overgaard M, Overgaard J. (2003) Prediction of normal tissue radiosensitivity from polymorphisms in candidate genes. *Radiother Oncol.* **69:**127-35.

Andreassen CN, Alsner J, Overgaard J. (2002) Does variability in normal tissue reactions after radiotherapy have a genetic basis--where and how to look for it? *Radiother Oncol.* **64:** 131-40.

Anscher MS, Kong FM, Marks LB, Bentel GC, Jirtle RL. (1997) Changes in plasma transforming growth factor beta during radiotherapy and the risk of symptomatic radiation-induced pneumonitis. *Int J Radiat Oncol Biol Phys.* **37:**253-8.

Armitage JO, Carbone PP, Connors JM, Levine A, Bennett JM, Kroll S. (2003) Treatment-related myelodysplasia and acute leukemia in non-Hodgkin's lymphoma patients. *J Clin Oncol.* **21:**897-906.

Au WW, Salama SA, Sierra-Torres CH. (2003) Functional characterization of polymorphisms in DNA repair genes using cytogenetic challenge assays. *Environ Health Perspect.* **111:**1843-50.

Awad MR, El-Gamel A, Hasleton P, Turner DM, Sinnott PJ, Hutchinson IV. (1998) Genotypic variation in the transforming growth factor-beta1 gene: association with transforming growth factor-beta1 production, fibrotic lung disease, and graft fibrosis after lung transplantation. *Transplantation.* **66:**1014-20.

Balducci L. (2000) Geriatric Oncology: Challenges for the new century. *Eur J Cancer.* **36**:1741-1754.

Balmain A, Harris CC. (2000) Carcinogenesis in mouse and human cells: parallels and paradoxes. *Carcinogenesis.* **21:**371-7.

Barber RC, Hickenbotham P, Hatch T, Kelly D, Topchiy N, Almeida GM, Jones GD, Johnson GE, Parry JM, Rothkamm K, Dubrova YE. (2006) Radiation-induced transgenerational alterations in genome stability and DNA damage. *Oncogene.* **25:**7336-42.

Barber R, Plumb MA, Boulton E, Roux I, Dubrova YE. (2002) Elevated mutation rates in the germ line of first- and second-generation offspring of irradiated male mice. *Proc Natl Acad Sci USA.* **99:**6877-82.

Bartelink H, Horiot JC, Poortmans P, Struikmans H, Van den Bogaert W, Barillot I, Fourquet A, Borger J, Jager J, Hoogenraad W, Collette L, Pierart M; European Organization for Research and Treatment of Cancer Radiotherapy and Breast Cancer Groups. (2001) Recurrence rates after treatment of breast cancer with standard radiotherapy with or without additional radiation. *N Engl J Med.* **345:**1378-87.

Basten GP, Duthie SJ, Pirie L, Vaughan N, Hill MH, Powers HJ. (2006) Sensitivity of markers of DNA stability and DNA repair activity to folate supplementation in healthy volunteers. *Br J Cancer.* **94:**1942-7.

Beltrami AP, Barlucchi L, Torella D, Baker M, Limana F, Chimenti S, Kasahara H, Rota M, Musso E, Urbanek K, Leri A, Kajstura J, Nadal-Ginard B, Anversa P. (2003) Adult cardiac stem cells are multipotent and support myocardial regeneration. *Cell.* **114:**763-76.

Bentzen SM. (2006) Preventing or reducing late side effects of radiation therapy: radiobiology meets molecular pathology. *Nat Rev Cancer.* **6:**702-13.

Bentzen SM, Dörr W, Anscher MS, Denhamc JD, Hauer-Jensen M, Marks LB, Williams J (2003) Normal tissue effects: reporting and analysis. *Sem Radiat Oncol.* **13:** 189-202.

Bentzen SM, Overgaard J. (1994) Patient-to-Patient Variability in the Expression of Radiation-Induced Normal Tissue Injury. *Semin Radiat Oncol.* **4:**68-80.

Bentzen SM, Overgaard J. (1993) Clinical manifestations of normal tissue damage. In *Basic Clinical Radiobiology*, 1st edition, Steel GG (editor). London, Edward Arnold Publishers. p89-98.

Bestor TH. (2000) The DNA methyltransferases of mammals. *Hum Mol Genet.* **9:**2395-402.

Bestor T, Laudano A, Mattaliano R, Ingram V. (1988) Cloning and sequencing of a cDNA encoding DNA methyltransferase of mouse cells. The carboxyl-terminal domain of the mammalian enzymes is related to bacterial restriction methyltransferases. *J Mol Biol.* **203:**971-83.

Biedermann KA, Sun JR, Giaccia AJ, Tosto LM, Brown JM. (1991) Scid mutation in mice confers hypersensitivity to ionizing radiation and a deficiency in DNA double-strand break repair. *Proc Natl Acad Sci USA.* **88:**1394-7.

Blount BC, Mack MM, Wehr CM, MacGregor JT, Hiatt RA, Wang G, Wickramasinghe SN, Everson RB, Ames BN. (1997) Folate deficiency causes uracil misincorporation into human DNA and chromosome breakage: implications for cancer and neuronal damage. *Proc Natl Acad Sci USA.* **94:**3290-5.

Bonnet D. (2005) Normal and leukaemic stem cells. *Br J Haematol.* **130**:469-479.

Boulton E, Cole C, Knight A, Cleary H, Snowden R, Plumb M. (2003) Low-penetrance genetic susceptibility and resistance loci implicated in the relative risk for radiation-induced acute myeloid leukemia in mice. *Blood.* **101:**2349-54.

Boulton E, Cleary H, Plumb M. (2002) Myeloid, B and T lymphoid and mixed lineage Thymic lymphomas in the irradiated mouse. *Carcinogenesis.* **23:**1079-1085.

Bourc'his D, Bestor TH. (2004) Meiotic catastrophe and retrotransposon reactivation in male germ cells lacking Dnmt3L. *Nature.* **431:**96-9.

Brem R, Hall J. (2005) XRCC1 is required for DNA single-strand break repair in human cells. *Nucleic Acids Res.* **33:**2512-20.

Bulaj ZJ, Griffen LM, Jorde LB, Edwards CQ, Kushner JP. (1996) Clinical and biochemical abnormalities in people heterozygous for hemochromatosis. *N Engl J Med.* **335:**1799-805.

Burger JA, Bürkle A. (2007) The CXCR4 chemokine receptor in acute and chronic leukaemia: a marrow homing receptor and potential therapeutic target. *Br J Haematol.* **137:**288-96.

Burrill W, Barber JB, Roberts SA, Bulman B, Scott D. (2000) Heritability of chromosomal radiosensitivity in breast cancer patients: a pilot study with the lymphocyte micronucleus assay. *Int J Radiat Biol.* **76:**1617-9.

Cartwright R, Tambini CE, Simpson PJ, Thacker J. (1998) The XRCC2 DNA repair gene from human and mouse encodes a novel member of the recA/RAD51 family. *Nucleic Acids Res.* **26:**3084-9.

Chalitchagorn K, Shuangshoti S, Hourpai N, Kongruttanachok N, Tangkijvanich P, Thong-ngam D, Voravud N, Sriuranpong V, Mutirangura A. (2004) Distinctive pattern of LINE-1 methylation level in normal tissues and the association with carcinogenesis. *Oncogene.* **23:**8841-6.

Chapple P, Prince HM, Quinn M, Bertoncello I, Juneja S, Wolf M, Januszewicz H, Brettell M, Gardyn J, Seymour C, Venter D. (1998) Peripheral blood CD34+ cell count reliably predicts autograft yield. *Bone Marrow Transplant.* **22:**125-30.

Chang WP, Little JB. (1992) Delayed reproductive death as a dominant phenotype in cell clones surviving X-irradiation. *Carcinogenesis.* **13:**923-8.

Chen J, Harrison DE. (2002) Quantitative trait loci regulating relative lymphocyte proportions in mouse peripheral blood. *Blood.* **99:**561-6.

Chen RZ, Pettersson U, Beard C, Jackson-Grusby L, Jaenisch R. (1998) DNA hypomethylation leads to elevated mutation rates. *Nature.* **395:**89-93.

Cheshier SH, Morrison SJ, Liao X, Weissman IL. (1999) In vivo proliferation and cell cycle kinetics of long-term self-renewing hematopoietic stem cells. *Proc Natl Acad Sci USA.* **96:**3120-5.

Cheung CC, Martin IC, Zenger KR, Donald JA, Thomson PC, Moran C, Buckley MF. (2004) Quantitative trait loci for steady-state platelet count in mice. *Mamm Genome.* **15:**784-97.

Christie DR, Bull CA, Gebski V, Langlands AO. (1995) Concurrent 5-fluorouracil, mitomycin C and irradiation in locally advanced cervix cancer. *Radiother Oncol.* **37:**181-9.

Cleary H, Boulton E, Plumb M. (2001) Allelic loss on chromosome 4 (Lyr2/TLSR5) is associated with myeloid, B-lympho-myeloid, and lymphoid (B and T) mouse radiation-induced leukemias. *Blood.* **98:**1549-54.

Clutton SM, Townsend KM, Walker C, Ansell JD, Wright EG. (1996) Radiation-induced genomic instability and persisting oxidative stress in primary bone marrow cultures. *Carcinogenesis.* **17:**1633-9.

Coates PJ, Lorimore SA, Lindsay KJ, Wright EG.J (2003) Tissue-specific p53 responses to ionizing radiation and their genetic modification: the key to tissue-specific tumour susceptibility? *Pathol.* **201:**377-88.

Cole CJ. (2005) Genetic and epigenetic factors in mouse radiation induced leukaemogenesis. PhD thesis. Department of Genetics. University of Leicester.

Colter DC, Sekiya I, Prockop DJ. (2001) Identification of a subpopulation of rapidly self-renewing and multipotential adult stem cells in colonies of human marrow stromal cells. *Proc Natl Acad Sci USA.* **98:**7841-5.

Connor JM, Ferguson-Smith MA. (eds) (1997) *Essential Medical Genetics*, 5th edition. St. Louis, Blackwell Sciences.

Coulombel L. (2004) Identification of hematopoietic stem/progenitor cells: strength and drawbacks of functional assays. *Oncogene.* **23:**7210-22.

Cox JD, Stetz J, Pajak TF. (1995) Toxicity criteria of the Radiation Therapy Oncology Group (RTOG) and the European Organization for Research and Treatment of Cancer (EORTC). *Int J Radiat Oncol Biol Phys.* **31:**1341-6.

Dainiak N. (2002) Hematologic consequences of exposure to ionizing radiation. *Exp Hematol.* **30:**513-28.

Danoy P, Sonoda E, Lathrop M, Takeda S, Matsuda F. (2007) A naturally occurring genetic variant of human XRCC2 (R188H) confers increased resistance to cisplatin-induced DNA damage. *Biochem Biophys Res Commun.* **352:**763-8.

Dante R, Dante-Paire J, Rigal D, Roizès G. (1992) Methylation patterns of long interspersed repeated DNA and alphoid repetitive DNA from human cell lines and tumors. *Anticancer Res.* **12:**559-63.

Davis AM, Dische S, Gerber L, Saunders M, Leung SF, O'Sullivan B. (2003) Measuring postirradiation subcutaneous soft-tissue fibrosis: state-of-the-art and future directions. *Semin Radiat Oncol.* **13:**203-13.

Dazzi F, Ramasamy R, Glennie S, Jones SP, Roberts I. (2006) The role of mesenchymal stem cells in haemopoiesis. *Blood Rev.* **20:**161-71.

de Haan G, Van Zant G. (1997) Intrinsic and extrinsic control of hemopoietic stem cell numbers: mapping of a stem cell gene. *J Exp Med.* **186:**529-36.

De Ruyck K, Van Eijkeren M, Claes K, Morthier R, De Paepe A, Vral A, De Ridder L, Thierens H. (2005a) Radiation-induced damage to normal tissues after radiotherapy in patients treated for gynecologic tumors: association with single nucleotide polymorphisms in XRCC1, XRCC3, and OGG1 genes and in vitro chromosomal radiosensitivity in lymphocytes. *Int J Radiat Oncol Biol Phys.* **62:**1140-9.

De Ruyck K, Wilding CS, Van Eijkeren M, Morthier R, Tawn EJ, Thierens H. (2005b) Microsatellite polymorphisms in DNA repair genes XRCC1, XRCC3 and XRCC5 in patients with gynecological tumors: association with late clinical radiosensitivity and cancer incidence. *Radiat Res.* **164:**237-44.

Dong VM, McDermott DH, Abdi R. (2003) Chemokines and diseases. *Eur J Dermatol.* **3:**224-30.

Dubrova YE, Plumb M, Gutierrez B, Boulton E, Jeffreys AJ. (2000) Transgenerational mutation by radiation. *Nature.* **405:**37.

Duthie SJ. (1999) Folic acid deficiency and cancer: mechanisms of DNA instability. *Br Med Bull.* **55:**578-92.

Duthie SJ, Hawdon A. (1998) DNA instability (strand breakage, uracil misincorporation, and defective repair) is increased by folic acid depletion in human lymphocytes in vitro. *FASEB J.* **12:**1491-7.

EBCTCG: Early Breast Cancer Trialists' Collaborative Group (2005) Effects of radiotherapy and of differences in the extent of surgery for early breast cancer on local recurrence and 15-year survival: an overview of the randomised trials. *Lancet.* **366:**2087-106.

Ehrhart EJ, Segarini P, Tsang ML, Carroll AG, Barcellos-Hoff MH. (1997) Latent transforming growth factor beta1 activation in situ: quantitative and functional evidence after low-dose gamma-irradiation. *FASEB J.* **11:**991-1002.

Ehrlich M. (2003) Expression of various genes is controlled by DNA methylation during mammalian development. *J Cell Biochem.* **88:**899-910.

Ehrlich M. (2002) DNA methylation in cancer: too much, but also too little. *Oncogene.* **21:**5400-13.

Ehrlich M, Buchanan KL, Tsien F, Jiang G, Sun B, Uicker W, Weemaes CM, Smeets D, Sperling K, Belohradsky BH, Tommerup N, Misek DE, Rouillard JM, Kuick R,

Hanash SM. (2001) DNA methyltransferase 3B mutations linked to the ICF syndrome cause dysregulation of lymphogenesis genes. *Hum Mol Genet.* **10:**2917-31.

Ehrlich M, Gama-Sosa MA, Huang LH, Midgett RM, Kuo KC, McCune RA, Gehrke C. (1982) Amount and distribution of 5-methylcytosine in human DNA from different types of tissues of cells. *Nucleic Acids Res.* **10:**2709-21.

Eichholzer M, Lüthy J, Moser U, Fowler B. (2001) Folate and the risk of colorectal, breast and cervix cancer: the epidemiological evidence. *Swiss Med Wkly.* **131:**539-49.

Esteller M. (2003) Profiling aberrant DNA methylation in hematologic neoplasms: a view from the tip of the iceberg. *Clin Immunol.* **109:**80-8.

Esteller M. (2002) CpG island hypermethylation and tumor suppressor genes: a booming present, a brighter future. *Oncogene.* **21:**5427-40.

Everson RB, Wehr CM, Erexson GL, MacGregor JT. (1988) Association of marginal folate depletion with increased human chromosomal damage in vivo: demonstration by analysis of micronucleated erythrocytes. *J Natl Cancer Inst.* **80:**525-9.

Feinberg AP, Ohlsson R, Henikoff S. (2006) The epigenetic progenitor origin of human cancer. *Nat Rev Genet.* **7:**21-33.

Fenech M. (2001) The role of folic acid and Vitamin B12 in genomic stability of human cells. *Mutat Res.* **475:** 57-67.

Fiets WE, van Helvoirt RP, Nortier JW, van der Tweel I, Struikmans H. (2003) Acute toxicity of concurrent adjuvant radiotherapy and chemotherapy (CMF or AC) in breast cancer patients. a prospective, comparative, non-randomised study. *Eur J Cancer.* **39:**1081-8.

Fijneman RJ, Vos M, Berkhof J, Demant P, Kraal G. (2004) Genetic analysis of macrophage characteristics as a tool to identify tumor susceptibility genes: mapping of three macrophage-associated risk inflammatory factors, marif1, marif2, and marif3. *Cancer Res.* **64:**3458-64.

Franks LM, Teich NM. (eds) (1997) Introduction to the cellular and molecular biology of human cancer, 3rd edition. Oxford, Oxford University Press.

Friedberg EC, Walker GC, Siede W. (1995) DNA repair and mutagenesis, 1st edition. Washington DC, ASM press.

Gama-Sosa MA, Midgett RM, Slagel VA, Githens S, Kuo KC, Gehrke CW, Ehrlich M. (1983) Tissue-specific differences in DNA methylation in various mammals. *Biochim Biophys Acta.* **740:**212-9.

Gaudet F, Rideout WM 3rd, Meissner A, Dausman J, Leonhardt H, Jaenisch R. (2004) Dnmt1 expression in pre- and postimplantation embryogenesis and the maintenance of IAP silencing. *Mol Cell Biol.* **24:**1640-8.

Gaudet F, Hodgson JG, Eden A, Jackson-Grusby L, Dausman J, Gray JW, Leonhardt H, Jaenisch R. (2003) Induction of tumors in mice by genomic hypomethylation. *Science.* **300:**489-92.

Gauldie J, Galt T, Bonniaud P, Robbins C, Kelly M, Warburton D. (2003) Transfer of the active form of transforming growth factor-beta 1 gene to newborn rat lung induces changes consistent with bronchopulmonary dysplasia. *Am J Pathol.* **163:**2575-84.

Geiger H, True JM, de Haan G, Van Zant G. (2001) Age- and stage-specific regulation patterns in the hematopoietic stem cell hierarchy. *Blood.* **98:**2966-72.

Giotopoulos G, Symonds RP, Foweraker K, Griffin M, Peat I, Osman A, Plumb M. (2007) The late radiotherapy normal tissue injury phenotypes of telangiectasia, fibrosis and atrophy in breast cancer patients have distinct genotype-dependent causes. *Br J Cancer.* **96:**1001-7.

Giotopoulos G, McCormick C, Cole C, Zanker A, Jawad M, Brown R, Plumb M. (2006) DNA methylation during mouse hemopoietic differentiation and radiation-induced leukemia. *Exp Hematol.* **34:**1462-70.

Giovannucci E. (2002) Epidemiologic studies of folate and colorectal neoplasia: a review. *J Nutr.* **132:**2350S-2355S.

Goll MG, Kirpekar F, Maggert KA, Yoder JA, Hsieh CL, Zhang X, Golic KG, Jacobsen SE, Bestor TH. (2006) Methylation of $tRNA^{Asp}$ by the DNA methyltransferase homolog Dnmt2. *Science.* **311:**395-8.

Goll MG, Bestor TH. (2005) Eukaryotic cytosine methyltransferases. *Annu Rev Biochem.* **74:**481-514.

Goode EL, Ulrich CM, Potter JD. (2002) Polymorphisms in DNA repair genes and associations with cancer risk. *Cancer Epidemiol Biomarkers Prev.* **11:**1513-30.

Grainger DJ, Heathcote K, Chiano M, Snieder H, Kemp PR, Metcalfe JC, Carter ND, Spector TD. (1999) Genetic control of the circulating concentration of transforming growth factor type beta1. *Hum Mol Genet.* **8:**93-7.

Greaves MF. (1996) The new biology of leukaemia. In *Leukaemia*, 6th edition, Henderson ES, Lister TA Greaves MF (editors). Philadelphia, WB Saunders Company. p34-45.

Gresner P, Gromadzinska J, Wasowicz W. (2007) Polymorphism of selected enzymes involved in detoxification and biotransformation in relation to lung cancer. *Lung Cancer.* **57:**1-25.

Grosovsky AJ, Parks KK, Giver CR, Nelson SL. (1996) Clonal analysis of delayed karyotypic abnormalities and gene mutations in radiation-induced genetic instability. *Mol Cell Biol.* **16:**6252-62.

Hadi MZ, Coleman MA, Fidelis K, Mohrenweiser HW, Wilson DM. (2000) Functional characterization of Ape1 variants identified in the human population. *Nucleic Acids Res.* **28:**3871–3879.

Hall EJ. (2000) The Physics and chemistry of Radiation absorption/DNA Strand breaks and Chromosomal Aberrations. In *Radiobiology for the radiobiologist*, 5th edition, Hall EJ (editor). Philadelphia, Lippincott Williams And Wilkins Publishers. p5-16/16-31.

Harper K, Lorimore SA, Wright EG. (1997) Delayed appearance of radiation-induced mutations at the Hprt locus in murine hemopoietic cells. *Exp Hematol.* **25:**263-9.

Heijmans BT, Boer JM, Suchiman HE, Cornelisse CJ, Westendorp RG, Kromhout D, Feskens EJ, Slagboom PE. (2003) A common variant of the methylenetetrahydrofolate reductase gene (1p36) is associated with an increased risk of cancer. *Cancer Res.* **63:**1249-53.

Henckaerts E, Langer JC, Snoeck HW. (2004) Quantitative genetic variation in the hematopoietic stem cell and progenitor cell compartment and in lifespan are closely linked at multiple loci in BXD recombinant inbred mice. *Blood.* **104:**374-9.

Henckaerts E, Geiger H, Langer JC, Rebollo P, Van Zant G, Snoeck HW. (2002) Genetically determined variation in the number of phenotypically defined hematopoietic progenitor and stem cells and in their response to early-acting cytokines. *Blood.* **99:**3947-54.

Hendry JH, Akahoshi M, Wang LS, Lipshultz SE, Stewart FA, Trott KR. (2008) Radiation-induced cardiovascular injury. *Radiat Environ Biophys.* **47:**189-93.

Herman H, Feil R. (2008) The Biology of Genomic Imprinting. In *Epigenetics*, 1st edition, Tost J (editor). Norfolk, Caister Academic Press. p249-271.

Hodgetts SI, Grounds MD. (2003) Irradiation of dystrophic host tissue prior to myoblast transfer therapy enhances initial (but not long-term) survival of donor myoblasts. *J Cell Sci.* **116:**4131-46.

Hoeijmakers JH. (2001) Genome maintenance mechanisms for preventing cancer. *Nature.* **411:**366-74.

Hoeller U, Borgmann K, Bonacker M, Kuhlmey A, Bajrovic A, Jung H, Alberti W, Dikomey E. (2003) Individual radiosensitivity measured with lymphocytes may be used to predict the risk of fibrosis after radiotherapy for breast cancer. *Radiother Oncol.* **69:**137-44.

Hu JJ, Smith TR, Miller MS, Lohman K, Case LD. (2002) Genetic regulation of ionizing radiation sensitivity and breast cancer risk. *Environ Mol Mutagen.* **39:**208-15.

Hu JJ, Smith TR, Miller MS, Mohrenweiser HW, Golden A, Case LD. (2001) Amino acid substitution variants of APE1 and XRCC1 genes associated with ionizing radiation sensitivity. *Carcinogenesis.* **22:**917-22.

Hu Z, Ma H, Chen F, Wei Q, Shen H. (2005) XRCC1 polymorphisms and cancer risk: a meta-analysis of 38 case-control studies. *Cancer Epidemiol Biomarkers Prev.* **14:**1810-8.

Humpe A, Riggert J, Vehmeyer K, Troff C, Hiddemann W, Köhler M, Wörmann B. (1997) Comparison of CD34+ cell numbers and colony growth before and after cryopreservation of peripheral blood progenitor and stem cell harvests: influence of prior chemotherapy. *Transfusion.* **37:**1050-7.

Hung RJ, Brennan P, Canzian F, Szeszenia-Dabrowska N, Zaridze D, Lissowska J, Rudnai P, Fabianova E, Mates D, Foretova L, Janout V, Bencko V, Chabrier A, Borel S, Hall J, Boffetta P. (2005) Large-scale investigation of base excision repair genetic polymorphisms and lung cancer risk in a multicenter study. *J Natl Cancer Inst.* **97:**567-76.

Ikuta K, Weissman IL. (1992) Evidence that hematopoietic stem cells express mouse c-kit but do not depend on steel factor for their generation. *Proc Natl Acad Sci USA.* **89:**1502-6.

Ishihara H, Tanaka I, Wan H, Nojima K, Yoshida K. (2004) Retrotransposition of limited deletion type of intracisternal A-particle elements in the myeloid leukemia Clls of C3H/He mice. *J Radiat Res.* **45:**25-32.

Jair KW, Bachman KE, Suzuki H, Ting AH, Rhee I, Yen RW, Baylin SB, Schuebel KE. (2006) De novo CpG island methylation in human cancer cells. *Cancer Res.* **66:**682-92.

Jawad M, Cole C, Zanker A, Giotopoulos G, Fitch S, Talbot CJ, Plumb M. (2008) QTL analyses of lineage-negative mouse bone marrow cells labelled with Sca-1 and c-Kit. *Mamm Genome.* **19:**190-8.

Jawad M, Giotopoulos G, Cole C, Plumb M. (2007a) Target cell frequency is a genetically determined risk factor in radiation leukaemogenesis. *Br J Radiol.* **80 Spec No 1:**56-62.

Jawad M, Giotopoulos G, Fitch S, Cole C, Plumb M, Talbot CJ. (2007b) Mouse bone marrow and peripheral blood erythroid cell counts are regulated by different autosomal genetic loci. *Blood Cells Mol Dis.* **38:**69-77.

Jawad M. (2006) Genetic Susceptibility to Radiation-Induced Acute Myeloid Leukaemia (r-AML). PhD thesis. Department of Genetics. University of Leicester.

Jawad M, Seedhouse CH, Russell N, Plumb M. (2006) Polymorphisms in human homeobox HLX1 and DNA repair RAD51 genes increase the risk of therapy-related acute myeloid leukemia. *Blood.* **108:**3916-8.

Johnson WG, Stenroos ES, Spychala JR, Chatkupt S, Ming SX, Buyske S. (2004) New 19 bp deletion polymorphism in intron-1 of dihydrofolate reductase (DHFR): a risk factor for spina bifida acting in mothers during pregnancy? *Am J Med Genet A.* **124:**339-45.

Jones PA, Baylin SB. (2007) The epigenomics of cancer. *Cell.* **128:**683-92.

Jones PA, Baylin SB. (2002) The fundamental role of epigenetic events in cancer. *Nat Rev Genet.* **3:**415-28.

Jones RJ, Celano P, Sharkis SJ, Sensenbrenner LL. (1989) Two phases of engraftment established by serial bone marrow transplantation in mice. *Blood.* **73:**397-401.

Kadhim MA, Lorimore SA, Hepburn MD, Goodhead DT, Buckle VJ, Wright EG. (1994) Alpha-particle-induced chromosomal instability in human bone marrow cells. *Lancet.* **344:**987-8.

Kadhim MA, Macdonald DA, Goodhead DT, Lorimore SA, Marsden SJ, Wright EG. (1992) Transmission of chromosomal instability after plutonium alpha-particle irradiation. *Nature.* **355:**738-40.

Kalinich JF, Catravas GN, Snyder SL. (1989) The effect of gamma radiation on DNA methylation. *Radiat Res.* **117:**185-97.

Kara I, Sazci A, Ergul E, Kaya G, Kilic G. (2003) Association of the C677T and A1298C polymorphisms in the 5,10 methylenetetrahydrofolate reductase gene in patients with migraine risk. *Brain Res Mol Brain Res.* **111:**84-90.

Kazazian HH Jr. (2004) Mobile elements: drivers of genome evolution. *Science.* **303:**1626-32.

Kazazian HH Jr, Moran JV. (1998) The impact of L1 retrotransposons on the human genome. *Nat Genet.* **19:**19-24.

Kesavan V, Pote MS, Batra V, Viswanathan G. (2003) Increased folate catabolism following total body gamma-irradiation in mice. *J Radiat Res (Tokyo).* **44:**141-4.

Kiel MJ, Yilmaz OH, Iwashita T, Yilmaz OH, Terhorst C, Morrison SJ. (2005) SLAM family receptors distinguish hematopoietic stem and progenitor cells and reveal endothelial niches for stem cells. *Cell.* **121:**1109-21.

Kim YI. (2004) Folate, colorectal carcinogenesis, and DNA methylation: lessons from animal studies. *Environ Mol Mutagen.* **44:**10-25.

King Roger JB. (editor) (2000) Cancer Biology, 2nd edition. Harlow, Pearson Prentice Hall.

Klerk M, Lievers KJ, Kluijtmans LA, Blom HJ, den Heijer M, Schouten EG, Kok FJ, Verhoef P. (2003) The 2756A>G variant in the gene encoding methionine synthase: its relation with plasma homocysteine levels and risk of coronary heart disease in a Dutch case-control study. *Thromb Res.* **110:**87-91.

Kobayashi S, Nishimura M, Shimada Y, Suzuki F, Matsuoka A, Sakamoto H, Hayashi M, Sofuni T, Sado T, Ogiu T. (1997) Increased sensitivity of scid heterozygous mice to ionizing radiation. *Int J Radiat Biol.* **72:**537-45.

Kodama K, Fujiwara S, Yamada M, Kasagi F, Shimizu Y, Shigematsu I. (1996) Profiles of non-cancer diseases in atomic bomb survivors. *World Health Stat Q.* **49:**7-16.

Kondo M, Wagers AJ, Manz MG, Prohaska SS, Scherer DC, Beilhack GF, Shizuru JA, Weissman IL. (2003) Biology of hematopoietic stem cells and progenitors: implications for clinical application. *Annu Rev Immunol.* **21:**759-806.

Koturbash I, Pogribny I, Kovalchuk O. (2005) Stable loss of global DNA methylation in the radiation-target tissue--a possible mechanism contributing to radiation carcinogenesis? *Biochem Biophys Res Commun.* **337:**526-33.

Kovalchuk O, Burke P, Besplug J, Slovack M, Filkowski J, Pogribny I. (2004) Methylation changes in muscle and liver tissues of male and female mice exposed to acute and chronic low-dose X-ray-irradiation. *Mutat Res.* **548:**75-84.

Ladiges WC. (2006) Mouse models of XRCC1 DNA repair polymorphisms and cancer. *Oncogene.* **25:**1612-9.

Lander E, Kruglyak L. (1995) Genetic dissection of complex traits: guidelines for interpreting and reporting linkage results. *Nat Genet.* **11:**241-247.

Lebailly P, Willett EV, Moorman AV, Roman E, Cartwright R, Morgan GJ, Wild CP. (2002) Genetic polymorphisms in microsomal epoxide hydrolase and susceptibility to adult acute myeloid leukaemia with defined cytogenetic abnormalities. *Br J Haematol.* **116:**587-94.

Lee E, Burgess G, Win N. (2005) Autoimmune hemolytic anemia and a further example of autoanti-Kpb. *Immunohematology.* **21:**119-21.

Leone G, Mele L, Pulsoni A, Equitani F, Pagano L. (1999) The incidence of secondary leukemias. *Haematologica.* **84:**937-45.

Li C, Wilson PB, Levine E, Barber J, Stewart AL, Kumar S. (1999) TGF-beta1 levels in pre-treatment plasma identify breast cancer patients at risk of developing post-radiotherapy fibrosis. *Int J Cancer.* **84:**155-9.

Libbus BL, Borman LS, Ventrone CH, Branda RF. (1990) Nutritional folate-deficiency in Chinese hamster ovary cells. Chromosomal abnormalities associated with perturbations in nucleic acid precursors. *Cancer Genet Cytogenetic.* **46:**231-42.

Limoli CL, Kaplan MI, Giedzinski E, Morgan WF. (2001) Attenuation of radiation-induced genomic instability by free radical scavengers and cellular proliferation. *Free Radic Biol Med.* **31:**10-9.

Lin JP, O'Donnell CJ, Levy D, Cupples LA. (2005) Evidence for a gene influencing haematocrit on chromosome 6q23-24: genome wide scan in the Framingham Heart Study. *J Med Genet.* **42:**75-9.

Little JB. (2003) Genomic instability and radiation. *J Radiol Prot.* **23:**173-81.

Liu N. (2002) XRCC2 is Required for the Formation of Rad51 Foci Induced by Ionizing Radiation and DNA Cross-Linking Agent Mitomycin C. *J Biomed Biotechnol.* **2:**106-113.

Loft S, Poulsen HE. (1996) Cancer risk and oxidative DNA damage in man. *J Mol Med.* **74:**297-312.

Lopez E, Guerrero R, Nunez MI, del Moral R, Villalobos M, Martínez-Galan J, Valenzuela MT, Munoz-Gamez JA, Oliver FJ, Martin-Oliva D, Ruiz de Almodovar JM (2005) Early and late skin reactions to radiotherapy for breast cancer and their correlation with radiation-induced DNA damage in lymphocytes. *Breast Cancer Res.* **7:**R690-8.

Lorimore SA, Coates PJ, Wright EG. (2003) Radiation-induced genomic instability and bystander effects: inter-related nontargeted effects of exposure to ionizing radiation. *Oncogene.* **22:**7058-69.

Lorimore SA, Pragnell IB, Eckmann L, Wright EG. (1990) Synergistic interactions allow colony formation in vitro by murine haemopoietic stem cells. *Leuk Res.* **14:**481-9.

Lyng FM, O'Reilly S, Cottell DC, Seymour CB, Mothersill C. (1996) Persistent expression of morphological abnormalities in the distant progeny of irradiated cells. *Radiat Environ Biophys.* **35:**273-83.

MacCallum DE, Hupp TR, Midgley CA, Stuart D, Campbell SJ, Harper A, Walsh FS, Wright EG, Balmain A, Lane DP, Hall PA. (1996) The p53 response to ionising radiation in adult and developing murine tissues. *Oncogene.* **13:**2575-87.

MacGregor JT, Schlegel R, Wehr CM, Alperin P, Ames BN. (1990) Cytogenetic damage induced by folate deficiency in mice is enhanced by caffeine. *Proc Natl Acad Sci U S A.* **87:**9962-5.

Mao JH, Balmain A. (2003) Genomic approaches to identification of tumour-susceptibility genes using mouse models. *Curr Opin Genet Dev.* **13:**14-9.

Marder BA, Morgan WF. (1993) Delayed chromosomal instability induced by DNA damage. *Mol Cell Biol.* **13:**6667-77.

Marley SB, Lewis JL, Davidson RJ, Roberts IA, Dokal I, Goldman JM, Gordon MY. (1999) Evidence for a continuous decline in haemopoietic cell function from birth: application to evaluating bone marrow failure in children. *Br J Haematol.* **106:**162-6.

Martin M, Lefaix J, Delanian S. (2000) TGF-beta1 and radiation fibrosis: a master switch and a specific therapeutic target? *Int J Radiat Oncol Biol Phys.* **47:**277-90.

Martin M, Vozenin MC, Gault N, Crechet F, Pfarr CM, Lefaix JL. (1997) Coactivation of AP-1 activity and TGF-beta1 gene expression in the stress response of normal skin cells to ionizing radiation. *Oncogene.* **15:**981-9.

Matsuo K, Suzuki R, Hamajima N, Ogura M, Kagami Y, Taji H, Kondoh E, Maeda S, Asakura S, Kaba S, Nakamura S, Seto M, Morishima Y, Tajima K. (2001) Association between polymorphisms of folate- and methionine-metabolizing enzymes and susceptibility to malignant lymphoma. *Blood.* **97:**3205-9.

Matsuura K, Nagai T, Nishigaki N, Oyama T, Nishi J, Wada H, Sano M, Toko H, Akazawa H, Sato T, Nakaya H, Kasanuki H, Komuro I. (2004) Adult cardiac Sca-1-positive cells differentiate into beating cardiomyocytes. *J Biol Chem.* **279:**11384-91.

Mayer C, Popanda O, Zelezny O, von Brevern MC, Bach A, Bartsch H, Schmezer P. (2002) DNA repair capacity after gamma-irradiation and expression profiles of DNA repair genes in resting and proliferating human peripheral blood lymphocytes. *DNA Repair (Amst).* **1:**237-50.

McDermott DH, Fong AM, Yang Q, Sechler JM, Cupples LA, Merrell MN, Wilson PW, D'Agostino RB, O'Donnell CJ, Patel DD, Murphy PM. (2003) Chemokine receptor mutant CX3CR1-M280 has impaired adhesive function and correlates with protection from cardiovascular disease in humans. *J Clin Invest.* **111:**1241-50.

McDermott DH, Halcox JP, Schenke WH, Waclawiw MA, Merrell MN, Epstein N, Quyyumi AA, Murphy PM. (2001) Association between polymorphism in the chemokine receptor CX3CR1 and coronary vascular endothelial dysfunction and atherosclerosis. *Circ Res.* **89:**401-7.

McGrath K, Palis J. (2008) Ontogeny of erythropoiesis in the mammalian embryo. *Curr Top Dev Biol.* **82:**1-22.

Mettler FA Jr, Gus'kova AK, Gusev I. (2007) Health effects in those with acute radiation sickness from the Chernobyl accident. *Health Phys.* **93:**462-9.

Meyn MS. (1999) Ataxia-telangiectasia, cancer and the pathobiology of the ATM gene. *Clin Genet.* **55:**289-304.

Midgley CA, Owens B, Briscoe CV, Thomas DB, Lane DP, Hall PA. (1995) Coupling between gamma irradiation, p53 induction and the apoptotic response depends upon cell type in vivo. *J Cell Sci.* **108:**1843-8.

Miki Y, Nishisho I, Horii A, Miyoshi Y, Utsunomiya J, Kinzler KW, Vogelstein B, Nakamura Y. (1992) Disruption of the APC gene by a retrotransposal insertion of L1 sequence in a colon cancer. *Cancer Res.* **52:**643-5.

Mock BA, Krall MM, Dosik JK. (1993) Genetic mapping of tumor susceptibility genes involved in mouse plasmacytomagenesis. *Proc Natl Acad Sci USA.* **90:**9499-503.

Monk M, Boubelik M, Lehnert S. (1987) Temporal and regional changes in DNA methylation in the embryonic, extraembryonic and germ cell lineages during mouse embryo development. *Development.* **99:**371-82.

Morgan WF. (2003a) Non-targeted and delayed effects of exposure to ionizing radiation: I. Radiation-induced genomic instability and bystander effects in vitro. *Radiat Res.* **159:**567-80.

Morgan WF. (2003b) Non-targeted and delayed effects of exposure to ionizing radiation: II. Radiation-induced genomic instability and bystander effects in vivo, clastogenic factors and transgenerational effects. *Radiat Res.* **159:**581-96.

Morison IM, Ramsay JP, Spencer HG. (2005) A census of mammalian imprinting. *Trends Genet.* **21:**457-65.

Morita H, Taguchi J, Kurihara H, Kitaoka M, Kaneda H, Kurihara Y, Maemura K, Shindo T, Minamino T, Ohno M, Yamaoki K, Ogasawara K, Aizawa T, Suzuki S, Yazaki Y. (1997) Genetic polymorphism of 5,10-methylenetetrahydrofolate reductase (MTHFR) as a risk factor for coronary artery disease. *Circulation.* **95:**2032-6.

Morrison SJ, Qian D, Jerabek L, Thiel BA, Park IK, Ford PS, Kiel MJ, Schork NJ, Weissman IL, Clarke MF. (2002) A genetic determinant that specifically regulates the frequency of hematopoietic stem cells. *J Immunol.* **168:**635-42.

Morse B, Rotherg PG, South VJ, Spandorfer JM, Astrin SM. (1988) Insertional mutagenesis of the myc locus by a LINE-1 sequence in a human breast carcinoma. *Nature.* **333:**87-90.

Moullan N, Cox DG, Angèle S, Romestaing P, Gérard JP, Hall J. (2003) Polymorphisms in the DNA repair gene XRCC1, breast cancer risk, and response to radiotherapy. *Cancer Epidemiol Biomarkers Prev.* **12:**1168-74.

Müller-Sieburg CE, Riblet R. (1996) Genetic control of the frequency of hematopoietic stem cells in mice: mapping of a candidate locus to chromosome 1. *J Exp Med.* **183:**1141-50.

Nakagawa H, Nuovo GJ, Zervos EE, Martin EW Jr, Salovaara R, Aaltonen LA, de la Chapelle A. (2001) Age-related hypermethylation of the 5' region of MLH1 in normal colonic mucosa is associated with microsatellite-unstable colorectal cancer development. *Cancer Res.* **61:**6991-5.

Narayan A, Tuck-Muller C, Weissbecker K, Smeets D, Ehrlich M. (2000) Hypersensitivity to radiation-induced non-apoptotic and apoptotic death in cell lines from patients with the ICF chromosome instability syndrome. *Mutat Res.* **456:**1-15.

Narayan A, Ji W, Zhang XY, Marrogi A, Graff JR, Baylin SB, Ehrlich M. (1998) Hypomethylation of pericentromeric DNA in breast adenocarcinomas. *Int J Cancer.* **77:**833-8.

NCRN (1998) Trial Standardisation of Breast Radiotherapy. *Clinical Trials and Statistics Unit.* Sutton, Surrey, UK: Institute of Cancer Research.

Ochiai K, Ozaki S, Tanino A, Watanabe S, Ueno T, Mitsui K, Toei J, Inada Y, Hirose S, Shirai T, Nishimura H. (2000) Genetic regulation of anti-erythrocyte autoantibodies and splenomegaly in autoimmune hemolytic anemia-prone new zealand black mice. *Int Immunol.* **12:**1-8.

Okada S, Nakauchi H, Nagayoshi K, Nishikawa S, Miura Y, Suda T. (1992) In vivo and in vitro stem cell function of c-kit- and Sca-1-positive murine hematopoietic cells. *Blood.* **80:**3044-50.

Okada S, Nakauchi H, Nagayoshi K, Nishikawa S, Nishikawa S, Miura Y, Suda T. (1991) Enrichment and characterization of murine hematopoietic stem cells that express c-kit molecule. *Blood.* **78:**1706-12.

Okano M, Bell DW, Haber DA, Li E. (1999) DNA methyltransferases Dnmt3a and Dnmt3b are essential for de novo methylation and mammalian development. *Cell.* **99:**247-57.

O'Sullivan B, Levin W. (2003) Late radiation-related fibrosis: pathogenesis, manifestations, and current management. *Semin Radiat Oncol.* **13:**274-89.

Paulsen M, Tierling S, Walter J (2008) DNA Methylation and the Mammalian Genome. In *Epigenetics*, 1st edition, Tost J. (editor). Norfolk, Caister Academic Press. p1-21.

Pavy JJ, Denekamp J, Letschert J, Littbrand B, Mornex F, Bernier J, Gonzales-Gonzales D, Horiot JC, Bolla M, Bartelink H. (1995) EORTC Late Effects Working Group. Late effects toxicity scoring: the SOMA scale. *Radiother Oncol.* **35**:11-5.

Pedersen-Bjergaard J, Pedersen M, Roulston D, Philip P. (1995) Different genetic pathways in leukemogenesis for patients presenting with therapy-related myelodysplasia and therapy-related acute myeloid leukaemia. *Blood.* **86:**3542-52.

Peled A, Petit I, Kollet O, Magid M, Ponomaryov T, Byk T, Nagler A, Ben-Hur H, Many A, Shultz L, Lider O, Alon R, Zipori D, Lapidot T. (1999) Dependence of human stem cell engraftment and repopulation of NOD/SCID mice on CXCR4. *Science.* **283:**845-8.

Pierce DA, Shimizu Y, Preston DL, Vaeth M, Mabuchi K. (1996) Studies of the mortality of atomic bomb survivors. Report 12, Part I. Cancer: 1950-1990. *Radiat Res.* **146:**1-27.

Pinar B, Lara PC, Lloret M, Bordon E, Nunez MI, Villalobos M, Guerrero R, Luna JD, Ruiz de Almodovar JM. (2007) Radiation-induced DNA damage as a predictor of long-term toxicity in locally advanced breast cancer patients treated with high-dose hyperfractionated radical radiotherapy. *Radiat Res.* **168:**415-22.

Plass C. (2002) Cancer epigenomics. *Hum Mol Genet.* **11:**2479-88.

Plumb JA, Strathdee G, Sludden J, Kaye SB, Brown R. (2000) Reversal of drug resistance in human tumor xenografts by 2'-deoxy-5-azacytidine-induced demethylation of the hMLH1 gene promoter. *Cancer Res.* **60:**6039-44.

Plumb M. (2003) Comments on the paper: Microsatellite instability in acute myelocytic leukaemia developed from A-bomb survivors--a biological perspective. *Int J Radiat Biol.* **79:**367-70.

Plumb M, Cleary H, Wright E. (1998) Genetic instability in radiation-induced leukaemias: mouse models. *Int J Radiat Biol.* **74:**711-20.

Pogribny I, Raiche J, Slovack M, Kovalchuk O. (2004) Dose-dependence, sex- and tissue-specificity, and persistence of radiation-induced genomic DNA methylation changes. *Biochem Biophys Res Commun.* **320:**1253-61.

Ponnaiya B, Cornforth MN, Ullrich RL. (1997) Radiation-induced chromosomal instability in BALB/c and C57BL/6 mice: the difference is as clear as black and white. *Radiat Res.* **147:**121-5.

Popanda O, Ebbeler R, Twardella D, Helmbold I, Gotzes F, Schmezer P, Thielmann HW, von Fournier D, Haase W, Sautter-Bihl ML, Wenz F, Bartsch H, Chang-Claude J. (2003) Radiation-induced DNA damage and repair in lymphocytes from breast cancer patients and their correlation with acute skin reactions to radiotherapy. *Int J Radiat Oncol Biol Phys.* **55:**1216-25.

Pravenec M, Zidek V, Zdobinska M, Kren V, Krenova D, Bottger A, van Zutphen LF, Wang J, St Lezin E. (1997) Mapping genes controlling hematocrit in the spontaneously hypertensive rat. *Mamm Genome.* **8:**387-9.

Preston DL, Shimizu Y, Pierce DA, Suyama A, Mabuchi K. (2003) Studies of mortality of atomic bomb survivors. Report 13: Solid cancer and noncancer disease mortality: 1950–1997. *Radiat Res.* **160:**381–407.

Ptasznik A, Urbanowska E, Chinta S, Costa MA, Katz BA, Stanislaus MA, Demir G, Linnekin D, Pan ZK, Gewirtz AM. (2002) Crosstalk between BCR/ABL oncoprotein and CXCR4 signaling through a Src family kinase in human leukemia cells. *J Exp Med.* **196:**667-78.

Qu G, Dubeau L, Narayan A, Yu MC, Ehrlich M. (1999) Satellite DNA hypomethylation vs. overall genomic hypomethylation in ovarian epithelial tumors of different malignant potential. *Mutat Res.* **423:**91-101.

Quarmby S, Fakhoury H, Levine E, Barber J, Wylie J, Hajeer AH, West C, Stewart A, Magee B, Kumar S. (2003) Association of transforming growth factor beta-1 single nucleotide polymorphisms with radiation-induced damage to normal tissues in breast cancer patients. *Int J Radiat Biol.* **79:**137-43.

Quinlan JG, Cambier D, Lyden S, Dalvi A, Upputuri RK, Gartside P, Michaels SE, Denman D. (1997) Regeneration-blocked mdx muscle: in vivo model for testing treatments. *Muscle Nerve.* **20:**1016-23.

Quinlan JG, Lyden SP, Cambier DM, Johnson SR, Michaels SE, Denman DL. (1995) Radiation inhibition of mdx mouse muscle regeneration: dose and age factors. *Muscle Nerve.* **18:**201-6.

Rafii S, O'Regan P, Xinarianos G, Azmy I, Stephenson T, Reed M, Meuth M, Thacker J, Cox A. (2002) A potential role for the XRCC2 R188H polymorphic site in DNA-damage repair and breast cancer. *Hum Mol Genet.* **11:**1433-8.

Raiche J, Rodriguez-Juarez R, Pogribny I, Kovalchuk O. (2004) Sex- and tissue-specific expression of maintenance and de novo DNA methyltransferases upon low dose X-irradiation in mice. *Biochem Biophys Res Commun.* **325:**39-47.

Randall K, Coggle JE. (1996) Long-term expression of transforming growth factor TGF beta 1 in mouse skin after localized beta-irradiation. *Int J Radiat Biol.* **70:**351-60.

Randall K, Coggle JE. (1995) Expression of transforming growth factor-beta 1 in mouse skin during the acute phase of radiation damage. *Int J Radiat Biol.* **68:**301-9.

Rithidech KN, Cronkite EP, Bond VP. (1999) Advantages of the CBA mouse in leukemogenesis research. *Blood Cells Mol Dis.* **25:**38-45.

Roberts SA, Spreadborough AR, Bulman B, Barber JB, Evans DG, Scott D. (1999) Heritability of cellular radiosensitivity: a marker of low-penetrance predisposition genes in breast cancer? *Am J Hum Genet.* **65:**784-94.

Robertson KD, Wolffe AP. (2000) DNA methylation in health and disease. *Nat Rev Genet.* **1:**11-9.

Robertson KD, Uzvolgyi E, Liang G, Talmadge C, Sumegi J, Gonzales FA, Jones PA. (1999) The human DNA methyltransferases (DNMTs) 1, 3a and 3b: coordinate mRNA expression in normal tissues and overexpression in tumors. *Nucleic Acids Res.* **27:**2291-8.

Rocha JL, Eisen EJ, Van Vleck LD, Pomp D. (2004) A large-sample QTL study in mice: II. Body composition. *Mamm Genome.* **15:**100-13.

Rodemann HP, Bamberg M. (1995) Cellular basis of radiation-induced fibrosis. *Radiother Oncol.* **35:**83-90.

Rogers PB, Plowman PN, Harris SJ, Arlett CF. (2000) Four radiation hypersensitivity cases and their implications for clinical radiotherapy. *Radiother Oncol.* **57:**143-54.

Rollins RA, Haghighi F, Edwards JR, Das R, Zhang MQ, Ju J, Bestor TH. (2006) Large-scale structure of genomic methylation patterns. *Genome Res.* **16:**157-63.

Ron E. (1998) Ionizing radiation and cancer risk: evidence from epidemiology. *Radiat Res.* **50(5 Suppl):**S30-41.

Rouleau C, Cui K, Feldman L. (2004) A functional erythropoietin receptor is necessary for the action of thrombopoietin on erythroid cells lacking c-mpl. *Exp Hematol.* **32:**140-8.

Rubin P, Constine LS, Fajardo LF, Phillips TL, Wasserman TH. (1995) RTOG Late Effects Working Group. Overview. Late Effects of Normal Tissues (LENT) scoring system. *Int J Radiat Oncol Biol Phys.* **31**:1041-2.

Sandovici I, Smith NH, Ozanne SE, Constancia M. (2008) The Dynamic Epigenome: The impact of the Environment on Epigenetic Regulation of Gene Expression and Developmental Programming. In *Epigenetics*, 1st edition, Tost J. (editor). Norfolk, Caister Academic Press. p343-370.

Sarbia M, Stahl M, von Weyhern C, Weirich G, Pühringer-Oppermann F. (2006) The prognostic significance of genetic polymorphisms (Methylenetetrahydrofolate Reductase C677T, Methionine Synthase A2756G, Thymidilate Synthase tandem repeat polymorphism) in multimodally treated oesophageal squamous cell carcinoma. *Br J Cancer*. **94:**203-7.

Savonet V, Maenhaut C, Miot F, Pirson I. (1997) Pitfalls in the use of several "housekeeping" genes as standards for quantitation of mRNA: the example of thyroid cells. *Anal Biochem.* **247:**165-7.

Schofield PN. (1998) Impact of genomic imprinting on genomic instability and radiation-induced mutation. *Int J Radiat Biol.* **74:**705-10.

Schultz-Hector S, Trott KR. (2007) Radiation-induced cardiovascular diseases: is the epidemiologic evidence compatible with the radiobiologic data? *Int J Radiat Oncol Biol Phys.* **67:**10-8.

Schulz WA. (2006) L1 retrotransposons in human cancers. *J Biomed Biotechnol.* **2006:**83672.

Sengupta AK, Ohhata T, Wutz A. (2008) X Chromosome Inactivation. In *Epigenetics*, 1st edition, Tost J (editor). Norfolk, Caister Academic Press. p273-301.

Shakespeare TP, Ferrier AJ, Holecek MJ, Jagavkar RS, Steven MJ. (1998) Difficulties using the Franco-Italian Glossary in assessing toxicity of cervical cancer treatment. *Int J Gynecol Cancer*. **8**:51-55.

Shanley S, McReynolds K, Ardern-Jones A, Ahern R, Fernando I, Yarnold J, Evans G, Eccles D, Hodgson S, Ashley S, Ashcroft L, Tutt A, Bancroft E, Short S, Smith I, Gui G; Royal Marsden NHS Foundation Trust, Barr L, Baildam A, Howell A, Royle G, Pierce L, Easton D, Eeles R. (2006) Acute chemotherapy-related toxicity is not increased in BRCA1 and BRCA2 mutation carriers treated for breast cancer in the United Kingdom. *Clin Cancer Res.* **12:**7033-8.

Sharp L, Little J. (2004) Polymorphisms in genes involved in folate metabolism and colorectal neoplasia: a HuGE review. *Am J Epidemiol.* **159:**423-43.

Shimizu Y, Pierce DA, Preston DL, Mabuchi K. (1999) Studies of the mortality of atomic bomb survivors. Report 12, part II. Noncancer mortality: 1950-1990. *Radiat Res.* **152:**374-89.

Sims JK, Magazinnik T, Houston SI, Wu S, Rice JC. (2008) Histone modifications and Epigenetics. In *Epigenetics*, 1st edition, Tost J. (editor). Norfolk, Caister Academic Press. p105-125.

Smith LG, Weissman IL, Heimfeld S. (1991) Clonal analysis of hematopoietic stem-cell differentiation in vivo. *Proc Natl Acad Sci USA.* **88:**2788-92.

Sokal RR, Rohlf FJ (eds) (1995) In *Biometry,* 3rd Edition. New York, USA: W.H. Freeman and Company.

Souhami RL, Tannock I, Hohenberger P, Horiot J-C. (eds) (2001) *The Oxford Textbook of Oncology,* 2nd edition. Oxford, Oxford University Press.

Spangrude GJ, Brooks DM. (1993) Mouse strain variability in the expression of the hematopoietic stem cell antigen Ly-6A/E by bone marrow cells. *Blood.* **82:**3327-32.

Spangrude GJ, Heimfeld S, Weissman IL. (1988) Purification and characterisation of mouse hematopoietic stem cells. *Science.* **241**:58-62.

Sproston AR, West CM, Hendry JH. (1997) Cellular radiosensitivity in human severe-combined-immunodeficiency (SCID) syndromes. *Radiother Oncol.* **42:**53-7.

Steel GG. (1993) Introduction: The significance of radiobiology for radiotherapy. In *Basic Clinical Radiobiology*, 1st edition, Steel GG (editor). London, Edward Arnold Publishers. p1-7.

Szilvassy SJ, Humphries RK, Lansdorp PM, Eaves AC, Eaves CJ. (1990) Quantitative assay for totipotent reconstituting hematopoietic stem cells by a competitive repopulation strategy. *Proc Natl Acad Sci USA.* **87:**8736-40.

Tadokoro Y, Ema H, Okano M, Li E, Nakauchi H. (2007) De novo DNA methyltransferase is essential for self-renewal, but not for differentiation, in hematopoietic stem cells. *J Exp Med.* **204:**715-22.

Taramelli R, Acquati F. (2004) The human genome project and the discovery of genetic determinants of cancer susceptibility. *Eur J Cancer.* **40:**2537-43.

Tavor S, Petit I, Porozov S, Avigdor A, Dar A, Leider-Trejo L, Shemtov N, Deutsch V, Naparstek E, Nagler A, Lapidot T. (2004) CXCR4 regulates migration and development of human acute myelogenous leukemia stem cells in transplanted NOD/SCID mice. *Cancer Res.* **64:**2817-24.

Tawa R, Kimura Y, Komura J, Miyamura Y, Kurishita A, Sasaki MS, Sakurai H, Ono T. (1998) Effects of X-ray irradiation on genomic DNA methylation levels in mouse tissues. *J Radiat Res (Tokyo).* **39:**271-8.

Tebbs RS, Flannery ML, Meneses JJ, Hartmann A, Tucker JD, Thompson LH, Cleaver JE, Pedersen RA. (1999) Requirement for the Xrcc1 DNA base excision repair gene during early mouse development. *Dev Biol.* **208:**513-29.

Thacker J, Zdzienicka MZ. (2004) The XRCC genes: expanding roles in DNA double-strand break repair. *DNA Repair (Amst).* **3:**1081-90.

Tilbrook PA, Klinken SP. (1999) The erythropoietin receptor. *Int J Biochem Cell Biol.* **31:**1001-5.

Toms JR (ed). (2004) CancerStats Monograph 2004. London, Cancer Research 138 UK. Ref Type: Report.

Tower RL, Spector LG. (2007) The epidemiology of childhood leukemia with a focus on birth weight and diet. *Crit Rev Clin Lab Sci.* **44:**203-42.

Travis LB, Weeks J, Curtis RE, Chaffey JT, Stovall M, Banks PM, Boice JD Jr. (1996) Leukemia following low-dose total body irradiation and chemotherapy for non-Hodgkin's lymphoma. *J Clin Oncol.* **14:**565-71.

Trivedi A, Hannan MA. (2004) Radiation and cardiovascular diseases. *J Environ Pathol Toxicol Oncol.* **23:**99–106.

Tuck-Muller CM, Narayan A, Tsien F, Smeets DF, Sawyer J, Fiala ES, Sohn OS, Ehrlich M. (2000) DNA hypomethylation and unusual chromosome instability in cell lines from ICF syndrome patients. *Cytogenet Cell Genet.* **89:**121-8.

Uchida N, Weissman IL. (1992) Searching for hematopoietic stem cells: evidence that Thy-1.1lo Lin- Sca-1+ cells are the only stem cells in C57BL/Ka-Thy-1.1 bone marrow. *J Exp Med.* **175:**175-84.

Ullrich RL, Davis CM. (1999) Radiation-induced cytogenetic instability in vivo. *Radiat Res.* **152:**170-3.

Van der Kogel AJ (1993) Cell proliferation in normal tissues/Radiobiology of normal tissues. In *Basic Clinical Radiobiology*, 1st edition, Steel GG (editor). London, Edward Arnold Publishers. p23-27/99-107-98.

Van der Put NM, Steegers-Theunissen RP, Frosst P, Trijbels FJ, Eskes TK, van den Heuvel LP, Mariman EC, den Heyer M, Rozen R, Blom HJ. (1995) Mutated methylenetetrahydrofolate reductase as a risk factor for spina bifida. *Lancet.* **346:**1070-1.

Van Emburgh BO, Robertson KD. (2008) DNA Methyltransferases and Methyl-CpG Binding Proteins as Multifunctional Regulators of Chromatin Structure and Development in Mammalian Cells. In *Epigenetics*, 1st edition, Tost J. (editor). Norfolk, Caister Academic Press. p24-61.

van Os R, Ausema A, Noach EJ, van Pelt K, Dontje BJ, Vellenga E, de Haan G. (2006) Identification of quantitative trait loci regulating haematopoietic parameters in B6AKRF2 mice. *Br J Haematol.* **132:**80-90.

Wada T, Nagata Y, Nagahisa H, Okutomi K, Ha SH, Ohnuki T, Kanaya T, Matsumura M, Todokoro K. (1995) Characterization of the truncated thrombopoietin variants. *Biochem Biophys Res Commun.* **213:**1091-8.

Wagers AJ, Sherwood RI, Christensen JL, Weissman IL. (2002) Little evidence for developmental plasticity of adult hematopoietic stem cells. *Science.* **297:**2256-9.

Wakeford R. (2004) The cancer epidemiology of radiation. *Oncogene.* **23:**6404-28.

Walsh CP, Bestor TH. (1999) Cytosine methylation and mammalian development. *Genes Dev.* **13:**26-34.

Wang N, Satoskar A, Faubion W, Howie D, Okamoto S, Feske S, Gullo C, Clarke K, Sosa MR, Sharpe AH, Terhorst C. (2004) The cell surface receptor SLAM controls T cell and macrophage functions. *J Exp Med.* **199:**1255-64.

Wang S, Basten CJ, Zeng ZB. (2001-2004) Windows QTL Cartographer 2.0. Department of Statistics, North Carolina State University, Raleigh, NC. (http://statgen.ncsu.edu/qtlcart/WQTLCart.htm)

Ward JF. (1988) DNA damage produced by ionizing radiation in mammalian cells: identities, mechanisms of formation, and reparability. *Prog Nucleic Acid Res Mol Biol.* **35:**95-125.

Ward JF. (1985) Biochemistry of DNA lesions. *Radiat Res Suppl.* **8:**S103-11.

Warner JK, Wang JCY, Hope KJ, Jin L, Dick JE. (2004) Concepts of leukaemic development. *Oncogene.* **23:** 7164-7177.

Watson GE, Pocock DA, Papworth D, Lorimore SA, Wright EG. (2001) In vivo chromosomal instability and transmissible aberrations in the progeny of haemopoietic stem cells induced by high- and low-LET radiations. *Int J Radiat Biol.* **77:**409-17.

Watson GE, Lorimore SA, Clutton SM, Kadhim MA, Wright EG. (1997) Genetic factors influencing alpha-particle-induced chromosomal instability. *Int J Radiat Biol.* **71:**497-503.

Watson GE, Lorimore SA, Wright EG. (1996) Long-term in vivo transmission of alpha-particle-induced chromosomal instability in murine haemopoietic cells. *Int J Radiat Biol.* **69:**175-82.

Williams RW, Gu J, Qi S, Lu L. (2001) The genetic structure of recombinant inbred mice: high-resolution consensus maps for complex trait analysis. *Genome Biol.* **2:** RESEARCH0046. (http://www.nervenet.org)

Wynn TA. (2008) Cellular and molecular mechanisms of fibrosis. *J Pathol.* **214:**199-210.

Xie S, Wang Z, Okano M, Nogami M, Li Y, He WW, Okumura K, Li E. (1999) Cloning, expression and chromosome locations of the human DNMT3 gene family. *Gene*. **236:**87-95.

Yang AS, Estécio MR, Doshi K, Kondo Y, Tajara EH, Issa JP. (2004) A simple method for estimating global DNA methylation using bisulfite PCR of repetitive DNA elements. *Nucleic Acids Res.* **32:**38.

Yilmaz OH, Kiel MJ, Morrison SJ. (2006) SLAM family markers are conserved among hematopoietic stem cells from old and reconstituted mice and markedly increase their purity. *Blood.* **107:**924-30.

Yoder JA, Walsh CP, Bestor TH. (1997) Cytosine methylation and the ecology of intragenomic parasites. *Trends Genet.* **13:**335-40.

Zhang SM, Willett WC, Selhub J, Hunter DJ, Giovannucci EL, Holmes MD, Colditz GA, Hankinson SE. (2003) Plasma folate, vitamin B6, vitamin B12, homocysteine, and risk of breast cancer. *J Natl Cancer Inst.* **95:**373-80.

Zijno A, Andreoli C, Leopardi P, Marcon F, Rossi S, Caiola S, Verdina A, Galati R, Cafolla A, Crebelli R. (2003) Folate status, metabolic genotype, and biomarkers of genotoxicity in healthy subjects. *Carcinogenesis.* **24:**1097-103.